

**THE EFFECTS OF SELECTED MEDICINAL PLANT
EXTRACTS ON ANTI-ADIPOGENESIS OF 3T3-L1
CELLS**



**A Thesis Submitted in Partial Fulfillment of the Requirements for the
Degree of Doctor of Philosophy in Biomedical Sciences
Suranaree University of Technology**

Academic Year 2018

ผลของสารสกัดสมุนไพรบางชนิดต่อกระบวนการยับยั้งการสร้างไขมันในเซลล์

3T3-L1



นางสาวธนาภรณ์ เสงประถม

วิทยานิพนธ์นี้เป็นส่วนหนึ่งของการศึกษาตามหลักสูตรปริญญาวิทยาศาสตรดุษฎีบัณฑิต

สาขาวิชาชีวเวชศาสตร์

มหาวิทยาลัยเทคโนโลยีสุรนารี

ปีการศึกษา 2561

**THE EFFECTS OF SELECTED MEDICINAL PLANT EXTRACTS
ON ANTI-ADIPOGENESIS OF 3T3-L1 CELLS**

Suranaree University of Technology has approved this thesis submitted in partial fulfillment of the requirements for the Degree of Doctor of Philosophy.

Thesis Examining Committee

Rungrodee Srisawat

(Assist. Prof. Dr. Rungrodee Srisawat)

Chairperson

G. Eumkeb.

(Assoc. Prof. Dr. Griangsak Eumkeb)

Member (Thesis Advisor)

Gordon Matthew Lowe

(Dr. Gordon Matthew Lowe)

Member (Thesis Co-Advisor)

Sajeera Kupittayanant

(Assoc. Prof. Dr. Sajeera Kupittayanant)

Member

P. Ngern

(Assist. Prof. Dr. Piyada Ngernsounnern)

Member

Santi Maensiri

(Prof. Dr. Santi Maensiri)

Vice Rector for Academic Affairs
and Internationalization

Worawat Meevasana

(Assoc. Prof. Dr. Worawat Meevasana)

Dean of Institute of Science

ธนาภรณ์ เสงประถม : ผลของสารสกัดสมุนไพรบางชนิดต่อกระบวนการยับยั้งการสร้างไขมันในเซลล์ 3T3-L1 (THE EFFECTS OF SELECTED MEDICINAL PLANT EXTRACTS ON ANTI-ADIPOGENESIS OF 3T3-L1 CELLS)

อาจารย์ที่ปรึกษา : รองศาสตราจารย์ เกษัชกร ดร.เกรียงศักดิ์ เอี่ยมเก็บ, 198 หน้า.

ภาวะโรคอ้วนเป็นปัญหาหลักทางด้านสาธารณสุขที่สำคัญทั่วโลก ภาวะโรคอ้วนสามารถบ่งชี้ได้จากการเพิ่มจำนวนและขนาดของเซลล์ไขมันเต็มวัย (แอดิโพไซต์) ที่พัฒนามาจากเซลล์ไขมันต้นกำเนิด (พรีแอดิโพไซต์) การศึกษาครั้งนี้มีวัตถุประสงค์เพื่อตรวจสอบฤทธิ์การยับยั้งกระบวนการสร้างและพัฒนาไปเป็นเซลล์ไขมันโดยใช้เซลล์ชนิด 3T3-L1 ของสารสกัดจากพืชสมุนไพร 4 ชนิด ได้แก่ 1) เพกา (*Oroxylum indicum*) 2) อบเชยเทศ (*Cinnamomum verum*) 3) ย่านาง (*Tiliacora triandra*) และ 4) เสาวรส (*Passiflora edulis*) โดยสารสกัดจากพืชที่มีฤทธิ์ที่ดีที่สุดในการยับยั้งกระบวนการพัฒนาไปเป็นเซลล์ไขมันชนิด 3T3-L1 จะถูกคัดเลือกเพื่อนำไปวิจัยต่อไป รวมถึงศึกษากลไกการออกฤทธิ์และตรวจหาสารประกอบทางเคมีที่สำคัญ ผลการศึกษาพบว่าสารสกัดจากพืชสมุนไพรทั้ง 4 ชนิด มีฤทธิ์ในการยับยั้งกระบวนการพัฒนาไปเป็นเซลล์ไขมันแอดิโพไซต์ชนิด 3T3-L1 โดยพบว่าสารสกัดจากเพกา (OIE) ที่ช่วงความเข้มข้นระหว่าง 50 ถึง 200 ไมโครกรัมต่อมิลลิลิตร มีฤทธิ์ในการยับยั้งที่ดีที่สุด โดยความเข้มข้นในช่วงนี้ไม่มีความเป็นพิษต่อเซลล์ นอกจากนี้การลดลงของระดับการสร้างไขมันในเซลล์ 3T3-L1 ที่ถูกใส่สารสกัดจากเพกา ได้รับการยืนยันจากการทดสอบด้วยเทคนิคฟูเรียร์ทรานส์ฟอร์มอินฟราเรดสเปกโทรสโกปี (FTIR) จากการวิเคราะห์หาองค์ประกอบทางเคมีของสารสกัดจากเพกา ด้วยเทคนิค LC-MS และ GC-MS พบสารกลุ่มฟลาโวนอยด์ (ได้แก่ ไบคาไลน์) และไฟโตสเตอรอล (ได้แก่ แกมมา ซิโตสเตอรอล) เป็นองค์ประกอบหลัก การศึกษากลไกการยับยั้งกระบวนการพัฒนาไปเป็นเซลล์ไขมันแอดิโพไซต์ได้ทำการศึกษาโดยการตรวจสอบการแสดงออกของยีนและโปรตีนที่เกี่ยวข้องกับกระบวนการพัฒนาไปเป็นเซลล์ไขมันแอดิโพไซต์ วัฏจักรเซลล์ การเผาผลาญกลูโคสและกิจกรรมของไมโทคอนเดรีย ผลการศึกษาพบว่าสารสกัดจากเพกาที่ความเข้มข้น 200 ไมโครกรัมต่อมิลลิลิตรสามารถยับยั้งการแสดงออกของเอ็มอาร์เอ็นเอ (mRNA) ที่เกี่ยวข้องกับกระบวนการพัฒนาไปเป็นเซลล์ไขมันแอดิโพไซต์ รวมถึง PPAR γ 2 และ SREBP-1c นำไปสู่การลดลงของการหลั่งเอนไซม์ Fatty acid synthetase (FAS) และ อดิโปเนคติน (adiponectin) นอกจากนี้ ที่ระดับความเข้มข้นเดียวกันนี้พบว่าสารสกัดจากเพกา สามารถทำให้การดำเนินของวัฏจักรเซลล์ไปสู่ระยะ G2/M ช้าลงและซีดีเคสอง (Cdk2) ลดลง ยิ่งไปกว่านั้นการทดลองพบว่าสารสกัดจากเพกา สามารถลดปฏิกิริยาฟอสโฟริ

เลขชั้นของโปรตีนตัวรับอินซูลิน ชนิดที่ 1 และ 2 (IRS1 และ IRS2) ส่งผลให้การรับกลูโคสเข้าเซลล์ และการแสดงออกของ GLUT4 ในวันที่ 12 ของการทดลองลดลงด้วย ในการทดลองศักย์ไฟฟ้าของ เยื่อหุ้มไมโทคอนเดรีย (MMP) พบว่า สารสกัดจากเพกาททำให้ระดับ MMP ในเซลล์ไขมันแอดิโพไซต์ที่ได้รับสารสกัดเพกา มีค่าสูงขึ้นและต่ำลงอย่างมีนัยสำคัญกว่าเซลล์ไขมันพรีแอดิโพไซต์ที่ได้รับสารสกัดเพกา ที่เวลา 24 ชั่วโมงและวันที่ 12 ของการทดลองตามลำดับ ($P < 0.05$) อย่างไรก็ตาม ในวันที่ 12 ของการทดลองยังพบว่าเซลล์ไขมันแอดิโพไซต์ที่ได้รับสารสกัดเพกา มีระดับ MMP สูงกว่าในขณะที่ระดับเอทีพี (ATP) ต่ำกว่าอย่างมีนัยสำคัญเมื่อเทียบกับกลุ่มที่ไม่ได้รับสารสกัดเพกา ภาพจากกล้องจุลทรรศน์อิเล็กตรอนแบบส่องผ่าน (TEM) พบว่าสารสกัดเพกาสามารถปกป้องการเสียหายของไมโทคอนเดรียในเซลล์ไขมันแอดิโพไซต์ โดยลักษณะทางสัณฐานวิทยาของไมโทคอนเดรียยังคงเหมือนกับในเซลล์ไขมันพรีแอดิโพไซต์ เมื่อเทียบกับเซลล์ไขมันแอดิโพไซต์ที่ไม่ได้รับสารสกัดเพกา โดยสรุปแล้วการศึกษาครั้งนี้พบว่า สารสกัดจากเพกามีฤทธิ์ต่อต้านกิจกรรมของ กระบวนการสร้างและพัฒนาไปเป็นเซลล์ไขมันผ่านปัจจัยที่ช่วยเปลี่ยนแปลงไปเป็นเซลล์ไขมันพรีแอดิโพไซต์ ได้แก่ การยับยั้งวงจรของเซลล์และลดการเกิด phosphorylation ของ kinase ยิ่งไปกว่านั้น สารสกัดจากเพกายังสามารถเพิ่มกิจกรรมของไมโทคอนเดรียได้อีกด้วย ดังนั้น สารสกัดจากเพกา จึงมีศักยภาพสูงในการพัฒนาในอนาคตเพื่อเป็นผลิตภัณฑ์เสริมอาหารเพื่อสุขภาพ ยาสมุนไพรหรือยาแผนปัจจุบัน สำหรับการป้องกันและรักษาภาวะไขมันในเลือดสูงและโรคอ้วน

สาขาวิชาปริคลินิก

ปีการศึกษา 2561

ลายมือชื่อนักศึกษา ชนภรณ์ ไข่งประดม

ลายมือชื่ออาจารย์ที่ปรึกษา IN

TANAPORN HENGPRATOM : THE EFFECTS OF SELECTED
MEDICINAL PLANT EXTRACTS ON ANTI-ADIPOGENESIS OF
3T3-L1 CELLS. THESIS ADVISOR : ASSOC. PROF. GRIANGSAK
EUMKEB, Ph.D. 198 PP.

*OROXYLUM INDICUM/CINNAMOMUM VERUM/TILIACTORA TRIANDRA/
PASSIFLORA EDULIS/CELL VIABILITY/ANTI-ADIPOGENESIS/3T3-L1
ADIPOCYTES*

Obesity is a major public health threat worldwide. It is characterized by an increase in the number and size of adipocytes. The present study aimed to screen the inhibitory effects of 4 selected medicinal plant extracts including 1) *Oroxylum indicum* (*O. indicum*), 2) *Cinnamomum verum* (*C. verum*), 3) *Tiliacora triandra* (*T. triandra*), and 4) *Passiflora edulis* (*P. edulis*) on adipogenesis using 3T3-L1 cells. The extract demonstrated the highest inhibitory effect on the development of 3T3-L1 adipocytes was chosen for further investigations. These consisted of determining the phytochemicals composition and mechanism of action. The results suggested that all of 4 selected medicinal plant extracts had anti-adipogenesis effects, but the most significant inhibitory effect was in *O. indicum extract* (OIE) at a concentrations of 50 to 200 µg/mL with no effect on the viability of 3T3-L1 cells. The reduction of lipid level in 3T3-L1 cells treated with OIE was confirmed by FTIR. The results from LC-MS and GC-MS revealed that the major phytochemical composition in OIE was composed of flavonoid (baicalein) and phytosterol (γ -sitosterol). The mechanism of action on anti-adipogenesis activity was evaluated through the study of adipogenic

transcription, cell cycle, glucose metabolism, and mitochondria activity. The OIE at 200 µg/mL inhibited adipogenic mRNA expression, including PPAR γ 2 and SREBP-1c led to decrease fatty acid synthetase (FAS) enzyme and adiponectin secretion. Also, the cell cycle transition to the G2/M phase was delayed and Cdk2 was decreased by OIE at this concentration. Furthermore, OIE decreased the phosphorylation of insulin receptor substrate 1 and 2 (IRS1 and IRS2) resulted in a decrease in glucose uptake level and GLUT4 expression at day 12. In mitochondrial activity experiment, the mitochondria membrane potential (MMP) level of OIE-treated differentiated cells was significantly higher, whereas lower than OIE-treated non-differentiated cells at 24 h and day 12 respectively ($P < 0.05$). Also, OIE-treated differentiated cells exhibited significantly higher MMP level, whereas lower ATP level compared to the untreated differentiated group at day 12, respectively. Transmission electron microscope results revealed that OIE could protect mitochondria deformation of differentiated cells, entirely similar to pre-adipocytes, compared to the untreated group. In summary, these findings provide evidence that OIE has anti-adipogenesis activity through adipogenic transcriptional factors, cell cycle inhibition, and decrease kinase phosphorylation. Furthermore, OIE can also improve mitochondria activity. Therefore, OIE exhibits a high potential for future development to be a novel health food supplement, herbal medicine, or modern drug for the prevention and treatment of hyperlipidemia and obesity.

School of Preclinic

Academic Year 2018

Student's Signature

T. Hengpratom

Advisor's Signature

G. Eumkeb

ACKNOWLEDGEMENTS

I would like to express my deepest and sincere gratitude to my thesis advisor, Assoc. Prof. Dr. Griangsak Eumkeb, for his excellent guidance, caring, encourages and supports throughout my time as a Ph.D. student.

My deepest appreciation is extended to my academic co-supervisor, Dr. Gordon Matthew Lowe for his excellent guidance, valuable advice, and kindly let me have wonderful research experience in life sciences laboratory at the Liverpool John Moores University.

I extend many thanks to my committee members, Assist. Prof. Dr. Rungrudee Srisawat, Assoc. Prof. Dr. Sajeera Kupittayanant, and Assist. Prof. Dr. Piyada Ngermsoungnern for their excellent advice and suggestions regarding this thesis.

I gratefully acknowledge to the Thailand Research Fund for financially supporting me throughout my studies through the Royal Golden Jubilee Ph.D. program (Grant No. PHD/0029/2556).

I would like to extend my sincere thanks to all staffs at Suranaree University of Technology and Liverpool John Moores University, many thanks go to my colleagues and friends who are always willing to help in every circumstance.

My acknowledgement cannot be completed without expressing my extreme gratitude to my lovely family who always supports, encourages and beside me in every moment during my studies.

Tanaporn Hengpratom

CONTENTS

	Page
ABSTRACT IN THAI.....	I
ABSTRACT IN ENGLISH	III
ACKNOWLEDGEMENTS.....	V
CONTENTS.....	VI
LIST OF TABLES	XIV
LIST OF FIGURES	XV
LIST OF ABBREVIATION.....	XVIII
CHAPTER	
I INTRODUCTION.....	1
1.1 Introduction.....	1
1.2 Research objectives.....	4
1.3 Research hypothesis.....	5
1.4 Scope and limitation of the study.....	5
1.5 Significant of the Study	8
1.6 References.....	8
II LITERATURE REVIEW	13
2.1 Significant of obesity and its therapeutic options	13
2.2 3T3-L1 cell culture model for adipogenesis study	14
2.3 History of 3T3-L1 cell	14

CONTENTS (Continued)

	Page
2.4 The stages of adipocyte differentiation.....	15
2.4.1 Molecular signals that drive adipogenesis at very early stage	16
2.4.2 Molecular signals that drive adipogenesis at early and intermediate stage.....	17
2.4.3 Molecular signals that drive adipogenesis at late stage	18
2.5 Role of transcriptional factors during differentiation	19
2.5.1 Peroxisome proliferator-activated receptors (PPARs).....	19
2.5.2 Sterol regulatory element-binding proteins (SREBPs).....	20
2.6 The stages of adipocyte differentiation.....	23
2.6.1 Glucose transporter 4 (GLUT4) and Insulin receptor.....	23
2.6.2 Fatty acid synthase (FAS)	24
2.7 Adipocyte-secreted adipocytokines	25
2.7.1 Adiponectin.....	25
2.7.2 Leptin	26
2.8 The role of mitochondria during adipogenesis	28
2.9 <i>Oroxylum indicum</i>	29
2.9.1 Key Features of <i>O. indicum</i>	29
of <i>O. indicum</i>	30
2.9.2 A summary of some chemical constitutes identified in different parts of <i>O. indicum</i>	30

CONTENTS (Continued)

	Page
2.10 <i>Cinnamomum verum</i>	31
2.10.1 Key features of <i>C. verum</i>	31
2.10.1 A summary of some chemical constituents identified in different parts of <i>C. verum</i>	32
2.11 <i>Passiflora edulis</i>	33
2.11.1 Key features of <i>P. edulis</i>	33
2.11.2 A summary of some chemical constituents identified in different parts of <i>P. edulis</i>	34
2.12 <i>Tiliacora triandra</i>	35
2.13 Flavonoids phytochemical properties related to lipid metabolism.....	35
2.14 References	40
III PLANT EXTRACTIONS, CYTOTOXICITY, AND LIPID ACCUMULATION OF FOUR MEDICINAL PLANTS	56
3.1 Abstract	56
3.2 Introduction	57
3.3 Materials	58
3.3.1 Plant specimens	58
3.3.2 Chemicals and reagents	59
3.3.3 Cell line	59

CONTENTS (Continued)

	Page
3.4 Method	60
3.4.1 Preparation of media used for 3T3-L1 cells differentiation.....	60
3.4.2 Procedures for 3T3-L1 cells differentiation.....	60
3.4.3 Plant extraction preparation	61
3.4.4 Cytotoxicity.....	61
3.4.5 Oil Red O staining	62
3.4.6 Statistical analysis.....	63
3.5 Results.....	63
3.5.1 Percentage yields of plant extracts.....	63
3.5.2 The effect of the extracts on cell viability in 3T3-L1 pre-adipocytes	64
3.5.3 The effect of the extracts on lipid accumulation in 3T3-L1 adipocytes.....	66
3.6 Discussion and conclusion.....	69
3.7 References.....	71
 IV SCREENING OF BIOACTIVE COMPOUNDS IN <i>O. INDICUM</i>	
FRUIT EXTRACT AND BIOCHEMICAL COMPOSITIONS OF	
3T3-L1 CELLS	74
4.1 Abstract.....	74
4.2 Introduction.....	76
4.3 Materials and Methods.....	78

CONTENTS (Continued)

	Page
4.3.1 Chemicals and reagents.....	78
4.3.2 Phytochemical screening.....	78
4.3.3 Total phenolic content determination (TPC)	79
4.3.4 Total flavonoid content determination (TFC).....	80
4.3.5 Gas chromatography-mass spectrometry (GC-MS) analysis.....	80
4.3.6 Liquid chromatography-tandem mass spectrometry (LC-MS/MS)	81
4.3.7 Fourier-transform Infrared Spectroscopy (FTIR) analysis	81
4.4 Results.....	82
4.4.1 The phytochemical composition, TPC and TFC.....	82
4.4.2 GC-MS quantification of volatiles compounds in OIE.....	83
4.4.3 LC-MS/MS quantification of selected flavonoids in OIE	86
4.4.4 Fourier-transform infrared (FTIR) spectral profiles	88
4.5 Discussion and conclusion.....	100
4.6 References.....	104
V EFFECT OF <i>O. INDICUM</i> EXTRACT ON ADIPONECTIN SECRETION, LIPASES ACTIVITY, AND MOLECULAR MECHANISM ON ANTI-ADIPOGENESIS	110
5.1 Abstract.....	110
5.2 Introduction.....	111
5.3 Materials and methods	113

CONTENTS (Continued)

	Page
5.3.1 Chemicals and reagents.....	113
5.3.2 Cell culture and treatment.....	113
5.3.3 Protein extraction and immunoblot analysis.....	114
5.3.4 Determination of adiponectin secreted from 3T3-L1 cells by ELISA	115
5.3.5 Immunocytochemistry for adiponectin.....	116
5.3.6 RNA extraction and mRNA expression analysis.....	116
5.3.7 Lipase activity.....	118
5.3.8 Statistical analysis.....	118
5.4 Results.....	118
5.4.1 Effect of OIE on adiponectin protein expression in 3T3-L1 cells.....	118
5.4.2 Effect of OIE on the secretion of adiponectin	121
5.4.3 Effect of OIE on adiponectin staining in 3T3-L1 cells.....	122
5.4.4 Effect of OIE on mRNA expression in 3T3-L cells	124
5.4.5 Effect of OIE on pancreatic lipase activity.....	125
5.5 Discussion and conclusion.....	127
5.6 References.....	130
VI EFFECT OF O. INDICUM EXTRACT ON ADIPONECTIN SECRETION, LIPASES ACTIVITY, AND MOLECULAR MECHANISM ON ANTI ADIPOGENESIS	135

CONTENTS (Continued)

	Page
6.1 Abstract.....	135
6.2 Introduction.....	137
6.3 Materials and methods	139
6.3.1 Chemicals and reagents.....	139
6.3.2 Cell culture.....	139
6.3.3 Cell cycle analysis.....	140
6.3.4 Protein extraction and immunoblot analysis.....	140
6.3.5 Immunocytochemistry	141
6.3.6 Flow cytometry	142
6.3.7 Confocal microscopy	142
6.3.8 ATP measurement.....	143
6.3.9 Electron microscopy	143
6.3.10 Statistical analysis.....	144
6.4 Results.....	145
6.4.1 Effect of OIE on inhibition of cell cycle progression.....	145
6.4.2 Effect of OIE on glucose metabolism.....	149
6.4.3 Effect of OIE on mitochondrial activity	152
6.5 Discussion and conclusion.....	160
6.6 References.....	164
VII CONCLUSION	171
APPENDICES	174

CONTENTS (Continued)

	Page
APPENDIX A STANDARD CURVE	175
APPENDIX B REAGENTS AND BUFFERS	178
APPENDIX C PLUBLICATION	183
CURRICULUM VITAE.....	198



LIST OF TABLES

Table	Page
2.1	Summarization of studies of lipid-lowering effects of OIE..... 31
2.2	Summarization of studies relating CVE on lipid metabolism 33
2.3	Summarization of studies relating PEE on lipid metabolism 34
3.1	Extraction yield of OIE, CVE, TTE, and PEE..... 64
4.1	Phytochemical composition, total phenolic content, and total flavonoid content of OIE..... 83
4.2	The relative concentrations of volatiles in OIE 84
4.3	Quantification of selected compounds in OIE..... 88
4.4	FTIR band assignments for functional groups found in the second derivative Spectra of 3T3-L1 cell 90

LIST OF FIGURES

Figure	Page
1.1	Scope and limitation of the studies 7
2.1	The conversion of 3T3-L1 pre-adipocytes to adipocytes 15
2.2	Major identified events of 3T3-L1 preadipocyte differentiation in chronological order 16
2.3	The mechanism of PPAR γ nuclear receptor 20
2.4	Summary of the present of the proteolytic activation SREBPs 22
2.5	Insulin promotes SREBP-1c processing 22
2.6	The signaling pathway of glucose transporter 4 and insulin receptor 24
2.7	Diagram of some proteins identified in adipocytes 27
2.8	Characteristics of <i>O. indicum</i> 30
3.1	The procedure for differentiation of 3T3-L1 cells 61
3.2	The effect of four medicinal extracts on the viability of 3T3-L1 preadipocytes 65
3.3	The effect of four medicinal extracts on the lipid accumulation in 3T3-L1 adipocytes 67
3.4	Microscopic imaging of intracellular lipid 3T3-L1 cells 68
4.1	The GC/MS chromatogram of the OIE 84
4.2	Multiple reaction monitoring (MRM) chromatograms of OIE and standard reference compounds 87

LIST OF FIGURES (Continued)

Figure	Page
4.3	Average original FTIR spectra (3000-950 cm ⁻¹) obtained from 3T3-L1 cells 89
4.4	Average the secondary derivative spectra of 3T3-L1 cells..... 93
4.5	The histogram of integrated areas of 3T3-L1 cells 95
4.6	Principal component analysis (PCA) of FTIR spectral ranges 3000-2800 cm ⁻¹ and 1800-950 cm ⁻¹ giving PCA score plot 97
4.7	Unsupervised hierarchical cluster analysis (UHCA) dendrogram achieved by cluster classifications of infrared spectra of 3T3-L1 cells..... 99
5.1	The effect of OIE on adiponectin protein expression 120
5.2	The effect of OIE on the secretion of adiponectin during differentiation..... 122
5.3	The effect of OIE on the secretion of adiponectin during differentiation..... 123
5.4	The effect of OIE on mRNA expression of PPAR γ 2, SREBP-1C, FAS, GLUT4, and LEP in 3T3-L1 cells 125
5.5	Inhibitory effects of OIE (%) at various concentrations lipase activity..... 126
6.1	The effect of the OIE on cell cycle progression in 3T3-L1 preadipocytes.... 146
6.2	The effect of the OIE on glucose metabolism in 3T3-L1 cells..... 150
6.3	The effect of the OIE on mitochondrial activity in 3T3-L1 cells 155
7.1	Schematic represents the partial mechanisms of the anti-adipogenesis of OIE on 3T3-L1 adipocytes 172

CHAPTER I

INTRODUCTION

1.1 Introduction

Obesity is a condition in which the body's energy reserves are stored in fatty tissue and increased to a point where it may have an adverse effect on health. On a global scale, obesity has reached epidemic proportions and is a major contributor to the global burden of chronic disease and disability. Currently, thirteen percent of the adult population was reported as being clinically obese (WHO, 2019; Yun, 2010). The statement is based on the collection and analysis of body mass index (BMI, kg/m^2) data. The BMI scales indicate that a BMI equal or over 25 are classified as overweight, but greater than or equal to 30 are classified as obese. In recent years, the incidence of obesity has risen at an alarming rate and is becoming a significant public health concern with incalculable social costs. Indeed, obesity facilitates the development of metabolic disorders such as diabetes, hypertension, and cardiovascular diseases in addition to chronic illnesses such as stroke, osteoarthritis, sleep apnea, some cancers, and inflammation-based pathologies (Bray, 2004; Chang et al., 2015; D'Adamo et al., 2015; Schienkiewitz et al., 2012) .

Pharmaceutical treatments commonly prescribed for obesity such as orlistat, phentermine, diethylpropion, fluoxetine, metformin, and thiazolidinediones have

potential long-term side-effects which have raised some safety concerns over these treatments (Rucker et al., 2007). At present, because of dissatisfaction of high costs and potentially hazardous side-effects, the potential of natural products for treating obesity is under exploration. This may be an excellent alternative strategy for developing future effective, safe anti-obesity drugs (Mayer et al., 2009). One avenue that is under current consideration is the use of natural products to target obesity with the hope of achieving success and reducing the toxic side-effects. The compounds must target the generation or apoptosis of adipose tissue. Recently resveratrol was found to have properties that can mimic caloric restriction (Lam et al., 2013). *Oroxylum indicum* (*O. indicum*) belong to the Bignoniaceae family is used in traditional food ingredient and medicine in Asia (Zeraik and Yariwake, 2010). The chemical constituents of *O. indicum*, including flavones, alkaloids, baicalein, chrysin, oroxylin A, and oroxylin B (Dinda et al., 2015; Uddin et al., 2003). Preliminary studies indicated that its pharmacological effects were primarily anti-microbial or anti-inflammatory (Mat Ali et al., 1998). Antioxidant activities were also reported. A less reported effect of this extract was its capacity to inhibit adipogenesis. Moreover, stem bark of this plant has been shown a protective effect on carbon tetrachloride-induced hepatotoxicity in the rat (Panda, 2011). *Cinnamomum verum* (J.) (*C. verum*), also known as Ceylon cinnamon or 'true cinnamon' is indigenous to Sri Lanka (Jayaprakasha and Rao, 2011). The studies have demonstrated many beneficial health effects of *C. verum*, such as anti-inflammatory properties, anti-microbial activity, blood glucose control, reducing cardiovascular disease, boosting cognitive function, and it may help reduce the risk of colon cancer (Gruenwald et al., 2010; Ouattara et al., 1997). One

important characteristic of this compound is that Cinnamon also significantly increase HDL and insulin level, but reduce body weight and LDL level in diabetic rats (Ranasinghe et al., 2012). *Tiliacora triandra* (*T. triandra*) or Yanang belongs to the *Menispermaceae* family. It is a vegetable used in many cuisines of the northeast of Thailand and Lao, especially in bamboo shoot soup. Phytochemical screening of the methanol extract showed the presence of alkaloid, flavonoid, tannin, and saponins. It also exhibited the property of having effective antioxidant activity. So, the apparent antioxidant activity suggests its potential usefulness in the prevention of some diseases (Rattana et al., 2010). *Passiflora edulis* (*P. edulis*) or passion fruit is the species most employed as a flavoring and as juice in the food industries. Most of the pharmacological investigations of *P. edulis* have been focused on its antioxidant activity due to its present expressive amount of flavonoids especially in leaves (Barbosa et al., 2008; Da Silva et al., 2013; Rudnicki et al., 2007; Zeraik and Yariwake, 2010; Zeraik et al., 2011). Moreover, several researchers have determined that established isoflavones and flavonoids derived from plant extracts such as genistein, naringenin, and quercetin all have anti-adipogenic effects on 3T3-L1, a preadipocyte cell line (Harmon and Harp, 2001; Hwang et al., 2005). Furthermore, the natural products and the 3T3-L1 cell line have been extensively used to study the potential role of apoptosis in adipocyte tissue growth to prevent or treat metabolic disorders (Hsu and Yen, 2006; Hwang et al., 2005; Singh and Kakkar, 2014; Sorisky et al., 2000). This cell line becomes one of the most intensively studied models because they are derived from a mouse embryo and are committed to the adipocyte lineage. In addition, the influences of

hormones and a transcriptional factor on adipocyte regulation and development may be studied (Moreno-Navarrete and Fernández-Real, 2017).

As mentioned above, a few studies have investigated the anti-adipogenesis effects of medicinal plant crude extracts as follow in 3T3-L1 pre-adipocyte cell line. In this study, we intended to investigate the impact of *O. indicum*, *C. verum*, *T. triandra*, and *P. edulis* on anti-adipogenesis activity. A more detailed study was undertaken using these cell lines to determine the effect on biochemical composition of cells, adipocytokine secretion, transcriptional regulation, cell cycle regulation, and mitochondria function in order to gain further insight into the molecular mechanisms whereby crude extracts may have to mediate its antiadipogenic action in vitro.

1.2 Research objectives

Accordingly, the overall objectives of the present thesis were:

- 1.2.1 To screen of four selected medicinal plant extracts for anti-adipogenesis activity. The extract that showed less intracellular lipid accumulation in 3T3-L1 adipocytes was chosen for further analysis.
- 1.2.2 To investigate the phytochemical compounds of *O. indicum* extract.
- 1.2.3 To investigate the effect of *O. indicum* extract on biochemical components of 3T3-L1 adipocytes using FTIR.
- 1.2.4 To investigate the effect of *O. indicum* extract on lipase activity, adipocytokines, and transcriptional factors involved during adipogenesis (PPAR γ 2 and SREBP-1c).

1.2.5 To explore the cells cycle progression and mitochondria function of 3T3-L1 cells during adipogenesis with and without *O. indicum* extract.

1.3 Research hypothesis

1.3.1 The medicinal plant crude extracts were not toxic to 3T3-L1 cells but appeared to have biological activity.

1.3.2 The extracts contained a high content of flavonoids compounds, including baicalein.

1.3.3 The extracts decreased lipid accumulation and adipocytokine expression by suppression of cell cycle progression and regulation of PPAR γ 2 and SREBP-1C transcriptional factors.

1.3.4 The extracts suppressed insulin signaling pathway by modulation at insulin receptor phosphorylation, glucose transporter 4, and glucose uptake level.

1.3.5 The extracts slowed down mitochondria activity at the early phase of adipocytes differentiation resulted in a decrease in lipogenesis.

1.4 Scope and limitations of the study

Initial experiments were performed using 3T3-L1 cells to establish any potential toxic effect of four medicinal plants extract including *O. indicum*, *C. verum*, *T. triandra*, and *P. edulis* and their impacts on lipid accumulation in adipocytes. Then, the plant extract that showed less lipid accumulation was selected to investigate their chemical composition and mechanisms of action. Phytochemical test of the extracts was performed by using a

simple screening test, LC-MS, and GC-MS. The biochemical components of cells were determined by using FTIR. The impact of the extracts on lipase activity was investigated *in vitro* using lipase of porcine pancreas type 2. According to the process of converting pre-adipocytes into adipocytes involved a series of tightly regulated events of the interplay between mediators of cell-cycle functions and differentiation-associated factors. Thus, cell cycle, cell cycle regulatory proteins (cdk2, cyclin A) were examined by flow cytometer and western immunoblotting, respectively. Fatty acid synthetase (FAS), glucose transporter (GLUT4), peroxisome proliferator-activated receptor-gamma 2 (PPAR γ 2), and sterol regulatory element-binding proteins 1 (SREBP-1c) transcriptional factors were measured by real-time PCR. Adiponectin secreted from the cells was measured using enzyme-linked immunosorbent assay (ELISA). The impact of the extract on mitochondria activity was measured by JC1-dye for mitochondria membrane potential and ATP luminescent for intracellular ATP level. The limitation of this study was only one medicinal plant extract that showed positive results on anti-adipogenesis was selected to investigate their mechanisms of action. The overviews of the studies were summarized in Figures 1.1.

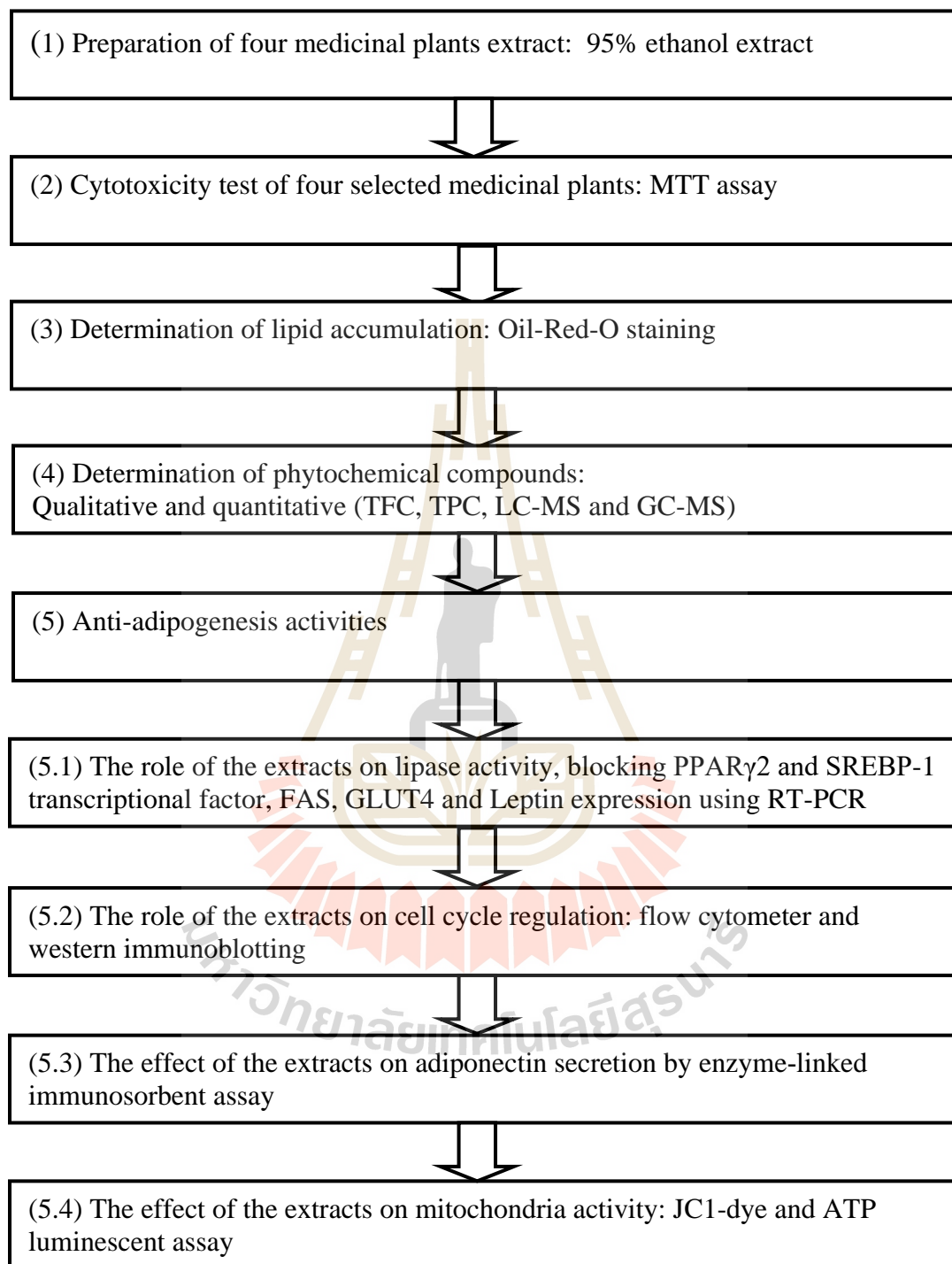


Figure 1.1 Scope and limitation of the studies.

1.5 Significance of the study

The research was expected to provide the following information:

1.5.1 The cytotoxicity data and potential use of selected four medicinal plants on anti-adipogenesis in 3T3-L1 adipocytes.

1.5.2 Insights on the potentialities of *O. indicum* extract on anti-adipogenesis in 3T3-L1 adipocytes.

1.5.3 The outcome from the study of mitochondria activity could have been used as scientific data for future therapeutic strategies to treat obesity by targeting mitochondria.

1.6 References

- Barbosa, P. R., Valvassori, S. S., Bordignon, C. L., Jr., Kappel, V. D., Martins, M. R., Gavioli, E. C., Quevedo, J., and Reginatto, F. H. (2008). The aqueous extracts of *Passiflora alata* and *Passiflora edulis* reduce anxiety-related behaviors without affecting memory process in rats. **Journal of Medicinal Food**. 11(2): 282-288.
- Bray, G. A. (2004). Medical Consequences of Obesity. **The Journal of Clinical Endocrinology and Metabolism**. 89(6): 2583-2589.
- Chang, C. J., Jian, D. Y., Lin, M. W., Zhao, J. Z., Ho, L. T., and Juan, C. C. (2015). Evidence in obese children: contribution of hyperlipidemia, obesity-inflammation, and insulin sensitivity. **PloS One**. 10(5): e0125935.

- D'Adamo, E., Guardamagna, O., Chiarelli, F., Bartuli, A., Liccardo, D., Ferrari, F., and Nobili, V. (2015). Atherogenic dyslipidemia and cardiovascular risk factors in obese children. **International Journal of Endocrinology**. 2015: 912047.
- Da Silva, J. K., Cazarin, C. B. B., Colomeu, T. C., Batista, Â. G., Meletti, L. M. M., Paschoal, J. A. R., Bogusz Júnior, S., Furlan, M. F., Reyes, F. G. R., Augusto, F., Maróstica Júnior, M. R., and de Lima Zollner, R. (2013). Antioxidant activity of aqueous extract of passion fruit (*Passiflora edulis*) leaves: *In vitro* and *in vivo* study. **Food Research International**. 53(2): 882-890.
- Dinda, B., SilSarma, I., Dinda, M., and Rudrapaul, P. (2015). *Oroxylum indicum* (L.) Kurz, an important Asian traditional medicine: from traditional uses to scientific data for its commercial exploitation. **Journal of Ethnopharmacology**. 161: 255-278.
- Gruenwald, J., Freder, J., and Armbruester, N. (2010). Cinnamon and Health. **Critical Reviews in Food Science and Nutrition**. 50(9): 822-834.
- Harmon, A. W., and Harp, J. B. (2001). Differential effects of flavonoids on 3T3-L1 adipogenesis and lipolysis. **American Journal of Physiology - Cell Physiology**. 280(4): C807-813.
- Hsu, C. L., and Yen, G. C. (2006). Induction of cell apoptosis in 3T3-L1 pre-adipocytes by flavonoids is associated with their antioxidant activity. **Molecular Nutrition and Food Research**. 50(11): 1072-1079.
- Hwang, J. T., Park, I. J., Shin, J. I., Lee, Y. K., Lee, S. K., Baik, H. W., Ha, J., and Park, O. J. (2005). Genistein, EGCG, and capsaicin inhibit adipocyte differentiation

- process via activating AMP-activated protein kinase. **Biochemical and Biophysical Research Communications**. 338(2): 694-699.
- Jayaprakasha, G. K., and Rao, L. J. (2011). Chemistry, biogenesis, and biological activities of *Cinnamomum zeylanicum*. **Critical Reviews in Food Science and Nutrition**. 51(6): 547-562.
- Lam, Y. Y., Peterson, C. M., and Ravussin, E. (2013). Resveratrol vs. calorie restriction: data from rodents to humans. **Experimental Gerontology**. 48(10): 1018-1024.
- Mat Ali, R., Houghton, P. J., Raman, A., and Houtt, J. R. (1998). Antimicrobial and antiinflammatory activities of extracts and constituents of *Oroxylum indicum* (L.) Vent. **Phytomedicine**. 5(5): 375-381.
- Mayer, M. A., Hocht, C., Puyo, A., and Taira, C. A. (2009). Recent advances in obesity pharmacotherapy. **Current Clinical Pharmacology**. 4(1): 53-61.
- Moreno-Navarrete, J. M., and Fernández-Real, J. M. (2017). Adipocyte differentiation. In: **Adipose Tissue Biology**. Springer, pp. 69-90
- Ouattara, B., Simard, R. E., Holley, R. A., Piette, G. J.-P., and Bégin, A. (1997). Antibacterial activity of selected fatty acids and essential oils against six meat spoilage organisms. **International Journal of Food Microbiology**. 37(2-3): 155-162.
- Panda, S. K. (2011). Phytochemical Analysis and Hepatoprotective Effect of Stem Bark of *Oroxylum indicum* (L) Vent. on Carbon Tetrachloride Induced Hepatotoxicity in Rat. **International Journal of Pharmaceutical and Biological Archive**. 2.

- Ranasinghe, P., Jayawardana, R., Galappaththy, P., Constantine, G., de Vas Gunawardana, N., and Katulanda, P. (2012). Efficacy and safety of 'true' cinnamon (*Cinnamomum zeylanicum*) as a pharmaceutical agent in diabetes: a systematic review and meta-analysis. **Diabetic Medicine**. 29(12): 1480-1492.
- Rattana, S., Padungkit, M., and Cushnie, B. (2010). *Phytochemical screening, flavonoid content, and antioxidant activity of Tiliacora triandra leaf extracts*. In: the Proceedings of the 2nd Annual International Conference of Northeast Pharmacy Research. pp. 60-63.
- Rucker, D., Padwal, R., Li, S. K., Curioni, C., and Lau, D. C. (2007). Long term pharmacotherapy for obesity and overweight: updated meta-analysis. **British Medical Journal**. 335(7631): 1194-1199.
- Rudnicki, M., de Oliveira, M. R., da Veiga Pereira, T., Reginatto, F. H., Dal-Pizzol, F., and Moreira, J. C. F. (2007). Antioxidant and antiglycation properties of *Passiflora alata* and *Passiflora edulis* extracts. **Food Chemistry**. 100(2): 719-724.
- Schienkiewitz, A., Mensink, G. B. M., and Scheidt-Nave, C. (2012). Comorbidity of overweight and obesity in a nationally representative sample of German adults aged 18-79 years. **BioMed Central Public Health**. 12(1): 658.
- Singh, J., and Kakkar, P. (2014). Oroxylin A, a constituent of *Oroxylum indicum* inhibits adipogenesis and induces apoptosis in 3T3-L1 cells. **Phytomedicine**. 21(12): 1733-1741.

- Sorisky, A., Magun, R., and Gagnon, A. M. (2000). Adipose cell apoptosis: death in the energy depot. **International Journal of Obesity and Related Metabolic Disorders** 24 Suppl 4: S3-7.
- Uddin, K., Sayeed, A., Islam, A., Rahman, A. A., Ali, A., Khan, G., and Sadik, M. G. (2003). Purification, Characterization and Cytotoxic Activity of Two Flavonoids from *Oroxylum Indicum* Vent. (Bignoniaceae). **Asian Journal of Plant Sciences**. 2(6): 515-518.
- WHO. (2019, May 28). Obesity and overweight. [On-line]. <https://www.who.int/en/news-room/fact-sheets/detail/obesity-and-overweight>.
- Yun, J. W. (2010). Possible anti-obesity therapeutics from nature-a review. **Phytochemistry**. 71(14-15): 1625-1641.
- Zeraik, M., and Yariwake, J. (2010). Quantification of isoorientin and total flavonoids in *Passiflora edulis* fruit pulp by HPLC-UV/DAD. **Microchemical Journal**. 96(1): 86-91.
- Zeraik, M. L., Serateyn, D., Deby-Dupont, G., Wauters, J.-N., Tits, M., Yariwake, J. H., Angenot, L., and Franck, T. (2011). Evaluation of the antioxidant activity of passion fruit (*Passiflora edulis* and *Passiflora alata*) extracts on stimulated neutrophils and myeloperoxidase activity assays. **Food Chemistry**. 128(2): 259-265.

CHAPTER II

LITERATURE REVIEW

2.1 Significant of obesity and its therapeutic options

Obesity is a serious health problem because it is implicated in various diseases, including type II diabetes, hypertension, coronary heart disease, and cancer (Kopelman, 2000). Obesity is characterized by increased adipose tissue mass that results from both adipocyte hyperplasia (increased fat cell number) and adipocyte hypertrophy (increased fat cell size) (Couillard et al., 2000). Proposed mechanisms for controlling obesity have been extended based on the energy balance between energy intake and expenditure. Although using weight-loss drugs or restrictive gastric surgery are common ways for treatment to manage obesity, recent progress has been made in the regulation of white fat tissue development at the cellular and molecular events. Recently, it was discovered that the amount of adipose tissue mass could be regulated by either inhibition of adipogenesis or induction of apoptosis (Roncari et al., 1981; Sorisky et al., 2000). It is necessary to understand the mechanisms responsible for adipocyte development for efforts to identify new and better therapeutic options to inhibit these processes. However, the study of adipocyte differentiation has been further hampered by the diffuse nature of adipogenesis *in vivo*; this has made it challenging to dissect regions of committed, which presumptive precursor cell from an embryo. So, *in vitro* cell line has provided preferably to identify the mechanism that regulates adipocyte differentiation

2.2 3T3-L1 cell culture model for adipogenesis study

The purpose of this study was related to the development of the adipocyte. Thus, it is essential to select a suitable model fit for the objectives and the experiments. Unfortunately, it would be difficult to control other systems which may interfere with the development of the adipocyte in vivo models. Hence, an in vitro study is the first step to achieve this goal and to reduce the interfering effect. 3T3-L1 cells are major preadipocyte cell line model, which has been used for many studies. The specific character of these cells is when treated with appropriate hormone or pharmacological agent it can only differentiate to adipocyte lineage, and during development, they also change in the expression of numerous genes reflected by the appearance of early, intermediate and late of mRNA, protein marker and triglyceride accumulation. Thus, 3T3-L1 cells seem to be quite useful in the identification of key molecular marker and transcription. This section below will describe the history of the 3T3-L1 cell line, the differentiation process from pre-adipocyte to adipocyte; factor represented in a different stage of adipocyte development and hormone produced from these cells.

2.3 History of 3T3-L1 cells

The 3T3-L1 cell line is the first and most commonly characterized in vitro model established to study adipogenesis. The 3T3-L1 cells were found in 1974 by two scientists, George Todaro and Howard Green (Green and Meuth, 1974). Selected clones of the original fibroblast stock obtained from 17- to 19-day Swiss 3T3 mouse embryos were able to convert to adipose cells in culture. The 3T3-L1 cells propagate under normal conditions having a fiblastic phenotype. In response to a confluent and contact-inhibited state with the appropriate stimulus, the morphologically-fibroblast-like pre-

adipocytes undergo conversion into round adipocytes accumulating fat in high serum mediums (Green and Kehinde, 1975). Figure 2.1 shows the morphology of undifferentiated cell (2A), 3T3-L1 pre-adipocytes after 10 days of differentiating (2B) and adipocytes stained with oil red o after 10 days of differentiating (2C). Cells differentiated from pre-adipocytes into adipocytes that had the morphology of mature adipocytes, characterized by a large quantity of lipids droplets in the cytoplasm. The lipids are stained red (Oliveira et al., 2013).

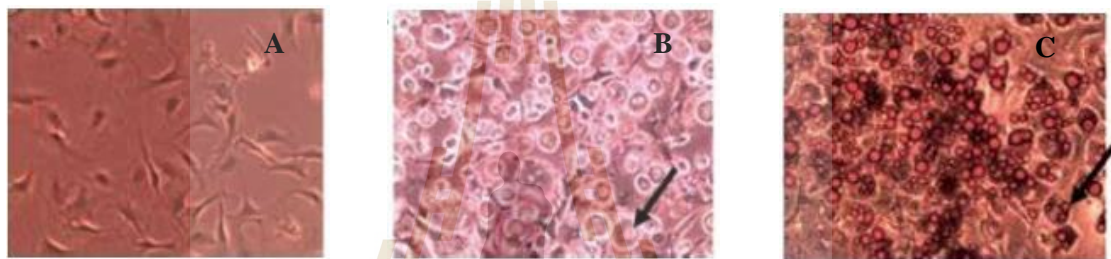


Figure 2.1 The conversion of 3T3-L1 pre-adipocytes to adipocytes.

(A) Undifferentiated cells (pre-adipocytes). (B) Cells after 10 days of differentiating. (C) Cells stained with oil red o after 10 days of differentiating. The arrows indicate an adipocyte with lipid droplets in the cytoplasm (Oliveira et al., 2013).

2.4 The stages of adipocyte differentiation

The differentiation process of converting pre-adipocyte to adipocyte involves a series of tightly regulated events of the interplay between mediators of cell-cycle functions and differentiation-associated factors (Avram et al., 2007). The stages of adipocyte differentiation in vitro models include the specific patterns of gene expression, which have been illustrated in Figure 2.2.

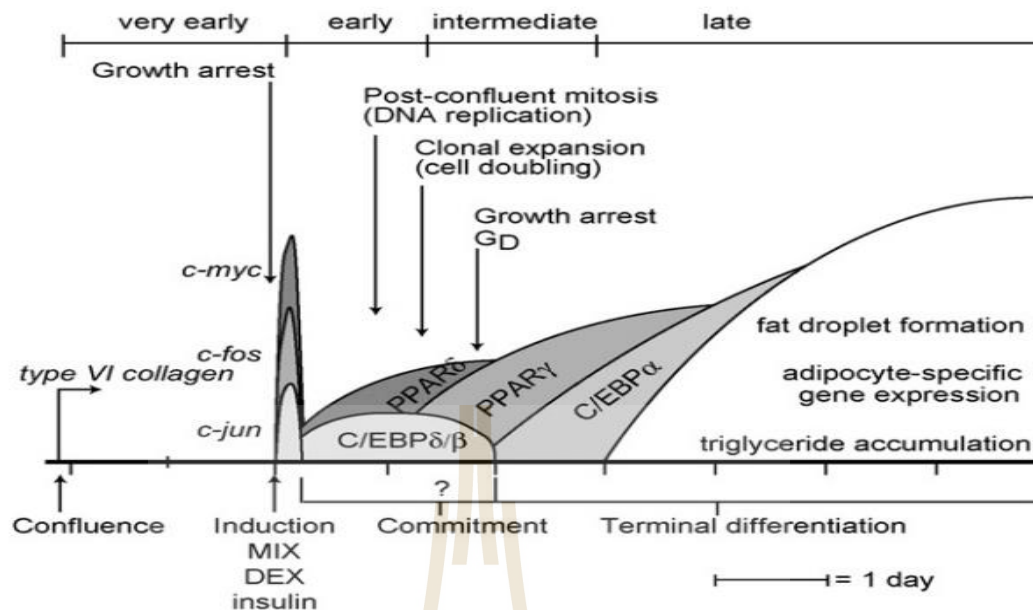


Figure 2.2 Major identified events of 3T3-L1 preadipocyte differentiation in chronological order. The major events are composed of a very early stage, early and intermediate stage, and late-stage (described below). Areas labeled by gene names represent periods of gene expression during the differentiation program (Avram et al., 2007).

2.4.1 Molecular signals that drive adipogenesis at a very early stage

After reaching confluence that no more space for cell growth and propagation, proliferating preadipocytes no longer multiply due to cell-cell contact inhibition. This crosstalk inhibition between cell signals post-confluent preadipocytes to become growth arrest at the G1/S phase of the cell cycle. Withdrawal of cell cycle in preadipocytes or growth arrest is necessarily a first step in the commitment of cultured preadipocytes toward terminal differentiation (Ailhaud et al., 1989). In addition, the transition process is associated with the expression of very early markers such as collagen type VI. However, the confluent 3T3-L1 pre-adipocytes at the arrest growth

stage can spontaneously differentiate into clusters of fat cells in the presence of fetal bovine serum-supplemented culture medium for several weeks. Moreover, the conversion process could be accelerated by an adipogenic cocktail, which different and varies in each cell type. The inducer for the differentiation of 3T3-L1 cells is composed of fetal bovine serum, insulin, dexamethasone, isobutylmethylxanthine. After the addition of inducer to 3T3-L1 cells for 1 hour, the expression of nuclear proto-oncogenes c-fos, c-jun, c-myc, and the transcription factors C/EBP β and C/EBP δ are observed (Zeng et al., 1997). C-myc has been involved in the ability of preadipocytes to respond to signals that stimulate DNA replication (mitogenesis). Based on their roles in other systems, c-fos and c-jun proteins are also thought to possess mitogenic properties. The transient expression of c-fos, c-myc, and c-jun disappear within 2 to 6 hours after induction (Zeng et al., 1997). C/EBP β and C/EBP δ probably play an important role as initiators of postconfluent mitosis and clonal expansion (Greenbaum et al., 1998; Zheng et al., 2005).

2.4.2 Molecular signals that drive adipogenesis in an early and intermediate stage

Before differentiation, growth-arrested preadipocytes received appropriate induction, undergo at least one round of DNA replication (post confluent mitosis) and cell doubling (clonal expansion), a process proposed to lead to the clonal amplification of committed cells (Cornelius et al., 1994). Then, two days after induction growth-arrested cells have the ability to differentiated in the absence of the DNA synthesis, and only arrested cells response to a proliferative effect of isobutylmethylxanthine (Scott et al., 1982). At this point afterward, the preadipocytes are already to be fully committed, and the key transcription factors, PPAR γ , and C/EBP α begin to rise before and during

this stage. The cells begin to express the late markers of adipocyte differentiation by day 3 and become spherical, accumulate fat droplets, which complete terminal differentiation by days 5 through days 7 (Yang et al., 2008).

2.4.3 Molecular signals that drive adipogenesis at a late-stage

From arrested cells to terminal differentiation, the adipocytes lose their capacity of cell division permanently by an irreversible withdrawal of cells from the cell cycle. During the terminal phase of differentiation, lipid metabolism specialized adipocytes in a culture markedly increase in de novo lipogenesis and acquire a sensitivity to insulin to fulfill the dramatic increment in lipid synthesis and hormonal responsiveness as they are *in vivo* (Gregoire et al., 1998). In this stage, the preadipocytes take on the characteristics of the mature adipocyte. About 10-100 folds of up-regulation of genes that are responsible for the glucose and lipid metabolism was measured in mRNA levels and protein activities during this stage, including ATP citrate lyase, malic enzyme, acetyl-CoA carboxylase, stearoyl-CoA desaturase, glycerol phosphate acyltransferase, glycerol-3-phosphate dehydrogenase, fatty acid synthase and glyceraldehyde-3-phosphate dehydrogenase (Paulauskis and Sul, 1988).

Alteration in the composition of cell membrane receptors drives differentiating adipocytes to function hormonally like mature fat cells to acquire both lipogenic and lipolytic properties. Insulin sensitivity is enhanced in response to the induced expression and number of insulin receptors and insulin-sensitive glucose transporters like GLUT-4 (Garcia de Herreros and Birnbaum, 1989). While the replacement of β 1-adrenergic receptors with the β 2- and β 3-adrenergic receptors increases in the total number of adrenoreceptors and a higher sensitivity to lipolysis stimuli (Fève et al., 1990). Further, scientific evidence has clarified that other than being storage depots,

adipocytes also secrete adipocytokines which function to regulate appetite, glucose and lipid metabolism and immunity to achieve intercommunication with other organs like hypothalamus, muscle, and liver (Kershaw and Flier, 2004; Walker et al., 2007). This established the role of the secretory cell to adipocytes. The adipocyte-secreted proteins, for instances adiponectin, leptin, resistin, and tumor necrosis factor- α , are crucial for homeostasis of multiple physiological processes (Avram et al., 2007; Gregoire, 2001).

2.5 Role of transcriptional factors during differentiation

2.5.1 Peroxisome proliferator-activated receptors (PPARs)

Peroxisome proliferator-activated receptors (PPARs) are identified as a group of nuclear hormone receptor (Feige et al., 2006). The family of PPARs is represented by the following three members: PPAR- α , PPAR- δ , and PPAR- γ . These receptors have an important role relating to lipid and glucose metabolism, fatty acid transport, adipocyte differentiation and inflammation (Shao et al., 2016; Varga et al., 2011; Wang et al., 2018). Peroxisome proliferator-activated receptor-gamma 2 (PPAR γ 2) is a subdivision of the PPAR γ family. It has a significant role in adipogenesis especially when activated by an agonist ligand in preadipocytes; a differentiation program is stimulated; in turn, morphological changes, lipid accumulation, and distinctive adipocyte gene expression take place (Barak et al., 1999; Tontonoz et al., 1994). *In vivo* study found that adipose selective knockout of PPAR γ 2 has reduced fat in mouse (Farmer, 2006). Similarly, normal mice exposed to a high fat diet has increased of PPAR γ 2 by 50% in adipose tissue (Vidal-Puig et al., 1996). The mechanism of PPAR γ initiated by ligands which can be a hormone, a free fatty acid, fatty acid derivative, or synthetic drugs binds to nuclear receptor then PPAR γ form heterodimers with the

retinoid X receptor (RXR). The heterodimers bind to sequence-specific PPAR response elements (PPREs) present in the DNA of target genes, activating transcription of these genes and thereby increasing protein expression (Figure 2.3) (Grommes et al., 2004).

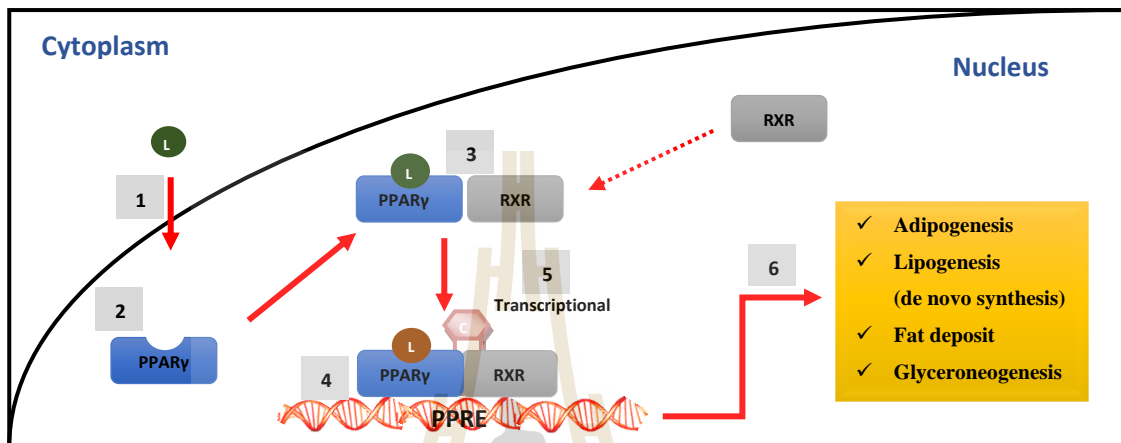


Figure 2.3 The mechanism of PPAR γ nuclear receptor. PPAR γ : Peroxisome proliferator-activated receptors-gamma, RXR: retinoids X receptor, PPRE: PPAR response elements (Grommes et al., 2004).

2.5.2 Sterol regulatory element-binding proteins (SREBPs)

SREBPs are grouped as a family of transcriptional factors mediating the expression levels of enzymes in cholesterol synthesis or uptake and fatty acid synthesis. These factors are proteins, which belong to the basic helix-loop-helix-leucine zipper family, translated in the endoplasmic reticulum (ER) as precursor proteins (Horton et al., 2002). Transcriptional activation of protein performs from ER to Golgi, where inactive SREBPs are cleaved and activated by SREBP cleavage-activating protein (SCAP). The activity of SCAP depends on the presence of insulin and the intracellular sterols levels. In response to the two signal stimulators (insulin and the intracellular sterols levels), the activation of SCAP is induced, leading to the production of active

forms of SREBP proteins. Exposed NH₂-terminal domain of the mature form of SREBPs, after translocation to the nucleus, binds to sterol response elements in the promoter/enhancer of multiple target genes for gene coding, in turn modulating lipogenic enzymes (Figure 2.4) (Matsuda et al., 2001).

SREBP-1 and SREBP-2 are two major isoforms with the former one further divided into SREBP-1a and SREBP-1c. Evaluation of individual isoforms suggest SREBP-1 may be selectively involved in activation of genes involved in fatty acid metabolism and de novo lipogenesis whereas SREBP-2 may be more selective for genes involved directly in cholesterol homeostasis (Horton et al., 1998; Pai et al., 1998). Overexpression of SREBP-1c in cultured preadipocytes activated genes involved in fatty acid and triglyceride syntheses such as Acetyl CoA Carboxylase and fatty acid synthase (FAS) (Noriega et al., 2012). These processes required the simultaneous addition of insulin and a high level of glucose (Figure 2.5) (Kim and Spiegelman, 1996; Shimano et al., 1997; Xu et al., 2013).

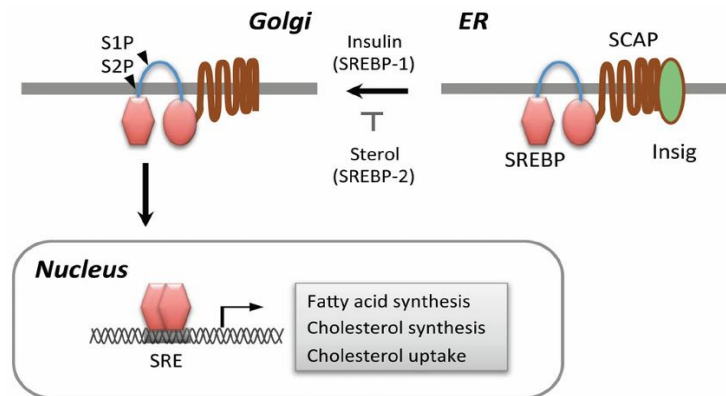


Figure 2.4 Summary of the present of the proteolytic activation SREBPs. SREBPs are synthesized as ER-anchored precursor forms in the ER. SREBPs are associated with the SREBP cleavage-activating protein (SCAP) and ER retention protein called Insig. In order to be activated, SREBP-SCAP complex should be dissociated from Insig, then migrate to the Golgi apparatus. SREBPs are sequentially cleaved by site 1 (S1P) and site 2 (S2P) proteases in the Golgi, which releases the N-terminal cytosolic portion of the protein, which enters the nucleus to act as the active transcription factor (Xu et al., 2013).

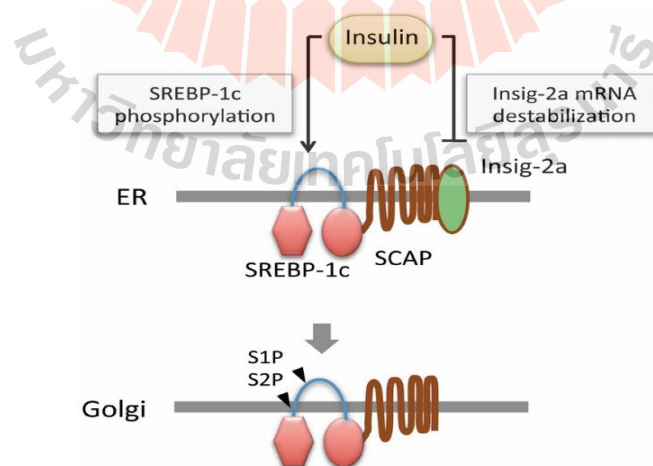


Figure 2.5 Insulin promotes SREBP-1c processing. Insulin induces AKT-mediated SREBP-1c phosphorylation, which stimulates the transport of SREBP-1c-SCAP

complex to the Golgi apparatus. Insulin also induces the degradation of Insig-2a mRNA to promote the Golgi transport and proteolytic processing of SREBP-1c (Xu et al., 2013).

2.6 The roles of the protein involved in lipid and glucose metabolism

2.6.1 Glucose transporter 4 (GLUT4) and Insulin receptor

Glucose is an important energy source for most cells for metabolism. The uptake of glucose into the cells is mediated by a family of integral membrane proteins, called glucose transporters. GLUT4 is highly expressed in adipose tissue and muscle. In lipid assimilation, GLUT-4 carries out metabolic functions by facilitating glucose transportation into the cells and exerting an effect on the metabolism of glucose removal and homeostasis. Insulin promotes the glucose uptake into adipocytes by stimulating the GLUT-4. Upon the activation of the insulin receptor, GLUT-4 protein concentrated in the intracellular membrane system is translocated to the plasma membrane by exocytosis from its cytosolic site. At the same time, the endocytosis of GLUT-4 is significantly inhibited to prevent the internalization of cycling GLUT-4 from the plasma membrane. The overall redistribution of GLUT-4 to the cell surface thus results in a 10-20-fold increase in glucose transport (Huang et al., 2008). Insulin signaling is initiated when insulin binds to its receptor, leads to a rapid conformational change in the receptor that eventuates in autophosphorylation of specific tyrosine residues receptor then recruitment sites for insulin receptor substrate (IRS) proteins. The PI-3 kinase is a target of IRS proteins, which converts the membrane lipid PIP2 to PIP3. When activated PIP3 subsequently activates PDK1 and Akt. Akt activated, plays a vital

role by linking Glut4 to the insulin signal transduction pathway shown in Figure 2.6 (Dasgupta et al., 2011).

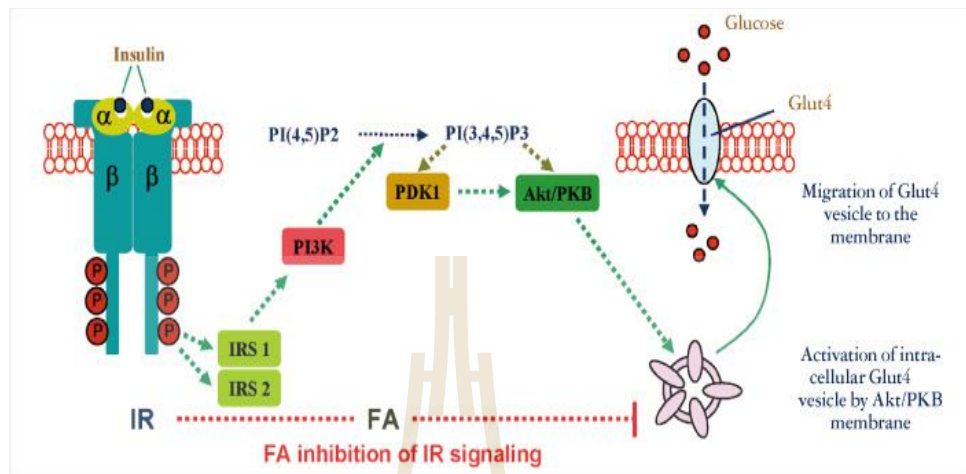


Figure 2.6 The signaling pathway of glucose transporter 4 and insulin receptor. Fatty acid (FA) has been reported to impair this pathway by producing defects in the insulin receptor (IR), insulin receptor substrate (IRS1), phosphatidylinositol 3-kinase (PI3K), phosphoinositide-dependent kinase1 (PDK1), Akt/protein kinase B (PKB), and glucose transporter 4 (Glut4) (Dasgupta et al., 2011).

2.6.2 Fatty acid synthase (FAS)

FAS is instrumental in catalyzing the formation of long-chain fatty acids (LCFA). Such products of de novo synthesis are the important source for the intracellular TG synthesis through esterifying with glycerol-3-phosphate (Ruderman et al., 1999). In fat tissues, FAS elongates the short-chain malonyl-CoA by the condensation with acetyl-CoA to form LCFAs such as palmitoyl-CoA and stearoyl-CoA. Referring to the malonyl-CoA regulatory mechanism, it is essential to confine the intracellular level of accumulated malonyl-CoA, of which an increase inhibits the activity of carnitine palmitoyl transferase1 (CPT1), an enzyme facilitating the uptake

of palmitoyl-CoA into the mitochondria for β -oxidation (fat burning), and contribute to the subsequent fatty acid synthesis, leading to enhanced fat deposit in tissues. Controversially, the FAS promote the fatty acid synthesis and fat accumulation on one side but lower the intracellular malonyl-CoA level to allow fat oxidation on the other sides, suggesting a FAS system could be a pivotal point for intervention via the regulation of both fat oxidation and accumulation (Kusunoki et al., 2006).

2.7 Adipocyte-secreted adipocytokines

2.7.1 Adiponectin

Adiponectin, abbreviated Acrp30, is a protein hormone produced mainly by mature adipocytes. In contrast to other polypeptide hormones, adiponectin is very abundant in circulation (Kadowaki and Yamauchi, 2005). This adipocyte-specific hormone, classified as good adipocytokine, has been shown to manipulate multiple metabolic processes, including glucose and fatty acid catabolism (Kadowaki and Yamauchi, 2005). Though it is produced in adipose tissue, adiponectin secretion was found to be decreased in obese and type 2 diabetic patients (Holst and Grimaldi, 2002). It is reported that circulating adiponectin levels are inversely related to insulin resistance and hyperinsulinemia, linking adiponectin to the development of metabolic syndrome (Weyer et al., 2001). Such as insulin resistance, glucose intolerance, and hyperlipidemia and increased susceptibility to vascular injury and atherosclerosis (Kubota et al., 2002).

Being a significant adipocyte secretory product, adiponectin in circulation exerts insulin-sensitizing, anti-inflammatory, and antiatherosclerotic effects as an endocrine factor while, within adipose tissue, it plays roles in differentiation, gene

expression, and biological function via autocrine and paracrine pathway (Lara-Castro et al., 2006). During adipocytes differentiation, the level of adiponectin mRNA elevates 100 folds. Experimentally, overexpression of adiponectin accelerates adipocytes differentiation leading to more significant lipid accumulation and higher insulin-responsive glucose transport activity in fully differentiated cells (Fu et al., 2005). It is further supported by in vivo study. Obese animals with adiponectin treatment have shown decreased levels of blood glucose and free fatty acids in plasma, and improved insulin sensitivity (Berg et al., 2002).

2.7.2 Leptin

Leptin is an important adipocyte-derived hormone well known for its major regulatory roles in satiety, metabolism, neuroendocrine function, and energy homeostasis (Friedman, 2002). This hormone is mainly synthesized by adipocytes as a product of the obese (*ob*) gene. Glucose homeostasis is regulated by leptin through multiple actions, including uterine, endocrine, and paracrine fashion and has action at distinct neural circuits. The hypothalamus is the major effector mediating the leptin effect on metabolism and satiety. Leptin receptors are found within the ventrobasal hypothalamus, which is known as appetite center. The binding of leptin to the receptors within the hypothalamus signals to the central nervous system (CNS) which produces a feeling of satiety. Thus, it works like a signal of negative energy balance.

The mechanism of leptin on 3T3-L1 cell line indicated that leptin does not act directly to induce adipocyte apoptosis, but can act directly to inhibit maturation of pre-adipocytes (Ambati et al., 2007). Anti-lipogenic and lipolytic effects of leptin during differentiated and mature adipocytes may have been partly mediated by suppressing the expression of PPAR γ and IGF-I genes (Kim et al., 2008). Leptin not only affects the

central nervous system but also affects peripheral tissues such as liver, muscle, and pancreas (Paz-Filho et al., 2012). The deficiency of functional leptin or its receptor has been investigated for the pathogenesis of insulin resistance and obesity in *ob/ob* or *db/db* mouse strains (Kahn and Flier, 2000). In leptin-deficient *ob/ob* mice, the administration of leptin ameliorate both glucose and insulin levels, and the insulin-sensitizing effect surpasses those seen in pair-fed mice. Increasing evidence supports that in nonadipose tissues (i.e., muscle and β -cells), lipid accumulation is lowered by leptin via enhanced fatty acid oxidation and reduced lipid synthesis, which would increase insulin sensitivity (Muoio et al., 1997). It was shown that leptin could reduce esterification and increase fatty acid oxidation in pancreatic islets and skeletal muscle (Kahn and Flier, 2000). Summarization of some proteins identified during/after differentiation of adipocytes showed in Figure 2.7.

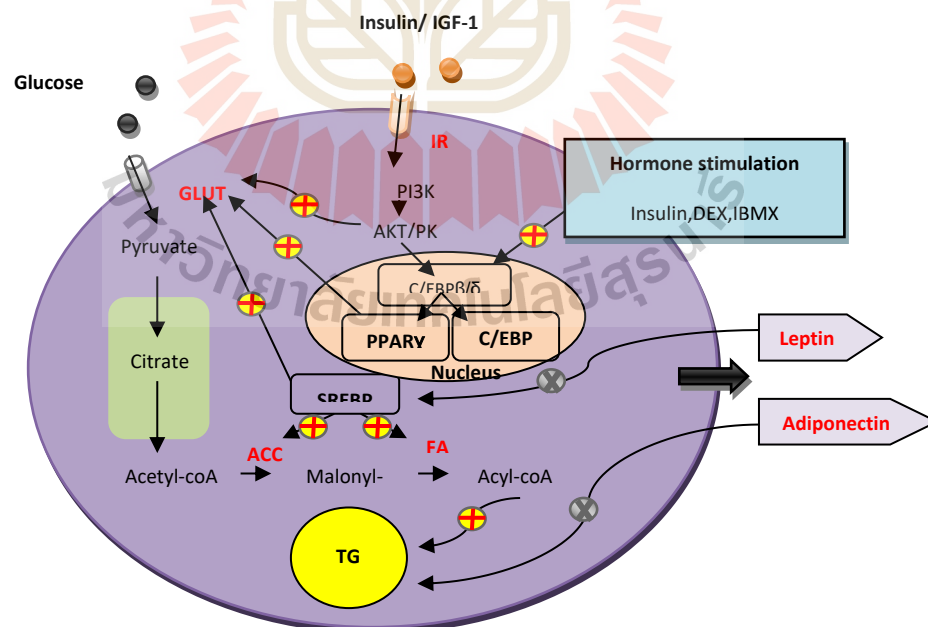


Figure 2.7 Diagram of some proteins identified in adipocytes.

2.8 The role of mitochondria during adipogenesis

As mentioned above, the ability of pre-adipocyte to differentiate into adipocyte influenced by the abundance of signaling genes, proteins, and hormone secreted by adipocyte. Since many protein and biochemical events are involved in the process of lipogenesis, mitochondria might be required to provide generous ATP to ensure the normal metabolism of lipid synthesis. The section below summarizes the current knowledge of mitochondria on cells differentiation.

In recent year, evidence has suggested that the regulation of mitochondria dynamic and function are essential for osteogenic and adipocyte differentiation. Mitochondria has a significant role in physiological response and involved in metabolic pathways by converting carbohydrate, lipids, and protein into ATP. During differentiation of 3T3-L1 adipocyte, it stimulates the mitochondria proliferation and s mitochondria morphology appeared to be dense and surrounded by the lipid droplet (Wilson-Fritch et al., 2003). Besides, expression of mitochondria mRNA in adipocytes such as pyruvate carboxylase (a key intermediate for triglyceride synthesis) increased about 16-fold and a component of pyruvate dehydrogenase complex increased about 20-fold compared to pre-adipocytes (Wilson-Fritch et al., 2003). In the study of Lu RH et al., demonstrated that ATP level was highest after treated with an adipogenic cocktail, then decreased accompanied with adipocyte differentiation (Lu et al., 2010). While extracellular ATP provides cell sensitivity to the adipogenic hormone in the pre-proliferating stages and stimulates adipocyte differentiation (Omatsu-Kanbe et al., 2006). Which suggests that the high level of ATP may start up the signal in adipogenesis. However, the role of mitochondria during cell differentiation is in its initial stages, more research of the molecular messengers linking mitochondria dynamic

and differentiation of adipocytes is still required. Thus, to find out more mechanism of the plant extract on anti-adipogenesis, it would be exciting to know how plant extracts impact on mitochondria in the 3T3-L1 model.

2.9 *Oroxylum indicum* (*O. indicum*)

2.9.1 Key Features of *O. indicum*

Being a member of the Bignoniaceae family, *Oroxylum* is a genus and under *indicum* species. *O. indicum* is well-known and widely found throughout the tropical area, including Southeast Asia and South Asia, mainly in the damp region and moist places in the forests (Harminder et al., 2011). This plant is a deciduous tree; small to medium-sized and may grow to 12 meters in height. The leaves are 90-180 cm long, 2-3 pinnate with 5 or more pairs of primary pinnae. The flowers are reddish-purple externally, but pale, pinkish-yellow on the inside. The tree fruit has long pods that curved downward, hang down from the branches. Fruits are flat capsules, 0.33-1 m long and 5-10 cm broad and sword-shaped. When the pod bursts open the seeds flutter to the ground, often traveling some distance, resembling butterflies. The plant flowers in June-July and bears fruits in November. The fresh root bark is soft and juicy; it is sweet, becoming bitter later. On drying, the bark shrinks adhere closely to the wood and become faintly fissured (Harminder et al., 2011). Characteristics of *O. indicum* showed in Figure 2.8.

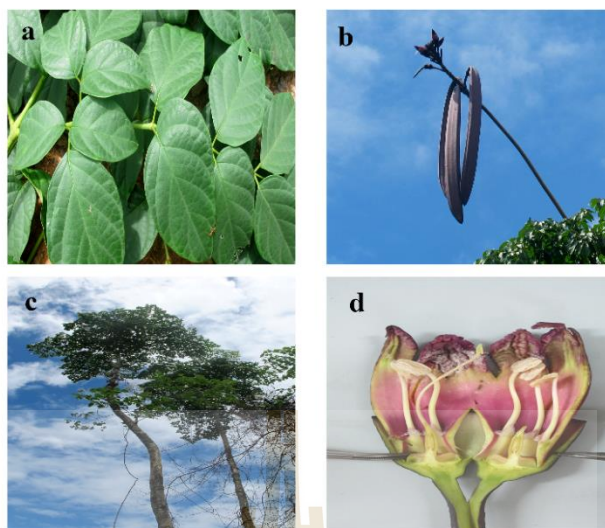


Figure 2.8 Characteristics of *O. indicum*, (a) leaves (b) Pod (c) trees (d) flowers

2.9.2 A summary of some chemical constituents identified in different parts of *O. indicum*

The evaluation of root bark of *O. indicum* performed by using RP-HPLC showed the presence of flavonoids oroxylin A, baicalein, and chrysin (Zaveri et al., 2008). The root of *O. indicum* was extracted with dichloromethane also showed flavonoid (baicalein, chrysin, oroxylin-A), naphthalenoids (lapachol) and steroid (β -sitosterol) (Mat Ali et al., 1998). The extract of stem bark (500 $\mu\text{g/mL}$) with 50% aqueous ethanol was reported to contain baicalin, baicalein, and chrysin (Singh and Kakkar, 2013). Also, the major chemical constituents of seeds of the plant also contain baicalein, chrysin, baicalein-7-O-glucoside, baicalein 7-O-diglucoside, and chrysin-7-O-diglucoside (Chen et al., 2003). The flavonoid baicalein is an active component in the methanolic extract of *O. indicum*, which represented approximately 4% of freeze-dried fruits (Roy et al., 2007). The result from identification of flavonoid from leaves of *O. indicum* by high-speed counter-current chromatography system (HPCCC) showed chrysin, baicalein, baicalein-7-O-glucoside, baicalein-7-O-diglucoside, chrysin-7-O-

glucuronide, baicalein-7-O-glucuronide, and a chrysin-diglucoside are the major chemical constituents (Yuan et al., 2008). Reviews relating *O. indicum* on lipid metabolism showed in table 2.1.

Table 2.1 Summary of studies of lipid-lowering effects of *O. indicum*.

Model of study	Treatment	Significant Result	Reference
In vitro studies			
3T3-L1 cells	Oroxylin A, (dose 20 μ M, 40 μ M)	Suppress intracellular lipid accumulation, downstream genes (FAS and LPL) along with adiponectin secretion.	(Singh and Kakkar, 2014)
3T3-L1 cells	Baicalein (dose 20 μ M)	Prevent the differentiation of pre-adipocytes to adipocyte during 4 days of induction	(Dunkhunthod et al., 2017)
In vivo studies			
Rats fed with high cholesterol-rich diet	<i>O. indicum</i> Extract (dose 200 mg/kg/day)	Exhibit good anti-obesity effect, blood sugar level, and body organ weights were also found to be significantly reduced as compared to the normal group.	(D'Mello et al., 2011)

2.10 *Cinnamomum verum* (*C. verum*)

2.10.1 Key features of *C. verum*

C. verum also known as Ceylon cinnamon or 'true cinnamon.' It belongs to Lauraceae family, which is widely distributed throughout tropical, subtropical India and Sri Lanka. The tree grows to 10–15 meters height and forms a very dense mat of fine roots in the topsoil. Leaves are stiff, vary in shape and size and petiole 1-2 cm long.

The young leaves of the lush bush, later turning dark green above with paler veins and pale grayish-green beneath. Individual flowers tiny, about 3 mm in diameter, pale yellow, with a fetid smell, each subtended by a small, ovate, hairy bract. Bark 8-10 mm thick, brown, rough, and cracks vertical line (NCCIH, 2009).

2.10.2 A summary of some chemical constituents identified in different parts of *C. verum*

Various kind of essential oils is significantly founded in different parts of cinnamon, which provide different pharmacological effects (Kaul et al., 2003). Other chemical components which can be isolated from this plant are phenolic and flavonoids compound (Rao and Gan, 2014). The isolation of violates from root bark performed by using gas chromatography showed that camphor is a major component of root bark (Senanayake et al., 1978). However, the roots of these plants contain chrysin, scutellarin-7-rutinoside, sitosterol, galactose, baicalein, biochanin-A, ellagic acid, oroxylin-A (Vangalapati et al., 2012). The stem of this plant is reported to contain 65 to 80 percent of cinnamaldehyde with 5 to 10 percent of eugenol (Bullerman et al., 1977). Leave of *C. verum* also contain cinnamaldehyde and eugenol 1 to 5 % and 70-95 % respectively. Trans-cinnamyl acetate and caryophyllene are major compounds located in fruits of *C. verum* (Bullerman et al., 1977). Moreover, the investigation of the extracts and their active compound with different of the solvent has been reported to possess antioxidant, anti-inflammatory, anti-diabetic activity, cholesterol and lipid-lowering effect (Rao and Gan, 2014). Reviews relating *C. verum* on lipid metabolism showed in table 2.2.

Table 2.2 Summary of studies relating *C. verum* on lipid metabolism

Model of study	Treatment	Significant Result	Reference
In vitro studies			
3T3-L1 cells	Supercritical fluid extracts of <i>C. verum</i> (SFC)	SFC significantly reduce the mRNA expression of the transcription factor PPAR γ , SREBP1c, down-regulated, ASC1, FAS, FATP1 and perilipin	(Park et al., 2013)
Human pancreatic α -amylase (HPA)	Isopropanol extracts of <i>C. verum</i> (leaves)	Reducing of postprandial hyperglycemia via control of starch breakdown.	(Ponnusamy et al., 2011)
In vivo studies			
Wistar rats fed a high-fructose diet to induce insulin resistance	Cinnamon extract (Cinnulin PF, 50 mg/kg daily)8 weeks	Reducing blood glucose, plasma insulin, triglycerides, total cholesterol, chylomicron-apoB48, VLDL-apoB100, and soluble CD36.	(Qin et al., 2010)

2.11 *Passiflora edulis* (*P. edulis*)

2.11.1 Key features of *P. edulis*

The genus *Passiflora*, comprising about 500 species, is the largest in the family Passifloraceae (the passionflower family). The species of this genus are distributed in the warm temperate and tropical regions. Several species are grown in the tropics for their edible fruits, the most widely grown being *P. edulis* Sims (Passion fruit or purple Granadilla). The plants of genus *Passiflora* are a group of the herbaceous or woody vine, mostly climbers with auxiliary tendrils. The leaf is blades 3-lobed with 2-5 cm petioles. It has a white and purple color of flowers. Fruits are dark purple when ripe

(Dhawan et al., 2004). *P. edulis* leaves extract resulted in improved wound healing and the inhibition of parasite growth. The aqueous extract of the root was effective against viruses (Noriega et al., 2012).

2.11.2 A summary of some chemical constituents identified in different parts of *P. edulis*

P. edulis has been reported to be rich in glycoside and contain other compounds such as phenols and alkaloid. A major component of leaves of *P. edulis* is flavone (isoorientin) and other contained glycoside (passiflorin), phenols, glycosyl flavonoids, cyanogenic and alkaloids (Bombardelli et al., 1975; Dhawan et al., 2004; Petry et al., 2001). Also, fruits of this plant also found 19% of flavone (isoorientin), carotenoids, and L-ascorbic acid (Zeraik and Yariwake, 2010). Reviews relating to *P. edulis* on lipid metabolism showed in table 2.3.

Table 2.3 Summary of studies relating *P. edulis* on lipid metabolism.

Model of study	Treatment	Significant Result	Reference
Pilot clinical study			
nineteen women, aged between 30- and 60-years cholesterol \geq 200 mg/dL	The flour of the passion fruit peel (pectin) (30g)	60 days it was observed a statistical reduction of the total cholesterol and LDL-cholesterol	(Ramos et al., 2007)
In vivo studies			
Hamster fed with high cholesterol-rich diet	<i>P. edulis</i> seed extract (5.73g/100g of diet)	Decreasing the levels of serum triglyceride, total serum cholesterol, and liver cholesterol	(Chau and Huang, 2005)

2.12 *Tiliacora triandra* (*T. triandra*)

T. triandra belongs to the Menispermaceae family, which has a Thai name call Ya Nang. It is a vegetable used in many cuisines of the northeast of Thailand and Lao, especially in bamboo shoot soup. Phytochemical screening of the methanol extract showed the presence of alkaloid, flavonoid, tannin, and saponins with anti-oxidant activity (Rattana et al., 2010). The study of acute and subchronic toxicities of the water extract from *T. triandra* showed that *T. triandra* does not cause acute or subchronic toxicities in either male or female rats during 90 days (Seewaboon et al., 2008). Although many people drink Yanang juice every day to decrease body weight or blood sugar, there is no scientific evidence to prove the exact effect and mechanism of *T. triandra* relate to lipid metabolism. At this point, *T. triandra* should have been studied.

2.13 Flavonoids phytochemical properties related to lipid metabolism

Flavonoids are a family of polyphenolic compounds, which occur naturally in fruits and plants. The structure of flavonoids is based upon 15 carbon atoms, 2 benzene rings joined by heterocyclic pyran ring. 6 majors subgroups of flavonoids composed of flavones, flavonols, flavanones, flavanone, isoflavones, and flavan-3-ols (Kumar and Pandey, 2013). The different between subgroups of flavonoids are at c rings position while within groups are the substitution of A and B rings. Several of the biological properties of flavonoids appear to be related to their structure. The biological properties of some flavonoids have been shown to relate to metabolic diseases such as anti-obesity and anti-diabetic (Kawser Hossain et al., 2016). Due to flavonoids cannot be synthesized by humans and animals. Thus the studies that interested in active phytochemical properties mostly came from the original natural source such as plants.

The paragraph below mentioned about the scientific evidence that shown a significant effect of dietary flavonoids from a natural source related to lipid action both in vivo and in-vitro models.

The effects of genistin and naringenin on the process of adipogenesis in the cell line 3T3-L1 have been studied (Harmon and Harp, 2001). The results indicated that genistein inhibited mitotic clonal expansion, triglyceride accumulation, and peroxisome proliferator-activated receptor-gamma expression, but naringenin had no such effect (Harmon and Harp, 2001). The effects of genistein, EGCG, and capsaicin on AMPK activation in 3T3-L1 cells have been studied. Interestingly, genistein (20-200 μM) significantly inhibited the process of adipocyte differentiation and led to apoptosis of mature adipocytes, further to this Genistein, EGCG, and capsaicin-stimulated intracellular ROS release. One explanation may be that AMPK, which regulating glucose and fat metabolism in the fat cell, liver, and muscle is activated through ER stress, which triggers ROS production (Hwang et al., 2005). Investigation of the effects of esculetin on 3T3-L1 adipocyte apoptosis and adipogenesis exhibited that esculetin caused a time- and dose-related increase in adipocyte apoptosis and a decrease in viability (Yang et al., 2008). Also, the studies using epigallocatechin gallate (EGCG) from *Camellia sinensis* demonstrated that EGCG at doses of 5-10 μM reduced fat accumulation and induced the expression of genes related to insulin sensitivity and 3T3-adipocytes differentiation at the early stage of differentiation (Sakurai et al., 2009). Furthermore, the previous finding revealed that body weight and waist circumference of obese patients were decreased by 4.6 and 4.48%, respectively, after 3 months taking green tea extract (Chantre and Lairon, 2002).

The effects of EGEC on thermogenesis and fat oxidation in obese men study exhibited that ECEG induced significantly lower respiratory quotient (Oliveira et al., 2013). Values but did not alter resting energy expenditure (EE) compared to the placebo (Boschmann and Thielecke, 2007). Narirutin and naringin did not show this effect on lipases from porcine pancreas and *Pseudomonas*. In animal experiments, the concentration of plasma triglyceride in rats fed a diet containing 10% hesperidin were significantly lower than those fed the control diet (Kawaguchi et al., 1997). The experimentation of some prenylflavonoids including glycyfl coumarin, glycerin, dehydroglyasperin C and dehydroglyasperin D from licorice extract indicated these flavonoids might be useful in preventing and ameliorating diabetes, abdominal obesity and preventing hypertension in mice (Mae et al., 2003).

The polyphenol fractions of *Salix matsudana* leave extract were shown to reduce hepatic cholesterol, inhibit palmitic acid uptake, and α -amylase activity in high-fat diet induced mice. Moreover, 1 mg/mL of this fraction enhanced norepinephrine induced lipolysis in the fat cell, but not effective in non-poly phenol fraction (Han et al., 2003). The inhibitory effect may be due to the inhibition of carbohydrate and lipid absorption from the small intestine through the inhibition of α -amylase and palmitic acid uptake into the small intestine or accelerating fat mobilization through enhancing norepinephrine-induced lipolysis in fat cells. To clarify the active substance in polyphenol fraction, Han and other, 2003 isolated 3 active substances they were identified as apigenin-7-O-d-glucoside which inhibited alpha-amylase activity, luteolin-7-O-d-glucoside, and chrysoeriol-7-O-d-glucoside both inhibited palmitic acid uptake into small intestinal brush border membrane. Moreover, these three flavonoid glucosides enhanced norepinephrine-induced lipolysis in fat cells. Although, the

mechanisms of three compounds are under investigation and the other active substance from polyphenol fraction remain unknown (Han et al., 2003). In 2005 Zheng and others founded 4 new active compounds from the leaves of this plant composed of Apigenin 7-O-beta-D-glucopyranuronide, luteolin 7-O-beta-D-glucopyranuronide, m-hydroxybenzyl beta-D-glucoside, and chrysoeriol 7-O-beta-D-glucopyranuronide. Most active compounds except chrysoeriol 7-O-beta-D-glucopyranuronide can inhibit the production of 12-hydroxy-5, 8, 10, 14-eicosatetraenoic acid (12-HETE), so they might be used for preventing thrombus and arteriosclerosis (Zheng et al., 2005). In 2013, Zuo and others found that the chemical compound from their leaves composed of eight active compounds (1) beta-Sitosterol, (2) 5,7-Dihydroxychromone-7-O-beta-D-glucopyranoside, (3) 2S-Helichrysin A, (4) 2R-Helichrysin A, (5) Luteolin-7-O-beta-D-glucoside, (6) Salicin, (7) Apigenin-7-O-beta-D-glucopyranside, (8) Lutelion-3'-methyl ether-7-O-beta-D-glucopyranside (Zuo et al., 2013). Thus, it is clear that there is a much active substance that has not been studied.

Also, previous research showed that the flavonoids of *P. frutescens* leaves (TFP) that mainly consisted of apigenin with a smaller amount of luteolin at doses of 50–200 mg/kg. Oral administration of TFP to hyperlipidemia rats was highly effective in decreasing the levels of serum total cholesterol (Darlington et al., 1998), triacylglycerols (D'Mello et al., 2011), low-density lipoprotein cholesterol (LDL-c), and adipose tissue lipid accumulation, increasing the levels of serum high-density-lipoprotein-cholesterol (HDL-c), adjusting metabolic disturbance of lipoprotein, increasing antioxidant enzyme activity and repressing development of atherosclerosis (Feng et al., 2011). In conjunction, the investigation of naringenin revealed that at a 0.003-0.012% supplementation in rats for 6 weeks caused a significant reduction of

total triglyceride, cholesterol in plasma and liver, adiposity and triglyceride contents in parametrial adipose tissue (Cho et al., 2011). Similarly, 3% of the diet containing naringenin significantly decreased both triglyceride and cholesterol by 50% in Western diet rats (Mulvihill et al., 2010). Furthermore, Wistar rats were fed with fenugreek ethyl acetate extract that contains three flavonoids (kaempferol 3-O-glycoside, apigenin-7-O-rutinoside, and naringenin) resulted in significantly lowered the plasma levels of total cholesterol (Darlington et al., 1998), triglycerides (D'Mello et al., 2011), and low-density lipoprotein cholesterol (LDL-C), while increasing the plasma level of high-density lipoprotein cholesterol (HDL-C) (Belguith-Hadriche et al., 2010). Also, naringenin (50 mg/kg body weight/day) supplementation showed decreased levels of plasma and tissue TC, TG and FFA, HMG-CoA reductase and collagen content and increased the levels of HDL and LPL with ethanol alone-fed rats (Jayachitra, 2012). However, previous research exhibited that naringenin at 50 mg/kg did not change the hormone levels in rats. Blood glucose, triglyceride, total, esterified, and free cholesterol, and high-density-lipoprotein-cholesterol concentrations were also unaffected by this compound (Szkudelska et al., 2007). The baicalin investigation showed that baicalin at 80 mg/kg BW significantly decreased the elevated serum cholesterol, free fatty acid, and insulin concentrations caused by the HFD in rats (Guo et al., 2009). Likewise, the effect of baicalein on metabolic syndrome induced by a high-fat diet in mice indicated that Baicalein protects mice from metabolic syndrome through an AMPK α 2-dependent mechanism involving multiple intracellular signaling pathways (Pu et al., 2012). However, more details about combination the effect of some flavonoids as mentioned above seems very interesting to study on lipid metabolism.

2.14 References

- Ailhaud, G., Dani, C., Amri, E. Z., Djian, P., Vannier, C., Doglio, A., Forest, C., Gaillard, D., Négrel, R., and Grimaldi, P. (1989). Coupling growth arrest and adipocyte differentiation. **Environmental Health Perspectives**. 80: 17-23.
- Ambati, S., Kim, H. K., Yang, J. Y., Lin, J., Della-Fera, M. A., and Baile, C. A. (2007). Effects of leptin on apoptosis and adipogenesis in 3T3-L1 adipocytes. **Biochemical Pharmacology**. 73(3): 378-384.
- Avram, M. M., Avram, A. S., and James, W. D. (2007). Subcutaneous fat in normal and diseased states 3. Adipogenesis: from stem cell to fat cell. **Journal of the American Academy of Dermatology**. 56(3): 472-492.
- Barak, Y., Nelson, M. C., Ong, E. S., Jones, Y. Z., Ruiz-Lozano, P., Chien, K. R., Koder, A., and Evans, R. M. (1999). PPAR gamma is required for placental, cardiac, and adipose tissue development. **Molecular Cell**. 4(4): 585-595.
- Belguith-Hadriche, O., Bouaziz, M., Jamoussi, K., El Feki, A., Sayadi, S., and Makni-Ayedi, F. (2010). Lipid-lowering and antioxidant effects of an ethyl acetate extract of fenugreek seeds in high-cholesterol-fed rats. **Journal of Agricultural and Food Chemistry**. 58(4): 2116-2122.
- Berg, A. H., Combs, T. P., and Scherer, P. E. (2002). ACRP30/adiponectin: an adipokine regulating glucose and lipid metabolism. **Trends in Endocrinology and Metabolism**. 13(2): 84-89.
- Bombardelli, E., Bonati, A., Gabetta, B., Martinelli, E. M., Mustich, G., and Danieli, B. (1975). Passiflorine, a new glycoside from *Passiflora edulis*. **Phytochemistry**. 14(12): 2661-2665.

- Boschmann, M., and Thielecke, F. (2007). The effects of epigallocatechin-3-gallate on thermogenesis and fat oxidation in obese men: a pilot study. **Journal of the American College of Nutrition**. 26(4): 389s-395s.
- Bullerman, L., Lieu, F., and Seier, S. A. (1977). Inhibition of growth and aflatoxin production by cinnamon and clove oils. Cinnamic aldehyde and eugenol. **Journal of Food Science**. 42(4): 1107-1109.
- Chantre, P., and Lairon, D. (2002). Recent findings of green tea extract AR25 (Exolise) and its activity for the treatment of obesity. **Phytomedicine**. 9(1): 3-8.
- Chau, C. F., and Huang, Y. L. (2005). Effects of the insoluble fiber derived from *Passiflora edulis* seed on plasma and hepatic lipids and fecal output. **Molecular Nutrition and Food Research**. 49(8): 786-790.
- Chen, L. J., Games, D. E., and Jones, J. (2003). Isolation and identification of four flavonoid constituents from the seeds of *Oroxylum indicum* by high-speed counter-current chromatography. **Journal of Chromatography A**. 988(1): 95-105.
- Cho, K. W., Kim, Y. O., Andrade, J. E., Burgess, J. R., and Kim, Y. C. (2011). Dietary naringenin increases hepatic peroxisome proliferators-activated receptor alpha protein expression and decreases plasma triglyceride and adiposity in rats. **European Journal of Nutrition**. 50(2): 81-88.
- Cornelius, P., MacDougald, O. A., and Lane, M. D. (1994). Regulation of adipocyte development. **Annual Review of Nutrition**. 14: 99-129.
- Couillard, C., Mauriège, P., Imbeault, P., Prud'homme, D., Nadeau, A., Tremblay, A., Bouchard, C., and Després, J. P. (2000). Hyperleptinemia is more closely

associated with adipose cell hypertrophy than with adipose tissue hyperplasia.

International Journal of Obesity. 24(6): 782-788.

D'Mello, P., Darji, K., and Shetgiri, P. (2011). Evaluation of antiobesity activity of various Plant extracts. **Pharmacognosy Journal.** 3(21): 56-59.

Darlington, G. J., Ross, S. E., and MacDougald, O. A. (1998). The role of C/EBP genes in adipocyte differentiation. **The Journal of Biological Chemistry.** 273(46): 30057-30060.

Dasgupta, S., Bhattacharya, S., Maitra, S., Pal, D., Majumdar, S. S., Datta, A., and Bhattacharya, S. (2011). Mechanism of lipid induced insulin resistance: activated PKCepsilon is a key regulator. **Biochimica et Biophysica Acta.** 1812(4): 495-506.

Dhawan, K., Dhawan, S., and Sharma, A. (2004). Passiflora: a review update. **Journal of Ethnopharmacology.** 94(1): 1-23.

Dunkhunthod, B., Thumanu, K., and Eumkeb, G. (2017). Application of FTIR microspectroscopy for monitoring and discrimination of the anti-adipogenesis activity of baicalein in 3T3-L1 adipocytes. **Vibrational Spectroscopy.** 89: 92-101.

Farmer, S. R. (2006). Transcriptional control of adipocyte formation. **Cell Metabolism.** 4(4): 263-273.

Feige, J. N., Gelman, L., Michalik, L., Desvergne, B., and Wahli, W. (2006). From molecular action to physiological outputs: peroxisome proliferator-activated receptors are nuclear receptors at the crossroads of key cellular functions. **Progress in Lipid Research.** 45(2): 120-159.

- Feng, L.-J., huan-yu, C., Ying, K.-J., Hua, J., and Dai, X.-Y. (2011). Hypolipidemic and antioxidant effects of total flavonoids of *Perilla frutescens* leaves in hyperlipidemia rats induced by high-fat diet. **Food Research International**. 44(1): 404-409.
- Feve, B., Emorine, L. J., Briend-Sutren, M. M., Lasnier, F., Strosberg, A. D., and Pairault, J. (1990). Differential regulation of beta 1- and beta 2-adrenergic receptor protein and mRNA levels by glucocorticoids during 3T3-F442A adipose differentiation. **The Journal of Biological Chemistry**. 265(27): 16343-16349.
- Friedman, J. M. (2002). The function of leptin in nutrition, weight, and physiology. **Nutrition Reviews**. 60(10 Pt 2): S1-14; discussion S68-84, 85-17.
- Fu, Y., Luo, N., Klein, R. L., and Garvey, W. T. (2005). Adiponectin promotes adipocyte differentiation, insulin sensitivity, and lipid accumulation. **Journal of Lipid Research**. 46(7): 1369-1379.
- Garcia de Herreros, A., and Birnbaum, M. J. (1989). The acquisition of increased insulin-responsive hexose transport in 3T3-L1 adipocytes correlates with expression of a novel transporter gene. **The Journal of Biological Chemistry**. 264(33): 19994-19999.
- Green, H., and Kehinde, O. (1975). An established preadipose cell line and its differentiation in culture. II. Factors affecting the adipose conversion. **Cell**. 5(1): 19-27.
- Green, H., and Meuth, M. (1974). An established pre-adipose cell line and its differentiation in culture. **Cell**. 3(2): 127-133.

- Greenbaum, L. E., Li, W., Cressman, D. E., Peng, Y., Ciliberto, G., Poli, V., and Taub, R. (1998). CCAAT enhancer-binding protein beta is required for normal hepatocyte proliferation in mice after partial hepatectomy. **The Journal of Clinical Investigation**. 102(5): 996-1007.
- Gregoire, F. M. (2001). Adipocyte differentiation: from fibroblast to endocrine cell. **Experimental Biology and Medicine**. 226(11): 997-1002.
- Gregoire, F. M., Smas, C. M., and Sul, H. S. (1998). Understanding adipocyte differentiation. **Physiological Reviews**. 78(3): 783-809.
- Grommes, C., Landreth, G. E., and Heneka, M. T. (2004). Antineoplastic effects of peroxisome proliferator-activated receptor gamma agonists. **The Lancet. Oncology**. 5(7): 419-429.
- Guo, H. X., Liu, D. H., Ma, Y., Liu, J. F., Wang, Y., Du, Z. Y., Wang, X., Shen, J. K., and Peng, H. L. (2009). Long-term baicalin administration ameliorates metabolic disorders and hepatic steatosis in rats given a high-fat diet. **Acta Pharmacologica Sinica**. 30(11): 1505-1512.
- Han, L. K., Sumiyoshi, M., Zheng, Y. N., Okuda, H., and Kimura, Y. (2003). Anti-obesity action of *Salix matsudana* leaves (Part 2). Isolation of anti-obesity effectors from polyphenol fractions of *Salix matsudana*. **Phytotherapy Research**. 17(10): 1195-1198.
- Harminder, Singh, V., and Chaudhary, A. K. (2011). A review on the taxonomy, ethnobotany, chemistry and pharmacology of *Oroxylum indicum* Vent. **Indian Journal of Pharmaceutical Sciences**. 73(5): 483-490.

- Harmon, A. W., and Harp, J. B. (2001). Differential effects of flavonoids on 3T3-L1 adipogenesis and lipolysis. **American Journal of Physiology-Cell Physiology**. 280(4): C807-813.
- Holst, D., and Grimaldi, P. A. (2002). New factors in the regulation of adipose differentiation and metabolism. **Current Opinion in Lipidology**. 13(3): 241-245.
- Horton, J. D., Goldstein, J. L., and Brown, M. S. (2002). SREBPs: activators of the complete program of cholesterol and fatty acid synthesis in the liver. **The Journal of Clinical Investigation**. 109(9): 1125-1131.
- Horton, J. D., Shimomura, I., Brown, M. S., Hammer, R. E., Goldstein, J. L., and Shimano, H. (1998). Activation of cholesterol synthesis in preference to fatty acid synthesis in liver and adipose tissue of transgenic mice overproducing sterol regulatory element-binding protein-2. **The Journal of Clinical Investigation**. 101(11): 2331-2339.
- Huang, H. L., Hong, Y. W., Wong, Y. H., Chen, Y. N., Chyuan, J. H., Huang, C. J., and Chao, P. M. (2008). Bitter melon (*Momordica charantia* L.) inhibits adipocyte hypertrophy and down regulates lipogenic gene expression in adipose tissue of diet-induced obese rats. **The British Journal of Nutrition**. 99(2): 230-239.
- Hwang, J. T., Park, I. J., Shin, J. I., Lee, Y. K., Lee, S. K., Baik, H. W., Ha, J., and Park, O. J. (2005). Genistein, EGCG, and capsaicin inhibit adipocyte differentiation process via activating AMP-activated protein kinase. **Biochemical and Biophysical Research Communications**. 338(2): 694-699.

- Jayachitra, J., Nalini, Namasivayam. (2012). Effect of naringenin (citrus flavanone) on lipid profile in ethanol induced toxicity in rats. **Journal of Food Biochemistry**. 36(4): 502-511.
- Kadowaki, T., and Yamauchi, T. (2005). Adiponectin and adiponectin receptors. **Endocrine Reviews**. 26(3): 439-451.
- Kahn, B. B., and Flier, J. S. (2000). Obesity and insulin resistance. **The Journal of Clinical Investigation**. 106(4): 473-481.
- Kaul, P. N., Bhattacharya, A. K., Rajeswara Rao, B. R., Syamasundar, K. V., and Ramesh, S. (2003). Volatile constituents of essential oils isolated from different parts of cinnamon (*Cinnamomum zeylanicum* Blume). **Journal of the Science of Food and Agriculture**. 83(1): 53-55.
- Kawaguchi, K., Mizuno, T., Aida, K., and Uchino, K. (1997). Hesperidin as an inhibitor of lipases from porcine pancreas and *Pseudomonas*. **Bioscience, Biotechnology, and Biochemistry**. 61(1): 102-104.
- Kawser Hossain, M., Abdal Dayem, A., Han, J., Yin, Y., Kim, K., Kumar Saha, S., Yang, G.-M., Choi, H. Y., and Cho, S.-G. (2016). Molecular mechanisms of the anti-obesity and anti-diabetic properties of flavonoids. **International Journal of Molecular Sciences**. 17(4): 569-569.
- Kershaw, E. E., and Flier, J. S. (2004). Adipose tissue as an endocrine organ. **The Journal of Clinical Endocrinology & Metabolism**. 89(6): 2548-2556.
- Kim, J. B., and Spiegelman, B. M. (1996). ADD1/SREBP1 promotes adipocyte differentiation and gene expression linked to fatty acid metabolism. **Genes & Development**. 10(9): 1096-1107.

- Kim, W. K., Lee, C. Y., Kang, M. S., Kim, M. H., Ryu, Y. H., Bae, K. H., Shin, S. J., Lee, S. C., and Ko, Y. (2008). Effects of leptin on lipid metabolism and gene expression of differentiation-associated growth factors and transcription factors during differentiation and maturation of 3T3-L1 preadipocytes. **Endocrine Journal**. 55(5): 827-837.
- Kopelman, P. G. (2000). Obesity as a medical problem. **Nature**. 404(6778): 635-643.
- Kubota, N., Terauchi, Y., Yamauchi, T., Kubota, T., Moroi, M., Matsui, J., Eto, K., Yamashita, T., Kamon, J., Satoh, H., Yano, W., Froguel, P., Nagai, R., Kimura, S., Kadowaki, T., and Noda, T. (2002). Disruption of adiponectin causes insulin resistance and neointimal formation. **The Journal of Biological Chemistry**. 277(29): 25863-25866.
- Kumar, S., and Pandey, A. K. (2013). Chemistry and biological activities of flavonoids: an overview. **The Scientific World Journal**. 2013: 162750.
- Kusunoki, J., Kanatani, A., and Moller, D. E. (2006). Modulation of fatty acid metabolism as a potential approach to the treatment of obesity and the metabolic syndrome. **Endocrine**. 29(1): 91-100.
- Lara-Castro, C., Luo, N., Wallace, P., Klein, R. L., and Garvey, W. T. (2006). Adiponectin multimeric complexes and the metabolic syndrome trait cluster. **Diabetes**. 55(1): 249-259.
- Lu, R. H., Ji, H., Chang, Z. G., Su, S. S., and Yang, G. S. (2010). Mitochondrial development and the influence of its dysfunction during rat adipocyte differentiation. **Molecular Biology Reports**. 37(5): 2173-2182.
- Mae, T., Kishida, H., Nishiyama, T., Tsukagawa, M., Konishi, E., Kuroda, M., Mimaki, Y., Sashida, Y., Takahashi, K., Kawada, T., Nakagawa, K., and Kitahara, M.

- (2003). A licorice ethanolic extract with peroxisome proliferator-activated receptor-gamma ligand-binding activity affects diabetes in KK-Ay mice, abdominal obesity in diet-induced obese C57BL mice and hypertension in spontaneously hypertensive rats. **The Journal of Nutrition**. 133(11): 3369-3377.
- Mat Ali, R., Houghton, P. J., Raman, A., and Hoult, J. R. (1998). Antimicrobial and antiinflammatory activities of extracts and constituents of *Oroxylum indicum* (L.) Vent. **Phytomedicine**. 5(5): 375-381.
- Matsuda, M., Korn, B. S., Hammer, R. E., Moon, Y. A., Komuro, R., Horton, J. D., Goldstein, J. L., Brown, M. S., and Shimomura, I. (2001). SREBP cleavage-activating protein (SCAP) is required for increased lipid synthesis in liver induced by cholesterol deprivation and insulin elevation. **Genes & Development**. 15(10): 1206-1216.
- Mulvihill, E. E., Assini, J. M., Sutherland, B. G., DiMattia, A. S., Khami, M., Koppes, J. B., Sawyez, C. G., Whitman, S. C., and Huff, M. W. (2010). Naringenin decreases progression of atherosclerosis by improving dyslipidemia in high-fat-fed low-density lipoprotein receptor-null mice. **Arteriosclerosis, Thrombosis, and Vascular Biology**. 30(4): 742-748.
- Muoio, D. M., Dohm, G. L., Fiedorek, F. T., Jr., Tapscott, E. B., and Coleman, R. A. (1997). Leptin directly alters lipid partitioning in skeletal muscle. **Diabetes**. 46(8): 1360-1363.
- NCCIH. (2009). **Cinnamomum verum** [On-line]. Available: Database Provider Name of Database|. (Report Number).| Retrieved Date Accessed|, from Publisher| URL

- Noriega, P., Mafud, D. d. F., Souza, B. d., Soares-Scott, M., Rivelli, D. P., Barros, S. B. d. M., and Bacchi, E. M. (2012). Applying design of experiments (DOE) to flavonoid extraction from *Passiflora alata* and *P. edulis*. **Revista Brasileira de Farmacognosia**. 22: 1119-1129.
- Oliveira, M. d., Luvizotto, R. d. A. M., Olimpio, R. M. C., Sibio, M. T. d., Silva, C. B. R., Conde, S. J., Padovani, C. R., and Nogueira, C. I. R. (2013). Modulation of thyroid hormone receptors, TR \pm and TR 2 , by using different doses of triiodothyronine (T3) at different times. **Arquivos Brasileiros de Endocrinologia & Metabologia**. 57: 368-374.
- Omatsu-Kanbe, M., Inoue, K., Fujii, Y., Yamamoto, T., Isono, T., Fujita, N., and Matsuura, H. (2006). Effect of ATP on preadipocyte migration and adipocyte differentiation by activating P2Y receptors in 3T3-L1 cells. **Biochemical Journal**. 393(Pt 1): 171-180.
- Pai, J. T., Guryev, O., Brown, M. S., and Goldstein, J. L. (1998). Differential stimulation of cholesterol and unsaturated fatty acid biosynthesis in cells expressing individual nuclear sterol regulatory element-binding proteins. **The Journal of Biological Chemistry**. 273(40): 26138-26148.
- Park, S.-J., Lee, I.-S., Lee, S.-P., and Yu, M.-H. (2013). Inhibition of adipocyte differentiation and adipogenesis by supercritical fluid extracts and marc from *Cinnamomum verum*. **Journal of Life Science**. 23(4): 510-517.
- Paulauskis, J. D., and Sul, H. S. (1988). Cloning and expression of mouse fatty acid synthase and other specific mRNAs. Developmental and hormonal regulation in 3T3-L1 cells. **The Journal of Biological Chemistry**. 263(15): 7049-7054.

- Paz-Filho, G., Mastronardi, C., Wong, M. L., and Licinio, J. (2012). Leptin therapy, insulin sensitivity, and glucose homeostasis. **Indian Journal of Endocrinology and Metabolism**. 16(Suppl 3): S549-555.
- Petry, R. D., Reginatto, F., de-Paris, F., Gosmann, G., Salgueiro, J. B., Quevedo, J., Kapczinski, F., Ortega, G. G., and Schenkel, E. P. (2001). Comparative pharmacological study of hydroethanol extracts of *Passiflora alata* and *Passiflora edulis* leaves. **Phytotherapy Research**. 15(2): 162-164.
- Ponnusamy, S., Ravindran, R., Zinjarde, S., Bhargava, S., and Ravi Kumar, A. (2011). Evaluation of traditional Indian antidiabetic medicinal plants for human pancreatic amylase inhibitory effect *in vitro*. **Evidence-Based Complementary and Alternative Medicine**. 2011: 515647.
- Pu, P., Wang, X. A., Salim, M., Zhu, L. H., Wang, L., Chen, K. J., Xiao, J. F., Deng, W., Shi, H. W., Jiang, H., and Li, H. L. (2012). Baicalein, a natural product, selectively activating AMPK α 2 and ameliorates metabolic disorder in diet-induced mice. **Molecular and Cellular Endocrinology**. 362(1-2): 128-138.
- Qin, B., Polansky, M., and Anderson, R. (2010). Cinnamon extract regulates plasma levels of adipose-derived factors and expression of multiple genes related to carbohydrate metabolism and lipogenesis in adipose tissue of fructose-fed rats. **Hormone and Metabolic Research**. 42(03): 187-193.
- Ramos, A. T., Cunha, M. A. L., Sabaa-Srur, A. U. O., Pires, V. C. F., Cardoso, A. A., Diniz, M. d. F. M., and Medeiros, C. C. M. (2007). Uso de *Passiflora edulis* f. flavicarpa na redução do colesterol. **Revista Brasileira de Farmacognosia**. 17: 592-597.

- Rao, P. V., and Gan, S. H. (2014). Cinnamon: a multifaceted medicinal plant. **Evidence-Based Complementary and Alternative Medicine**. 2014: 642942.
- Rattana, S., Phadungkit, M., and Cushnie, B. (2010). Phytochemical screening, flavonoid content and antioxidant activity of *Tiliacora triandra* leaf extracts. **The 2nd Annual International Conference of Northeast Pharmacy Research, Mahasarakham University, Maha Sarakham, Thailand**, pp. 60-63, February 2010.
- Roncari, D. A., Lau, D. C., and Kindler, S. (1981). Exaggerated replication in culture of adipocyte precursors from massively obese persons. **Metabolism: Clinical and Experimental**. 30(5): 425-427.
- Roy, M. K., Nakahara, K., Na, T. V., Trakoontivakorn, G., Takenaka, M., Isobe, S., and Tsushida, T. (2007). Baicalein, a flavonoid extracted from a methanolic extract of *Oroxylum indicum* inhibits proliferation of a cancer cell line *in vitro* via induction of apoptosis. **Pharmazie**. 62(2): 149-153.
- Ruderman, N. B., Saha, A. K., Vavvas, D., and Witters, L. A. (1999). Malonyl-CoA, fuel sensing, and insulin resistance. **The American Journal of Physiology**. 276(1): E1-e18.
- Sakurai, N., Mochizuki, K., Kameji, H., Shimada, M., and Goda, T. (2009). (-)-Epigallocatechin gallate enhances the expression of genes related to insulin sensitivity and adipocyte differentiation in 3T3-L1 adipocytes at an early stage of differentiation. **Nutrition**. 25(10): 1047-1056.
- Scott, R. E., Florine, D. L., Wille, J. J., Jr., and Yun, K. (1982). Coupling of growth arrest and differentiation at a distinct state in the G1 phase of the cell cycle: GD.

Proceedings of the National Academy of Sciences of the United States of America. 79(3): 845-849.

Seewaboon, S., Nirush, L., Umarat, S., Amornat, T., Anongnad, N., and Nadthaganya, S. (2008). Acute and subchronic toxicity study of the water extract from *Tiliacora triandra* (Colebr.) Diels in rats. **Songklanakarin Journal of Science and Technology.** 30 (5): 611-619.

Senanayake, U. M., Lee, T. H., and Wills, R. B. H. (1978). Volatile constituents of cinnamon (*Cinnamomum zeylanicum*) oils. **Journal of Agricultural and Food Chemistry.** 26(4): 822-824.

Shao, X., Wang, M., Wei, X., Deng, S., Fu, N., Peng, Q., Jiang, Y., Ye, L., Xie, J., and Lin, Y. (2016). Peroxisome proliferator-activated receptor-gamma: Master regulator of adipogenesis and obesity. **Current Stem Cell Research & Therapy.** 11(3): 282-289.

Shimano, H., Shimomura, I., Hammer, R. E., Herz, J., Goldstein, J. L., Brown, M. S., and Horton, J. D. (1997). Elevated levels of SREBP-2 and cholesterol synthesis in livers of mice homozygous for a targeted disruption of the SREBP-1 gene. **The Journal of Clinical Investigation.** 100(8): 2115-2124.

Singh, J., and Kakkar, P. (2013). Modulation of liver function, antioxidant responses, insulin resistance and glucose transport by *Oroxylum indicum* stem bark in STZ induced diabetic rats. **Food and Chemical Toxicology.** 62: 722-731.

Singh, J., and Kakkar, P. (2014). Oroxylin A, a constituent of *Oroxylum indicum* inhibits adipogenesis and induces apoptosis in 3T3-L1 cells. **Phytomedicine.** 21(12): 1733-1741.

- Sorisky, A., Magun, R., and Gagnon, A. M. (2000). Adipose cell apoptosis: death in the energy depot. **International Journal of Obesity and Related Metabolic Disorders**. 24 Suppl 4: S3-7.
- Szkudelska, K., Nogowski, L., Nowicka, E., and Szkudelski, T. (2007). *In vivo* metabolic effects of naringenin in the ethanol consuming rat and the effect of naringenin on adipocytes *in vitro*. **Journal of Animal Physiology and Animal Nutrition**. 91(3-4): 91-99.
- Tontonoz, P., Hu, E., Graves, R. A., Budavari, A. I., and Spiegelman, B. M. (1994). mPPAR gamma 2: tissue-specific regulator of an adipocyte enhancer. **Genes & Development**. 8(10): 1224-1234.
- Vangalapati, M., Sree Satya, N., Surya Prakash, D. V., and Avanigadda, S. (2012). A review on pharmacological activities and clinical effects of *Cinnamon* species. **Research Journal of Pharmaceutical, Biological and Chemical Sciences**. 3(1): 653-663.
- Varga, T., Czimmerer, Z., and Nagy, L. (2011). PPARs are a unique set of fatty acid regulated transcription factors controlling both lipid metabolism and inflammation. **Biochimica et Biophysica Acta**. 1812(8): 1007-1022.
- Vidal-Puig, A., Jimenez-Liñan, M., Lowell, B. B., Hamann, A., Hu, E., Spiegelman, B., Flier, J. S., and Moller, D. E. (1996). Regulation of PPAR gamma gene expression by nutrition and obesity in rodents. **The Journal of Clinical Investigation**. 97(11): 2553-2561.
- Walker, C. G., Zariwala, M. G., Holness, M. J., and Sugden, M. C. (2007). Diet, obesity and diabetes: a current update. **Clinical Science**. 112(2): 93-111.

- Wang, Q. A., Zhang, F., Jiang, L., Ye, R., An, Y., Shao, M., Tao, C., Gupta, R. K., and Scherer, P. E. (2018). Peroxisome proliferator-activated receptor gamma and its role in adipocyte homeostasis and thiazolidinedione-mediated insulin sensitization. **Molecular and Cellular Biology**. 38(10): e00677-17.
- Weyer, C., Funahashi, T., Tanaka, S., Hotta, K., Matsuzawa, Y., Pratley, R. E., and Tataranni, P. A. (2001). Hypoadiponectinemia in obesity and type 2 diabetes: close association with insulin resistance and hyperinsulinemia. **The Journal of Clinical Endocrinology and Metabolism**. 86(5): 1930-1935.
- Wilson-Fritch, L., Burkart, A., Bell, G., Mendelson, K., Leszyk, J., Nicoloso, S., Czech, M., and Corvera, S. (2003). Mitochondrial biogenesis and remodeling during adipogenesis and in response to the insulin sensitizer rosiglitazone. **Molecular and Cellular Biology**. 23(3): 1085-1094.
- Xu, X., So, J. S., Park, J. G., and Lee, A. H. (2013). Transcriptional control of hepatic lipid metabolism by SREBP and ChREBP. **Seminars in Liver Disease**. 33(4): 301-311.
- Yang, J. Y., Della-Fera, M. A., Rayalam, S., Ambati, S., Hartzell, D. L., Park, H. J., and Baile, C. A. (2008). Enhanced inhibition of adipogenesis and induction of apoptosis in 3T3-L1 adipocytes with combinations of resveratrol and quercetin. **Life Sciences**. 82(19-20): 1032-1039.
- Yuan, Y., Hou, W., Tang, M., Luo, H., Chen, L.-J., Guan, Y. H., and Sutherland, I. A. (2008). Separation of flavonoids from the leaves of *Oroxylum indicum* by HSCCC. **Chromatographia**. 68(11): 885-892.

- Zaveri, M., Khandhar, A., and Jain, S. (2008). Quantification of baicalein, chrysin, biochanin-A and ellagic acid in root bark of *Oroxylum indicum* by RPHPLC with UV detection. **Eurasian Journal of Analytical Chemistry**. 3(2): 245-257.
- Zeng, G., Dave, J. R., and Chiang, P. K. (1997). Induction of proto-oncogenes during 3-deazaadenosine-stimulated differentiation of 3T3-L1 fibroblasts to adipocytes: mimicry of insulin action. **Oncology Research**. 9(4): 205-211.
- Zeraik, M., and Yariwake, J. (2010). Quantification of isoorientin and total flavonoids in *Passiflora edulis* fruit pulp by HPLC-UV/DAD. **Microchemical Journal**. 96(1): 86-91.
- Zheng, Y. N., Zhang, J., Han, L. K., Sekiya, K., Kimura, Y., and Okuda, H. (2005). Effects of compounds in leaves of *Salix matsudana* on arachidonic acid metabolism. **Journal of the Pharmaceutical Society of Japan**. 125(12): 1005-1008.
- Zuo, F. H., Wu, G. J., Li, J. J., Zhou, G. P., Fu, H. Z., and Liao, Y. Y. (2013). Chemical constituents of *Salix matsudana* leaf. **Journal of Chinese Medicinal Materials**. 36(12): 1959-1962.

CHAPTER III

PLANT EXTRACTIONS, CYTOTOXICITY, AND LIPID ACCUMULATION OF FOUR MEDICINAL PLANTS

3.1 Abstract

Obesity is often attributed by increasing storage of the excess energy in the form of adipocyte intracellular triglyceride. Many medicinal plants, including *O. indicum*, *C. verum*, *T. triandra*, and *P. edulis* has been widely studied for various medicinal approaches in anti-obesity ailment. However, the role of anti-adipogenesis of the extracts is little known. Therefore, the present study aimed to evaluate and compare anti-adipogenesis activities of *O. indicum* extract (OIE), *C. verum* extract (CVE), *T. triandra* extract (TTE), and *P. edulis* extract (PEE) in 3T3-L1 adipocytes. Plants were extracted with 95% of ethanol using soxhlation. The highest percentage yield was 18.39% w/w found in OIE. The mouse cell line 3T3-L1 was used to establish potential toxic effects of the extracts. The cells were exposed to various concentrations of the extracts (50, 100, 150, 200, 250, 500, 1,000, 1,500 $\mu\text{g}/\text{mL}$) for 48 h and were assessed by MTT. The viability of 3T3-L1 cells (%) was not significantly decreased after exposure to 200 and 150 $\mu\text{g}/\text{mL}$ of OIE for 2 days compared to controls ($p > 0.05$). Both CVE and TTE displayed no apparent effect on cell viability up to the concentration of 150 $\mu\text{g}/\text{mL}$ of each extract. While, PEE at a concentration range from 50 to 1500 $\mu\text{g}/\text{mL}$ did not alter the viability of 3T3-L1 cells.

In a separate study, the inhibitory effect of extracts on lipid accumulation in 3T3-L1 cells was also investigated. The concentration of 150 $\mu\text{g/mL}$ (no effect on the viability of cells) of all plant extracts exhibited significantly reduced lipid accumulation in 3T3-L1 adipocytes compared to the controls ($P < 0.05$). However, among four plant extracts, OIE showed the most potently suppressed lipid accumulation approximately 35 % and 52 % at 150 and 200 $\mu\text{g/mL}$, respectively. In the same way, microscopic observation of Oil Red O and hematoxylin-stained cells displayed that the OIE decreased Oil Red O stained droplets of mature adipocytes in a dose-dependent manner. Therefore, the findings of this study could provide the rationale for future studies on the mechanism of anti-adipogenesis property of OIE.

3.2 Introduction

Adipocytes is important for energy storage in addition to serving as a heat insulator (white adipose tissue) and utilize chemical energy to generate heat (brown adipose tissue) (Britannica, 2018). The expansion of adipose depots can be driven either by the increase in adipocyte size (hypertrophy) or by the formation of new adipocytes from precursor differentiation in the process of adipogenesis (hyperplasia) (Ghaben and Scherer, 2019). Adipocyte expansion through adipogenesis has been implicated in increased risks of obesity (de Simone and D'Addeo, 2008). Although using weight loss drugs is a common way to treat obesity, long-term pharmacological treatment has been reported to generate many side-effects (de Simone and D'Addeo, 2008; Thurairajah et al., 2005). This has led to innovative research using natural products to combat obesity in the hope of safe and novel treatment. Potential sources of natural anti-obesity have been found in various part of the plants, including leaves, fruits,

seeds, bark, and roots (Karri et al., 2019). In recent years, natural compounds like flavonoids and polyphenolics have shown the most significant role in body weight control (Karri et al., 2019). Although, the various phytochemical constituents from the plants have shown different types of pharmacological effects. The most common mechanism is by regulating lipid profile and inhibiting pancreatic lipase (Karri et al., 2019).

O. indicum (fruits), *C. verum* (stem), *T. triandra* (leaves), and *P. edulis* (leaves) are widely found throughout Southeast Asia, including Thailand. Many studies have been reported anti-oxidant effects (Phadungkit et al., 2010; Rudnicki et al., 2007), anti-adipogenesis effect (Park et al., 2013), anti-obesity effect (Chau and Huang, 2005; D'Mello et al., 2011), anti-diabetic (Ponnusamy et al., 2011), and anti-inflammatory (Rao and Gan, 2014). This indicates the pharmacological effects of four medicinal plant extracts in correlation with metabolic diseases. To find out the most remarkable therapeutic potential on adipogenesis activity from those plant extracts. This study aimed to investigate and compare the anti-adipogenesis activity of *O. indicum*, *C. verum*, *T. triandra*, and *P. edulis* crude extracts on 3T3-L1 adipocytes. The extracts that showed less intracellular lipid accumulation in 3T3-L1 adipocytes was chosen for further analysis.

3.3 Materials

3.3.1 Plant specimens

O. indicum (fruits), *C. verum* (stem), *T. triandra* (leaves), and *P. edulis* (leaves) fresh samples were purchased from Wang Nam Khiao District, Nakhon Ratchasima province, Thailand. During July to September 2015. The voucher

specimens (SOI0808U) were deposited at the flora of Suranaree University of Technology Herbarium and authenticated by Dr. Santi Wattatana, a lecturer and a plant biologist at Institute of Science, Suranaree University of Technology, Thailand.

3.3.2 Chemicals and reagents

Dulbecco's modified eagle's medium with high glucose (DMEM), penicillin, streptomycin, bovine calf serum (BCS), N-2-hydroxyethylpiperazine-N-2-ethane sulfonic acid (HEPES), and 3-(4,5-Dimethylthiazol-2-yl)-2,5-diphenyltetrazolium bromide (MTT) were purchased from GIBCO Invitrogen (Grand Island, NY, USA). Fetal bovine serum (FBS) was acquired from Hyclone (Logan, UT, USA). Dexamethasone was obtained from G Bioscience (St. Louis, MO, USA). Insulin solution from bovine, Isobutylmethylxanthine (IBMX), dimethyl sulphoxide (DMSO), and simvastatin were obtained from Sigma-Aldrich (St. Louis, MO, USA).

3.3.3 Cell line

3T3-L1 mouse embryonic fibroblasts were purchased from the American type culture collection (ATCC) (Manassas, VA, USA). The 3T3-L1 preadipocytes were cultured in Dulbecco's modified eagle's medium (DMEM) with high glucose, supplemented with 10 % v/v of bovine calf serum (BCS), 100 U/mL of penicillin and 100 µg/mL of streptomycin until reaching about 70-80 % confluent. Cells were maintained at 37 °C in a 95 % humidified with 5 % of CO₂ atmosphere throughout the experiments. The standard protocol followed the guideline from ATCC.

3.4 Methods

3.4.1 Preparation of media used for 3T3-L1 cell differentiation

The media used for adipogenesis of 3T3-L1 cells was prepared from 3 different formulas including 1) pre-adipocyte expansion media (90% of Dulbecco's modified eagle's medium (DMEM), and 10 % of bovine calf serum), 2) differentiation media (90 % of DMEM, 10 % of fetal bovine serum (FBS), 1.0 μ M of dexamethasone, 0.5 mM of isobutylmethylxanthine (IBMX), and 1.0 μ g/mL of insulin, and 3) adipocyte maintenance media (90 % of DMEM, 10 % of FBS, and 1.0 of μ g/mL insulin). All media contained 100 μ g/mL of streptomycin and 100 U/mL of penicillin.

3.4.2 Procedure for 3T3-L1 cell differentiation

3T3-L1 pre-adipocytes were cultured in pre-adipocyte expansion media. At two days after 3T3-L1 cells are at 70-80 % confluent, the cells were stimulated to differentiate with differentiation media for two days. From day 4 onwards, the differentiation media were replaced by adipocyte maintenance media (Figure 3.1). These media were changed every two days until the cells were harvested. On day 12 after the cells were differentiated (gauged by visible lipid droplet > 90 % of the control group), cells were collected for lipid measurement. Each experiment was repeated three times. The extract of medicinal plants was dissolved in 100 % of DMSO to a stock concentration (1.5 g/mL) and stored at -20 °C. The stock of the extracts was added to into induction media and maintenance media at various concentrations across the differentiation period until the cells were harvested. The final volume of DMSO in each media was 0.1 % v/v.

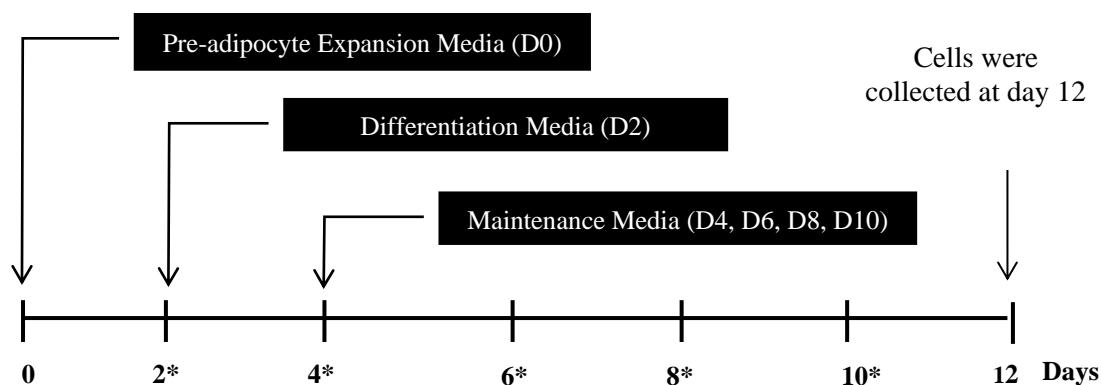


Figure 3.1 The procedure for the differentiation of 3T3-L1 cells.

*The extracts were added during cell differentiation at day 2, 4, 6 and 8.

3.4.3 Plants extract preparation

O. indicum (fruits), *C. verum* (stem), *T. triandra* (leaves), and *P. edulis* (leaves) fresh samples were washed thoroughly with tap water, then cut into small pieces and air-dried in an oven at 40 °C for 2 days. The dried pieces were then pulverized in a mechanical grinder to a coarse powder and were kept in a moisture-free container at room temperature. Plants dry powder (500 g) were extracted with 95 % of ethanol by soxhlation for 8 h. The extract was filtered through Whatman filter paper (number 1) and concentrated using a rotary evaporator at 50 °C under vacuum to remove the ethanol. The remaining extract was stored at -80 °C until required. Subsequently, the sample was lyophilized in a freeze dryer (LABCONCO), automatic mode, vacuum 240×10^{-3} mBar, and collector at -55 °C. The extracted powder was stored at -20 °C until required. The extract was resuspended in the media containing 0.1 % v/v DMSO (vehicle) and added to the cells at different concentrations.

3.4.4 Cytotoxicity

The cytotoxic effect of the medicinal plant extracts on the proliferation of 3T3-L1 preadipocytes was determined by 3-(4, 5-dimethylthiazol-2-yl)-2, 5-

diphenyltetrazolium bromide (MTT) assay. A pre-confluent of 3T3-L1 preadipocytes were seeded in 96-well plates at a density of 5×10^3 cells/well. Two days after reaching confluence, cells were treated with *O. indicum* extract (OIE), *C. verum* extract (CVE), *T. triandra* extract (TTE), and *P. edulis* extract (PEE) at concentrations ranging from 0 μ L to 1,500 μ L. Both treated and control cells were incubated for a further 48 h. At the end of the treatment period, the cell viability was assessed by using the MTT assay. The culture media were removed, and 100 μ L of MTT solution (0.5 mg/mL in phosphate buffer saline) was added, then incubated at 37 °C for 4 h. After incubation, 150 μ L of DMSO was added to dissolve formazan crystal. The absorbance of the intracellular formazan is proportional to the number of viable cells present was determined at 540 nm against a blank media (Benchmark Plus, Bio-Rad, Japan). The percentage of formazan product was calculated to determine the cytotoxicity following the equation below.

$$\begin{aligned} & \% \text{ Cell viability} \\ & = \left(\frac{\text{The optical density of the cells treated with the extract}}{\text{The optical density of the cells treated without treatment}} \right) \times 100 \end{aligned}$$

3.4.5 Oil Red O staining

The intracellular triglyceride content was determined using an Oil Red O staining. Briefly, on day 12, cells were washed with PBS and fixed with 1 mL/well of 10 % (v/v) formalin for 1 h at room temperature. After fixation, the cells were washed, and 500 μ L of 0.5 % of the Oil Red O solution was added. The cells were incubated for 30 min at room temperature. The Oil Red O solution was removed by gentle aspiration, and the cells were washed with PBS. The nucleus was then stained with 0.10% (w/v) hematoxylin. Fat droplets were observed under an inverted microscope at an

appropriate magnification. To determine the percent of lipid accumulation, the cells were extracted with 250 μL of isopropanol and 200 μL of the eluted solution was transferred to a new 96 well plate. The absorbance was measured at 490 nm with a microplate spectrophotometer. The simvastatin at 1.67 $\mu\text{g}/\text{mL}$ was used as a positive control.

3.4.6 Statistical analysis

All experiments were performed in triplicate. Data were expressed as a mean \pm standard error of the mean (SEM). The statistical significances difference between treatment and control groups of cell viability and the amount of lipid accumulation were analyzed by One-way analysis of variance (ANOVA) with a Turkey's HSD post-hoc test (SPSS v 23). Values were considered statistically significant when $P < 0.05$, and data were representative of at least three independent experiments ($n \geq 3$).

3.5 Results

3.5.1 Percentage yields of plant extracts

The percentage yields of crude extracts from OIE, CVE, TTE, and PEE are shown in Table 3.1. It showed that the high percentage yield was found in the 95 % ethanol of OIE (18.39 % w/w), CVE (18.33 % w/w), TTE (11.81 % w/w), and PEE (9.71 % w/w), respectively.

Table 3.1 Extraction yields of OIE, CVE, TTE, and PEE.

Plant samples	Fresh weight (g)	Dry weight (g)	Yield (g)	Yield (%w/w)
OIE	1,000	133.40	24.53	18.39
CVE	1,000	150.67	27.62	18.33
TTE	1,500	198.24	23.41	11.81
PEE	1,500	223.45	21.71	9.71

The percentage yield of the extract was calculated from extraction yield (g) x 100/dry weight (g). All plant samples were extracted with 95 % ethanol.

3.5.2 The effect of the extracts on cell viability in 3T3-L1 pre-adipocytes

To evaluate the cytotoxicity of the extracts on 3T3-L1 pre-adipocytes, an MTT assay was conducted. Cells were incubated for 48 h with a concentration between 50 to 1,500 $\mu\text{g/mL}$ of OIE, CVE, TTE, and PEE. As shown in the Figures 3.2B and C, both CVE and TTE at concentration ranging 50 to 150 $\mu\text{g/mL}$ did not alter the viability of pre-adipocytes, while the cytotoxicity effect was more pronounced at higher concentration (200 to 1,500 $\mu\text{g/mL}$) (Figures 3.2B and C). The concentration of OIE between 250 to 1,500 $\mu\text{g/mL}$ showed a significant reduction ($P < 0.05$) in the viability of pre-adipocytes with the IC_{50} at $882.68 \pm 47.99 \mu\text{g/mL}$ (Figure 3.2A). However, the viability of cells treated with lower doses of the extract (50 to 200 $\mu\text{g/mL}$) was not significantly different compared to non-treated cells ($P > 0.05$). Although cytotoxicity effect of OIE, CVE, and TTE exhibited at a concentration of 250 $\mu\text{g/mL}$, the results of

PEE showed differently. PEE at a concentration between 50 to 1,500 $\mu\text{g/mL}$ did not show toxic to pre-adipocytes, alternatively, was significantly increased in pre-adipocytes proliferation ($P < 0.05$) compared with the control cells. However, increasing concentration of PEE seems to effect to pre-adipocytes number. Therefore, a non-toxic concentration range of OIE, CVE, TTE, and PEE were chosen for 3T3-L1 cell treatment in the lipid accumulation studies.

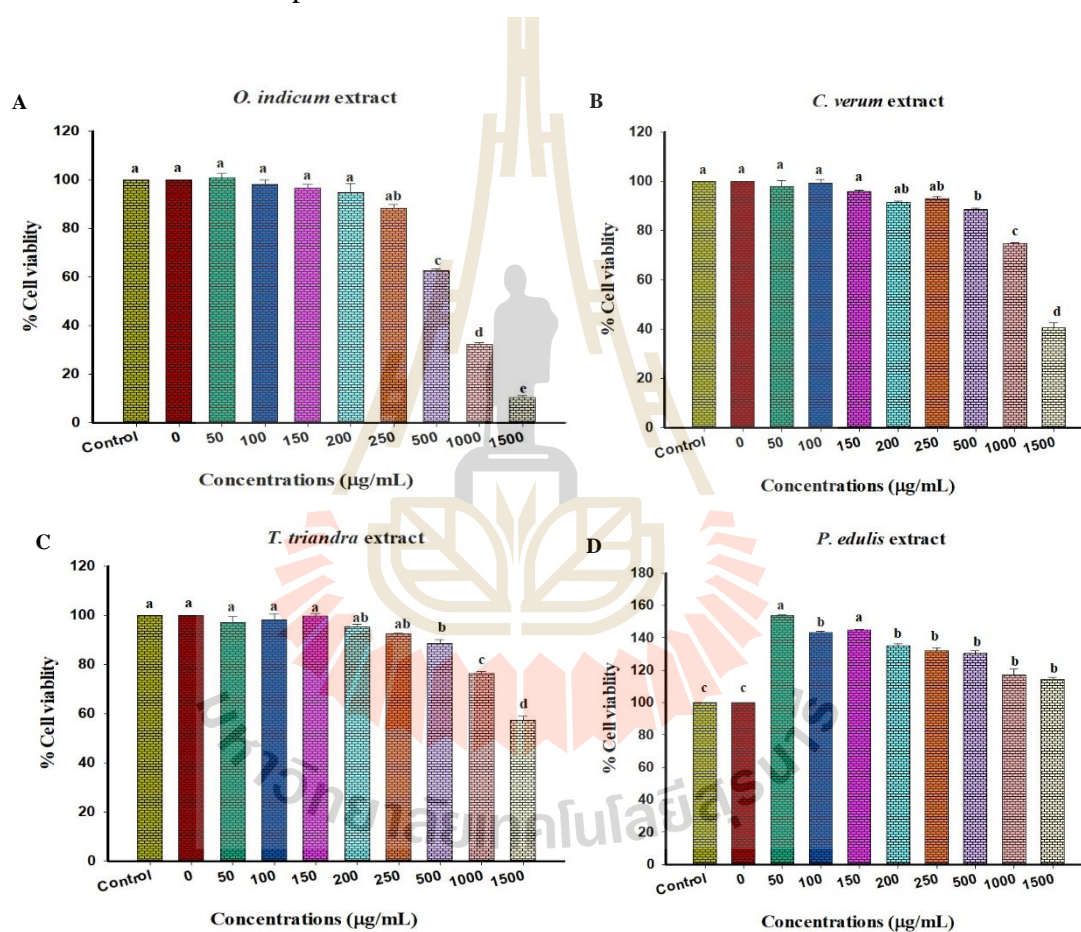


Figure 3.2 The effect of four medicinal extracts on the viability of 3T3-L1 preadipocytes. Cells were assessed by MTT. Control = Normal control; 0 = Vehicle control (0.1 % DMSO); (A) OIE; (B) CVE; (C) TTE; (D) PEE. Values are Means \pm SEM ($n = 3$ replicates). A significant difference was observed (Tukey's HSD test, $P <$

0.05) and are represented in the Figure with the letters from a to e. Bars annotated with the different letters are significantly different in each group.

3.5.3 The effect of the extracts on lipid accumulation in 3T3-L1 adipocytes

During the differentiation of 3T3-L1 pre-adipocytes into adipocytes, the cells were treated with 0 to 200 $\mu\text{g}/\text{mL}$ of OIE, CVE, TTE, and PEE. The intracellular lipid concentration was determined using Oil Red O staining. The 3T3-L1 pre-adipocytes, when exposed to the differentiation media, resulted in a significant increase in lipid accumulation compared to pre-adipocytes ($P < 0.05$) (Figure 3.3). However, the addition of OIE, CVE, TTE, and PEE at 200 $\mu\text{g}/\text{mL}$ significantly decreased the intracellular lipid accumulation by approximately 52 %, 27 %, 35 %, 29 %, respectively, compared to the 3T3-L1 adipocytes (control) ($P < 0.05$). The IC_{50} and IC_{60} values of OIE on lipid accumulation were 201.26 ± 10.00 and 237.72 ± 14.96 $\mu\text{g}/\text{mL}$, respectively (Figure 3.3A). Also, the cholesterol-lowering drug, simvastatin exhibited an IC_{60} at a concentration of 1.67 $\mu\text{g}/\text{mL}$. The effect of simvastatin is 142 times greater than OIE. According to our results, OIE showed the strongest on inhibiting lipid accumulation during adipocytes differentiation without any effect on the viability of cells. Thus OIE was selected for 3T3-L1 cell treatment in the subsequent studies.

In order to gain more evidence that OIE could affect lipid accumulation in differentiated 3T3-L1 cells, pre-adipocytes and adipocytes were stained with Oil Red O and hematoxylin and observed by a light microscope (Figure 3.4). Untreated adipocytes displayed an increase in size and number of prominent lipid droplets (Figure 3.4b). While adipocytes treated with simvastatin exhibited tiny and diffuse lipid droplets (Figure 3.4h). The 200 $\mu\text{g}/\text{mL}$ OIE treated adipocytes displayed smaller size

and number of lipid droplets that seemed to be focused on one part of the cell (Figure 4g).

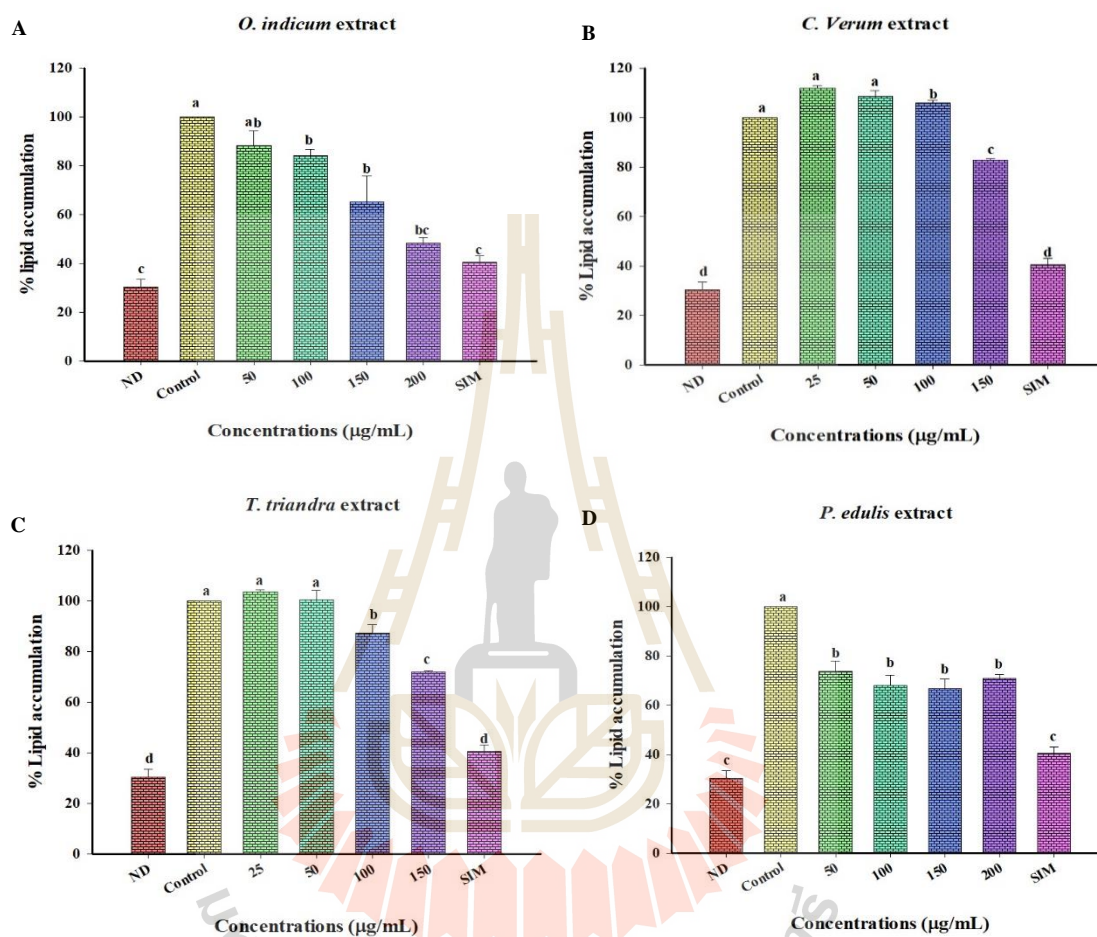


Figure 3.3 The effect of four medicinal plant extracts on the lipid accumulation in 3T3-L1 adipocytes. ND = non-differentiated cells (pre-adipocytes); Control = vehicle control; SIM (1.67) = Simvastatin at 1.67 µg/mL (a positive control); (A) OIE; (B) CVE; (C) TTE; (D) PEE. Values are Means \pm SEM (n = 3 replicates). A significant difference between each group was indicated by a different superscript letter (Tukey's HSD test, $P < 0.05$).

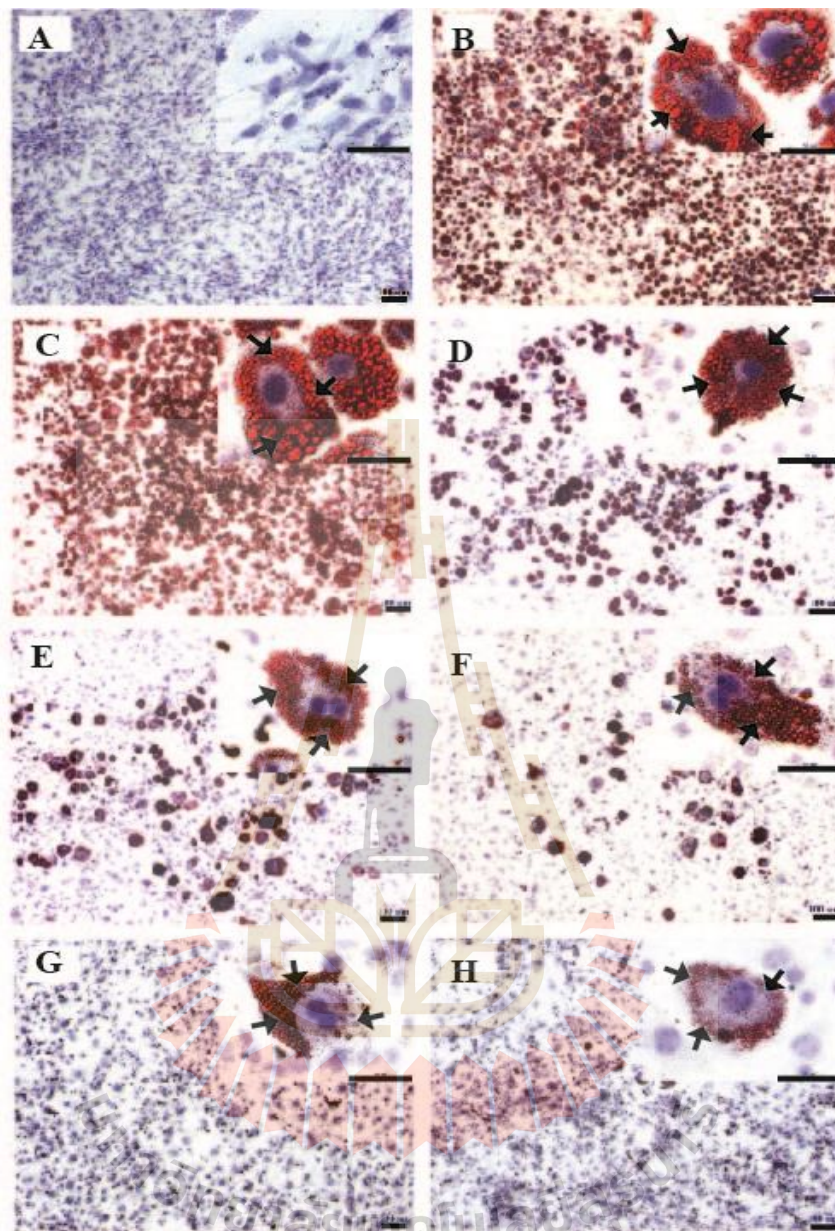


Figure 3.4 Microscopic imaging of intracellular lipid. 3T3-L1 cells were stained with Oil Red O and hematoxylin. The lipid droplets are stained in red and nuclei are stained in blue color. The arrows indicate the adipocyte with lipid droplets. The amount and size of lipid droplets are enlarged in untreated adipocytes (B and C). A = non-differentiated cells (pre-adipocytes); B = differentiated cells (untreated adipocytes); C = vehicle control; D, E, F and G = differentiated cells treated with OIE at the dose 50

$\mu\text{g/mL}$, 100 $\mu\text{g/mL}$, 150 and 200 $\mu\text{g/mL}$, respectively; H = simvastatin at 1.67 $\mu\text{g/mL}$ (original magnification at x40, scale bar; 100 μm and inset view at x400, scale bar; 50 μm).

3.6 Discussion and conclusion

Adipocyte formation and activity appear to play a central role in the development of obesity (Nawrocki and Scherer, 2005). Therefore, it becomes a primary target for treating obesity. Usually, the using of natural resources has increased, which based on safety and cost when compared with synthetic drugs or surgery (Chang, 2000; Clegg et al., 2003). Thus, this study investigated the effect of the OIE, CVE, TTE, and PEE on anti-adipogenesis in 3T3-L1 adipocytes. 3T3-L1 cell line toxicity test was conducted to investigate concentrations of four medicinal plant extracts that caused no detrimental effects on cells or cell viability. Therefore, the number of viable cells was estimated using MTT methods to ensure that these concentrations did not adversely affect 3T3-L1 cells. These studies indicated there was the dose-dependent effect of OIE, CVE, and TTE upon the viability of preadipocyte, ranging from a concentration of 250 $\mu\text{g/mL}$ to 1500 $\mu\text{g/mL}$. At a lower dose (0-150 $\mu\text{g/mL}$) of CVE or TTE and 0-200 $\mu\text{g/mL}$ of OIE, there was no significant difference from the control ($P > 0.05$). On the other hand, PEE was significantly increased the viability of cells at concentration range 50 to 1,500 $\mu\text{g/mL}$ compared to control ($P < 0.05$). Similarly, Osma et al. reported that the ethanolic extract of *P. edulis* leaves at 25 to 400 $\mu\text{g/mL}$ increased the viability of HepG2 cells. However, cells viability was decreased by increasing the exposure time (72 h) in all the concentrations (Osma, 2018). Although no major impact on the viability of the cells was observed at lower doses of four plant extracts, there may have been

some toxicology changes to the cells. One further observation was that in the adipogenesis assay did of 4 different extracts between dose 50 to 200 $\mu\text{g/mL}$ and 25 to 150 $\mu\text{g/mL}$ (Figure 3.3). This study finds that at concentration range 50 to 200 $\mu\text{g/mL}$ of OIE indicates a dose-dependent decrease in lipid accumulation and at 200 $\mu\text{g/mL}$ shows 52% of lipid reduction compared with the control (Figure 3.3A, 3.4G). While PEE at dose 200 $\mu\text{g/mL}$ exhibits a reduction of approximately 29 % of lipid. CVE and TTE at the dosage between 25 $\mu\text{g/mL}$ and 150 $\mu\text{g/mL}$ exhibited anti-adipogenesis effect by 17% and 28% lipid accumulation decreasing, respectively. These findings suggest that even OIE at lower doses can display higher anti-adipogenesis properties than CVE, TTE, and PEE. One explanation for the reduction of lipid could be that the chemical components of different extracts may have a different mechanism of action which inhibits the differentiation of preadipocytes. A previous study reported that the fruit of *O. indicum* was rich in flavonoids, such as baicalein (Roy et al., 2007). At a concentration of 20 μM baicalein could prevent the differentiation of preadipocyte to adipocyte during the first 4 days of induction (Madsen et al., 2003). In fact, there was evidence to support the suggestion that baicalein inhibited a cell cycle regulator and promoted cell cycle arrest at the G0/G1 phase and suppressed m-TOR signaling pathway leads to inhibit adipogenic factor (Seo et al., 2014). Interestingly, the effect of OIE at 200 $\mu\text{g/mL}$ on lipid accumulation of 3T3-L1 adipocytes was not significantly different from cells treated with 1.67 $\mu\text{g/mL}$ of simvastatin (Figure 3.3A). This observation is consistent with those of Nicholson et al. indicates that statin, including pitavastatin and simvastatin at 5 μM inhibits adipocyte differentiation by blocking *PPAR γ* expression and activating *pref-1* expression (Nicholson et al., 2007). These findings provide evidence that the statins have pleiotropic effects, not only do they have

a direct effect on the reduction of plasma cholesterol, but also have a role in anti-adipogenesis effect. These results suggest that the OIE primarily inhibit adipogenesis and lipid accumulation in adipocytes 3T3-L1. These may be due to the flavonoids in OIE act on biochemical molecules in the cells leads to inhibit the differentiating process of 3T3-L1 preadipocytes.

3.7 References

- Britannica, T. E. o. E. (2018, 06, 2018). Adipose cell. [On-line]. 09, 2019, Available: <https://www.britannica.com/science/adipose-cell>.
- Chang, J. (2000). Medicinal herbs: drugs or dietary supplements? **Biochemical Pharmacology**. 59(3): 211-219.
- Chau, C. F., and Huang, Y. L. (2005). Effects of the insoluble fiber derived from *Passiflora edulis* seed on plasma and hepatic lipids and fecal output. **Molecular Nutrition & Food Research**. 49(8): 786-790.
- Clegg, A., Colquitt, J., Sidhu, M., Royle, P., and Walker, A. (2003). Clinical and cost effectiveness of surgery for morbid obesity: a systematic review and economic evaluation. **International Journal of Obesity and Related Metabolic Disorders**. 27(10): 1167-1177.
- D'Mello, P., Darji, K., and Shetgiri, P. (2011). Evaluation of antiobesity activity of various plant extracts. **Pharmacognosy Journal**. 3(21): 56-59.
- de Simone, G., and D'Addeo, G. (2008). Sibutramine: balancing weight loss benefit and possible cardiovascular risk. **Nutrition, Metabolism, and Cardiovascular Diseases**. 18(5): 337-341.

- Ghaben, A. L., and Scherer, P. E. (2019). Adipogenesis and metabolic health. **Nature Reviews Molecular Cell Biology**. 20(4): 242-258.
- Karri, S., Sharma, S., Hatware, K., and Patil, K. (2019). Natural anti-obesity agents and their therapeutic role in management of obesity: A future trend perspective. **Biomedicine and Pharmacotherapy**. 110: 224-238.
- Madsen, L., Petersen, R. K., Sorensen, M. B., Jorgensen, C., Hallenborg, P., Pridal, L., Fleckner, J., Amri, E. Z., Krieg, P., Furstenberger, G., Berge, R. K., and Kristiansen, K. (2003). Adipocyte differentiation of 3T3-L1 preadipocytes is dependent on lipoxygenase activity during the initial stages of the differentiation process. **The Biochemical Journal**. 375(Pt 3): 539-549.
- Nawrocki, A. R., and Scherer, P. E. (2005). Keynote review: the adipocyte as a drug discovery target. **Drug Discovery Today**. 10(18): 1219-1230.
- Nicholson, A. C., Hajjar, D. P., Zhou, X., He, W., Gotto, A. M., Jr., and Han, J. (2007). Anti-adipogenic action of pitavastatin occurs through the coordinate regulation of PPARgamma and Pref-1 expression. **British Journal of Pharmacology**. 151(6): 807-815.
- Osma, J. (2018). Citotoxic and apoptotic activity of extracts from leaves and juice of *Passiflora edulis*. **Journal of Liver Research Disorder and Therapy**. 4(2): 67-71.
- Park, S.-J., Lee, I.-S., Lee, S.-P., and Yu, M.-H. (2013). Inhibition of adipocyte differentiation and adipogenesis by supercritical fluid extracts and marc from *Cinnamomum verum*. **Journal of Life Science**. 23(4): 510-517.

- Phadungkit, M., Rattarom, R., and Rattana, S. (2010). Phytochemical screening, antioxidant, antibacterial and cytotoxic activities of *Knema angustifolia* extracts. **Journal of Medicinal Plants Research**. 4(13): 1269-1272.
- Ponnusamy, S., Ravindran, R., Zinjarde, S., Bhargava, S., and Ravi Kumar, A. (2011). Evaluation of traditional Indian antidiabetic medicinal plants for human pancreatic amylase inhibitory effect *in vitro*. **Evidence-Based Complementary and Alternative Medicine**. 2011: 515647.
- Rao, P. V., and Gan, S. H. (2014). Cinnamon: a multifaceted medicinal plant. **Evidence-Based Complementary and Alternative Medicine**. 2014: 642942.
- Roy, M. K., Nakahara, K., Na, T. V., Trakoontivakorn, G., Takenaka, M., Isobe, S., and Tsushida, T. (2007). Baicalein, a flavonoid extracted from a methanolic extract of *Oroxylum indicum* inhibits proliferation of a cancer cell line *in vitro* via induction of apoptosis. **Pharmazie**. 62(2): 149-153.
- Rudnicki, M., de Oliveira, M. R., da Veiga Pereira, T., Reginatto, F. H., Dal-Pizzol, F., and Moreira, J. C. F. (2007). Antioxidant and antiglycation properties of *Passiflora alata* and *Passiflora edulis* extracts. **Food Chemistry**. 100(2): 719-724.
- Seo, M. J., Choi, H. S., Jeon, H. J., Woo, M. S., and Lee, B. Y. (2014). Baicalein inhibits lipid accumulation by regulating early adipogenesis and m-TOR signaling. **Food and Chemical Toxicology**. 67: 57-64.
- Thurairajah, P. H., Syn, W. K., Neil, D. A., Stell, D., and Haydon, G. (2005). Orlistat (Xenical)-induced subacute liver failure. **European Journal of Gastroenterology and Hepatology**. 17(12): 1437-1438.

CHAPTER IV

SCREENING OF BIOACTIVE COMPOUNDS IN *O.* *INDICUM* FRUIT EXTRACT AND BIOCHEMICAL COMPOSITION OF 3T3-L1 CELLS

4.1 Abstract

O. indicum is found throughout the Asian countries, including Thailand. It has much beneficial biological activity such as antioxidant, anti-inflammatory, antidiabetic, and hepatoprotective properties. However, there is little information report on the phytochemical constituents that can act as an anti-adipogenesis activity of 3T3-L1 cells. Therefore, the present study aimed to evaluate the phytochemical contents of *O. indicum* extract (OIE) and biomolecular change in 3T3-L1 adipocytes. Initial studies examined the chemical components of OIE, total phenolic content (TPC), and total flavonoid content (TFC), followed by gas chromatography and mass spectrometry (GC-MS) and liquid chromatography-tandem mass spectrometry (LC-MS/MS). Apart from this, Fourier transforms infrared (FTIR) was used to monitor and discriminate biomolecular changes caused by the potential anti-adipogenesis effect of the OIE on 3T3-L1 adipocytes. Chemical screening methods indicated that OIE was composed of flavonoids, alkaloids, steroids, glycoside, and tannins. As consequences, high TPC and TFC were found in the extracts. 26 volatile oils were identified in OIE by GC/MS. The most abundant volatile (> 10% of total concentration) are included γ -sitosterol, 2-

cyclohexen-1-one and 2-methyl-, benzeneethanol and 4-hydroxy-, and 3-hydroxy-2-methylbenzaldehyde, respectively. Evaluation of the flavonoid compounds in OIE using LC-MS/MS technique revealed that 20 mg/mL of the OIE exhibited 657.01 µg/mL of baicalein while the amounts of quercetin and apigenin were found at 1.10 µg/mL and 1.21 µg/mL, respectively. The inhibitory effect of the OIE on lipid accumulation in 3T3-L1 cells was conducted using FTIR microspectroscopy. The signal intensity and the integrated areas relating to lipids, lipid esters, nucleic acids, glycogen, and carbohydrates of the OIE-treated 3T3-L1 adipocytes were significantly lower than the untreated 3T3-L1 adipocytes ($P < 0.05$). Principal component analysis (PCA) indicated four distinct clusters for the FTIR spectra of 3T3-L1 adipocytes based on biomolecular changes (lipids, proteins, nucleic acids, and carbohydrates). This observation was confirmed using Unsupervised hierarchical cluster analysis (UHCA). These findings provide evidence that the OIE derived from the fruit pods of the plant is not only contain various potential substances, but also has the potential to inhibit lipids and carbohydrate accumulation in adipocytes. These results suggest that OIE can be used as a potential natural source with anti-adipogenic properties which may be exploited for the management of the overweight or obese.

4.2 Introduction

A natural product, such as plant extracts has been the most dominant phytochemical resources for drug discovery (Thomford et al., 2018). It is well known that the medicinal value of plants depends on the presence of biologically active ingredients with their pharmacological activity. *O. indicum* belongs to the Bignoniaceae family; it is a valuable medicinal plant widely found in Asian tropical and sub-tropical (Dinda et al., 2015). In Thailand, it is called Pheka (central), Litmai (northern), and Linfaa (north-eastern) (Rasadah, 2001). Many studies have reported antioxidant (Palasuwan et al., 2005), anti-inflammatory (Tran et al., 2015), anti-diabetic (Singh and Kakkar, 2013), and hepatoprotective (Joshi et al., 2011) properties in *O. indicum* and its isolated compounds. The previous study reported the chemical constitutions in fruits of *O. indicum* including flavonoids (baicalein, chrysin, oroxylin A, and oroxylin B) (Dinda et al., 2015; Uddin et al., 2003). The study of Singh (2014) and Seo (2014) revealed that isolated compounds found in *O. indicum* such as oroxylin A (Singh and Kakkar, 2014) and baicalein (Seo et al., 2014). The OIE had a pharmacological effect on adipocytes differentiation by down-regulated the expression of the large transcriptional factors and enhanced levels of pro-apoptotic proteins in 3T3-L1 cells. One aspect that has not been considered is the impact of *O. indicum* on the composition of biomolecules such as lipids and proteins which may have significant roles in the development of the adipocyte.

Fourier-transform infrared spectroscopy (FTIR) has been extensively applied to medical research due to its rapid and high sensitivity to detect the difference of functional groups belonging to tissue components such as lipids, proteins and nucleic acids (Dritsa et al., 2014). Previous research showed that FTIR was used for

determination of fatty acid in human abdominal fat (Bortolotto et al., 2005), monitoring level of glucose, protein, triglyceride, cholesterol, and lipoproteins in plasma and serum (Délérís and Petibois, 2003). Additionally, it had been successfully applied in the characterization of the molecular features of human atherosclerotic lesions because during the critical stages; the spectra were very sensitive to the structure of biological molecules (Manoharan et al., 1993). Besides, it had been demonstrated that FTIR microspectroscopy was a useful technique for assessing the biochemical changes in tissues (Movasaghi et al., 2008).

Although OIE has a varying pharmacological properties depending on which part of the plant it is derived from. A more detail insight into the chemical composition and biomolecular component during adipocyte development are still limited. Therefore, this study aimed to provide bioactive compounds of the extract. Initial experiments were performed using simple screening, GC-MS, and LC-MS. Also, the biochemical changes in the differentiated cells were examined using FTIR.

4.3 Materials and Methods

4.3.1 Chemicals and reagents

(+)-Catechin and gallic acid were purchased from Merck (Darmstadt, Germany). Quercetin, apigenin, kaempferol, baicalein, and biochanin A was obtained from INDOFINE Chemical Company (Hillsborough, NJ).

4.3.2 Phytochemical screening

The phytochemical screening was measured according to a previously published method with slight modifications (Rauf et al., 2013; Yadav and Agarwala, 2011). The stock concentration of the OIE (10 mg/mL) was prepared and tested for the presence of bioactive phytochemical compounds, including total phenolics, flavonoids, alkaloids, steroids, glycosides, tannin, and saponins.

Test for flavonoids

In brief, 1 mL of the OIE was mixed with 2 mL of 2 % of NaOH. The lead acetate test was also used operated. In this case, 1 mL of the OIE was mixed with 2 mL of 10 % w/v lead acetate solution. The formation of a yellow precipitate indicates the presence of flavonoids.

Test for alkaloids

Mayer's and Wagner's test was performed. Briefly, 1 mL of the OIE was added to 2 mL of 1 % HCl and heated. A few drops of Mayer's and Wagner's reagents were added to the mixture. The presence of turbidity of the resulting precipitate is evidence of alkaloids.

Test for steroids

The steroids containing in OIE were investigated. In short, 1 mL of the OIE was mixed with 2 mL of chloroform and H₂SO₄. The presence of red color in the lower chloroform layer resulting in the existence of steroids.

Test for Glycoside

Salkowski's test was done. In brief, 2 mg of the OIE was mixed with 2 mL of chloroform and a few drops of H₂SO₄. A reddish-brown color indicates the presence of a glycoside.

Test for tannin

The Gelatin test was performed. To summarise, 1 mL of the OIE was added to 2 mL of 1 % gelatin solution. The development of white precipitate indicates the presence of tannin.

Test for saponin

The foam test was done. Shortly, 5 mL of the OIE was shaken for 5 min. The formation of stable foam indicates the presence of saponin.

4.3.3 Total phenolic content determination (TPC)

The total phenolic content of OIE was determined by the method of Folin-Ciocalteu (Kohoude et al., 2017). In brief, 20 µL of extract (0.625 mg/mL) or a standard solution of gallic acid (0-7.5 µg/mL) were added into 100 µL of Folin-Ciocalteu reagent. The mixture was incubated at room temperature for 6 min, prior to the addition of 7.5 % (w/v) of Na₂CO₃. After 1 h of incubation at room temperature, the absorbance was recorded at 760 nm against a 100 % DMSO blank. TPC of the sample was expressed as mg of gallic acid equivalents (GAE) per gram of dry weight.

4.3.4 Total flavonoid content determination (TFC)

The total flavonoid content was measured according to a previously published with slight modifications (Jing et al., 2010). Briefly, a 25 μL of extract (3 mg/mL) or a standard solution of catechin (0-200 $\mu\text{g}/\text{mL}$) were added into 125 μL of deionized water followed by the addition of 10 μL of 5 % NaNO_2 . This was incubated at room temperature. After 6 min, 15 μL of 10% AlCl_3 was added. Upon mixing the reaction was allowed to proceed for 5 min, then 50 μL of 1 M NaOH was added. The absorbance of the mixture was determined at 595 nm versus prepared 100 % DMSO blank. The concentration of total flavonoids contained in OIE was expressed as milligrams of catechin equivalent (CE) per gram of dry extract.

4.3.5 Gas chromatography-mass spectrometry (GC-MS) analysis

The ethanolic extract obtained from the fruits of *O. indicum* was subjected to gas chromatography and mass spectroscopy for the determination of volatile bioactive compounds (Gokhale et al., 2017). The GC-MS analysis of the sample was carried out using BRUKER 450 GC and 320 MS. RTX 5MS capillary column (30 m x 0.25 mm, fused silica 0.25 μm) was used for the analysis. The operating conditions of the column were as follows: 1) Gas chromatography; oven temperature program from 110 $^\circ\text{C}$, at rate 0 $^\circ\text{C}/\text{min}$ withholding time of 2 min and from 200 $^\circ\text{C}$, at rate 10 $^\circ\text{C}/\text{min}$ withholding time of 3 min, and the final temperature was 280 $^\circ\text{C}$, at rate 5 $^\circ\text{C}$ and kept for 24 min. The injector temperature was maintained at 250 $^\circ\text{C}$, column flow 1.0 mL/min Helium, injection split 1:5. 2) Mass spectrometry; ion source temperature 200 $^\circ\text{C}$, scan mode ranges from 45 to 500 masses, electron energy 70 eV. The identification of extract was performed by comparing the mass spectra with data from NIST (National Institute of Standards and Technology, US) mass spectral library 2008.

4.3.6 Liquid chromatography-tandem mass spectrometry (LC-MS/MS) analysis

The analysis of phytochemical compounds in OIE was performed on the Agilent Technologies 1290 series HPLC with Agilent Technologies 6490 series electrospray ionization triple-quadrupole MS/MS with electrospray ionization (ESI) (Rojsanga et al., 2017). The injection volume for all samples was 5 μ L. The separation was achieved using a Zorbax Rapid Resolution High Definition (RRHD) SB-C18 (2.1 mm id \times 150 mm, 1.8 μ m) (Agilent Technologies) and thermostated at 25 $^{\circ}$ C, with a flow rate of 0.2 mL/min of mobile phase whose composition was: A = 1 % aqueous formic acid, B = 1 % formic acid in acetonitrile. The solvent gradient was starting with 30 % solvent B at 10 min and 100% solvent B at 30 min. 0.01 mg/mL of quercetin, apigenin, kaempferol, baicalein, and biochanin A were dissolved in 100 % of methanol solution and used as standard reference compounds. 20 mg/mL of OIE was dissolved in 100 % of methanol and keep in the dark at 4 $^{\circ}$ C before analysis.

4.3.7 Fourier-transform Infrared Spectroscopy (FTIR) analysis

The effect of OIE on general biochemical composition of 3T3-L1 adipocytes was conducted using FTIR; the method applied from Dunkhunthod et al. (Dunkhunthod et al., 2017). Briefly, on day 10, cells were collected and centrifuged at 4000 \times g for 5 min, then washed with 0.85% w/v NaCl and centrifuged at 4000 \times g for 5 min. Cell pellets were dropped onto a window slide (MirrIR, Kevley Technologies) and dried for 30 min in a desiccator to eliminate the excess water. The dried cells were stored in a desiccator until analysis using FTIR.

FTIR spectra were recorded using a spectroscopy facility, at the Synchrotron Light Research Institute (Public Organization), Thailand. FTIR spectra were acquired

with a Bruker Vertex 70 spectrometer coupled with a Bruker Hyperion 2000 microscope (Bruker Optics Inc., Ettlin-Gen, Germany) equipped with a nitrogen-cooled MCT (HgCdTe) detector with a $36 \times$ IR. The spectra were obtained in the reflection mode with the wavenumber range of $4000\text{-}600\text{ cm}^{-1}$, using an aperture size of $50\text{ }\mu\text{m} \times 50\text{ }\mu\text{m}$, with a resolution of 6 cm^{-1} . Each spectrum was collected at 64 scans. OPUS 7.2 software (Bruker Optics Ltd, Ettlingen, Germany) was used to acquire FTIR spectral data and control instrument system.

The spectral range between $3000\text{-}2800\text{ cm}^{-1}$ and $1800\text{-}850\text{ cm}^{-1}$ was identified by Principal Component Analysis (PCA) using variants of the Unscrambler 9.7 software (CAMO Software AS, Oslo, Norway). The preprocessing of the spectra was performed by second derivative transformations using the Savitzky-Golay algorithm (nine smoothing points) and normalized with extended multiplicative signal correction (EMSC). Score plots (3D) and loading plots were used to represent the different classes of data and relations among variables of the data set, respectively.

The FTIR spectra data sets were submitted to the Unsupervised Hierarchical Cluster Analysis (UHCA), to collect similar spectra in groups or clusters, using the OPUS 7.2 software (Bruker). Cluster analysis was performed on the second derivatives, and vector normalizes spectra using Ward's algorithm.

4.4 Results

4.4.1 The phytochemical composition, TPC and TFC

The phytochemical compounds of OIE were positive for flavonoids, alkaloids, steroids, glycoside, and tannin, but no saponin observed in OIE. The concentration of

TPC and TFC presented in OIE were 51.483 ± 0.766 mg GAE/g and 34.191 ± 2.473 mg CE/g of dry weight, respectively (Table 4.1).

Table 4.1 Phytochemical composition, total phenolic content, and total flavonoid content of OIE.

The phytochemical composition, TPC and TFC	Results
Flavonoids	+
Alkaloids	+
Steroids	+
Glycoside	+
Tannins	+
Saponin	-
Total phenolic content (TPC)	51.48 ± 0.77 (mg GAE/g)*
Total flavonoids content (TFC)	34.19 ± 2.47 (mg CE/g)*

(+) = positive test; (-) = negative test

*The TPC and TFC of the dry weight of OIE. These were calculated from the calibration curve of the standard. The data are expressed as the mean \pm SEM of three independent experiments performed in triplicate (n = 9).

4.4.2 GC-MS quantification of volatile compounds in OIE

Twenty-six volatiles were identified in OIE by GC/MS (Figure 4.1) including γ -Sitosterol, 2-cyclohexen-1-one and 2-methyl-, benzeneethanol and 4-hydroxy-, 3-hydroxy-2-methylbenzaldehyde were the most abundant volatiles, those concentrations amounts were 17.19 %, 15.28 %, 13.33 % and 11.18 % of the total concentration of the

26 detected volatiles, respectively (Table 4.2). Also, cyclobutanecarboxylic acid, decyl ester (8.82 %) was the next abundant volatiles. 2-furancarboxaldehyde and 5(hydroxymethyl)-, Glycerol 1-monopalmitate, Beta-Monolinolein, n-Decanoic acid, Campesterol, Nonanoic acid, Stigmasterol, 1,6-Dihydro-5-(2-hydroxyethyl)-4-methyl-6-oxopyrimidine, 2-Dodecenoic acid, Dotriacontane, Dodecanoic acid, and Glycerol 1,3-dipalmitate, the concentrations were in ranges between 1-5 % of total volatiles concentration.

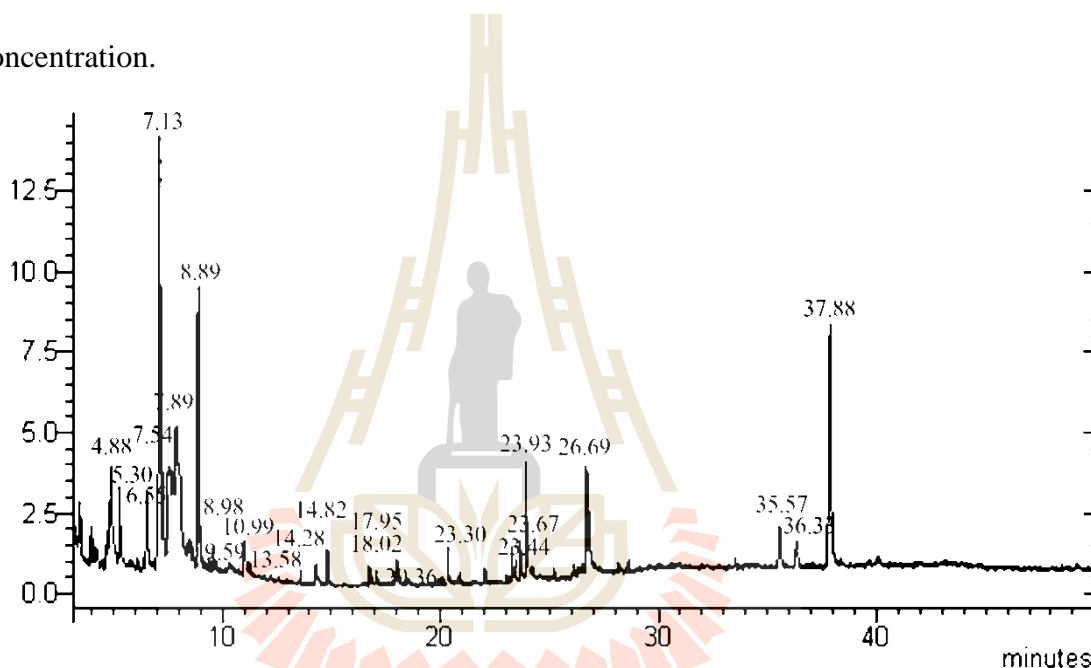


Figure 4.1 The GC/MS chromatogram of the OIE.

Table 4.2 Relative concentrations of volatiles in OIE.

Volatiles	Retention time	Peak Area (%)
2-Furancarboxaldehyde, 5(hydroxymethyl)-	4.879	4.86
Nonanoic acid	5.295	2.28
n-Decanoic acid	6.546	2.82

Table 4.2 Relative concentrations of volatiles in OIE (Continued)

Volatiles	Retention time	Peak Area (%)
2-Cyclohexen-1-one, 2-methyl-	7.130	15.28
2-Dodecenoic acid	7.296	1.33
Benzeneethanol, 4-hydroxy-	7.539	13.33
3-Hydroxy-2-methylbenzaldehyde	7.881	11.18
Cyclobutanecarboxylic acid, decyl ester	8.893	8.82
Dodecanoic acid	8.983	1.15
Ethyl N-(o-anisyl) formimidate	9.586	0.40
1,6-Dihydro-5-(2-hydroxyethyl)-4-methyl-6-oxopyrimidine	10.987	1.39
Tetradecanoic acid	11.255	0.21
Hexadecanoic acid, methyl ester	13.579	0.28
n-Hexadecanoic acid	14.278	0.66
Hexadecanoic acid, ethyl ester	14.824	0.99
Phytol	17.086	0.39
Linoleic acid ethyl ester	17.951	0.58
Linolenic acid ethyl ester	18.082	0.57
Glycerol 1,3-dipalmitate	20.358	1.13
Linolelaidic acid, methyl ester	23.301	0.79
9,12,15-Octadecatrienoic acid, 2-phenyl-1,3-dioxan-5-yl ester	23.437	0.52

Table 4.2 Relative concentrations of volatiles in OIE (Continued)

Volatiles	Retention time	Peak Area (%)
Dotriacontane	23.669	1.29
Glycerol 1-monopalmitate	23.934	4.37
Beta-Monolinolein	26.699	4.09
Campesterol	35.565	2.48
Stigmasterol	36.333	1.48
gamma-Sitosterol	37.876	17.19
Total		100

4.4.3 LC-MS/MS quantification of selected flavonoids in OIE

The identification of phytochemical compounds in the OIE was performed by using LC-MS/MS. Figure 4.2 presents the MRM chromatograms of the OIE compared to the reference compounds, including quercetin (RT~9.2 min), apigenin (RT~10.8 min), kaempferol (RT~11.2 min), baicalein (RT~11.6 min), and biochanin A (RT~16.2 min). It was shown that quercetin, apigenin, and baicalein were identified in the OIE (Figure 4.1B). Besides, the OIE also exhibited other prominent peaks at RT ~1.8, 2.2, and 15.2 min. The result from MRM data quantification of 20 mg/mL of the OIE exhibited 657.01 $\mu\text{g/mL}$ of baicalein while the amounts of quercetin and apigenin were found to be quite low at 1.10 $\mu\text{g/mL}$ and 1.21 $\mu\text{g/mL}$, respectively (Table 4.3). However, kaempferol and biochanin A were not detected in the OIE.

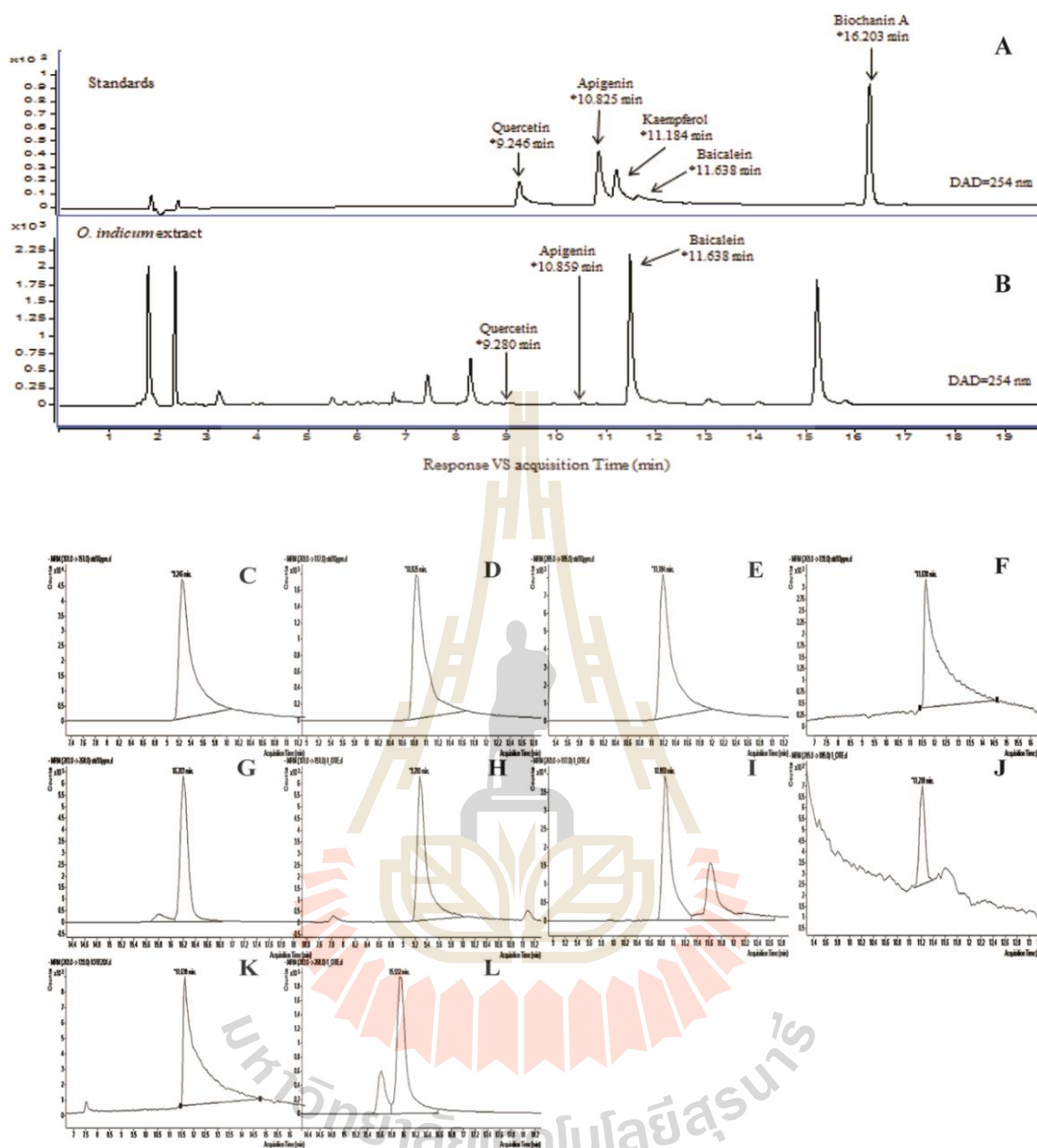


Figure 4.2 Multiple reaction monitoring (MRM) chromatograms of the OIE and standard reference compounds. (A) Mixtures of standard reference compounds, (B) and (H) to (L) Chromatography of OIE, (C) Chromatography of quercetin, (D) Chromatography of apigenin, (E) Chromatography of kaempferol, (F) Chromatography of baicalein, (G) Chromatography of biochanin A.

Table 4.3 Quantification of Flavonoid compounds in OIE.

Compounds	Quercetin	Apigenin	Kaempferol	Baicalein	Biochanin A
	(301-->151)	(269-->117)	(285-->185)	(269-->139)	(283-->268)
			ND		ND
OIE (20 mg/mL)	1.10 μg/mL	1.21 μg/mL	(Detection limit = 0.55 μg/mL)	657.01 μg/mL	(Detection limit = 0.11 μg/mL)

ND = Not detected

4.4.4 Fourier-transform infrared spectroscopy (FTIR) spectra profiles

FTIR spectra

FTIR microspectroscopy was used to determine the biochemical composition of pre-adipocytes, adipocytes, and adipocytes treated with either, simvastatin or OIE. For each treatment, FTIR spectra between wavelengths, 3000-950 cm^{-1} were obtained and are shown in Figure 4.3. The Spectra was converted to second derivatives to allow a more detailed comparison of the four groups. These were further separated into three distinct areas: (1) the lipid regions (3000-2800 cm^{-1}), (2) the protein regions (1700-1500 cm^{-1}) and (3) carbohydrate and nucleic acid regions (1300-950 cm^{-1}). The FTIR band assignments found in secondary derivative spectra in 3T3-L1 cells are shown in Table 4.4.

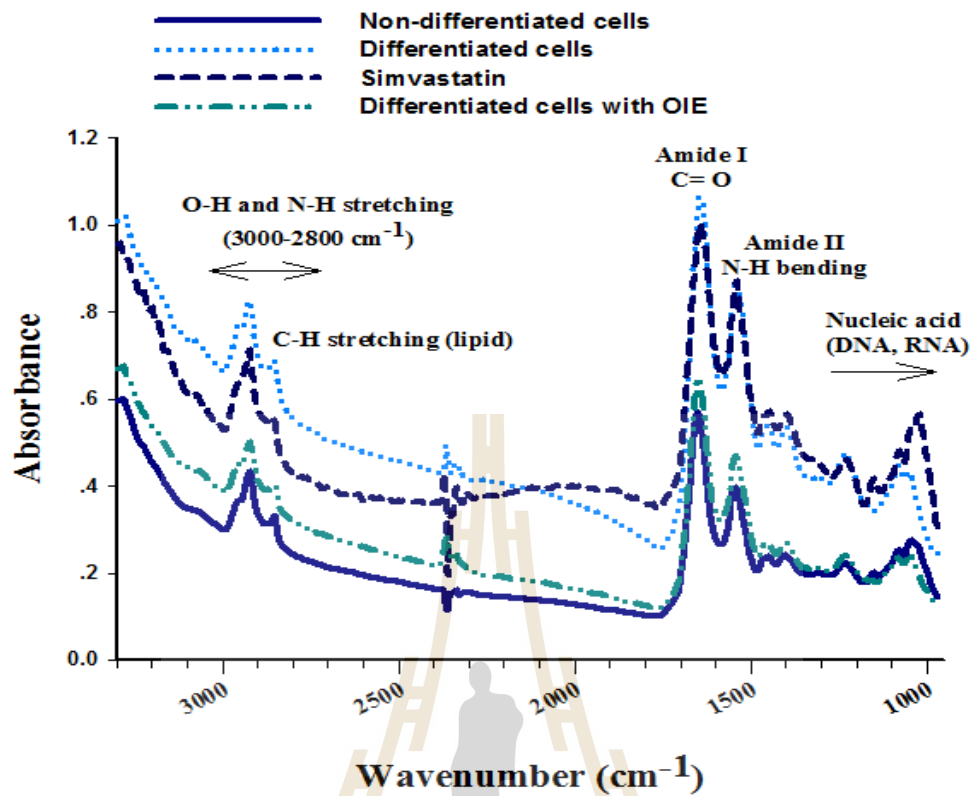


Figure 4.3 Average original FTIR spectra (3000-950 cm^{-1}) obtained from 3T3-L1 cells. The raw spectra of non-differentiated cells (preadipocytes) ($n = 62$), differentiated cells (untreated adipocytes) ($n = 92$), simvastatin and OIE treated 3T3-L1 adipocytes ($n = 47$) for 10 day.

Table 4.4 FTIR band assignments for functional groups found in the second derivative spectra of 3T3-L1 cells (Garip et al., 2009; Kucuk Baloglu et al., 2015).

2nd derivative spectra (cm⁻¹)	Band assignment
2962	Asymmetrical stretching (C-H) from methyl (-CH ₃) groups of lipids
2924	Asymmetrical stretching (C-H) from methylene (-CH ₂) groups of lipids
2854	Symmetrical stretching (C-H) from methylene (-CH ₂) groups of lipids
1740	(C=O) of ester functional groups primarily from lipid and fatty acids
1647	Amide I protein (C=O stretching)
1543	Amide II protein (N-H bending, C-H stretching)
1462	Asymmetrical deformation (CH ₂) _{scissor} from methylene (-CH ₂) groups of lipids
1400	Symmetrical stretching (COO ⁻) associated with symmetrical in-plane deformation bend (CH ₃) of proteins
1234	Asymmetrical stretching (PO ₂ ⁻) mainly nucleic acids with the little contribution from phospholipids
1153	Asymmetrical stretching (CO-O-C) of glycogen, other carbohydrates and nucleic acids

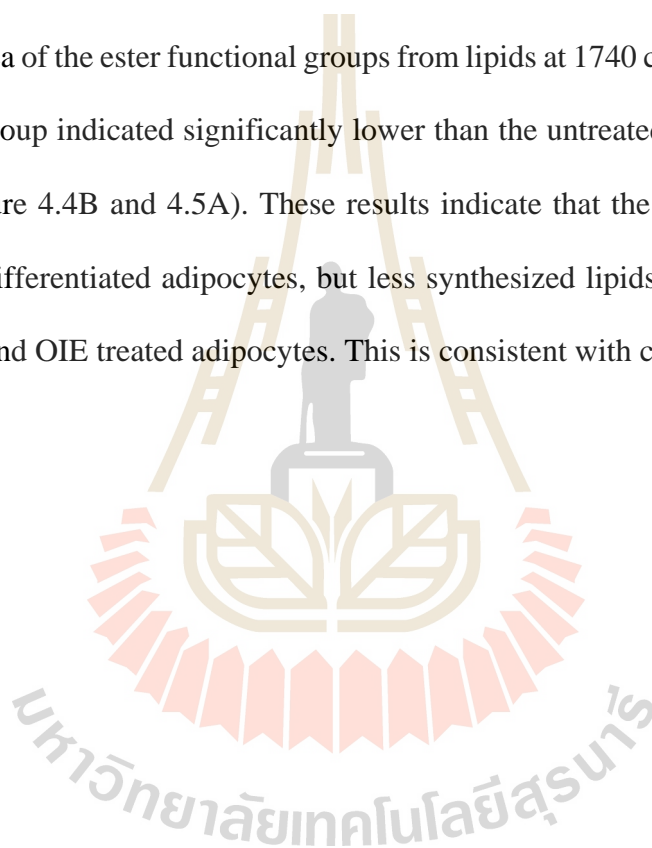
Table 4.4 FTIR band assignments for functional groups found in the second derivative spectra of 3T3-L1 cells (Garip et al., 2009; Kucuk Baloglu et al., 2015) (Continued).

2nd derivative spectra (cm-1)		Band assignment
1080	Symmetrical stretching (PO_2^-) of the phosphodiester backbone of nucleic acids (DNA and RNA) and phospholipids	
1018	(C-O) vibration from glycogen and other carbohydrates	

The second derivative spectra in the lipid region

The spectra in the high-frequency region at $3000\text{-}2800\text{ cm}^{-1}$ correspond to the symmetrical and asymmetrical vibrations of -CH groups of the lipid. The average second derivative spectra of 3T3-L1 cells under different experimental conditions exhibited triplet dominant lipid absorbance bands at 2962 cm^{-1} , 2924 cm^{-1} and 2854 cm^{-1} which are attributed to asymmetrical stretching from the methyl and methylene groups of lipids, and symmetrical stretching from methylene groups of lipids, respectively (Figure 4.4A). Also, the dominant peak relevant to the lipid occurred in the lower wavenumber region at 1740 cm^{-1} , which is assigned to C=O stretches of the ester functional groups from lipids and fatty acids (Figure 4.4A). The band centered at 2924 cm^{-1} and 1740 cm^{-1} of adipocyte were clearly separated from pre-adipocyte and treated cells, as shown in Figure 4.3A and 4.3B respectively. The decrease in signal intensity and area of the peaks (at 2962 cm^{-1} and 2924 cm^{-1}), which reflected an absorption peak of lipids of the OIE-treated adipocytes, presented less than untreated adipocytes (Figure 4.4A).

Then, we calculated the ratio of the integrated area of several functional groups, including CH₂ (2938-2906 cm⁻¹, centered at 2924 cm⁻¹)/CH₃ (2973-2954 cm⁻¹, centered at 2962 cm⁻¹) asymmetric stretching that belongs to lipids. The results showed that the ratio of the integrated area of the lipids region in the OIE-treated adipocytes displayed significantly less than the untreated adipocytes group ($P < 0.05$) and almost the same area as a simvastatin-treated group (Figure 4.5A). In the same way, the integrated area of the ester functional groups from lipids at 1740 cm⁻¹ in the OIE-treated adipocytes group indicated significantly lower than the untreated adipocytes group ($P < 0.05$) (Figure 4.4B and 4.5A). These results indicate that the lipid accumulation is seen in the differentiated adipocytes, but less synthesized lipids are observed in both simvastatin and OIE treated adipocytes. This is consistent with cellular studies (Figure 3.5).



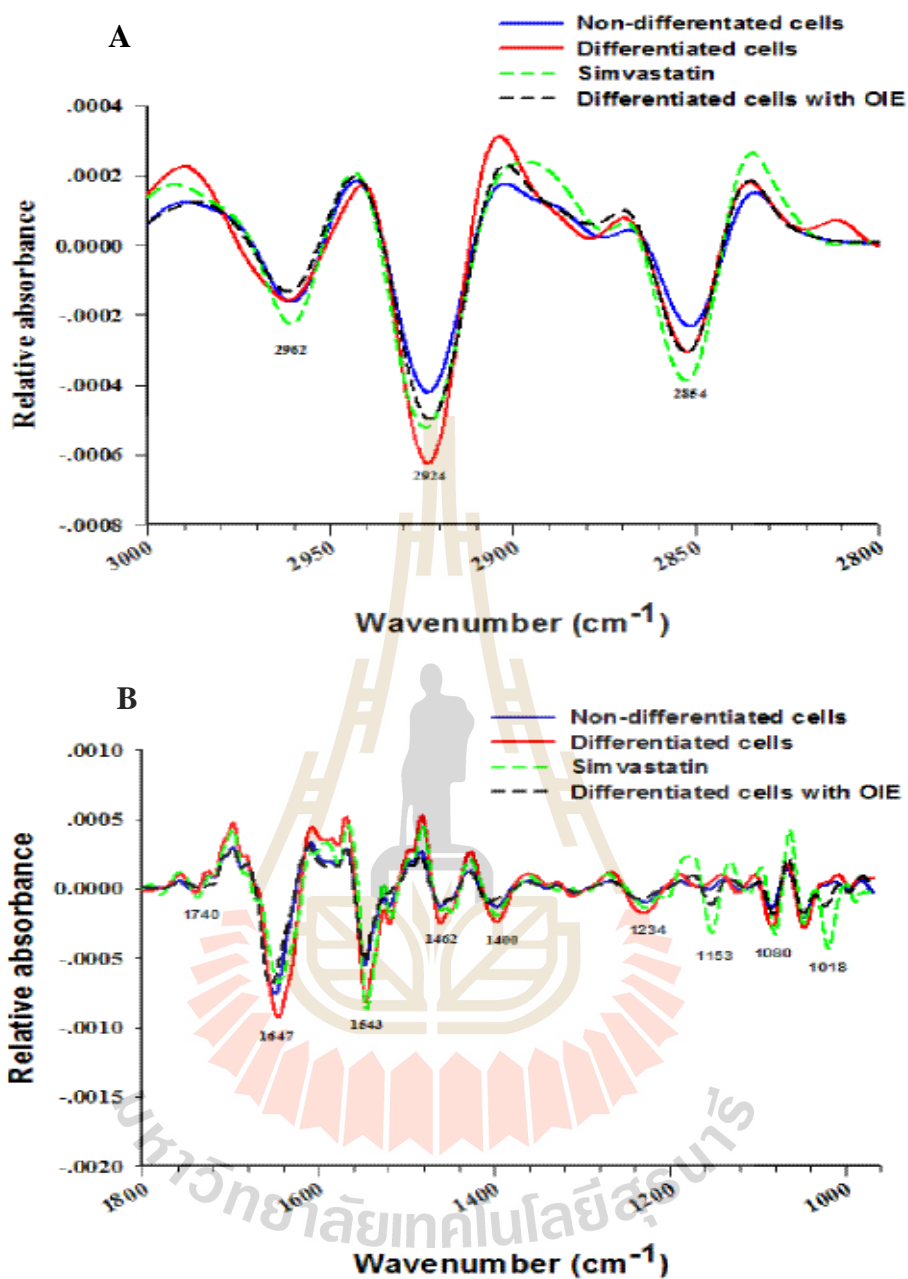


Figure 4.4 Average the secondary derivative spectra of 3T3-L1 cells. The second derivative spectra of non-differentiated cells (pre-adipocytes), differentiated cells (untreated adipocytes), simvastatin and OIE-treated differentiated cells for 10 days. The data are represented in two regions: **(a)** lipid regions ($3000\text{-}2800\text{ cm}^{-1}$) and **(b)** protein, nucleic acid, glycogen and other carbohydrate regions ($1800\text{-}950\text{ cm}^{-1}$).

The second derivative spectra in the protein region

The major contributor in the spectrum ranges from 1700-1500 cm^{-1} , which are attributed to an absorption peak of proteins amide I and II. The ratio of integrated area of several functional groups, including CH_2 asymmetric stretching (2938-2906 cm^{-1} , centered at 2924 cm^{-1})/amide I (1674-1624 cm^{-1} , centered at 1647 cm^{-1}) that belong to proteins of the OIE-treated adipocytes displayed little less integral area ratio than the untreated adipocytes group but not a significant difference ($P > 0.05$) (Figure 4.5B)

The second derivative spectra in the carbohydrate and nucleic acid region

The signal intensity and area of the peaks of the OIE-treated adipocytes at 1153 cm^{-1} and 1018 cm^{-1} which are attributed to an absorption peak of C–O vibrations from glycogen and other carbohydrates. Undoubtedly exhibited less than untreated 3T3-L1 adipocytes (Figure 4.4B) and displayed significantly less integral area than untreated adipocytes ($P < 0.05$) and nearly the same level as the simvastatin-treated group (Figure 4.5B). The functional group of PO_2 stretching mode from mainly nucleic acids at 1234 cm^{-1} and 1080 cm^{-1} regions of the OIE-treated adipocytes displayed signal intensity and areas less than the untreated and simvastatin-treated adipocytes ($P < 0.05$) (Figure 4.4B and 4.5B). This confirms significant differences between the OIE treated and non-treated adipocytes.

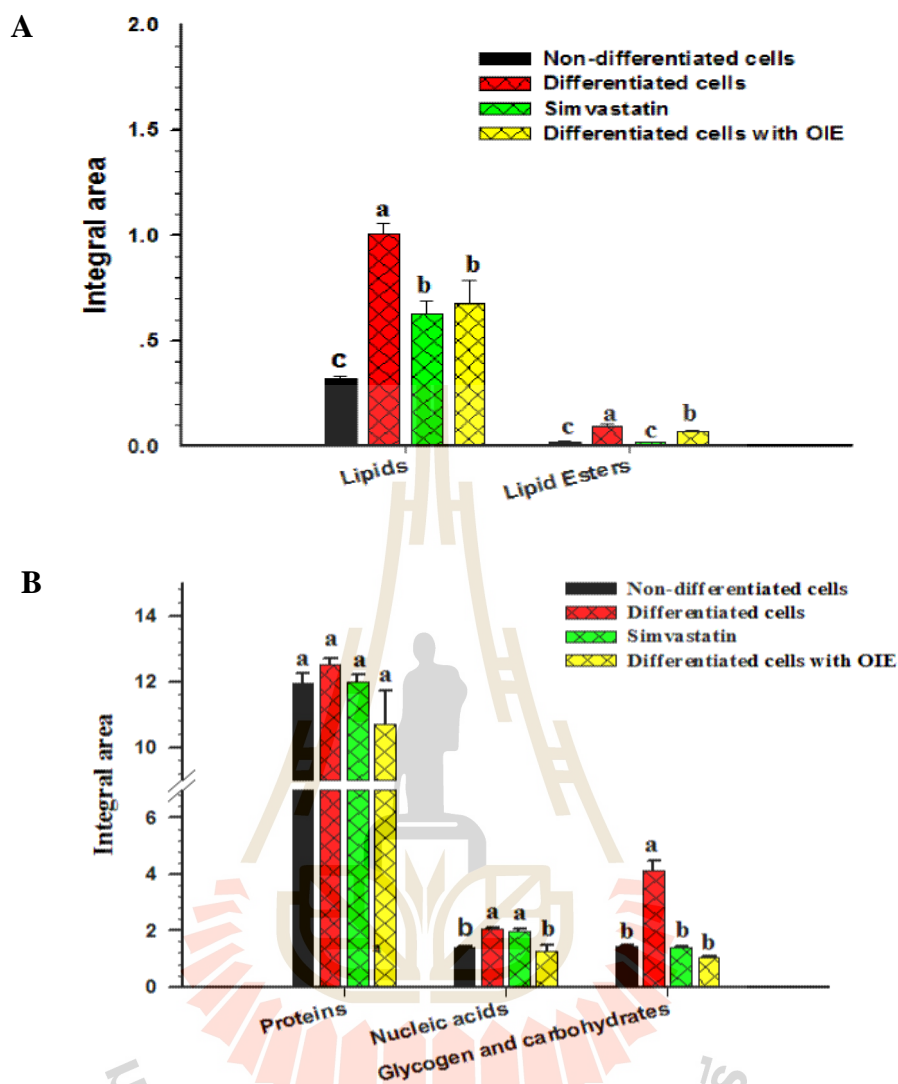


Figure 4.5 The histogram of integrated areas of 3T3-L1 cells. The integrated area from the second derivative data of non-differentiated cells (pre-adipocytes), differentiated cells (untreated adipocytes), simvastatin- and OIE-treated differentiated cells. (A) Integral area of lipids and lipid esters. (B) Integral area of proteins, nucleic acids, glycogen, and carbohydrates. The results reported as means \pm SEM ($n = 3$). Significant differences were observed (Tukey's HSD test, $P < 0.05$) and are represented in the Figure with the letters from a to c. Bars annotated with the different letter are significantly different.

PCA

The PCA was performed to distinguish the data sets acquired from pre-adipocyte, untreated adipocyte, simvastatin- and OIE-treated adipocytes. The PCA results were obtained from a second derivative spectra range at 3000-2800 cm^{-1} and 1700-950 cm^{-1} . The results from 2-dimensional PCA clustering (Figure 4.6A) clearly reveal distinct separation of cluster spectra according to the difference in cell composition, the clusters of untreated adipocytes were separated from the clusters of simvastatin and OIE-treated adipocytes along PC1 (41%). Likewise, the clusters of pre-adipocytes were distinguished from OIE-treated adipocytes along PC2 (14%). Also, the spectrum band which most influences to the clustering could be examined through the PCA loading plots (Figure 4.6B). PC1 loading plot was discriminated by the loading spectra at 2920 cm^{-1} and 2850 cm^{-1} caused by the C-H stretching and at 1153 cm^{-1} and 1022 cm^{-1} resulting from the C-O vibrations from glycogen and other carbohydrates, which separated the negative score plot of the untreated adipocytes from the positive score plot of simvastatin and OIE-treated adipocytes.

This result illustrated and confirmed that untreated adipocytes had a higher lipid and carbohydrate contents than simvastatin and OIE-treated adipocytes. Moreover, the negative PC2 loading in the lipid region (centered at 2920 cm^{-1} and 2854 cm^{-1} , 1485 cm^{-1}) revealed that preadipocytes and OIE-treated adipocytes exhibited different properties. These results are consistent with the second derivative spectra results in the previous section.

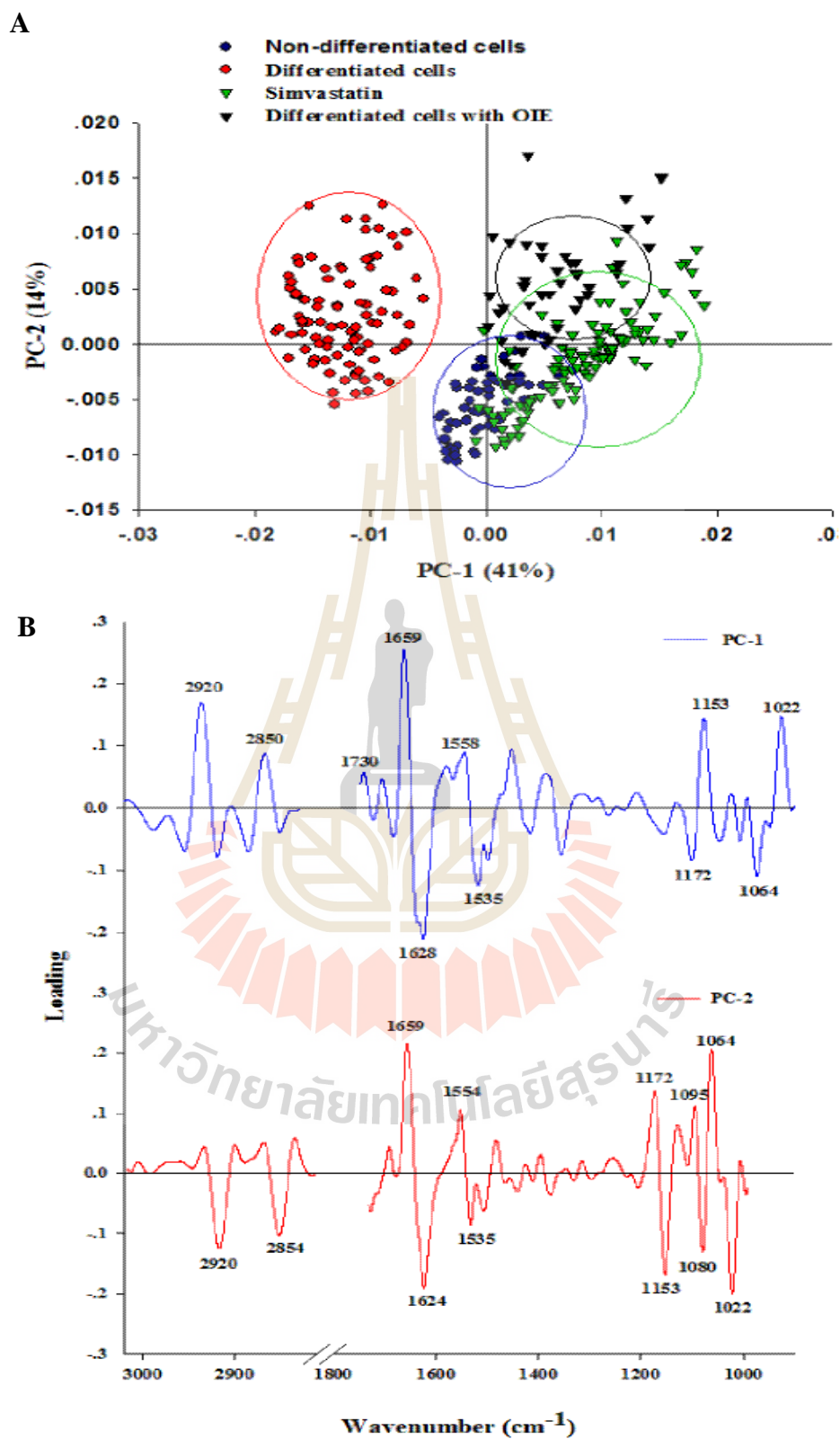


Figure 4.6 Principal component analysis (PCA) of FTIR spectral ranges 3000-2800 cm^{-1} and 1800-950 cm^{-1} giving PCA score plot. (A) PCA loading plot, (B) The 2D PCA

score plots showed the clustering separation spectra between 3T3-L1 non-differentiated cells, differentiated cells, simvastatin, and OIE-treated differentiated cells for 10 days. The biomarker differences over a spectral range of samples are identified by PC1 and PC2 loading plots.

UHCA

UHCA was used to determine the spectral similarity within groups and between groups of preadipocytes, untreated adipocytes, simvastatin- and OIE-treated adipocytes. The spectral similarity regarding relative distance is illustrated in the dendrogram (Figure 4.7), which was obtained from second derivative spectral data and Ward's algorithm. The results exhibited that the first cluster of pre-adipocyte, branch A, was clearly separated from other groups (branch B). Additionally, the branch B that was corresponding to spectra of untreated adipocytes (branch B2), OIE-treated- (branch B1.1) and simvastatin-treated (branch B1.2) adipocytes was obviously distinguished. The spectra of branch B1 is composed of two subgroups revealing a closer similarity between OIE- and simvastatin-treated adipocytes. Cluster analysis employed Ward's algorithm using second derivatives, and vector normalization, over the spectral ranges $3000\text{-}2800\text{ cm}^{-1}$ and $1800\text{-}950\text{ cm}^{-1}$. The smaller the relative distance indicates further similarity of the spectra. The spectra from the same group were classified into the same cluster. Regarding the result in Figure 4.5a, the lipid amount of pre-adipocytes as expected was the lowest ($P < 0.05$).

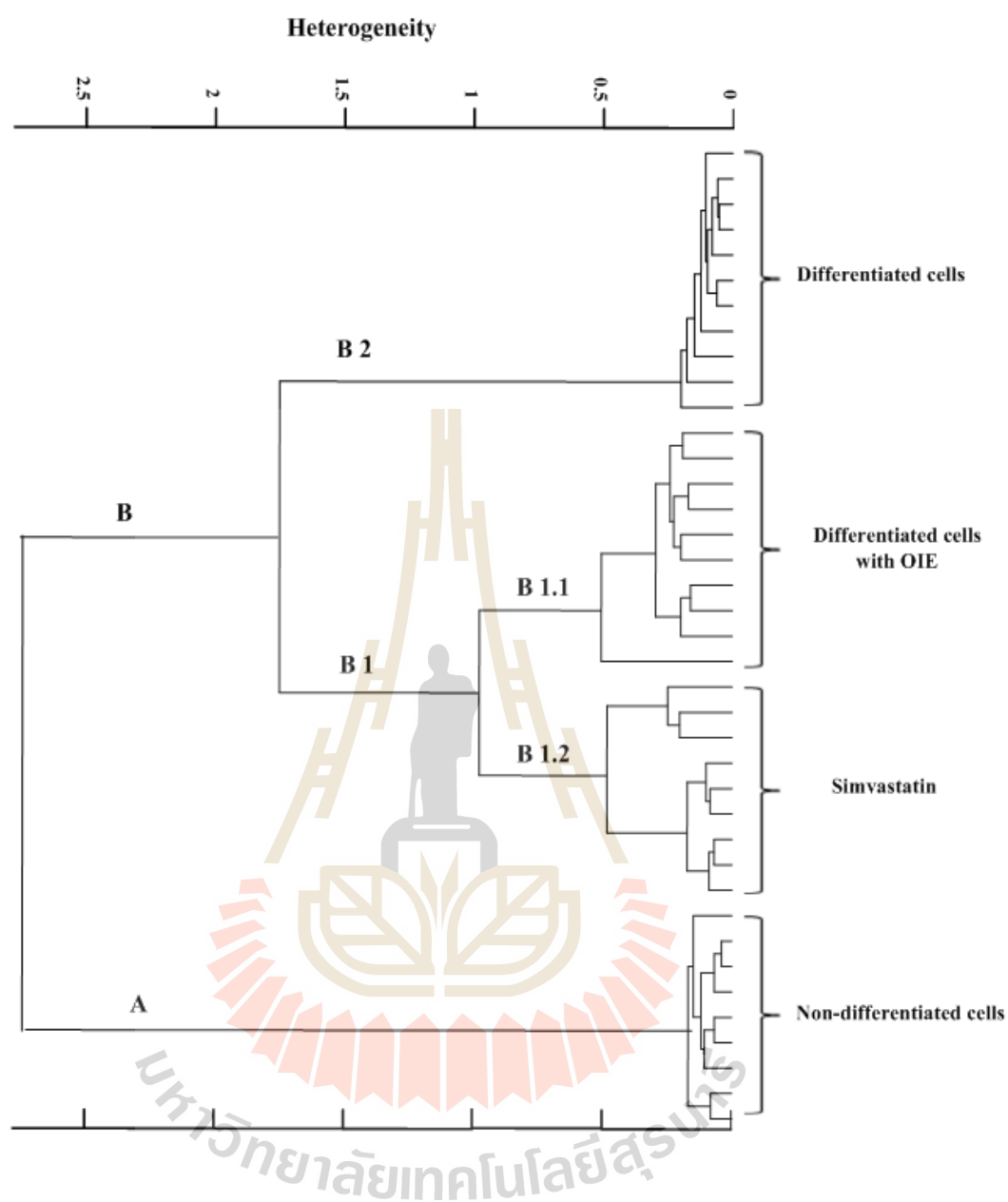


Figure 4.7 Unsupervised hierarchical cluster analysis (UHCA) dendrogram achieved by cluster classifications of infrared spectra of 3T3-L1 cells. Non-differentiated cells (pre-adipocytes), differentiated cells (untreated adipocytes), simvastatin, and OIE-treated differentiated cells using second derivative spectra data set.

4.5 Discussion and conclusion

Natural products from plants is an important natural resource for the discovery of the new drugs, due to their chemical diversity, which may potentially be functional against many diseases. In this study, 3T3-L1 pre-adipocytes had been treated with the OIE to investigate adipogenesis in these cells. Thus, it is important to know the phytochemical constitutes of OIE, which would possibly impact on adipocytes development. The study on qualitative phytochemical screening revealed the presence of flavonoids, alkaloids, steroids, glycoside, and tannin were observed in the OIE. The results are related to the results carried out from GC-MS and LC-MS analysis. The results of GC-MS profiles of OIE can be grouped in four major volatile compounds including;

1) Fatty acids and glyceride: Fatty acid consists of a straight chain of carbon atoms with hydrogen atoms along the length of the chain at one end of the chain and a carboxyl group at the other end. Fatty acids, in combination with glycerol in the form of mono-, di- and triglyceride (Britannica, 2019). Fatty acids and glycerides which found in OIE included of nonanoic acid, n-decanoic acid, 2-dodecenoic acid, decanoic acid, tetradecanoic acid, n-hexadecanoic acid, glycerol 1,3-dipalmitate, glycerol 1-monopalmitate, and beta-monolinolein. However, the amount of fatty acid and glycerides compounds found in OIE were very low (0.21- 4.37 %).

2) Steroids: steroids are characterized by a molecular structure of 17 carbon atoms arranged in four rings (Clayton, 2019). Steroids obtained from OIE included campesterol, stigmasterol, and gamma-sitosterol. Interestingly, in this study, we found the gamma-sitosterol, which was the main constituent of the OIE, accounting for 17.19 % of the total compound content. This major compound was previously displayed

antidiabetic activity (Balamurugan et al., 2011; Balamurugan et al., 2012). Oral administration of γ -sitosterol (20 mg/kg body weight) for 21 days in STZ-induced diabetic rats resulted in a significant decrease in blood glucose, total serum cholesterol, triglycerides, and very-low-density lipoprotein-cholesterol levels coupled with an elevation of high-density lipoprotein cholesterol levels in diabetic rats (Balamurugan et al., 2011). The mechanism was by closing K^+ ATP channel and released insulin from the islets of the pancreas (Balamurugan et al., 2011). Although, the previous result suggested that plants, where γ -sitosterol was found, had been useful in antidiabetic. However, many reports showed their cytotoxicity against cancer cells (Endrini et al., 2015; Sirikhansaeng et al., 2017; Sundarraj et al., 2012). Therefore, toxicity to plants containing a high amount of γ -sitosterol should be considered to ensure for the safety use.

3) Aromatic hydrocarbon: aromatic hydrocarbon is hydrocarbons containing one or more aromatic rings (Speight, 2017). In this study we found 3 groups of aromatic hydrocarbon compounds in OIE including 3.1) Furan (2-Furancarboxaldehyde, 5(hydroxymethyl)-), 3.2) Benzene (Benzeneethanol, 4-hydroxy-, 3-Hydroxy-2-methylbenzaldehyde, Ethyl N-(o-anisyl) formimidate, 9,12,15-Octadecatrienoic acid, 2-phenyl-1,3-dioxan-5-yl ester), and 3.3) Pyrimidine (1,6-Dihydro-5-(2-hydroxyethyl)-4-methyl-6-oxopyrimidine). In this study, Benzeneethanol, 4-hydroxy- (13.33 %) was presented dominantly among the aromatic hydrocarbon compound in OIE. The study of Lee (2011) found that tyrosol or benzeneethanol, 4-hydroxy- was a major bioactive phenolic compound present in *Rhodiola crenulata* extracts could suppress of adipogenesis and lipid accumulation through modulation of pentose phosphate pathway (Lee et al., 2011). Moreover, the previous study found that tyrosol and its metabolites

from olive oil exhibited antioxidant in human endothelial cells and anti-inflammatory in-ear edema mouse model (Muriana et al., 2017).

4) Others: Other compounds which found in OIE were including 4.1) ketone (2-cyclohexen-1-one, 2-methyl-), 4.2) esters (cyclobutanecarboxylic acid, decyl ester, hexadecanoic acid, methyl ester, hexadecanoic acid, ethyl ester, linoleic acid ethyl ester, linoleic acid, methyl ester), 4.3) acyclic diterpene alcohols (phytol), 4.4) alkane (dotriacontane). While, the study of Jadhav (2018) reported that methanolic extract of *O. indicum* fruits showed the presence of hexadecanoic acid, methyl ester, 9-octadecynoic acid, methyl ester, 9-octadecenoic acid, methyl ester, (E)-, and octadecanoic acid, methyl ester (Jadhav, 2018). Although there are some different type of ester compounds found in the previous study but did not show up in this study. The possible explanation for the difference in a variety of the compounds maybe because they are using the maceration technique, different solvents, and different in LC-MS operations.

Evaluation of the flavonoid compounds in OIE using LC MS/MS technique revealed that the OIE contained quercetin, apigenin, and baicalein. The MRM mode, which was used for the data quantification showed that 657.01 $\mu\text{g/mL}$ of baicalein was the most dominate flavone found in 20 mg/mL of OIE. While quite low amounts of quercetin and apigenin were identified in the OIE (1.10 $\mu\text{g/mL}$ and 1.21 $\mu\text{g/mL}$ respectively), these results are in accordance with the previous report that baicalein is the major component of methanolic extract of the fruits of *O. indicum* (Roy et al., 2007). Many studies found that baicalein could inhibit lipid accumulation and adipocyte differentiation by suppressing adipogenic factors such as PPAR γ and C/EBP α through m-TOR signaling pathway (Seo et al., 2014), enhanced the expression of COX-2 (Cha

et al., 2006) in 3T3-L1 fibroblasts. Moreover, 20 mg/kg body weight of baicalein decreased food intake, adipose tissue, and body weight of diet-induced obese mice (Min et al., 2018).

Although FTIR microspectroscopy has previously been used to characterize biochemical composition in medical research studies (Manoharan et al., 1993; Pijanka et al., 2010; Vongsvivut et al., 2013), this is the first study using FTIR to demonstrate on the biochemical profile of OIE treated adipocyte. These results indicated that the lipids, lipid esters, nucleic acids, glycogen, and carbohydrates of the OIE-treated adipocytes were significantly decreased compared to untreated adipocytes (Fig. 4.5a and 4.5b). These results are in agreement with the previous report that the anti-adipogenesis activity of baicalein, the lipid, glycogen and carbohydrate spectral band of baicalein treated 3T3-L1 adipocytes is lower than untreated adipocyte (Dunkhunthod et al., 2017). On the other hand, the nucleic acid content of cells was shown to be reduced in OIE treatment, however, not significantly different compared to preadipocytes. The PCA analysis clearly showed the separation of cluster spectral of untreated-adipocyte from simvastatin, OIE, and preadipocyte along PC1 (41 %). Determination spectral similarity by UHCA dendrogram was consistent with our previous results that untreated adipocyte was obviously separate from the other groups. These findings support the cellular studies in chapter III, which suggest that the OIE has an impact on adipocyte. These may be because of the various compounds such as γ -sitosterol, benzeneethanol, 4-hydroxy- or tyrosol, and baicalein in OIE effect on biochemistry lead to inhibit adipocyte differentiation. Although FTIR provided the preliminary evidence regarding biochemical changing in a different stage of 3T3-L1 cells, more research is needed to clarify the mechanism of action of OIE.

4.6 References

- Balamurugan, R., Duraipandiyan, V. and Ignacimuthu, S. (2011). Antidiabetic activity of γ -sitosterol isolated from *Lippia nodiflora* L. in streptozotocin induced diabetic rats. **European Journal of Pharmacology**. 667(1): 410-418.
- Balamurugan, R., Stalin, A. and Ignacimuthu, S. (2012). Molecular docking of gamma-sitosterol with some targets related to diabetes. **European Journal of Medicinal Chemistry**. 47(1): 38-43.
- Bortolotto, J. W., Reis, C., Ferreira, A., Costa, S., Mottin, C. C., Souto, A. A. and Guaragna, R. M. (2005). Higher content of trans fatty acids in abdominal visceral fat of morbidly obese individuals undergoing bariatric surgery compared to non-obese subjects. **Obesity Surgery**. 15(9): 1265-1270.
- Britannica, T. E. o. E. (2019, 20/02/2019). Fatty acid. [On-line]. 16/06, 2019, Available: <https://www.britannica.com/science/fatty-acid>.
- Cha, M. H., Kim, I. C., Lee, B. H. and Yoon, Y. (2006). Baicalein inhibits adipocyte differentiation by enhancing COX-2 expression. **Journal of Medicinal Food**. 9(2): 145-153.
- Clayton, R. H. K. R. B. (2019, 20/02/2019). Steroids. [On-line]. 16, 2019, Available: <https://www.britannica.com/science/steroid>.
- Déléris, G. and Petibois, C. (2003). Applications of FT-IR spectrometry to plasma contents analysis and monitoring. **Vibrational Spectroscopy**. 32(1): 129-136.
- Dinda, B., SilSarma, I., Dinda, M. and Rudrapaul, P. (2015). *Oroxylum indicum* (L.) Kurz, an important Asian traditional medicine: from traditional uses to scientific data for its commercial exploitation. **Journal of Ethnopharmacology**. 161: 255-278.

- Dritsa, V., Pissaridi, K., Koutoulakis, E., Mamarelis, I., Kotoulas, C. and Anastassopoulou, J. (2014). An infrared spectroscopic study of aortic valve. a possible mechanism of calcification and the role of magnesium salts. **In Vivo (Athens, Greece)**. 28(1): 91-98.
- Dunkhunthod, B., Thumanu, K. and Eumkeb, G. (2017). Application of FTIR microspectroscopy for monitoring and discrimination of the anti-adipogenesis activity of baicalein in 3T3-L1 adipocytes. **Vibrational Spectroscopy**. 89: 92-101.
- Endrini, S., Rahmat, A., Ismail, P. and Taufiq-Yap, Y. (2015). Cytotoxic effect of γ -sitosterol from Kejibeling (*Strobilanthes crispus*) and its mechanism of action towards c-myc gene expression and apoptotic pathway. **Medical Journal of Indonesia**. 23(4): 203-208.
- Garip, S., Gozen, A. C. and Severcan, F. (2009). Use of fourier transform infrared spectroscopy for rapid comparative analysis of *Bacillus* and *Micrococcus* isolates. **Food Chemistry**. 113(4): 1301-1307.
- Gokhale, M., Gautam, D. and Khanna, A. (2017). A comparative GC-MS analysis of bioactive compounds in the different fractions of root extract of *Oroxylum indicum* (L.) Vent. **Analytical Chemistry Letters**. 7(3): 410-420.
- Jadhav. (2018). GC-MS screening of some bioactive compounds from methanolic extract of medicinally relevant wild edible plant parts. **Asian Journal of Pharmaceutical and Clinical Research**. 6 (1):136-139.
- Jing, L. J., Mohamed, M., Rahmat, A. and Bakar, M. F. A. (2010). Phytochemicals, antioxidant properties and anticancer investigations of the different parts of several gingers species (*Boesenbergia rotunda*, *Boesenbergia pulchella* var

- attenuata* and *Boesenbergia armeniaca*). **Journal of Medicinal Plants Research**. 4(1): 027-032.
- Joshi, S. V., Vyas, B. A., Shah, P. D., Shah, D. R., Shah, S. A. and Gandhi, T. R. (2011). Protective effect of aqueous extract of *Oroxylum indicum* Linn. (root bark) against DNBS-induced colitis in rats. **Indian Journal of Pharmacology**. 43(6): 656-661.
- Kohoude, M. J., Gbaguidi, F., Agbani, P., Ayedoun, M. A., Cazaux, S. and Bouajila, J. (2017). Chemical composition and biological activities of extracts and essential oil of *Boswellia dalzielii* leaves. **Pharmaceutical Biology**. 55(1): 33-42.
- Kucuk Baloglu, F., Garip, S., Heise, S., Brockmann, G. and Severcan, F. (2015). FTIR imaging of structural changes in visceral and subcutaneous adiposity and brown to white adipocyte transdifferentiation. **The Analyst**. 140(7): 2205-2214.
- Lee, O. H., Kwon, Y. I., Apostolidis, E., Shetty, K. and Kim, Y. C. (2011). Rhodiola-induced inhibition of adipogenesis involves antioxidant enzyme response associated with pentose phosphate pathway. **Phytotherapy Research**. 25(1): 106-115.
- Manoharan, R., Baraga, J. J., Rava, R. P., Dasari, R. R., Fitzmaurice, M. and Feld, M. S. (1993). Biochemical analysis and mapping of atherosclerotic human artery using FT-IR microspectroscopy. **Atherosclerosis**. 103(2): 181-193.
- Min, W., Wu, M., Fang, P., Yu, M., Shi, M., Zhang, Z. and Bo, P. (2018). Effect of baicalein on GLUT4 translocation in adipocytes of diet-induced obese mice. **Cellular Physiology and Biochemistry**. 50(2): 426-436.

- Movasaghi, Z., Rehman, S. and ur Rehman, D. I. (2008). Fourier transform infrared (FTIR) spectroscopy of biological tissues. **Applied Spectroscopy Reviews**. 43(2): 134-179.
- Muriana, F. J. G., Montserrat-de la Paz, S., Lucas, R., Bermudez, B., Jaramillo, S., Morales, J. C., Abia, R. and Lopez, S. (2017). Tyrosol and its metabolites as antioxidative and anti-inflammatory molecules in human endothelial cells. **Food and Function**. 8(8): 2905-2914.
- Palasuwan, A., Soogarun, S., Lertlum, T., Pradniwat, P. and Wiwanitkit, V. (2005). Inhibition of heinz body induction in an in vitro model and total antioxidant activity of medicinal Thai plants. **Asian Pacific Journal of Cancer Prevention**. 6(4): 458-463.
- Pijanka, J. K., Kumar, D., Dale, T., Yousef, I., Parkes, G., Untereiner, V., Yang, Y., Dumas, P., Collins, D., Manfait, M., Sockalingum, G. D., Forsyth, N. R. and Sulé-Suso, J. (2010). Vibrational spectroscopy differentiates between multipotent and pluripotent stem cells. **The Analyst**. 135(12): 3126-3132.
- Rasadah, M. A. (2001). *Oroxylum indicum* (L.) Kurz.In. Leiden, The Netherlands, Backhuys.
- Rauf, A., Jan, M., Rehman, W. and Muhammad, N. (2013). Phytochemical, phytotoxic and antioxidant profile of *Caralluma tuberculata* N. E. Brown. **Wudpecker Journal of Pharmacy and Pharmacology**. 2(2): 21-25.
- Rojsanga, P., Bunsupa, S., Brantner, A. H. and Sithisarn, P. (2017). Comparative phytochemical profiling and in vitro antioxidant activity of extracts from raw materials, tissue-cultured plants, and callus of *Oroxylum indicum* (L.) Vent. **Evidence-Based Complementary and Alternative Medicine**. 2017.

- Roy, M. K., Nakahara, K., Na, T. V., Trakoontivakorn, G., Takenaka, M., Isobe, S. and Tsushida, T. (2007). Baicalein, a flavonoid extracted from a methanolic extract of *Oroxylum indicum* inhibits proliferation of a cancer cell line in vitro via induction of apoptosis. **Die Pharmazie**. 62(2): 149-153.
- Seo, M. J., Choi, H. S., Jeon, H. J., Woo, M. S. and Lee, B. Y. (2014). Baicalein inhibits lipid accumulation by regulating early adipogenesis and m-TOR signaling. **Food and Chemical Toxicology**. 67: 57-64.
- Singh, J. and Kakkar, P. (2013). Modulation of liver function, antioxidant responses, insulin resistance and glucose transport by *Oroxylum indicum* stem bark in STZ induced diabetic rats. **Food and Chemical Toxicology**. 62: 722-731.
- Singh, J. and Kakkar, P. (2014). Oroxylin A, a constituent of *Oroxylum indicum* inhibits adipogenesis and induces apoptosis in 3T3-L1 cells. **Phytomedicine**. 21(12): 1733-1741.
- Sirikhansaeng, P., Tanee, T., Sudmoon, R. and Chaveerach, A. (2017). Major phytochemical as γ -sitosterol disclosing and toxicity testing in *Lagerstroemia* species. **Evidence-Based Complementary and Alternative Medicine**. 2017.
- Speight, J. G. (2017). Chapter 2 - Organic chemistry. In: Speight, J. G. (Ed.). **Environmental Organic Chemistry for Engineers**. Butterworth-Heinemann, pp. 43-86
- Sundarraj, S., Thangam, R., Sreevani, V., Kaveri, K., Gunasekaran, P., Achiraman, S. and Kannan, S. (2012). γ -Sitosterol from *Acacia nilotica* L. induces G2/M cell cycle arrest and apoptosis through c-Myc suppression in MCF-7 and A549 cells. **Journal of Ethnopharmacology**. 141(3): 803-809.

- Thomford, N. E., Senthebane, D. A., Rowe, A., Munro, D., Seele, P., Maroyi, A. and Dzobo, K. (2018). Natural products for drug discovery in the 21st century: innovations for novel drug discovery. **International Journal of Molecular Sciences**. 19(6).
- Tran, T. V., Malainer, C., Schwaiger, S., Hung, T., Atanasov, A. G., Heiss, E. H., Dirsch, V. M. and Stuppner, H. (2015). Screening of Vietnamese medicinal plants for NF-kappaB signaling inhibitors: assessing the activity of flavonoids from the stem bark of *Oroxylum indicum*. **Journal of Ethnopharmacology**. 159: 36-42.
- Uddin, K., Sayeed, A., Islam, A., Rahman, A. A., Ali, A., Khan, G. and Sadik, M. G. (2003). Purification, characterization and cytotoxic activity of two flavonoids from *Oroxylum indicum* Vent. (Bignoniaceae). **Asian Journal of Plant Sciences**. 2(6): 515-518.
- Vongsvivut, J., Heraud, P., Gupta, A., Puri, M., McNaughton, D. and Barrow, C. J. (2013). FTIR microspectroscopy for rapid screening and monitoring of polyunsaturated fatty acid production in commercially valuable marine yeasts and protists. **The Analyst**. 138(20): 6016-6031.
- Yadav, R. and Agarwala, M. (2011). Phytochemical analysis of some medicinal plants. **Journal of Phytology**. 3(12): 10-114.

CHAPTER V

EFFECT OF *O. INDICUM* EXTRACT ON ADIPONECTIN SECRETION, LIPASES ACTIVITY, AND MOLECULAR MECHANISM ON ANTIADIPOGENESIS

5.1 Abstract

O. indicum is regarded as traditional food with medicinal properties medicine and is used widely throughout Asia. It has been previously demonstrated that *O. indicum* extract (OIE) was able to suppress the differentiation of 3T3-L1 preadipocytes to adipocytes. However, the mechanism underlying the anti-adipogenesis of this plant has not been fully investigated. The present study was aimed to explore the impact of OIE at 50 to 200 µg/mL on the molecular mechanism involved in the anti-adipogenic activity in 3T3-L1 cells, and the impact of the OIE on lipase activity was also investigated. The morphology and biochemistry of the cells at day 12 were investigated and compared to the relevant controls. Adiponectin was measured using enzyme-linked immunosorbent assay (ELISA). The mRNA expression of peroxisome proliferator-activated receptor-gamma 2 (PPAR γ 2), sterol regulatory element-binding proteins 1c (SREBP-1c), fatty acid synthetase (FAS), glucose transporter (GLUT4), and leptin in adipocytes were determined by real-time PCR. The results demonstrated that the OIE at 200 µg/mL exhibited strongest suppression on intracellular lipid accumulation. The levels of adiponectin were dramatically increased in the untreated adipocytes, whereas significantly decreased in

the 200 µg/mL OIE-treated adipocytes ($P < 0.05$). Expression of the mRNAs revealed that OIE-treated adipocytes at 200 µg/mL significantly inhibited the expression of PPAR γ 2, SREBP-1c, and lowered the expression level of GLUT4, FAS, and leptin compared to the control ($P < 0.05$). The OIE also demonstrated a dose-dependent inhibitory effect upon lipase activity compared to control ($P < 0.05$). These findings suggest that OIE inhibits adipocyte differentiation along with the down-regulation of PPAR γ 2, SREBP-1c, and GLUT4 leading to the decrease in the expression of FAS and adipokine (leptin and adiponectin). Thus, OIE might be developed for hyperlipidemia and obesity prevention.

5.2 Introduction

Obesity is a major health problem and is associated with increasing the risk of cardiovascular disease, certain cancers, and type 2 diabetes (Goran et al., 2003). The prevalence of obesity is a global problem, with 13% of the adult population reported as being clinically obese (WHO, 2019). Adipogenesis can be described as a highly regulated process in which stem cells are converted to mature adipocytes through two processes, commitment, and differentiation (Church et al., 2012). An increase in the size and number of adipocytes is thought to be important risk factors for the future development of obesity (Landgraf et al., 2015; Parlee et al., 2014). Moreover, during the development of adipocyte and *de novo* lipogenesis, various adipokines and transcriptional factors appear to be important in this circumstance (Tontonoz et al., 1994). The current strategies for the prevention and treatment of obesity focus on increasing physical activity, reducing calorific intake and pharmacological treatments such as orlistat (Chan and Woo, 2010). Another approach would be to limit

adipogenesis by inhibiting both the proliferation and differentiation of adipocytes. Plant extracts have been screened to identify compounds that can suppress adipogenesis (Jang et al., 2017). One such plant extract that has attracted much interest is *O. indicum*. *O. indicum* is a plant that is found throughout Asian countries. It has been used as traditional medicine for many years (Siddiqui et al., 2012). The previous study revealed that fruit of *O. indicum* extract (OIE) at 200 µg/mL exhibited anti-adipogenesis property and reduced intracellular lipid level in the adipocyte. Furthermore, OIE demonstrated a non-toxic effect on cell viability up to the dose of 200 µg/mL (Hengpratom et al., 2018). Also, an animal study suggested that oral intake of 200 mg/kg body weight of the OIE for 28 days was safe in diabetic and normal rats (Kaldate et al., 2011; Singh and Kakkar, 2013).

Adiponectin is a hormone secreted from adipocytes. Previous studies have found that the importance of adiponectin is involved in the proliferation and differentiation of 3T3-L1 pre-adipocytes (Fu et al., 2005) and human pre-adipocytes (do Carmo Avides et al., 2008). As a result, it is raising C/EBP α and PPAR γ gene expression during adipogenesis, and consequently increasing lipid accumulation and glucose transportation in adipocytes. Thus, controlling of adiponectin could be a potential target to inhibit adipogenesis. According to the previous research finding, the OIE exhibited the anti-adipogenesis effect on 3T3-L1 adipocyte and caused a changing of some biochemical component of the cells measured by FTIR (Hengpratom et al., 2018). However, there is no report on whether the OIE effects on adipokines or is involved in transcriptional regulation. Thus, the aim of the present study was to investigate the potential function of the OIE on adiponectin secretion and explored the molecular mechanism underlying anti-adipogenesis effects of the OIE in 3T3-L1 cells.

5.3 Materials and Methods

5.3.1 Chemicals and reagents

Mouse anti-mouse adiponectin antibody was purchased from Abcam (Cambridge, MA, USA), HRP-conjugated goat anti-mouse IgG was obtained from Santa Cruz (CA, USA). RNA extraction and purification kit were purchased from Promega (Madison, WI, USA). Lipase from porcine pancreas type 2, 4-Nitrophenyl dodecanoate (pNP), and orlistat were purchased from Sigma-Aldrich (St. Louis, USA). Protease inhibitor cocktail was obtained from Roche (Mannheim, Germany).

5.3.2 Cell Culture and Treatment

Cell culture was carried out as a previous study (Dunkhunthod et al., 2017). Shortly, 3T3-L1 pre-adipocytes were cultured in Dulbecco's Modified Eagle's medium (DMEM) containing 10 % calf bovine serum (CBS) (GIBCO, Grand Island, NY, USA). At two days after confluence (day 0), the cells were stimulated to differentiate with DMEM containing 10 % fetal bovine serum (FBS) (Hyclone, Logan, UT, USA), 1.0 μ M of dexamethasone (G Bioscience, St. Louis, MO, USA), 0.5 mM of isobutylmethylxanthine and 1.0 μ g/mL of insulin for two days. From day 4 onwards, the differentiation media were replaced by 10 % FBS/DMEM media containing 1.0 μ g/mL of insulin. These media were changed every two days until the cells were harvested. All media contained 100 μ g/mL of streptomycin and 100 U/mL of penicillin (GIBCO). Cells were maintained at 37 °C in a 95 % humidified with 5 % of CO₂ atmosphere.

For the treatment of pre-adipocytes, the cells were seeded in a 6-well plate at the density of 1.5×10^5 cells/well. The cells were allowed to adhere to the plate for 48 h and were then divided into 8 groups; 1) non-differentiated cells (pre-adipocytes); 2)

untreated differentiated cells (untreated adipocytes, nontreated adipocytes, control); 3) differentiated cells treated with 0.1 % DMSO (vehicle control, DMSO-treated adipocytes); 4) differentiated cells treated with 1.67 $\mu\text{g}/\text{mL}$ simvastatin (positive control, SIM-treated adipocytes); 5-8) differentiated cells treated with 50, 100, 150, and 200 $\mu\text{g}/\text{mL}$ OIE (OIE-treated adipocytes), respectively. On day 12 after the cells were differentiated (gauged by visible lipid droplet > 90 % of the control group), the media and the cells were collected for RNA extraction, protein quantification, and immunocytochemistry detection. Each experiment was repeated three times.

5.3.3 Protein Extraction and Immunoblot Analysis

The expression of adiponectin protein in control and OIE-treated cells was determined by Western immunoblotting. The cells were washed 3 times with cold 0.1 M phosphate buffer saline (PBS) and were lysed in cold lysis buffer (10 mM Tris-HCl, 150 mM NaCl, 0.5 % Triton X-100, 1 mM EDTA, and 100 mM PMSF, pH 7.2) containing protease inhibitor cocktail (Roche, Mannheim, Germany). The protein concentrations were measured using a bovine serum albumin (BSA) protein assay kit following the company description (Thermo Scientific, Rockford, Winnebago, USA). The lysates (20 μg , each) were subjected to SDS-PAGE on 15 % polyacrylamide gel. After electrophoresis, the proteins were transferred to nitrocellulose membrane (GE Healthcare, Piscataway, NJ, USA). The membranes were then blocked with 5 % skimmed milk in 0.1 M PBS contains 0.1 % Tween-20 (PBST) for 1 h at room temperature, followed by washing with PBST. The membranes were subsequently incubated with mouse anti-mouse adiponectin antibody (Abcam, Cambridge, MA, USA) (1:1000 in PBS), overnight at 4 °C. Negative controls were performed by omitting the primary antibody or using the pre-absorbed one. After extensive washing,

the membranes were incubated with HRP-conjugated goat anti-mouse IgG (Santa Cruz, CA, USA) (1:2000 in PBS) for 1 h at room temperature, followed by washing with PBST. The antigen-antibody complex was visualized by adding a DAB kit (Vector Laboratories, Burlingame, CA, USA). Analysis of intensities of the adiponectin protein bands was quantified using ImageJ software under the same pixel area. The data were normalized using β -actin as an internal control. The experiments were repeated using cells from 3 different individuals.

5.3.4 Determination of Adiponectin Secreted From 3T3-L1 Cells by ELISA

The level of adiponectin secreted from 3T3-L1 adipocytes was performed as previously described with some modifications (Ngermsoungnern and Ngermsoungnern, 2016). At day 12, the culture media were collected from control and OIE-treated groups and centrifuged at 10,000 x g for 10 min at 4 °C. Supernatants containing antigen were collected. Subsequently, 100 μ L of 100 μ g/mL of the antigen and human adiponectin peptide (Abcam) which served as a standard were diluted with ELISA coating buffer, coated onto the ELISA plates, and incubated overnight at 4 °C. The plates were blocked for non-specific binding with 0.25 % BSA in 0.01 M PBS, pH 7.2 for 1 h at 37 °C and subsequently incubated with mouse anti-mouse adiponectin antibody (1:3000 in PBS). Negative controls were performed by omitting the primary antibody or using the pre-absorbed one. The plates were washed twice with PBST and then incubated with HRP-conjugated goat anti-mouse IgG (1:3000 in PBS) for 1 h at 37 °C, followed by washing. Finally, the tetramethylbenzidine substrate (Sigma-Aldrich, St. Louis, MO, USA) was added for developing a color reaction. The reactions were stopped by adding 1 N H₂SO₄, and the color was then read spectrophotometrically at 450 nm. The sensitivity

of the assay was 0.1 ng/mL. The intra-assay coefficient of variation was 2.4 %, and the inter-assay coefficient of variation was 5.9 %.

5.3.5 Immunocytochemistry for Adiponectin

At day 12, 3T3-L1 pre-adipocytes and adipocytes were collected, washed with cold PBS, fixed for 15 min in cold acetone, and washed with PBST. After blocking with 4 % of BSA for 1 h at room temperature, the cells were washed and incubated with anti-adiponectin antibody (1:200 in PBS), overnight at 4 °C. After extensive washing, Alexa 488-conjugated goat anti-mouse IgG (1:500) was applied to the samples and incubated for 1 h at room temperature. After washing thoroughly with PBS, the cells were double-stained with Hoechst 33342 (nucleus stain) (1:3000) for 10 min and washed twice. Finally, the cells were visualized using fluorescence microscopy.

5.3.6 RNA Extraction and mRNA Expression Analysis

The RNA extraction and purification were performed by the RNA cell miniprep system following the manufacturer protocol (Promega, Madison, WI, USA). The culture medium was removed from cells, and the cells were washed twice with 0.1 M PBS. After that, 250 µL of lysis buffer was added to each well. The cells were transferred to sterile microcentrifuge tubes, added with 85 µL of 100 % isopropanol, and then mixed for 5 sec. The cells were subsequently transferred to a ReliaPrep™ Minicolumn and centrifuged at 12,000 rpm for 2 min. The liquid in the collection tubes was discarded, followed by an adding of 500 µL RNA wash solution. The tubes were then centrifuged at 12,000 rpm for 2 min at 25 °C. Freshly prepared DNase I (30 µL) was then applied and incubated for 15 min at room temperature. Column wash solution (200 µL) was then added to the ReliaPrep™ Minicolumn and centrifuged at 12,000 rpm for 2 min, followed by adding of 500 µL RNA wash solution and centrifuged at 12,000

rpm for 2 min. The columns were then placed into new tubes, RNA wash solution (300 μ L) was added and then centrifuged at 12,000 rpm for 2 min. The columns were placed into the collection tubes, followed by an adding of 15 μ L nuclease-free water, and centrifuged at 12,000 rpm for 2 min. The purified total RNA was calculated from the concentration obtained at 260 nm using a NanoDrop.

The expression of adiponectin gene levels was conducted by quantitative real-time PCR (RT-PCR). RNA-directed SYBR Green real-time PCR master mix was used in the PCR reaction according to the manufacturer's instructions (Toyobo, Osaka, Japan). Total RNA at 50 ng was prepared for the PCR reaction, then subjected to 45 cycles of amplification (denaturation at 95 °C for 5 sec, annealing at 60 °C for 10 sec, and extension at 74 °C for 15 sec). Primers used for amplifying PPAR γ 2 were 5'-TgT CTC ATA ATg CCA TCA ggT TTg-3' (Forward) and 5'-gAT AAC gAA Tgg TgA TTT gTC TgT-3' (Reverse), for amplifying SREBP-1c were 5'-CTg TTg gTg CTC gTC TCC T-3' (Forward) and 5'-TTg CgA TgC CTC Cag AAg TA-3' (Reverse), and for amplifying FAS were 5'-ATC CTg gCT gAC gAA gAC TC-3' (Forward) and 5'-TgC TgC TgA ggT Tgg AgA g-3' (Reverse). In addition, primers used for amplification of GLUT4 were 5'-ggg TCC TTA CgT CTT CCT TCT-3' (Forward) and 5'-CCT CTg gTT TCA ggC ACT TT-3' (Reverse), of leptin were 5'-ggA TCA ggT TTT gTg gTg CT-3' (Forward) and 5'-TTg Tgg CCC ATA AAg TCC TC-3' (Reverse), and of β -actin which was used as the reference gene were 5'-ACA TCT gCT ggA Agg Tgg AC-3' (Forward) and 5'-ggT ACC ACC ATg TAC CCA gg-3' (Reverse). All gene expression results were expressed as fold changes of threshold cycle (Ct) value relative to controls using the $2^{-\Delta\Delta C_t}$ methods.

5.3.7 Lipase activity

Measurement of lipase activity was performed as previously described with slight modifications (Guo et al., 2016). In brief, lipase of porcine pancreas type 2 was dissolved in distilled water at 5 mg/mL, then the solution was centrifuged at 10,000 xg for 5 min, and the supernatant was used. pNP laurate was applied as a reaction substrate, and 100 mM of Tris buffer pH 8.2 was employed in reaction buffer. 0.1 % (w/v) of pNP laurate stock was dissolved in 5 mM of sodium acetate (pH 5.0) containing 1% Triton X-100, and the solution was heated to 80 °C and cooled to room temperature. The reaction buffer was added to the well then lipase and OIE were added respectively. The reaction was initiated by adding the substrate solution. The mixtures were incubated at 37 °C and measured at 409 nm using a microplate spectrophotometer. Orlistat at 12.5 to 100 µg/mL was used as a positive control. The inhibition rate (%) was described as $(1 - (\text{OD}_{\text{sample}} - \text{OD}_{\text{sample blank}}) / \text{OD}_{\text{control}}) \times 100$.

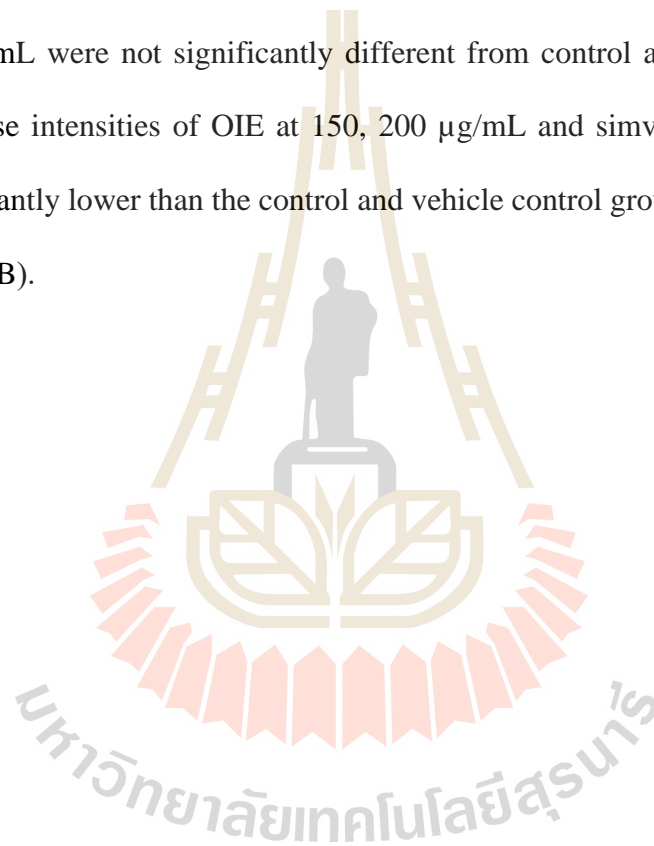
5.3.8 Statistical analysis

All the data were expressed as the mean \pm standard deviation of the mean (Mean \pm SD). The difference values between adiponectin protein levels, the number of adiponectin secretions, and gene expressions compared between treatment and control groups were analyzed using one-way analysis of variance (ANOVA) with a Turkey's HSD post-hoc test (SPSS v 23). Values were considered statistically significant when $P < 0.05$, and data were representative of three independent experiments ($n = 3$). Most of the experiments were performed in triplicate.

5.4 Results

5.4.1 Effect of OIE on adiponectin protein expression in 3T3-L1 cells

Adiponectin is known as an insulin-sensitizing hormone which produced and secreted from white adipocytes. On day 12, the cells were harvested, and the lysates were subjected to Western immunoblotting for adiponectin expression. Adiponectin expressed in 3T3-L1 preadipocytes and adipocytes were identified at 30 kDa. A recombinant human adiponectin protein, which served as the positive control, showed the same molecular weight. The intensities of adiponectin protein bands of OIE at 50 and 100 $\mu\text{g/mL}$ were not significantly different from control adipocytes ($P > 0.05$), although these intensities of OIE at 150, 200 $\mu\text{g/mL}$ and simvastatin-treated groups were significantly lower than the control and vehicle control groups ($P < 0.05$) (Figure 5.1A and 5.1B).



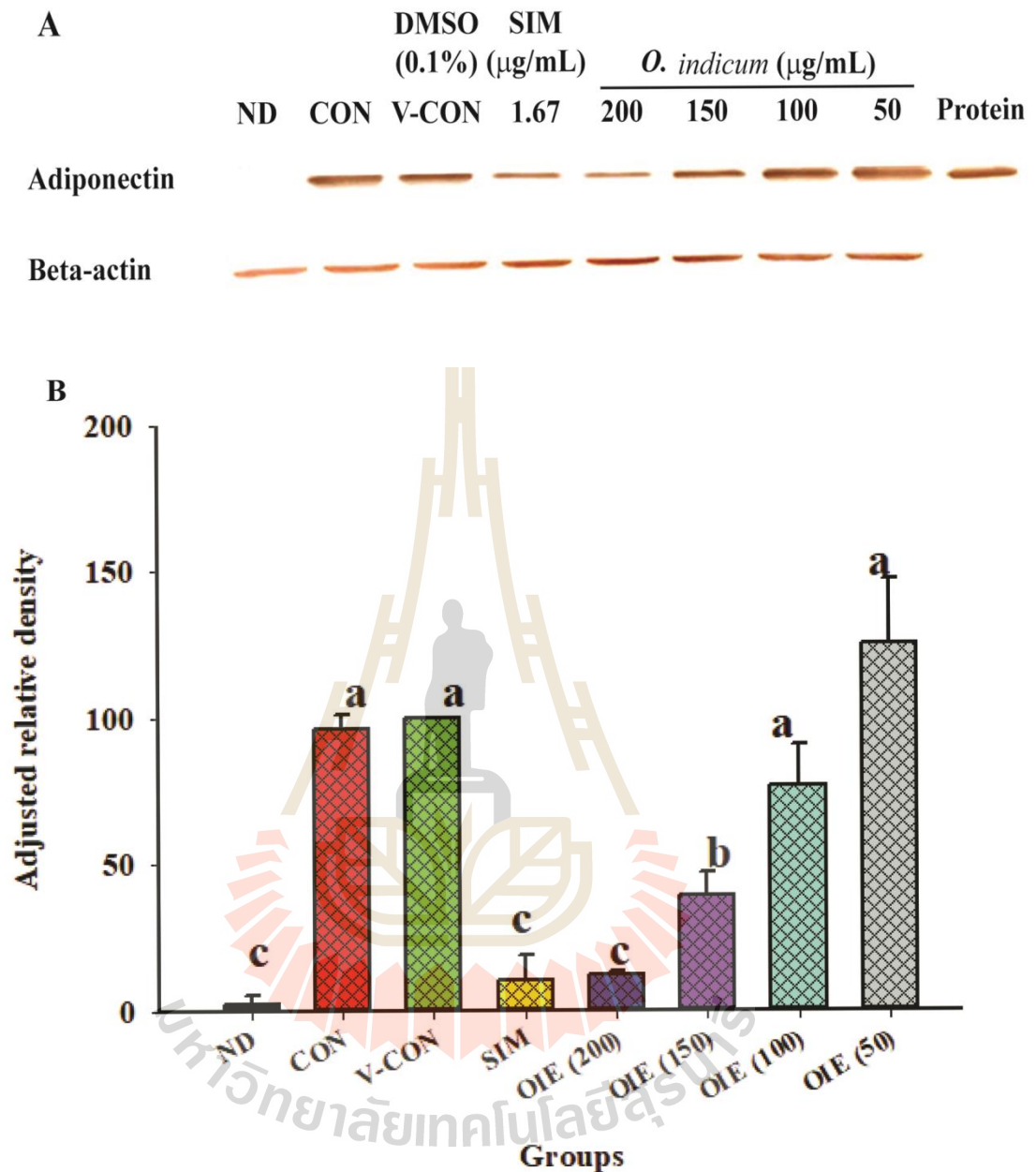
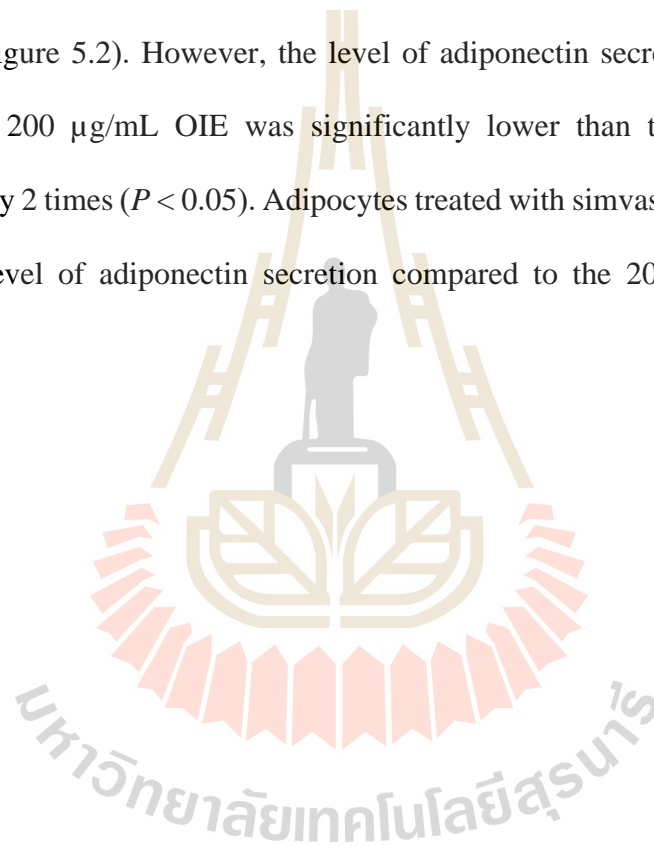


Figure 5.1 The effect of OIE on adiponectin protein expression. (A) The images of adiponectin protein expression. ND = Non-differentiated cells (pre-adipocytes), CON = Untreated adipocytes, V-CON = Differentiated cells with 0.1 % DMSO (Vehicle control), OIE (200) = OIE at 200 $\mu\text{g/mL}$, OIE (150) = OIE at 150 $\mu\text{g/mL}$, OIE (100) = OIE at 100 $\mu\text{g/mL}$, OIE (50) = OIE at 50 $\mu\text{g/mL}$, SIM = Simvastatin at 1.67 $\mu\text{g/mL}$. (B) Comparison of the intensity of adiponectin protein expression among 8 groups. All

values are presented as the mean \pm SD for three replicated. Means with the different superscript are significantly different from each other (Tukey's HSD test, $P < 0.05$).

5.4.2 Effect of OIE on the secretion of adiponectin

On day 12, the media were collected for the measuring of the adiponectin level. The level of adiponectin secretion was significantly elevated in control, vehicle control, 50, 100, and 150 $\mu\text{g/mL}$ OIE-treated group compared to the non-differentiated group ($P < 0.05$, Figure 5.2). However, the level of adiponectin secretion from adipocytes treated with 200 $\mu\text{g/mL}$ OIE was significantly lower than the control group for approximately 2 times ($P < 0.05$). Adipocytes treated with simvastatin showed a similar decreasing level of adiponectin secretion compared to the 200 $\mu\text{g/mL}$ OIE-treated group.



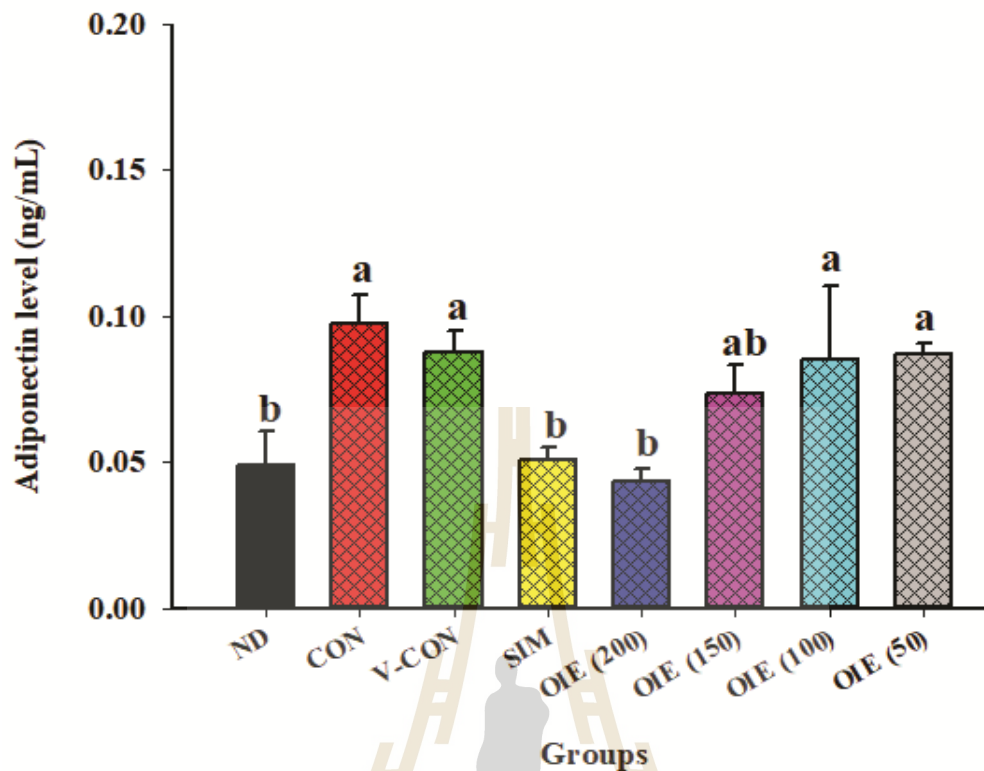


Figure 5.2 The effect of OIE on the secretion of adiponectin during differentiation. ND = Non-differentiated cells (pre-adipocytes); CON = Untreated adipocytes; V-CON = Differentiated cells with 0.1% DMSO (vehicle control), OIE (200) = OIE at 200 $\mu\text{g/mL}$, OIE (150) = OIE at 150 $\mu\text{g/mL}$, OIE (100) = OIE at 100 $\mu\text{g/mL}$, OIE (50) = OIE at 50 $\mu\text{g/mL}$, SIM = Simvastatin at 1.67 $\mu\text{g/mL}$. All values are presented as the mean \pm SD for three replicated. Means with the different superscript are significantly different from each other (Tukey's HSD test, $P < 0.05$).

5.4.3 Effect of OIE on adiponectin staining in 3T3-L1 cells

Adiponectin was found to be localized in the cytoplasm of the 3T3-L1 cells (Figure 5.3). There was a few localization of the adiponectin in the non-differentiated cells (Figure 5.3B). The adiponectin was detected in the control (Figure 5.3C) and vehicle control groups (Figure 5.3D). In contrast, when the cells were treated with 50

to 200 $\mu\text{g}/\text{mL}$ OIE during differentiation (Figure 5.3E-5H), the OIE at 200 $\mu\text{g}/\text{mL}$ caused the lowest localization of the adiponectin in the cells (Figure 5.3E).

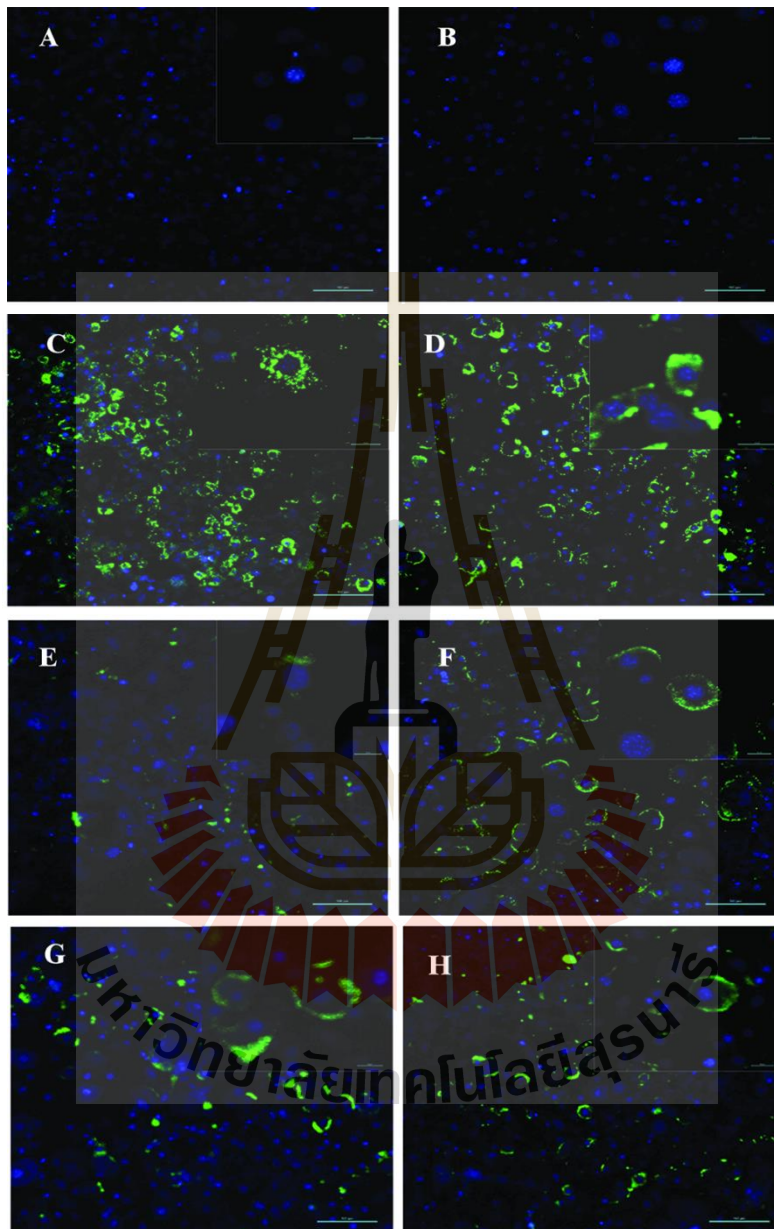


Figure 5.3 The effect of OIE on the localization of the adiponectin in the 3T3-L1 cells. The adiponectin is stained in green color, and nuclei are stained in blue color. (A) Negative control shows no staining of the adiponectin in the cells, (B) A few staining of the adiponectin in the Non-differentiated cells (Pre-adipocytes), (C) Staining of the adiponectin is observed in the untreated differentiated cells, (D) Differentiated cells

treated with 0.1 % DMSO (vehicle control), Differentiated cells treated with OIE at **(E)** 200 $\mu\text{g}/\text{mL}$, **(F)** 150 $\mu\text{g}/\text{mL}$, **(G)** 100 $\mu\text{g}/\text{mL}$, **(H)** 50 $\mu\text{g}/\text{mL}$. Scale bar: 100 μm .

5.4.4 Effect of OIE on mRNA expression in 3T3-L1 cells

To clarify the mechanism underlying anti-adipogenesis of the OIE, expression levels of mRNA of PPAR γ 2, SREBP-1C, FAS, GLUT4, and LEP were studied. The vehicle control group exhibited significantly increased in PPAR γ 2, SREBP-1C mRNA expression by 10 folds and 5 folds, respectively ($P < 0.05$) compared to the non-differentiated group. A similar pattern was observed in FAS, GLUT4, and LEP by more than 10 times higher in the vehicle control group compared to the non-differentiated group (Figure 5.4). The mRNA expression level in the cells treated with 200 $\mu\text{g}/\text{mL}$ OIE was significantly decreased approximately 1/2 times compared to the vehicle control group ($P < 0.05$). These results suggest that OIE can inhibit adipogenesis via inhibition of the changing of mRNA level.

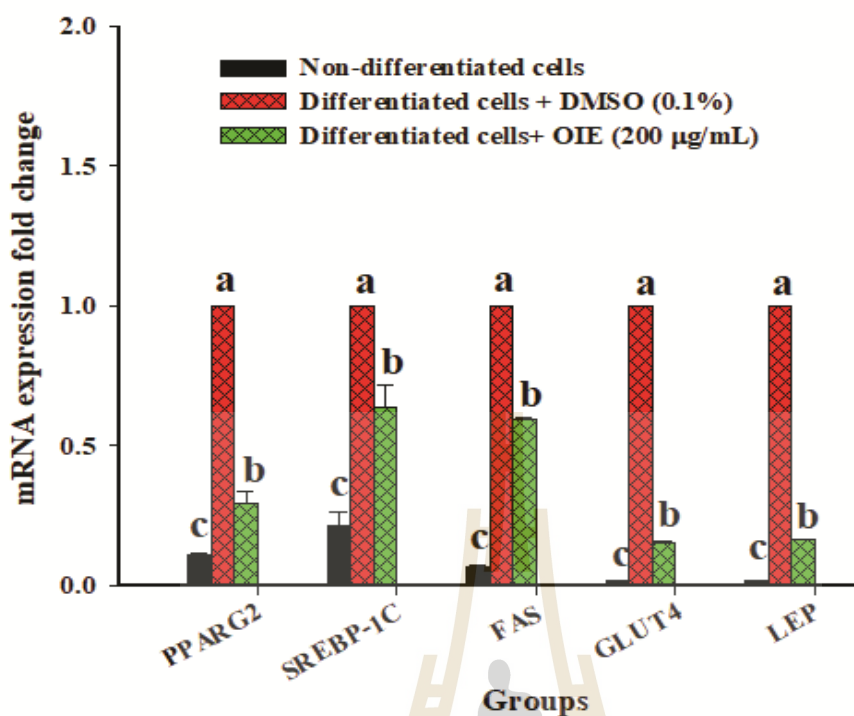


Figure 5.4 The effect of OIE on mRNA expression of PPAR γ 2 (PPAR G2), SREBP-1c, FAS, GLUT4, and LEP in 3T3-L1 cells. The expression values were normalized to the β -actin. The results are presented as the mean \pm SD for three triplicated. Means with the different superscript are significantly different from each other (Tukey's HSD test, $P < 0.05$).

5.4.5 Effect of OIE on pancreatic lipase activity

Pancreatic lipase is an enzyme responsible for the hydrolysis of lipid into free fatty acid and glycerol. The OIE concentrations between 100 to 1250 $\mu\text{g/mL}$ displayed significantly higher inhibitory lipase activity than those of the controls ($P < 0.05$) (Figure 5.5). Moreover, the IC_{50} of OIE for the inhibition of pancreatic lipase was $1062.04 \pm 32.21 \mu\text{g/mL}$. While the inhibitory effect of the positive control orlistat at 12.5 to 100 $\mu\text{g/mL}$, demonstrated an IC_{50} at $38.78 \pm 9.55 \mu\text{g/mL}$. Under those circumstances, the potential strength of orlistat on lipase activity inhibition is approximately 27 times greater than the OIE. These results suggested that the inhibitory

implications of the OIE on pancreatic lipase activity increased in a dose-dependent manner.

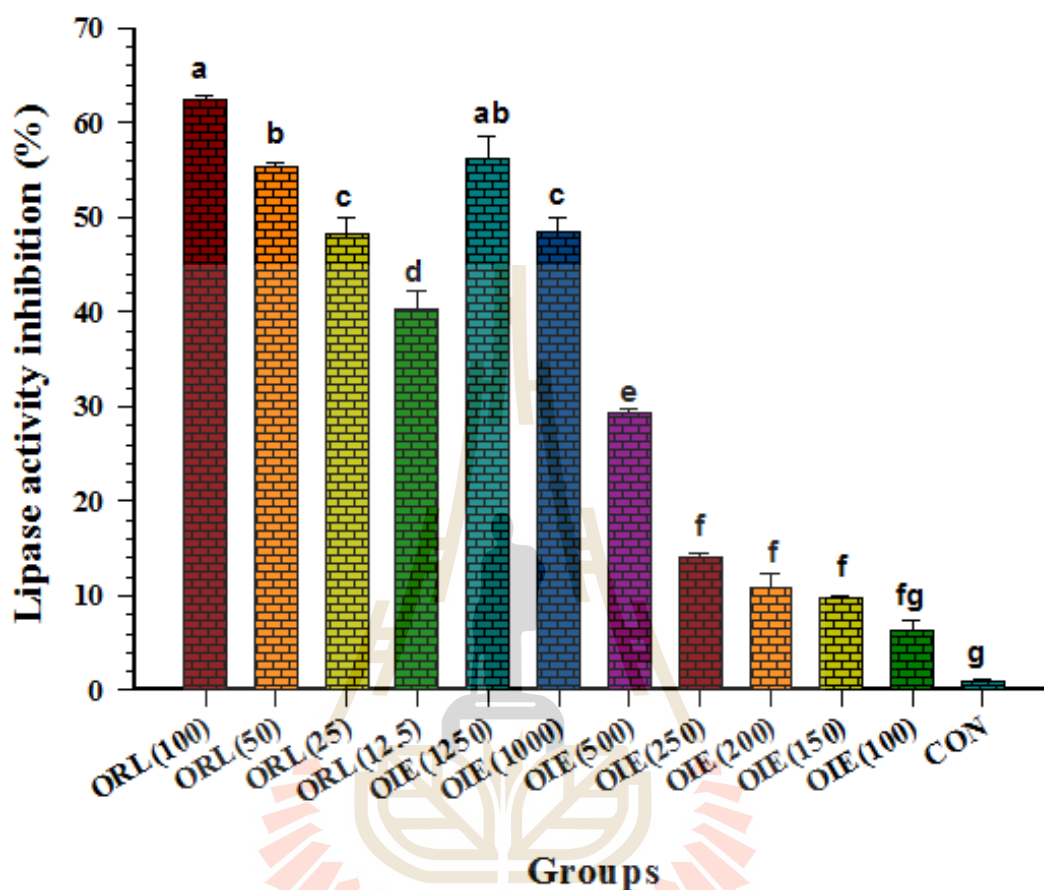


Figure 5.5 Inhibitory effects of OIE (%) at various concentrations on lipase activity. CON = Control; OIE (100) = OIE at 100 $\mu\text{g}/\text{mL}$; ORL (12.5) = Orlistat at 12.5 $\mu\text{g}/\text{mL}$. Orlistat was used as a positive control. Values are represented as Means \pm SD ($n = 3$). Significant differences are observed (Tukey's HSD test, $P < 0.05$) and are represented in the Figure with letters from a to g. Bars annotated with the different letter are significantly different.

5.5 Discussion and conclusion

This study found that the OIE inhibited the differentiation of pre-adipocytes, and retained the fibroblastic morphology almost the same as those of pre-adipocyte stage. While the non-treated adipocytes and vehicle control showed numerous lipid in their cytoplasm. In addition, the media of non-treated adipocytes or vehicle control was changed to yellow color as this would indicate a drop in PH. However, no significant change in the color of the media was observed in pre-adipocytes and adipocytes treated with simvastatin or the OIE. The possible explanation is that adipocytes may have an active metabolic stage and secrete numerous factors of adipokine.

At the molecular level, elevation in protein localization, secretion and mRNA expression level of adiponectin was observed in control and vehicle control adipocytes, which was related to adipogenesis and cellular lipid accumulation. These findings are consistent with Ikeda et al., that the mRNA expression of adiponectin in 3T3-L1 cells increases throughout the maturation process of adipocytes (Ikeda et al., 2011). Apart from this, Fu et al. reported that adiponectin caused the proliferation and differentiation of pre-adipocytes to adipocytes through promoting prolonged transcriptional factors in the process of cell differentiation (Fu et al., 2005). These findings lead us to believe that these genes can be used as adipocyte maturation markers and can help to maintain the size of the adipocytes. However, adipocytes treated with 200 $\mu\text{g}/\text{mL}$ of OIE was significantly decreased in localization and secretion of the adiponectin protein and mRNA expression compared to the control adipocytes (Seo et al., 2014). The possible explanation can be that the OIE delay the progression of cell proliferation and cause adiponectin level lower than the control group. In particular, it was shown that 12.5 μM of baicalein, a flavone presented in the fruit-OIE, was able to block the G0/G1 phase of

the 3T3-L1 cell cycle induction to adipocytes at 24 h. Moreover, numerous studies revealed that the inhibitory effect of the crude extract or their compounds on the differentiation of adipocytes caused by the inhibition of the cell cycle (Kim et al., 2011; Tang et al., 2003).

In vitro studies suggested that adipogenesis occurred in 2 major steps, including the recruitment and proliferation of preadipocytes followed by their subsequent differentiation into mature fat cells. Differentiation was accompanied by the sequential expression of key transcription factors that direct the adipogenic program. Peroxisome proliferator-activated receptor-gamma 2 (PPAR γ 2) is playing a crucial role in the differentiation program (Gregoire, 2001). The mechanism of PPAR γ was initiated by ligands, which could be a hormone, a free fatty acid, fatty acid, derivative or synthetic drugs which bound to the nuclear receptor. The PPAR γ then formed heterodimers with the retinoid X receptor (RXR), thereby increasing of adipogenic genes and protein expression, including leptin and GLUT4 (Grommes et al., 2004). SREBP-1c is a transcriptional factor mediating the expression levels of genes involved in fatty acid metabolism and *de novo* lipogenesis (Matsuda et al., 2001). An *in vitro* study found that overexpression of SREBP-1c in cultured preadipocytes activated genes involved in fatty acid and triglyceride syntheses such as Acetyl CoA Carboxylase (ACC) and fatty acid synthase (FAS) (Horton et al., 2003). This research selected the most effective concentration of the OIE for studying the mRNA expression of adipocyte gene. These results showed that at 200 μ g/mL of OIE significantly prevented up-regulation of PPAR γ 2 and SREBP-1c genes compared to the control mature adipocytes. It was noteworthy that PPAR γ was essential for normal adipocyte differentiation, and PPAR γ knockdown largely prevented the adipogenic differentiation of 3T3-L1 cells

(Liao et al., 2007). Thus, OIE could mediate lipogenesis either via the delayed of cell cycle progression or modulation of PPAR γ and SREBP-1c genes. This study also detected the expression of GLUT4, which facilitates glucose transportation into the cells, and FAS, a product of *de novo* synthesis, which is the important source for the intracellular triglyceride synthesis. The results indicated that adipocytes treated with the OIE significantly inhibited an increase in both GLUT4 and FAS expression along with PPAR γ , SREBP-1c, and leptin genes compared to the untreated adipocytes.

To further elucidate the biochemical potential of OIE, *in vitro* pancreatic lipase assay was performed as part of this study. Pancreatic lipase is an enzyme responsible for breakdown triglycerides into glycerol and fatty acid in the gastrointestinal tract. When lipase activity is inhibited, triacylglycerol cannot cross the intestinal brush border membrane leading to a decrease in the uptake of lipids into the human body. Lipase became a target for research groups attempting to prevent obesity or metabolic syndrome (Dunkhunthod et al., 2017; Guo et al., 2016). Orlistat, a known lipase inhibitor is a drug for treating obesity, was used in this study as a positive control. The results of this study indicated that OIE demonstrated as inhibition of pancreatic lipase between doses of 100-1250 $\mu\text{g/mL}$ (IC_{50} of $1062.04 \pm 32.21 \mu\text{g/mL}$), presumably 27 times less potential strengths than orlistat. The dose of OIE that inhibited pancreatic lipase was possibly similar concentration which induced the decrease in viability of pre-adipocytes (IC_{50} of $882.68 \pm 47.99 \mu\text{g/mL}$). It would be tempting to speculate that this was the mechanism of action of OIE regarding the growth and differentiation of 3T3-L1 cells. However, a study by Roh and Jung indicated that several plant extracts could inhibit pancreatic lipase but had minimal effect on the viability of 3T3-L1 cells

(Roh and Jung, 2012). In light of this research, the association of lipase inhibition and cell viability is somewhat diminished.

In summary, these findings provide evidence that the potential anti-adipogenesis mechanism of the OIE can be by downregulation of PPAR γ 2 and lipogenic genes controlling adipogenesis including SREBP-1c, FAS, and GLUT4 leads to diminishing adipokines marker secretion from adipocytes (adiponectin and leptin). Moreover, the OIE primarily exerted inhibition of lipase activity on the cell-free vitro assay. Thus, the OIE may be developed as a new natural resource for a lipid-lowering herbal medicine or a novel drug.

5.6 References

- Chan, R. S. M., and Woo, J. (2010). Prevention of overweight and obesity: how effective is the current public health approach. **International Journal of Environmental Research and Public Health**. 7(3): 765-783.
- Church, C., Horowitz, M., and Rodeheffer, M. (2012). WAT is a functional adipocyte? **Adipocyte**. 1(1): 38-45.
- do Carmo Avides, M., Domingues, L., Vicente, A., and Teixeira, J. (2008). Differentiation of human pre-adipocytes by recombinant adiponectin. **Protein Expression and Purification**. 59(1): 122-126.
- Dunkhunthod, B., Thumanu, K., and Eumkeb, G. (2017). Application of FTIR microspectroscopy for monitoring and discrimination of the anti-adipogenesis activity of baicalein in 3T3-L1 adipocytes. **Vibrational Spectroscopy**. 89: 92-101.

- Fu, Y., Luo, N., Klein, R. L., and Garvey, W. T. (2005). Adiponectin promotes adipocyte differentiation, insulin sensitivity, and lipid accumulation. **Journal of Lipid Research**. 46(7): 1369-1379.
- Goran, M. I., Ball, G. D., and Cruz, M. L. (2003). Obesity and risk of type 2 diabetes and cardiovascular disease in children and adolescents. **Journal of Clinical Endocrinology & Metabolism**. 88(4): 1417-1427.
- Gregoire, F. M. (2001). Adipocyte differentiation: from fibroblast to endocrine cell. **Experimental Biology and Medicine**. 226(11): 997-1002.
- Grommes, C., Landreth, G. E., and Heneka, M. T. (2004). Antineoplastic effects of peroxisome proliferator-activated receptor γ agonists. **The Lancet Oncology**. 5(7): 419-429.
- Guo, X., Liu, J., Cai, S., Wang, O., and Ji, B. (2016). Synergistic interactions of apigenin, naringin, quercetin and emodin on inhibition of 3T3-L1 preadipocyte differentiation and pancreas lipase activity. **Obesity Research & Clinical Practice**. 10(3): 327-339.
- Hengpratom, T., Lowe, G. M., Thumanu, K., Suknasang, S., Tiomyom, K., and Eumkeb, G. (2018). *Oroxylum indicum* (L.) Kurz extract inhibits adipogenesis and lipase activity in vitro. **BMC Complementary and Alternative Medicine**. 18(1): 177.
- Horton, J. D., Shimomura, I., Ikemoto, S., Bashmakov, Y., and Hammer, R. E. (2003). Overexpression of sterol regulatory element-binding protein-1a in mouse adipose tissue produces adipocyte hypertrophy, increased fatty acid secretion, and fatty liver. **The Journal of Biological Chemistry**. 278(38): 36652-36660.

- Ikeda, Y., Hama, S., Kajimoto, K., Okuno, T., Tsuchiya, H., and Kogure, K. (2011). Quantitative comparison of adipocytokine gene expression during adipocyte maturation in non-obese and obese rats. **Biological & Pharmaceutical Bulletin**. 34(6): 865-870.
- Jang, M.-K., Yun, Y.-R., Kim, J.-H., Park, M.-H., and Jung, M. H. (2017). Gomisins N inhibits adipogenesis and prevents high-fat diet-induced obesity. **Scientific Reports**. 7: 40345-40345.
- Kaldate, P., Tenpe, C., and Yeole, P. (2011). **Antidiabetic activity of leaves of *Oroxylum indicum* in alloxan-induced diabetic rats.**
- Kim, C. Y., Le, T. T., Chen, C., Cheng, J. X., and Kim, K. H. (2011). Curcumin inhibits adipocyte differentiation through modulation of mitotic clonal expansion. **The Journal of Nutritional Biochemistry**. 22(10): 910-920.
- Landgraf, K., Rockstroh, D., Wagner, I. V., Weise, S., Tauscher, R., Schwartze, J. T., Loffler, D., Buhligen, U., Wojan, M., Till, H., Kratzsch, J., Kiess, W., Bluher, M., and Korner, A. (2015). Evidence of early alterations in adipose tissue biology and function and its association with obesity-related inflammation and insulin resistance in children. **Diabetes**. 64(4): 1249-1261.
- Liao, W., Nguyen, M. T., Yoshizaki, T., Favellyukis, S., Patsouris, D., Imamura, T., Verma, I. M., and Olefsky, J. M. (2007). Suppression of PPAR-gamma attenuates insulin-stimulated glucose uptake by affecting both GLUT1 and GLUT4 in 3T3-L1 adipocytes. **American Journal of Physiology-Endocrinology and Metabolism**. 293(1): E219-227.
- Matsuda, M., Korn, B. S., Hammer, R. E., Moon, Y. A., Komuro, R., Horton, J. D., Goldstein, J. L., Brown, M. S., and Shimomura, I. (2001). SREBP cleavage-

activating protein (SCAP) is required for increased lipid synthesis in liver induced by cholesterol deprivation and insulin elevation. **Genes & Development**. 15(10): 1206-1216.

Ngernsoungnern, A., and Ngernsoungnern, P. (2016). Localization of ghrelin-like peptide in the gastrointestinal tract of the golden apple snail (*Pomacea canaliculata*) and changing of its concentration during fasting. **Acta Histochemica**. 118(3): 244-251.

Parlee, S. D., Lentz, S. I., Mori, H., and MacDougald, O. A. (2014). Quantifying size and number of adipocytes in adipose tissue. **Methods in Enzymology**. 537: 93-122.

Roh, C., and Jung, U. (2012). Screening of crude plant extracts with anti-obesity activity. **International Journal of Molecular Sciences**. 13(2): 1710-1719.

Seo, M. J., Choi, H. S., Jeon, H. J., Woo, M. S., and Lee, B. Y. (2014). Baicalein inhibits lipid accumulation by regulating early adipogenesis and m-TOR signaling. **Food and Chemical Toxicology**. 67: 57-64.

Siddiqui, W. A., Ahad, A., Ganai, A., Sareer, O., Najm, M., Kausar, M., and Mohd, M. (2012). Therapeutic potential of *Oroxylum indicum*: a review. **Journal of Pharmaceutical Research**. 2: 163-172.

Singh, J., and Kakkar, P. (2013). Modulation of liver function, antioxidant responses, insulin resistance and glucose transport by *Oroxylum indicum* stem bark in STZ induced diabetic rats. **Food and Chemical Toxicology**. 62: 722-731.

Tang, Q. Q., Otto, T. C., and Lane, M. D. (2003). Mitotic clonal expansion: a synchronous process required for adipogenesis. **Proceedings of the National Academy of Sciences of the United States of America**. 100(1): 44-49.

- Tontonoz, P., Hu, E., and Spiegelman, B. M. (1994). Stimulation of adipogenesis in fibroblasts by PPAR gamma 2, a lipid-activated transcription factor. **Cell**. 79(7): 1147-1156.
- WHO. (2019, May 28). Obesity and overweight. [On-line]. <https://www.who.int/en/news-room/fact-sheets/detail/obesity-and-overweight>.



CHAPTER VI

EFFECT OF *O. INDICUM* EXTRACT ON CELL CYCLE INHIBITION, GLUCOSE METABOLISM, AND MITOCHONDRIA FUNCTION

6.1 Abstract

The differentiation of adipocytes requires crosstalk between cell cycle regulation and metabolic control. This study attempted to investigate the mechanisms of *O. indicum* extract (OIE) on cell cycle regulation, glucose metabolism, and mitochondria function of 3T3-L1 cells. The effect of the OIE on cell cycle progression was measured by flow cytometry along with observing the expression of the cycle regulator (Cdk2) by immunoblotting. To assess the effect of the OIE on glucose metabolism, the amount of glucose uptake (2-NBDG) influenced by insulin was determined. As well as, the protein tyrosine phosphorylation (PY20) and glucose transporter4 (GLUT4) expression in OIE-treated- (OIE-treated adipocytes) and untreated-differentiated 3T3-L1 cells (untreated adipocytes) were determined by immunoblotting assay. Mitochondria are also essential to metabolic processes, This study investigated mitochondrial activity using JC-1, and mitochondria mass by MitoTracker Green (MTG) staining fluorescence dyes. Finally, cellular ATP concentration was measured using an ATP chemiluminescence assay. The results indicated that OIE-treated at 50 to 200 $\mu\text{g/mL}$ in the early phase of adipogenesis resulted in significant inhibition of the cell cycle into the G2/M phase

compared to untreated adipocytes. These results were confirmed by a significant decrease in the expression of Cdk2 in 200 µg/mL OIE-treated adipocytes compared with untreated adipocytes ($P < 0.05$). Tyrosine kinase (IRS-1/IRS-2) activity of 200 µg/mL OIE-treated adipocytes was significantly reduced compared to untreated adipocytes at day 12 ($P < 0.05$). GLUT4 protein was significantly increased in both treated- and untreated-adipocytes at day 12 compared to preadipocytes ($P < 0.05$). These results were correlated with the immunofluorescence staining of GLUT4, which showed highly expressed in the cell membrane of these cells. However, OIE-treated adipocytes exhibited significantly lower GLUT4 level compared to untreated adipocytes ($P < 0.05$). Furthermore, adipocytes treated with OIE were significantly decreased glucose uptake level at day 12 compared to adipocytes at 24 h. Suggesting that OIE treatment can modify how differentiated 3T3-L1 cells obtain their glucose. Other mitochondrial activity experiments, the mitochondria membrane potential (MMP) of OIE-treated adipocytes was significantly decreased at 24 h, whereas increased at day 12 compared to untreated-adipocytes ($P < 0.05$). Moreover, OIE caused significant reduction in intracellular ATP of OIE-treated adipocytes compared to other adipocytes groups ($P < 0.05$). Transmission electron microscope results exhibited that OIE could protect mitochondria deformation of OIE-treated adipocytes, entirely similar to pre-adipocytes (non-differentiated cells), compared to the untreated adipocytes. These results suggest that 200 µg/mL of OIE suppresses adipogenesis through cell cycle inhibition, decreases the phosphorylation of IRS-1 and IRS-2, leading to a decrease in glucose uptake to the cells. Interestingly, treatment with OIE can improve mitochondrial activity and morphology compared to mature untreated adipocytes. These results provide evidence that OIE affects anti-adipogenesis through

1) inhibits cells cycle progression, 2) reduces the phosphorylation activity of IRS-1 and IRS-2. Moreover, it slows down the mitochondrial activity at the early phase of cell differentiation leading to a decrease in lipogenesis.

6.2 Introduction

3T3-L1 pre-adipocytes has been extensively used for the study of adipogenesis, defined as the process by which preadipocytes get differentiated into adipocytes (Ruiz-Ojeda et al., 2016). The transformation of 3T3-L1 pre-adipocytes to adipocytes is initiated by various stimulators in the differentiation media, which include 3-isobutyl-1-methylxanthine (IBMX), dexamethasone (DEX), and insulin. Once cells receive these stimulators, cells proliferate to confluence such that there is no more space for cell growth and propagation. Proliferating of pre-adipocytes no longer multiply due to cell-cell contact inhibition. Post-confluent pre-adipocytes become growth-arrested at the G1/S phase of the cell cycle (Ailhaud et al., 1989). The re-entry of growth-arrested pre-adipocytes into the cell cycle and the completion of several rounds of clonal expansion are the first steps in the process of adipogenesis (Camp et al., 2002).

The differentiation of pre-adipocyte into mature adipocytes requires a complex interaction of metabolic pathways. Glucose transporter isoform 4 (GLUT4) is the main insulin-responsive glucose transporter, and it is located predominantly in muscle and fat cells (Assimacopoulos-Jeannet et al., 1995). Binding of the insulin to the insulin receptor (IR) initiates a signaling cascade that results in the translocation of the insulin-sensitive glucose transporter protein 4 to the plasma membrane which leads to the facilitated diffusion of glucose into the cell (Deshmukh, 2016). Roberts et al. found that the earliest changes in the process of cell differentiation were associated with an

increased in the utilization of glucose via glycolysis (Roberts et al., 2009) and glucose was converted to pyruvate which was imported into the mitochondria to join TCA cycle. Citrate formed in the TCA cycle is transported into the cytosol where it is converted to acetyl-CoA, which is an essential precursor for fatty acid synthesis. Thus, glucose synergizes with insulin is an important factor for glycolytic and lipogenic partway (Glimcher and Lee, 2009).

Furthermore, most of the adenosine triphosphate (ATP) synthesized during glucose metabolism is produced in the mitochondria through oxidative phosphorylation (Bertram et al., 2006). The previous study found that 20 to 30 folds of mitochondria protein were increased during the differentiation of 3T3-L1 cells, together with increased expression of lipogenic enzymes (Wilson-Fritch et al., 2003). The recent research revealed that hepatic mitochondrial dysfunction was associated with obesity and diabetes. Adipocytes are also vital endocrine organs and the secretion of adiponectin that regulated lipid and glucose metabolism. (Scherer et al., 1995).

In this regard, natural compounds would be an attractive target for the discovery of new anti-obesity drugs. From the previous chapter, I had found that OIE remarkably inhibited the differentiation and prevented morphologically deformed of adipocytes. These results lead us to believe that OIE may involve the preliminary stages of adipocyte development. Besides, OIE can inhibit the expression of PPAR γ 2, leading to decreased expression of adipokine and lipogenic enzymes. So, this chapter was studying the effect of OIE on the cell cycle, mitochondrial function, and glucose metabolism in 3T3-L1 cells.

6.3 Materials and Methods

6.3.1 Chemicals and reagents

Anti Cdk2 (D-12) antibody, anti-pTyr (PY20) antibody, anti-Glut4, anti- β -actin (C4), anti-mouse IgGk (BP-HRP), anti-mouse IgGk (BP-FITC) were purchased from Santa Cruz Biotechnology (Wembley, London, UK).

6.3.2 Cell culture

Cell culture was carried as previously described (Dunkhunthod et al., 2017). Shortly, 3T3-L1 pre-adipocytes were cultured in Dulbecco's Modified Eagle's medium (DMEM) containing 10 % calf bovine serum (CBS) (GIBCO, Grand Island, NY, USA). At two days after confluence (day 0), the cells were stimulated to differentiate with DMEM containing 10 % fetal bovine serum (FBS) (Hyclone, Logan, UT, USA), 1.0 μ M of dexamethasone (G Bioscience, St. Louis, MO, USA), 0.5 mM of isobutyl methylxanthine (IBMX) and 1.0 μ g/mL of insulin for two days. From day 4 onwards, the differentiation media were replaced by 10 % FBS/DMEM media containing 1.0 μ g/mL of insulin. These media were changed every two days until the cells were harvested. All media contained 100 μ g/mL of streptomycin and 100 U/mL of penicillin (GIBCO). Cells were maintained at 37 °C in a 95 % humidified with 5 % of CO₂ atmosphere.

For the treatment of pre-adipocytes, the cells were seeded in a 6-well plate at the density of 1.5×10^5 cells/well. The cells were allowed to adhere to the plate for 48 h and were then divided into 6 groups; 1) non-differentiated cells (pre-adipocytes); 2) untreated differentiated cells treated with 0.1% DMSO (vehicle control, untreated adipocytes); 4-6) differentiated cells treated with 50, 100, 150, and 200 μ g/mL OIE (OIE-treated adipocytes), respectively. 24 h after the cells were induced to differentiate;

the cells were collected for cell cycle analysis and protein quantification. For a further experiment, the cells were collected on day 12 for protein quantification, immunocytochemistry, flow cytometry, and TEM analysis.

6.3.3 Cell cycle analysis

Post confluent 3T3-L1 preadipocytes were stimulated with differentiation media in the presence of OIE (50 to 200 $\mu\text{g}/\text{mL}$) for 24 h. The cells were collected by trypsinization and washed twice with phosphate-buffered saline (PBS). The cells were then fixed in 80 % of ethanol and stored at $-20\text{ }^{\circ}\text{C}$ for 1 h. The fixed cells were washed twice with ice-cold PBS. The cells were stained with 50 μL of RNaseA (0.1unit/ mL) and 150 μL of PI (50 $\mu\text{g}/\text{mL}$) at $37\text{ }^{\circ}\text{C}$ for 1 h. The fluorescence intensity of the PI stained cells was measured using the BD Accuri C6 flow cytometer. The data from 25,000 cells per sample were analyzed using FlowJo software and the Dean-Jett-Fox model.

6.3.4 Protein extraction and immunoblot analysis

The expression of Cdk2, PY20, and Glut4 proteins in control and OIE-treated cells was determined by Western immunoblotting. The cells were washed 3 times with cold 0.1 M phosphate buffer saline (PBS) and were lysed in cold lysis buffer (10 mM Tris-HCl, 150 mM NaCl, 0.5 % Triton X-100, 1 mM EDTA, and 100 mM PMSF, pH 7.2) containing protease inhibitor cocktail (Roche, Mannheim, Germany). The protein concentrations were measured using a bovine serum albumin (BSA) protein assay kit following the company description (Thermo Scientific, Rockford, Winnebago, USA). The lysates (50 μg , each) were separated on 12 % Mini-PROTEAN TGX stain-free pre-cast gels. After electrophoresis, the proteins were transferred to PVDF using the Trans-Blot Turbo system (Bio-Rad, Watford, UK). The membranes were then blocked with 5

% skimmed milk in 0.1 M PBS contains 0.1 % Tween-20 (PBST) for 1 h at room temperature, followed by washing with PBST. The membranes were subsequently incubated with mouse monoclonal antibody (anti-Cdk2, anti-PY20, and anti-Glut4) (1:1000 in PBS), overnight at 4 °C. After extensive washing, the membranes were incubated with mouse IgGκ light chain binding protein (m-IgGκ BP) conjugated to horseradish peroxidase (HRP) (1:3000 in PBS) for 1 h at room temperature, followed by washing with PBST. The antigen-antibody complex was developed with the enhanced chemiluminescence (ECL) substrate solution for 5 min (Bio-Rad, Watford, UK). Analysis of intensities of the adiponectin protein bands was quantified using ImageJ software under the same pixel area. The data were normalized using β-actin as an internal control. The experiments were repeated using cells from 3 different individuals.

6.3.5 Immunocytochemistry

At day 12, 3T3-L1 pre-adipocytes and adipocytes were collected, washed with cold PBS, fixed for 15 min in cold acetone, and washed with PBST. After blocking with 4 % of BSA for 1 h at room temperature, the cells were washed and incubated with anti-Glut4 antibody (1:200 in PBS) overnight at 4 °C. After extensive washing, mouse IgGκ conjugated with fluorescein isothiocyanate (FITC) (1:500) was applied to the samples and incubated for 90 min at room temperature. After washing thoroughly with PBS, the cells were double-stained with DAPI (nucleus stain) (1:1000) for 5 min in the dark and washed twice with PBS. Finally, the cells were visualized using fluorescence microscopy (Leica DMI6000B).

6.3.6 Flow cytometry

Flow cytometry was used to detect glucose concentration and mitochondria activity in 3T3-L1 cells. At 24 h after inducing cells with differentiation media and at day 12, 3T3-L1 pre-adipocytes, adipocytes, and 200 $\mu\text{g}/\text{mL}$ OIE-treated adipocytes were collected and washed twice with PBS. Then, cells were incubated with fluorescence dye for 60 min, including 0.1 mM of 2-NBDG for glucose uptake and 10 μM of JC-1 for mitochondria membrane potential (MMP). Then, cells were washed twice with phosphate-buffered saline (PBS). Labeled cells were collected (keep in the dark) and analyzed using flow cytometer with excitation 488 nm. All data were recorded and analyzed using BD accuri C6 software. The data were presented as the median fluorescent signals for 10,000 cells. The JC-1 red/green fluorescence ratio of the dye in the mitochondria indicated the state of the mitochondria polarization, whereas the higher of the ratio was more J aggregates were formed (Gruenwald et al.), and the lower was the few red J aggregates were formed.

6.3.7 Confocal microscopy

The MitoTracker green fluorescent dye was used to label mitochondria within 3T3-L1 cells. At day 12, the culture media were removed and the cells were incubated with 200 nM of MitoTracker green fluorescent dye for 45 min at 37 °C. Then, the cells were carefully washed with culture media and trypsinized. Labeling cells were separated and deposited onto the Shandon cytoslide glass slide by using Shandon cytospin 4 cytocentrifuge, following manufactured protocol (Thermo Fisher Scientific). Briefly, 200 μL of each sample was loaded in the Shandon cytofunnel chamber and spin at 1,000 rpm for 5 min to allow for complete fluid absorption. The cells were then allowed to dry at room temperature and applied mounting medium to the surface of the

slide, then tipped the coverslip onto the mounting medium. The images were obtained using a Zeiss 510 Meta laser scanning microscope, mounted on an Axiovert 200M BP computer-controlled inverted microscope. The Argon ion laser was used with an excitation wavelength of 488 nm, and the images were captured at x10 and x20 magnification.

6.3.8 ATP measurement

ATP level was measured as previously described with some modifications (Kapoor et al., 2017). At day 12, the media were removed, and the cells were washed twice with 1 M of cold PBS. The level of ATP released was then determined using the ATP bioluminescent somatic cell assays kit (Sigma-Aldrich, Dorset, UK). 50 μ L of ATP releasing reagent stock with 450 μ L of ultrapure water was added directly to the cells and incubated for 5 minutes. Then, 20 μ L of mixed samples were taken to the 96 well plates, followed by adding 80 μ L of ultrapure water. Finally, 100 μ L of the luciferase assay mix was added to the sample. The amount of light emission was then measured using a microplate luminometer. ATP concentration (0 to 200 nM) was determined from the standard curve. The protein concentrations in each well were used to normalize to the ATP content (nM/mg of proteins). The amount of ATP (nM/mg of protein) was determined in triplicates (n = 3).

6.3.9 Transmission Electron Microscopy (TEM)

At day 12, the cells were dissociated with 0.25% trypsin at 37 °C for 3 - 5 min, and the digestion was stopped with culture medium containing FBS. The cells were transferred into 10 mL tube, centrifuged at 1,200 rpm for 8 min, washed in a pre-cooling PBS (4 °C) after discarding the supernatant and then centrifuged at 1,200 rpm for 8 min. After discarding the supernatant, added 2.5 % glutaraldehyde in 0.1M

phosphate buffer to the cells, then the cells were fixed at 4 °C for overnight. The cells were rinsed three times with 0.1M phosphate buffer (pH7.2) for 15 min each, followed by post-fixation with 1 % osmium tetroxide (OsO₄) in dH₂O. Fixed samples were dehydrated, embedded in epoxy resin (Electron Microscopy Sciences), and polymerized at 60 °C for 24 h. The blocks were ultra-thin-sectioned at 60 nm with a diamond knife using an RMC ultramicrotome. The sections were placed on copper grids and stained with 2 % uranyl acetate at room temperature for 15 min and then rinsed with distilled water, followed by secondary staining with lead stain solution (SPI-CHEM) at room temperature for 15 min. The grids were observed under a Transmission Electron Microscope (FEI Model TECNAI G² 20S-TWIN) at an acceleration voltage of 120 kV.

6.3.10 Statistical analysis

All the data were expressed as the mean \pm standard deviation of the mean (Mean \pm SD). The difference values between adiponectin protein levels, the number of adiponectin secretions, and gene expressions compared between treatment and control groups were analyzed using one-way analysis of variance (ANOVA) with a Turkey's HSD post-hoc test (SPSS v 23). Values were considered statistically significant when $P < 0.05$, and data were representative of three independent experiments ($n = 3$). Most of the experiments were performed in triplicate.

6.4 Results

6.4.1 Effect of OIE on inhibition of cell cycle progression

The effect of the OIE on cell cycle of 3T3-L1 cells is shown in Figure 6.1A and 6.1B. When 3T3-L1 preadipocytes were induced to differentiate with isobutyl methylxanthine (IBMX), dexamethasone, and insulin, the cells enter into S and G2/M phase within 24 h following induction (Figure 6.1A). Further analysis revealed that differentiated cells transformed from G1 and S phase to the G2 phase (36% cells in G2 phase). In contrast, treatment with OIE at concentrations 200, 150, 100, and 50 $\mu\text{g}/\text{mL}$ significantly arrested cells in the G0/G1 phase (10.3 %, 10.8 %, 14.4 %, and 18.7 % cells in G2 phase, respectively) compared to controls ($P < 0.01$) (Figure 6.1A and B). This observation may be explained that the OIE has an impact on the expression of cell cycle regulators in the formation of adipocytes. At doses of 150 and 200 $\mu\text{g}/\text{mL}$, OIE significantly affected the expression of Cdk2 in the differentiating cells (Figure 6.1C and 6.1D). These results suggest that OIE may inhibit cell cycle entry into the G2/M phase of 3T3-L1 cells. OIE has the potential to inhibit the initiation of mitotic clonal expansion (MCE), which is a significant step for cell differentiation. Thus, this mechanism may play an important role in adipogenesis suppression.

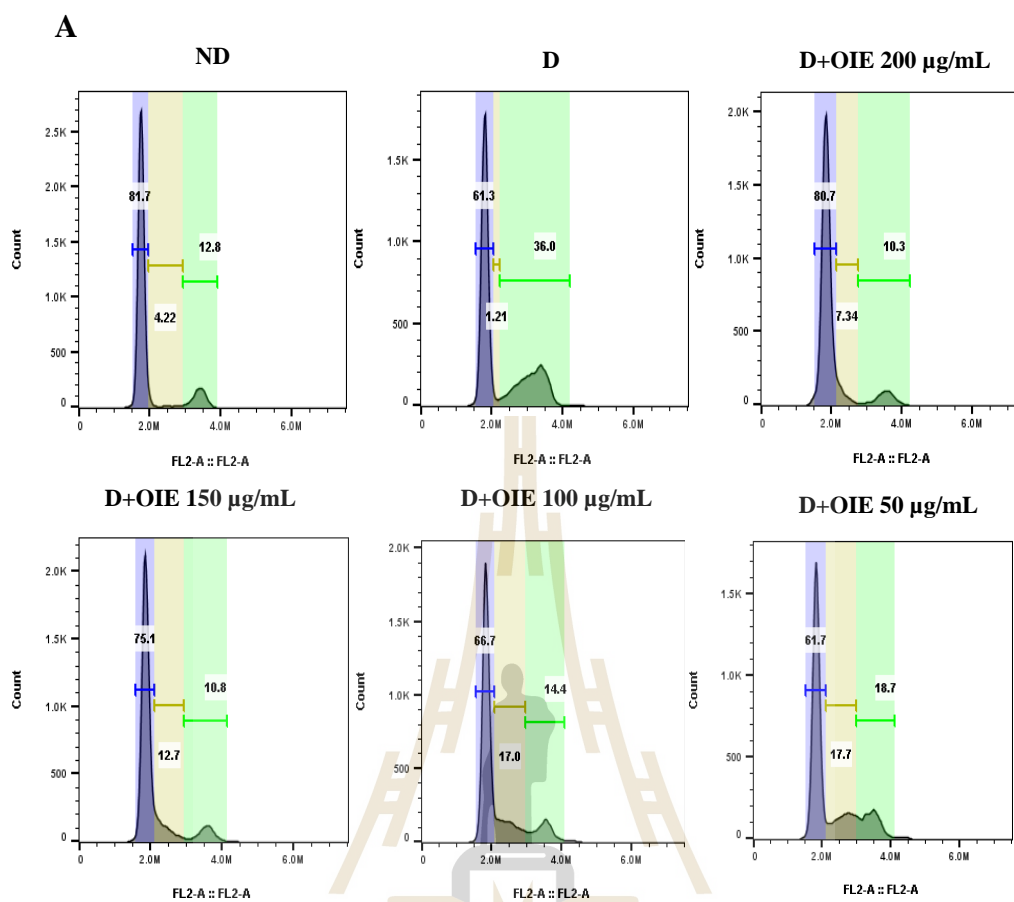


Figure 6.1 The effect of the OIE on cell cycle progression in 3T3-L1 preadipocytes.

(A) 3T3-L1 cells were treated by differentiation media in the presence of OIE at concentration 50 to 200 µg/mL for 24 h. ND = Non-differentiated cells (pre-adipocytes), CON = Differentiated cells with 0.1 % DMSO, OIE (200) = OIE at 200 µg/mL, OIE (150) = OIE at 150 µg/mL, OIE (100) = OIE at 100 µg/mL, OIE (50) = OIE at 50 µg/mL.

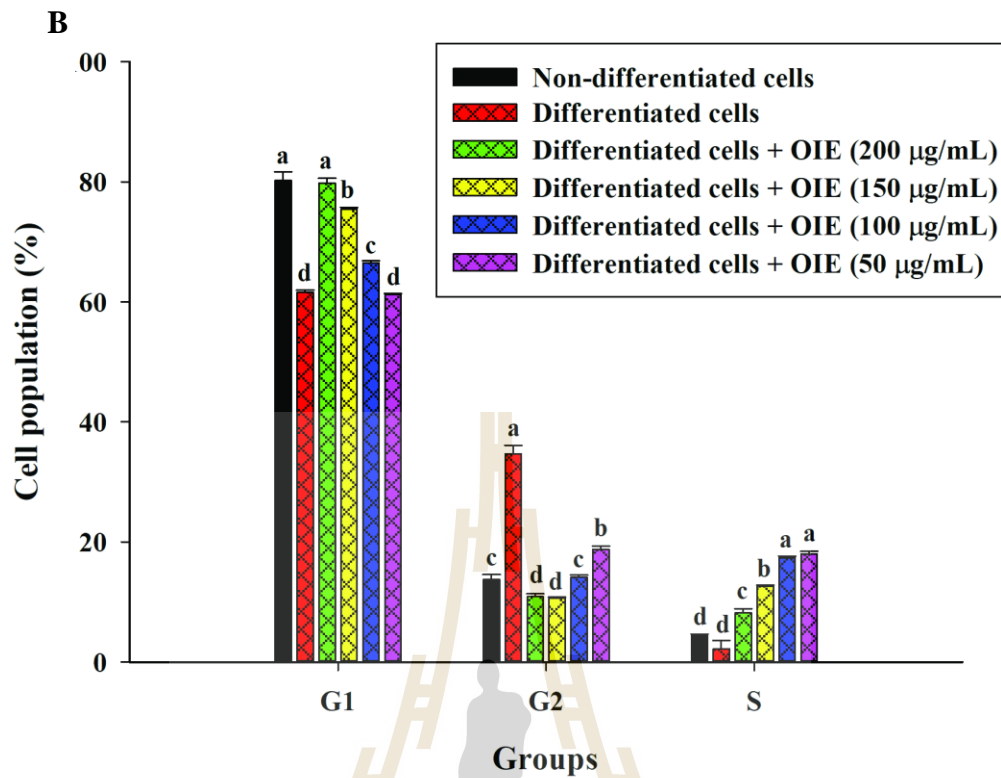


Figure 6.1 The effect of the OIE on cell cycle progression in 3T3-L1 preadipocytes (Continued). **(B)** The percentage of the cell population in the G0/G1, S, and G2/M phases of the cell cycle was determined by Flow Jo software. The result reported as means \pm SD value ($n = 3$). The different superscript alphabets are significantly different from each other. Results were analyzed by ANOVA and Tukey's Post-hoc test ($P < 0.05$).

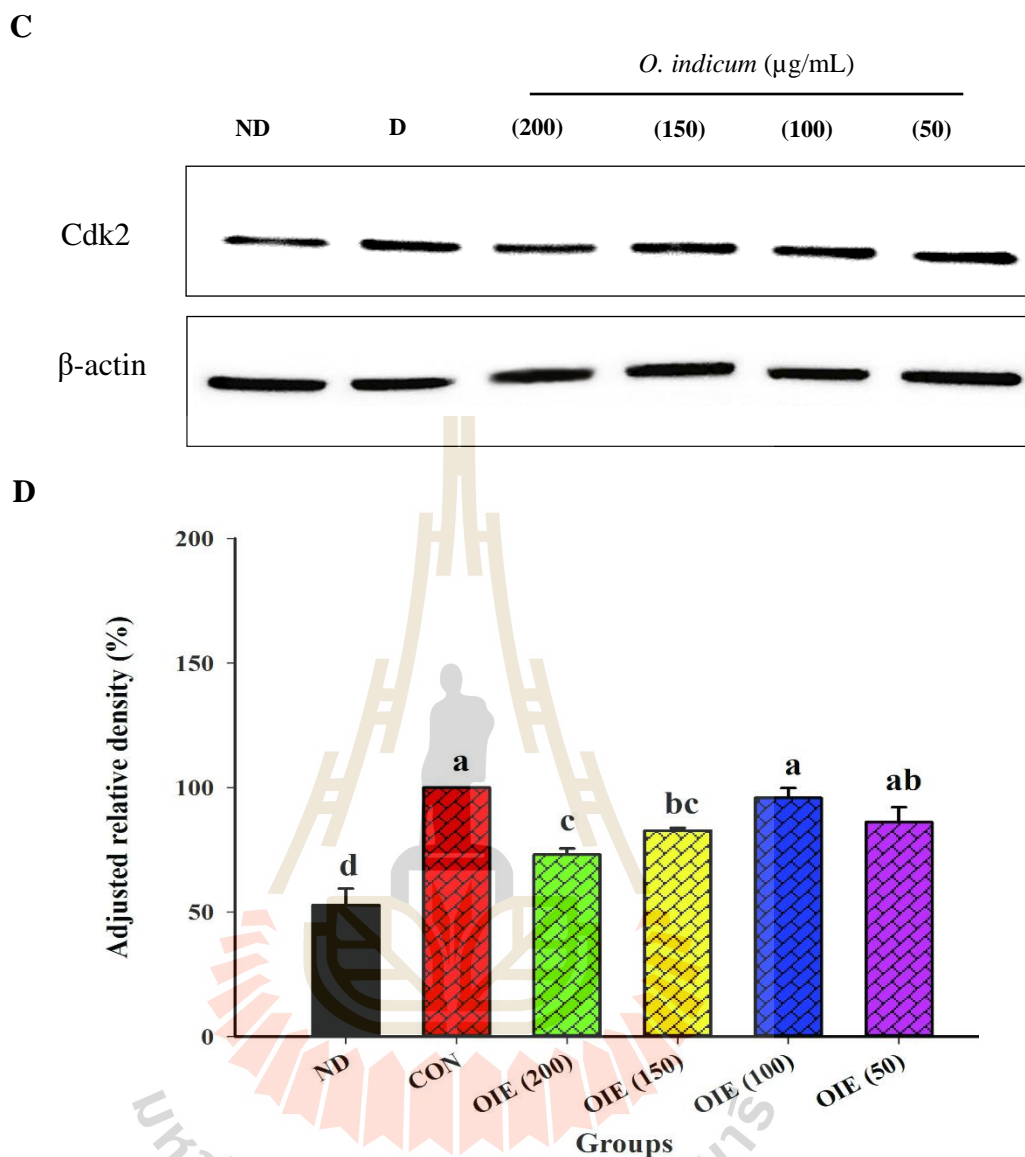


Figure 6.1 The effect of the OIE on cell cycle progression in 3T3-L1 preadipocytes (Continued). (C) Whole-cell lysates were immunoblotted with the anti-Cdk2 antibody. (D) Comparison of the intensity of Cdk2 protein expression among 6 groups. ND = Non-differentiated cells (pre-adipocytes), CON = Differentiated cells with 0.1 % DMSO, OIE (200) = OIE at 200 $\mu\text{g/mL}$, OIE (150) = OIE at 150 $\mu\text{g/mL}$, OIE (100) = OIE at 100 $\mu\text{g/mL}$, OIE (50) = OIE at 50 $\mu\text{g/mL}$. The result reported as means \pm SD value ($n = 3$). The different superscript alphabets are significantly different from each other. Results were analyzed by ANOVA and Tukey's Post-hoc test ($P < 0.05$).

6.4.2 Effect of OIE on glucose metabolism

To determine the effect of the OIE on glucose metabolism, this thesis evaluated the expression of glucose transporter 4 (GLUT4), assessed glucose uptake and tyrosine phosphorylation in differentiating 3T3-L1 cells. The addition of 1.0 $\mu\text{g/mL}$ of insulin in the media-induced the tyrosine phosphorylation of three major bands with apparent molecular masses of 181, 164, and 91 kDa, respectively at both 24 hour and 12 days following differentiation (Figure 6.2A and 6.2B). These proteins were consistent with insulin activity. However, OIE effectively reduced the phosphorylation of these proteins at day 12 and slightly decreased at 24 h. Furthermore, the expression of Glut4 was increased in differentiated cells and appeared to elevate at the plasma membrane of the cells at day 12 (Figure 6.2C). Treatment with OIE resulted in a 40 % reduction of the GLUT 4 expression compared to untreated adipocytes (Figure 6.2A and 6.2B). In a parallel experiment, pre-adipocytes and adipocytes treated with OIE were two folds significantly increased uptake of 2-NBDG compared to untreated control cells at 24 h ($P < 0.05$), Figure 6.2D). At day 12, the amount of glucose uptake in differentiated cells treated with OIE significantly reduced when compared within the same groups at 24 h and 48 h ($P < 0.05$). One explanation for this is that OIE may diminish the activity of tyrosine kinases leading to a reduction of GLUT4 expression in the plasma. Although OIE had highly elevated glucose uptake in both 3T3-L1 undifferentiated and differentiated cells at 24 h and 48 h. However, at day 12 in differentiated cells treated with OIE had less of an effect on glucose uptake.

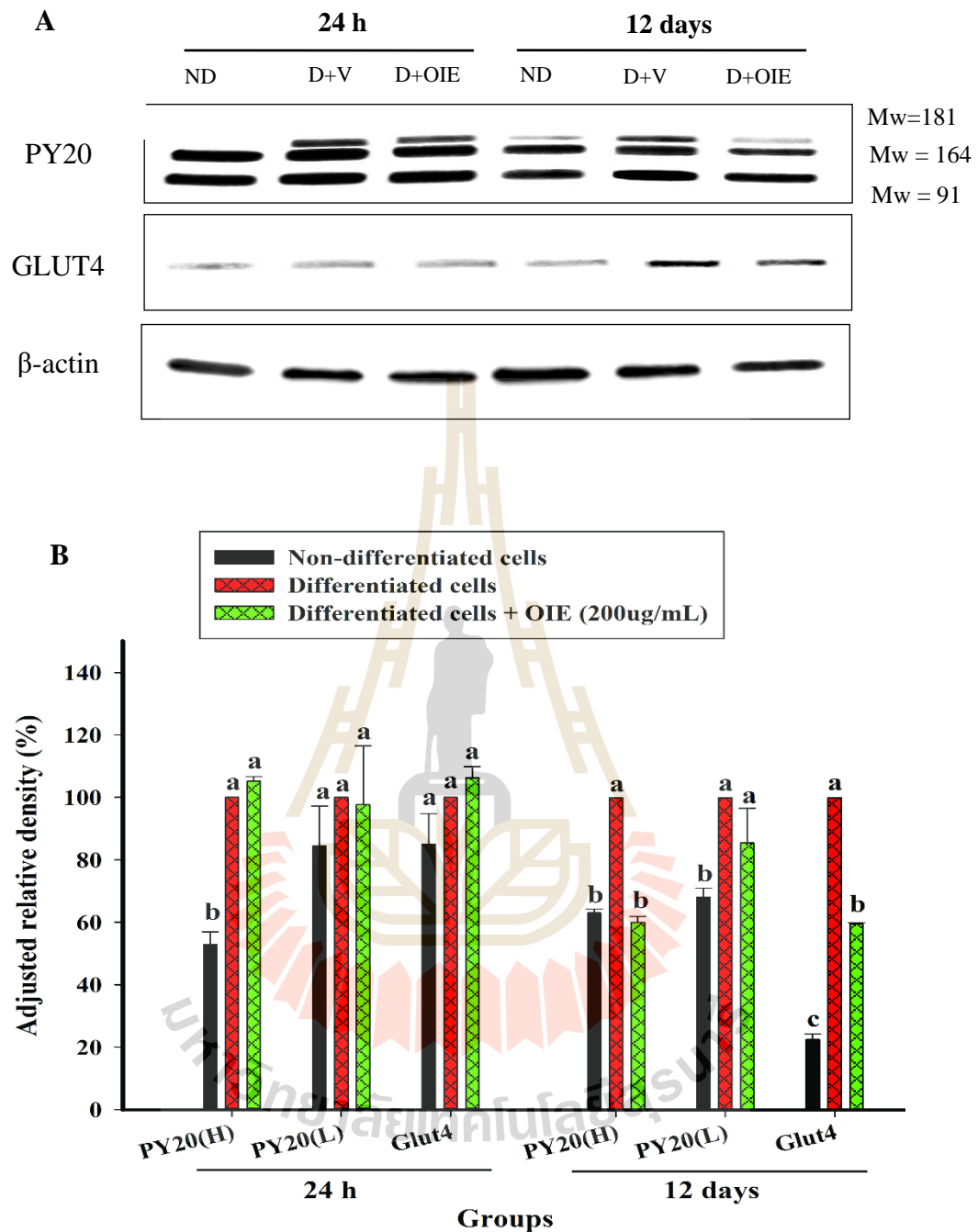


Figure 6.2 The effect of OIE on glucose metabolism in 3T3-L1 cells. **(A)** Whole-cell lysates were immunoblotted with anti-phosphotyrosine antibody and anti-glucose transporter4 at 24 h and 12 days. **(B)** Comparison of the relative intensity of PY20 and Glut4 proteins expression among 6 groups. The result reported as means \pm SD value (n

= 3). The different superscript alphabets are significantly different from each other. Results were analyzed by ANOVA and Tukey's Post-hoc test ($P < 0.05$) (Continued).

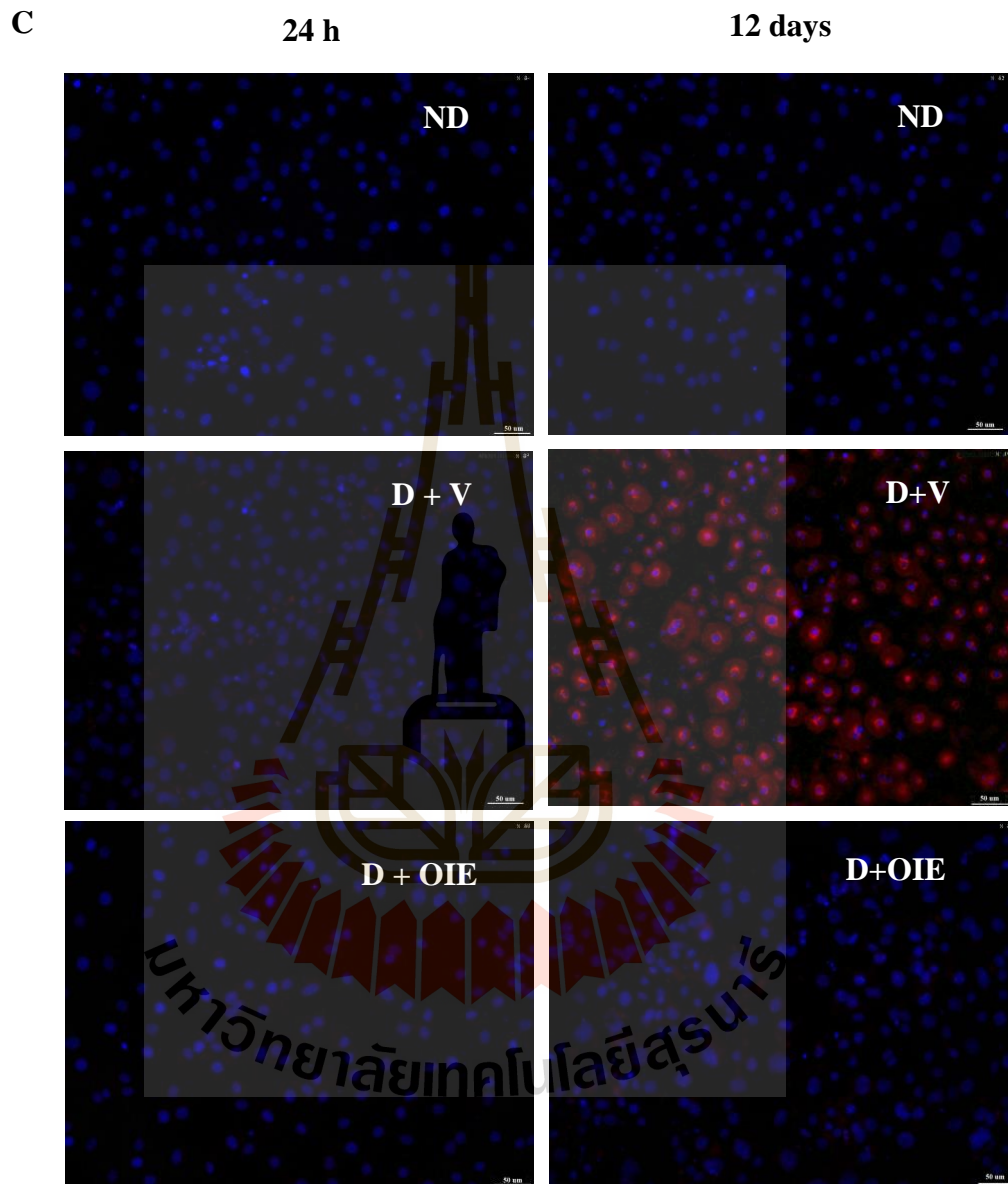


Figure 6.2 The effect of OIE on glucose metabolism in 3T3-L1 cells (Continued). (C) Fluorescence microscopic imaging of co-immunostaining between glucose-transporter4 (Gruenwald et al.) and nuclei (blue), scale bar; 50 μ m. ND = Non-differentiated cells (pre-adipocytes), D+V = Differentiated cells with 0.1% DMSO, D+OIE (200) = Differentiated cells with OIE at 200 μ g/mL.

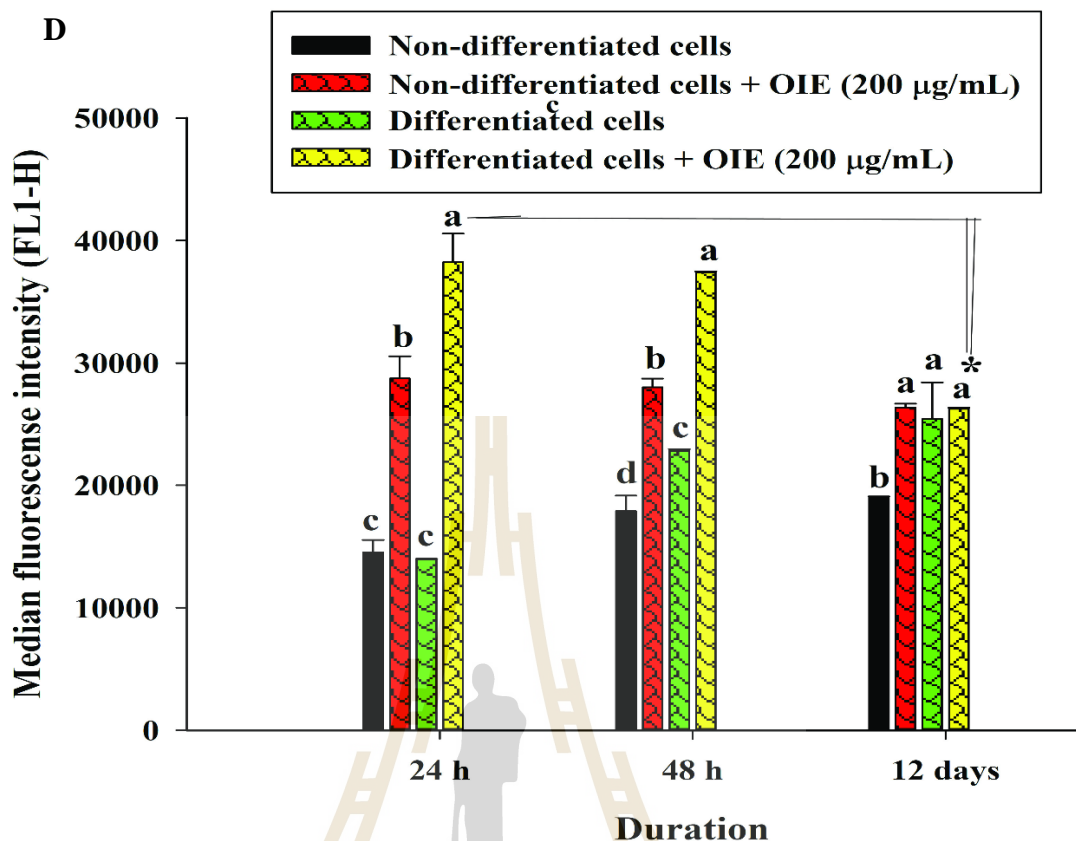


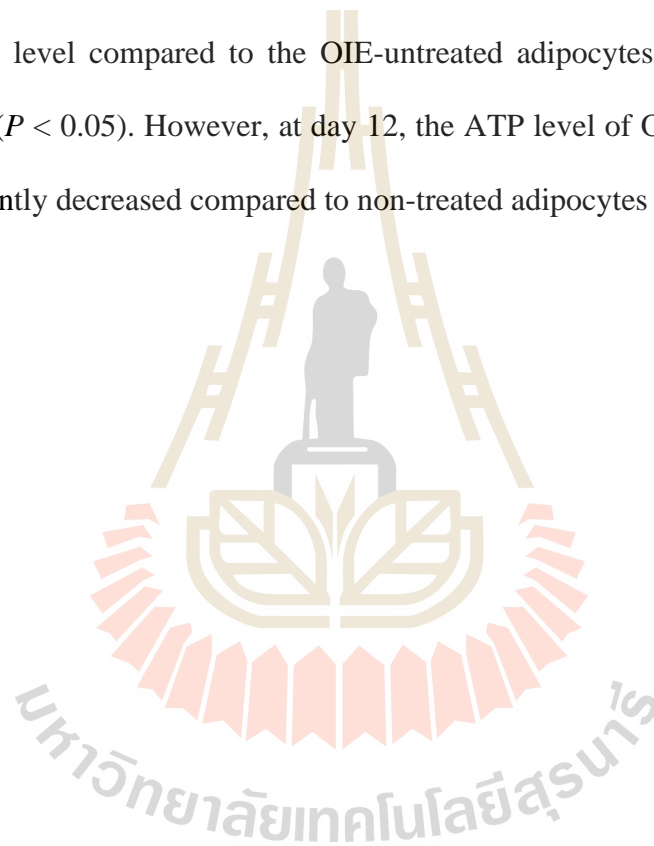
Figure 6.2 The effect of OIE on glucose metabolism in 3T3-L1 cells (Continued). **(D)** Glucose uptake in 3T3-L1 cells was determined by 2-NBDG at 24 h, 48 h, and 12 days. The result reported as means \pm SD value ($n = 3$). The different superscript alphabets are significantly different from each other. Results were analyzed by ANOVA and Tukey's Post-hoc test ($P < 0.05$). * The different of glucose uptake in differentiated cells treated with 200 $\mu\text{g}/\text{mL}$ of OIE during 24 h, 48 h and 12 days were analyzed by the Paired T-test ($P < 0.05$).

6.4.3 Effect of OIE on mitochondrial activity

To evaluate the effect of the OIE on mitochondrial activity, the mitochondrial membrane potential (MMP), intracellular ATP production, mitochondrial mass, and morphology were determined (Figure 6.3). The JC-1 dye was used for monitoring mitochondrial membrane. In the cytoplasm, the dye exhibited green fluorescence (JC-

1 monomer); however, when the dyes enter into the mitochondria where it accumulated and started forming reversible complexes called JC-1 aggregates. These JC-1 aggregates exhibited excitation and emission in the red spectrum. Fluorescence staining revealed that JC-1 monomer (green) and JC-1 aggregates were displayed in all samples. However, JC-1 aggregates in differentiated cells treated with 200 $\mu\text{g}/\text{mL}$ of OIE and non-differentiated cells were less pronounced compared to the differentiated control group (Figure 6.3A). This result is consistent with the flow cytometry data regarding MMP. The increasing of MMP (red/green fluorescence ratio) was demonstrated in differentiated cells, while treatment with 200 $\mu\text{g}/\text{mL}$ at 24 h significantly reduced the ratio ($P < 0.05$) (Figure 6.3B). However, a noticeable reduction of MMP was found in all samples at day 12, especially in differentiated control cells (untreated adipocytes). Furthermore, the cellular ATP level was determined at day 12, highest intracellular concentration of ATP level was found in adipocytes (untreated and vehicle control) and was significant ($P < 0.05$) reduced in adipocytes treated with OIE (Figure 6.3C). MitoTracker dyes have been used for detecting a mitochondrial mass. This fluorescent dye is linking to thiol groups in the mitochondria, and its produce green fluorescence under excitation 488 nm. The results showed that untreated adipocytes displayed a decrease in the intensity of the labeling mitochondrial (Figure 6.3D). Whereas the intensity seemed to increase in long treatment with 200 $\mu\text{g}/\text{mL}$ of the OIE, and it was similar to preadipocytes treated with and without OIE. This study explored the morphology of mitochondria by TEM. The results showed that mitochondria of preadipocytes with and without-OIE were gathered around the nucleus, and the morphology was mainly short, but the cristae were clearly observed (Figure 6.3E). In contrast, the mitochondria of untreated adipocytes had become more condensed,

slender shape with reduced of cristae mitochondria and uniformly distributed in the cytoplasm. While OIE-treated adipocytes could recover mitochondria mass and morphology compared to the untreated preadipocytes. These results suggest that mitochondrial plays an important role during 3T3-L1 differentiation. During the adipocyte differentiation process of untreated pre-adipocytes at 24 h, the cells had an increase in MMP. Whereas, OIE-treated adipocytes showed significantly lower and higher MMP level compared to the OIE-untreated adipocytes at 24 h and day 12, respectively ($P < 0.05$). However, at day 12, the ATP level of OIE-treated adipocytes was significantly decreased compared to non-treated adipocytes ($P < 0.05$).



A

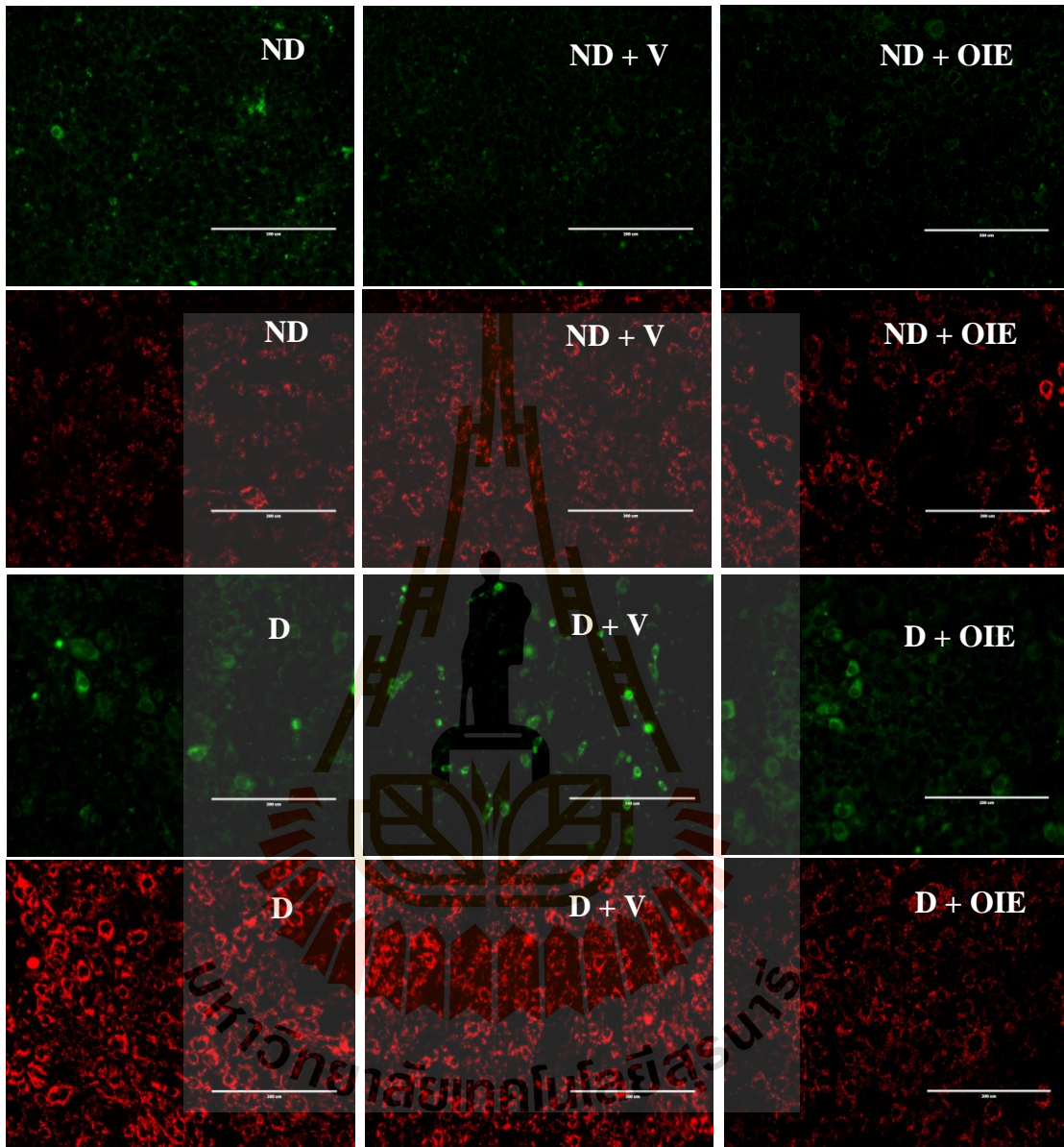


Figure 6.3 The effect of OIE on mitochondrial activity in 3T3-L1 cells. (A) 3T3-L1 cells were stained with JC-1 dye at 24 h and 12 days. The data were reported as the ratio of red aggregates (FL-2 channel) to green monomer (FL-1 channel). ND = Non-differentiated cells (pre-adipocytes), ND+V = non-differentiated cells with 0.1% DMSO, ND+OIE = non-differentiated cells with 200 $\mu\text{g}/\text{mL}$ of OIE, D = Differentiated

cells, D+V = Differentiated cells with 0.1% DMSO, D+OIE = Differentiated cells with OIE at 200 $\mu\text{g}/\text{mL}$ (Continued).

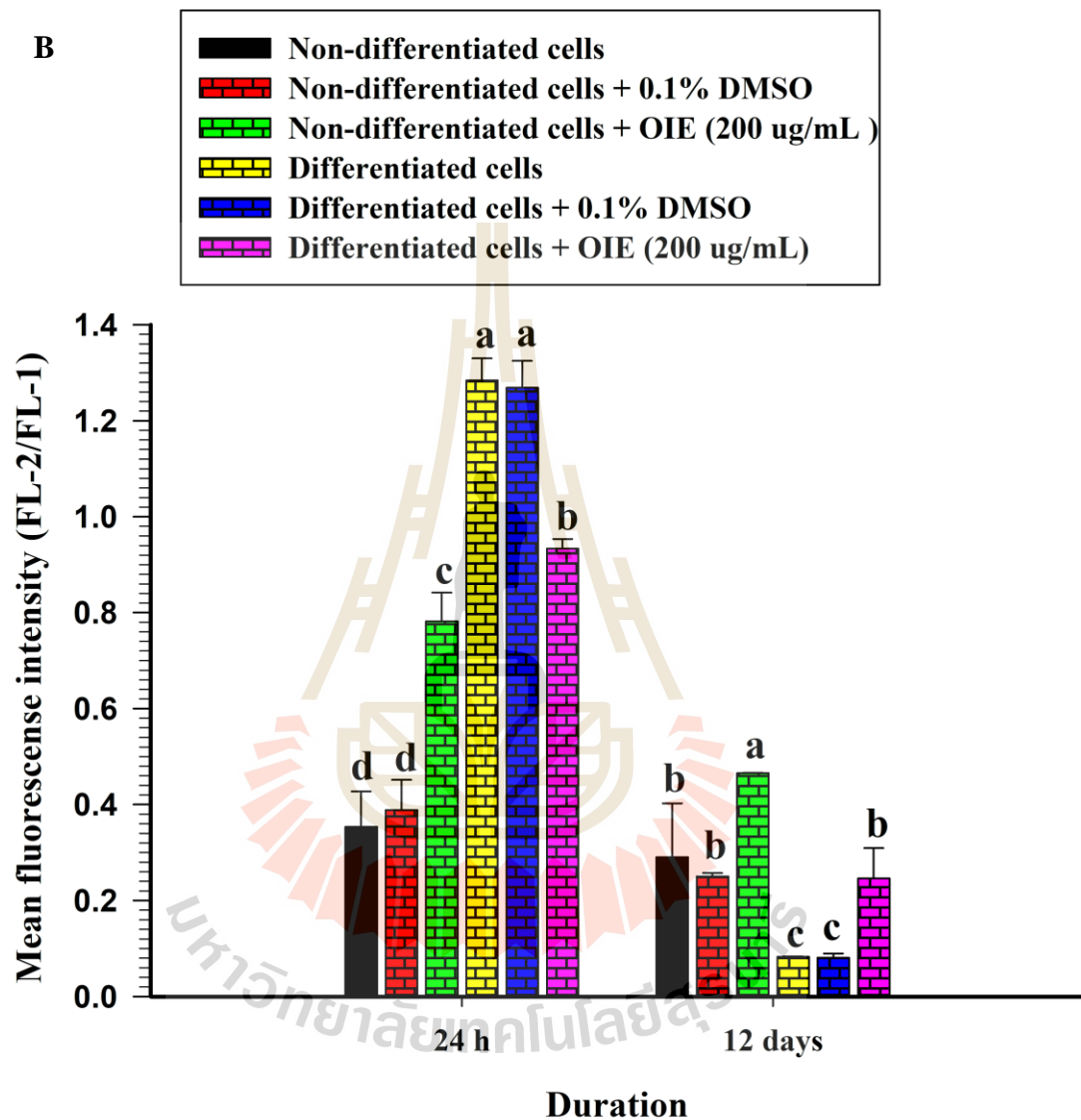


Figure 6.3 The effect of OIE on mitochondrial activity in 3T3-L1 cells (Continued).

(B) Imaging of cells labeling JC-1 at 24 h to vitalized mitochondria. J-monomer is visible as green and J-aggregates visible as red, scale bar; 200 μm . The result reported as means \pm SD value ($n = 3$). The different superscript alphabets are significantly

different from each other. Results were analyzed by ANOVA and Tukey's Post-hoc test ($P < 0.05$) (Continued).

C

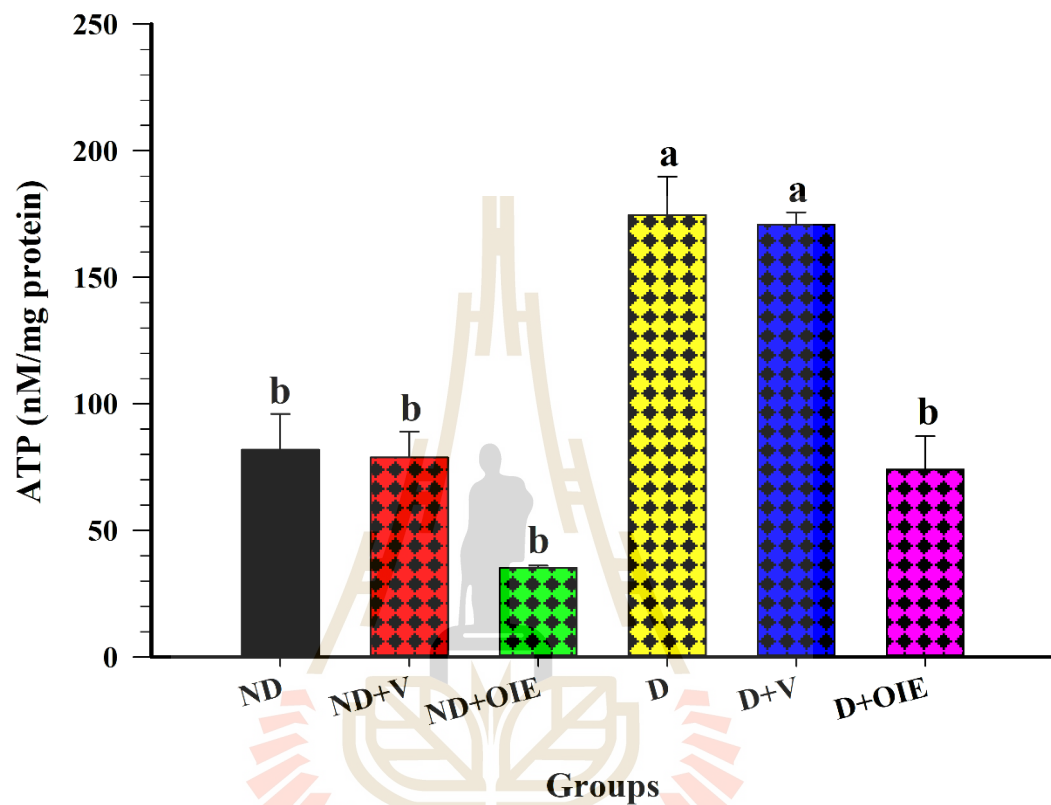


Figure 6.3 The effect of OIE on mitochondrial activity in 3T3-L1 cells (Continued). (C) ATP measurement was determined by ATP bioluminescent at day 12. The result reported as means \pm SD value ($n = 3$). The different superscript alphabets are significantly different from each other. Results were analyzed by ANOVA and Tukey's Post-hoc test ($P < 0.05$).

D

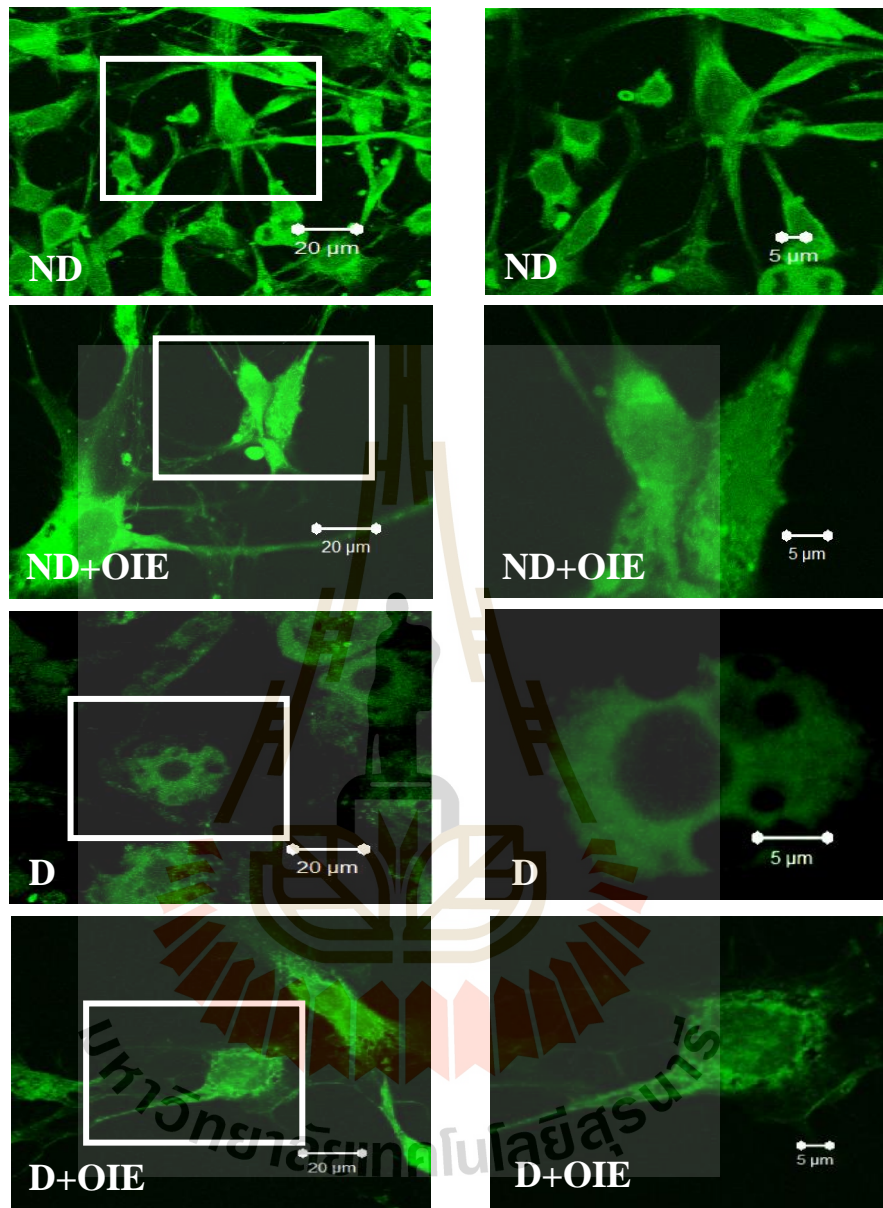


Figure 6.3 The effect of OIE on mitochondrial activity in 3T3-L1 cells (Continued).

(D) Confocal microscopic imaging of mitochondria labeling with MitoTracker dyes (green) at day 12 scale bar; 20 μm and 5 μm . ND = Non-differentiated cells (pre-adipocytes), ND+V = non-differentiated cells with 0.1% DMSO, ND+OIE = non-differentiated cells with 200 $\mu\text{g}/\text{mL}$ of OIE, D = Differentiated cells, D+V =

Differentiated cells with 0.1% DMSO, D+OIE = Differentiated cells with OIE at 200 $\mu\text{g}/\text{mL}$ (Continued).

E

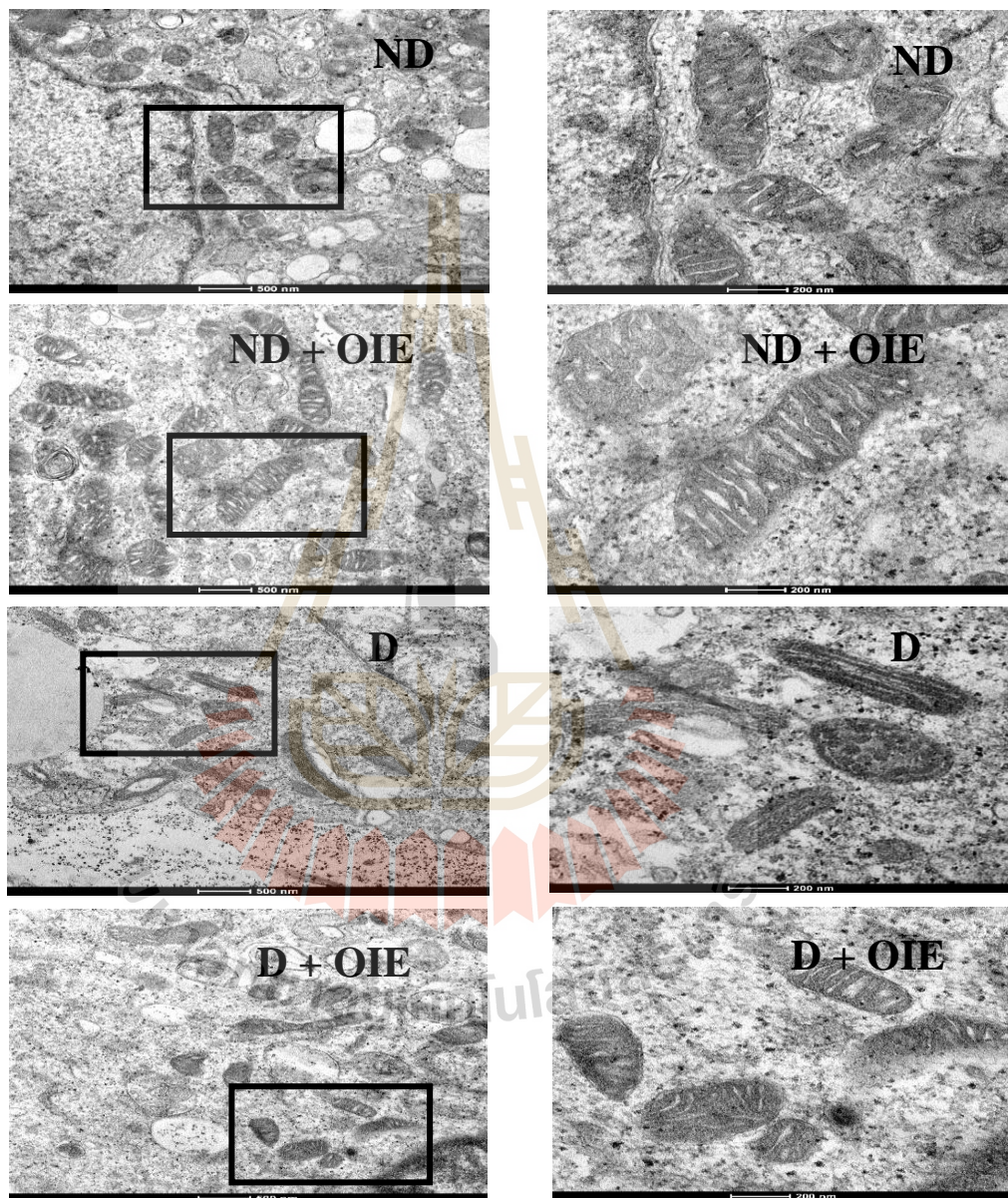


Figure 6.3 The effect of OIE on mitochondrial activity in 3T3-L1 cells (Continued).

(E) Transmission electron micrographs of mitochondria in 3T3-L1 cells. The left images (scale bar, 500 nm) show a lower magnification of the right images (scale bar, 200 nm). ND = Non-differentiated cells (pre-adipocytes), ND+V = non-differentiated

cells with 0.1% DMSO, ND+OIE = non-differentiated cells with 200 $\mu\text{g}/\text{mL}$ of OIE, D = Differentiated cells, D+V = Differentiated cells with 0.1% DMSO, D+OIE = Differentiated cells with OIE at 200 $\mu\text{g}/\text{mL}$ (Continued).

6.5 Discussion and conclusion

In the present study, our findings provide evidence that the agents, including isobutylmethylxanthine (IBMX), dexamethasone (DEX), and insulin can significantly induce growth-arrested 3T3-L1 cells to re-entry to the S and G2/M phase during the first 24 h of the cell cycle progression. The inducing agents enhance the differentiation by stimulating an increase in cellular cAMP. This can stimulate the production of several adipogenic transcriptional factors, including C/EBP α and PPAR γ (Parsons et al., 1988; Tae et al., 1995). However, the OIE at doses of 50-200 $\mu\text{g}/\text{mL}$ blocked the cell cycle at the G1/S stage, and this was subsequently confirmed by a significant decrease in the expression of Cdk2, a protein involved in the transition of G1/S to S/G2. Thus, these findings suggest that OIE blocks an important adipogenic event. As well as, other studies reported that natural products which inhibited adipocyte differentiation acted through a similar mechanism (Khalilpourfarshbafi et al., 2019; Tang et al., 2003).

The insulin signaling pathway contributes to the initiation of cell cycle progression during early adipogenesis (Kwon et al., 2012). When insulin binds to the insulin receptor at the cell surface, it activates tyrosine kinase activity, leading to autophosphorylation and phosphorylation of several receptor substrates (Solow et al., 1999). To understand the effect of the OIE on the insulin pathway and glucose metabolism, this research evaluated the level of tyrosine phosphorylation, GLUT4, and glucose uptake. The results showed that the protein tyrosine kinase activity was

apparent in the differentiated cells with or without OIE at 24 h. However, at day 12, the phosphorylation of proteins with molecular weights corresponding to 181 and 164 kDa was diminished by treatment with OIE. Whereas, this process of protein with MW at 91 kDa was not different compared to the differentiated control cells. The proteins with molecular masses of 181, 164, and 91 kDa correspond to the IRS-2, IRS-1, and IR β -subunit, respectively (Dupont et al., 1998; Eldar-Finkelman and Krebs, 1997; Miki et al., 2001). These results suggest that OIE may influence the activity of insulin and thus, the uptake of glucose. The increasing phosphorylation of IRS-1 and IRS-2 may activate many different signaling pathways, including phosphatidylinositol-3-kinase (PI3 kinase) and AKT pathway (Siddle, 2012). The activation of PI3 and AKT pathway has been suggested to be part of the signal transduction pathway for insulin-induced GLUT4 redistribution (Hajiaghaalipour et al., 2015). GLUT4 has long been known to be an insulin-responsive glucose transporter. This study found that GLUT4 was slightly expressed in the same amount in all groups at 24 h. These observations are in substantial agreement with the study of Jackson et al., that at the early part of differentiation, the expression of GLUT4 is low, but increase to reach a peak at day 9 (Jackson et al., 2017). Similarly, in this investigation, GLUT4 was significantly increased and highly expressed to the cell membrane in untreated adipocytes at day 12. The cells treated with OIE displayed a lower concentration of GLUT4. These findings lead me to believe that the cells are insensitive to insulin and may act on GLUT4 expression and glucose uptake. One suggestion is that OIE inhibits the phosphorylation of IRS-1 and IRS-2, leading to a decrease in GLUT4 protein expression and translocation to the membrane compared to the OIE-untreated adipocytes. If GLUT4 expression is compromised, this would have an impact on glucose uptake and intracellular glucose concentrations.

Differentiated control cells (nontreated or untreated adipocytes) gradually increased their glucose uptake compared to undifferentiated cells at 48 h and day 12, respectively. Whereas, differentiated cells treated with OIE significantly increased glucose uptake level by 2 folds compared to untreated differentiated cells. It was also observed that OIE-treated pre-adipocytes also had significantly increased in the glucose uptake. This exploration implies that the presence of insulin can stimulate the tyrosine kinase activity at the insulin receptor, results in autophosphorylation and initiate of other cell signaling pathways cause an increase in GLUT4 localization at the plasma membrane. However, OIE treated pre-adipocytes significantly increased glucose uptake level by 2-folds with no effect on GLUT4 expression. This may be explained as cells treated with OIE may use GLUT1 and is less dependent on GLUT4. In fact, in adipose tissue, GLUT1 is expressed along with GLUT4 (Shetty et al., 1993). Some of the antidiabetic drugs such as rosiglitazone and thiazolidinediones in both basal and insulin stages increase glucose uptake along with GLUT1, but no effect on GLUT4 expression (Ciaraldi and Henry, 1997; Nugent et al., 2001). Also, Berberine is a major alkaloid component of *Rhizoma coptidis*, has shown promising effect in up-regulation of GLUT-1 expression level by stimulating ERK pathway in 3T3-L1 cells (Cok et al., 2011; Kim et al., 2007).

Mitochondria are considered as the powerhouses of the cell (Tait and Green, 2012). In human white adipocytes, mitochondria produce > 95% cellular ATP which required for cell metabolism and other general cellular processes (Kaaman et al., 2007). Previous studies had demonstrated that during adipogenesis, mitochondria were present at number 19 folds greater than 3T3-L1 pre-adipocyte (Kim et al., 2004). Similarly, this investigating found that the level of mitochondria membrane potential (MMP) was significantly increased during differentiation at early 24 h. However, when cells

become mature adipocytes at day 12, the MMP level was dramatically decreased, while the ATP level was shown in a different way (Figure 6.3C). Additionally, confocal microscopy revealed that the adipocytes mitochondria displayed pale green fluorescence, which represents the mitochondrial mass. Moreover, the morphology of adipocytes mitochondria was elongated. This finding is consistent with the previous study that during cells differentiation, the mitochondria continuously switch their morphology from globular to elongated mitochondria via mitochondrial fusion (Lee et al., 2019). Accordingly, mitochondria undergo dynamic remodeling during differentiation, and thus, mitochondrial morphology and metabolism are changed. Although a massive increase in the number and activity of mitochondria beginning in the early adipogenesis (Kaaman et al., 2007). This is because mitochondria provide the key substrate necessary for lipogenesis (Rosen and Spiegelman, 2006). However, the study of Goldman et al. confirmed that mature adipocytes contained very few mitochondria compared to the cells undergoing in the differentiation process (Goldman et al., 2011). The decreasing of mitochondria content likely reflects the decrease needs for lipogenesis in the mature white adipocyte and the changing of mitochondria morphology could disrupt to their function (Cogliati et al., 2016; Hackenbrock, 1966; Kim et al., 2004). In the same way, the altered mitochondrial morphology in adipocytes was observed in this study. Thus, these findings lend support to the assumption that at the early phase of differentiation, untreated differentiated cells need a lot of ATP production for lipogenesis as shown increasing of MMP level at 24 h, while the fusion of adipocyte mitochondrial at day 12 takes effect to the mitochondria activity results in a decrease in the MMP level. Apart from this, an increasing ATP level in adipocytes may be explained that the mitochondria have been compromised, and then, the cell

switches to glycolysis. However, ATP generated from the glycolysis pathway may not be enough for the cells. Thus, cells try to keep homeostasis by increasing glucose uptake level. On the other hand, OIE-treated adipocytes exhibited significantly lower and higher MMP level compared to untreated adipocytes at 24 h and day 12, respectively. These results suggest that OIE may slow the cell division and cell growth and not much use of ATP, like preadipocytes, leads to lipogenesis reduction. Moreover, the mitochondria mass and morphology are virtually similar to preadipocytes mitochondria. In conclusion, the anti-adipogenic activity of OIE was achieved through the inhibition of cell cycle progression and reduced the expression of protein IRS-1 and IRS-2 resulted in a decrease in the glucose uptake level. Furthermore, OIE slowed down the mitochondrial activity of the early phase of cell differentiation caused lipogenesis reduction, which was similar to the preadipocytes stage.

6.6 References

- Ailhaud, G., Dani, C., Amri, E. Z., Djian, P., Vannier, C., Doglio, A., Forest, C., Gaillard, D., Négre, R., and Grimaldi, P. (1989). Coupling growth arrest and adipocyte differentiation. **Environmental Health Perspectives**. 80: 17-23.
- Arruda, A. P., Pers, B. M., Parlakgöl, G., Güney, E., Inouye, K., and Hotamisligil, G. S. (2014). Chronic enrichment of hepatic endoplasmic reticulum-mitochondria contact leads to mitochondrial dysfunction in obesity. **Nature Medicine**. 20(12): 1427-1435.
- Assimacopoulos-Jeannet, F., Brichard, S., Rencurel, F., Cusin, I., and Jeanrenaud, B. (1995). In vivo effects of hyperinsulinemia on lipogenic enzymes and glucose

- transporter expression in rat liver and adipose tissues. **Metabolism**. 44(2): 228-233.
- Bertram, R., Gram Pedersen, M., Luciani, D. S., and Sherman, A. (2006). A simplified model for mitochondrial ATP production. **Journal of Theoretical Biology**. 243(4): 575-586.
- Camp, H. S., Ren, D., and Leff, T. (2002). Adipogenesis and fat-cell function in obesity and diabetes. **Trends in Molecular Medicine**. 8(9): 442-447.
- Ciaraldi, T., and Henry, R. R. (1997). Thiazolidinediones and their effects on glucose transporters. **European Journal of Endocrinology**. 137(6): 610-612.
- Cogliati, S., Enriquez, J. A., and Scorrano, L. (2016). Mitochondrial Cristae: Where Beauty Meets Functionality. **Trends in Biochemical Sciences**. 41(3): 261-273.
- Cok, A., Plaisier, C., Salie, M. J., Oram, D. S., Chenge, J., and Louters, L. L. (2011). Berberine acutely activates the glucose transport activity of GLUT1. **Biochimie**. 93(7): 1187-1192.
- Deshmukh, A. S. (2016). Insulin-stimulated glucose uptake in healthy and insulin-resistant skeletal muscle. **Hormone Molecular Biology and Clinical Investigation**. 26(1): 13-24.
- Dunkhunthod, B., Thumanu, K., and Eumkeb, G. (2017). Application of FTIR microspectroscopy for monitoring and discrimination of the anti-adipogenesis activity of baicalein in 3T3-L1 adipocytes. **Vibrational Spectroscopy**. 89: 92-101.
- Dupont, J., Derouet, M., Simon, J., and Taouis, M. (1998). Nutritional state regulates insulin receptor and IRS-1 phosphorylation and expression in chicken. **American Journal of Physiology**. 274(2): E309-316.

- Eldar-Finkelman, H., and Krebs, E. G. (1997). Phosphorylation of insulin receptor substrate 1 by glycogen synthase kinase 3 impairs insulin action. **Proceedings of the National Academy of Sciences of the United States of America**. 94(18): 9660-9664.
- Glimcher, L. H., and Lee, A.-H. (2009). From sugar to fat: How the transcription factor XBP1 regulates hepatic lipogenesis. **Annals of the New York Academy of Sciences**. 1173 Suppl 1(Suppl 1): E2-E9.
- Goldman, S. J., Zhang, Y., and Jin, S. (2011). Autophagic degradation of mitochondria in white adipose tissue differentiation. **Antioxidants and Redox Signaling**. 14(10): 1971-1978.
- Gruenwald, J., Freder, J., and Armbruester, N. (2010). Cinnamon and Health. **Critical Reviews in Food Science and Nutrition**. 50(9): 822-834.
- Hackenbrock, C. R. (1966). Ultrastructural bases for metabolically linked mechanical activity in mitochondria: I. Reversible ultrastructural changes with change in metabolic steady state in isolated liver mitochondria. **The Journal of Cell Biology**. 30(2): 269-297.
- Hajiaghaalipour, F., Khalilpourfarshbafi, M., and Arya, A. (2015). Modulation of glucose transporter protein by dietary flavonoids in type 2 diabetes mellitus. **International Journal of Biological Sciences**. 11(5): 508-524.
- Jackson, R. M., Griesel, B. A., Gurley, J. M., Szweda, L. I., and Olson, A. L. (2017). Glucose availability controls adipogenesis in mouse 3T3-L1 adipocytes via up-regulation of nicotinamide metabolism. **The Journal of Biological Chemistry**. 292(45): 18556-18564.

- Kaaman, M., Sparks, L. M., van Harmelen, V., Smith, S. R., Sjolín, E., Dahlman, I., and Arner, P. (2007). Strong association between mitochondrial DNA copy number and lipogenesis in human white adipose tissue. **Diabetologia**. 50(12): 2526-2533.
- Kapoor, R. V., Coyle, R., Staton, C. A., Brown, N. J., and Vaidyanathan, S. (2017). Influence of washing and quenching in profiling the metabolome of adherent mammalian cells: a case study with the metastatic breast cancer cell line MDA-MB-231. **Analyst**. 142(11): 2038-2049.
- Khalilpourfarshbafi, M., Gholami, K., Murugan, D. D., Abdul Sattar, M. Z., and Abdullah, N. A. (2019). Differential effects of dietary flavonoids on adipogenesis. **European Journal of Nutrition**. 58(1): 5-25.
- Kim, B. W., Choo, H. J., Lee, J. W., Kim, J. H., and Ko, Y. G. (2004). Extracellular ATP is generated by ATP synthase complex in adipocyte lipid rafts. **Experimental and Molecular Medicine**. 36(5): 476-485.
- Kim, S. H., Shin, E. J., Kim, E. D., Bayarara, T., Frost, S. C., and Hyun, C. K. (2007). Berberine activates GLUT1-mediated glucose uptake in 3T3-L1 adipocytes. **Biological and Pharmaceutical Bulletin**. 30(11): 2120-2125.
- Kwon, J. Y., Seo, S. G., Heo, Y. S., Yue, S., Cheng, J. X., Lee, K. W., and Kim, K. H. (2012). Piceatannol, natural polyphenolic stilbene, inhibits adipogenesis via modulation of mitotic clonal expansion and insulin receptor-dependent insulin signaling in early phase of differentiation. **Journal of Biological Chemistry**. 287(14): 11566-11578.
- Lee, J. E., Seo, B. J., Han, M. J., Hong, Y. J., Hong, K., Song, H., Lee, J. W., and Do, J. T. (2019). Changes in the expression of mitochondrial morphology-related

genes during the differentiation of murine embryonic stem cells. **BioRxiv**: 644906.

Miki, H., Yamauchi, T., Suzuki, R., Komeda, K., Tsuchida, A., Kubota, N., Terauchi, Y., Kamon, J., Kaburagi, Y., Matsui, J., Akanuma, Y., Nagai, R., Kimura, S.-i., Tobe, K., and Kadowaki, T. (2001). Essential Role of Insulin Receptor Substrate 1 (IRS-1) and IRS-2 in Adipocyte Differentiation. **Molecular and Cellular Biology**. 21(7): 2521–2532.

Nugent, C., Prins, J. B., Whitehead, J. P., Savage, D., Wentworth, J. M., Chatterjee, V. K., and O'Rahilly, S. (2001). Potentiation of glucose uptake in 3T3-L1 adipocytes by PPAR gamma agonists is maintained in cells expressing a PPAR gamma dominant-negative mutant: evidence for selectivity in the downstream responses to PPAR gamma activation. **Molecular Endocrinology**. 15(10): 1729-1738.

Parsons, W. J., Ramkumar, V., and Stiles, G. L. (1988). Isobutylmethylxanthine stimulates adenylate cyclase by blocking the inhibitory regulatory protein, Gi. **Molecular Pharmacology**. 34(1): 37-41.

Roberts, L. D., Virtue, S., Vidal-Puig, A., Nicholls, A. W., and Griffin, J. L. (2009). Metabolic phenotyping of a model of adipocyte differentiation. **Physiological Genomics**. 39(2): 109-119.

Rosen, E. D., and Spiegelman, B. M. (2006). Adipocytes as regulators of energy balance and glucose homeostasis. **Nature**. 444(7121): 847-853.

Ruiz-Ojeda, F. J., Ruperez, A. I., Gomez-Llorente, C., Gil, A., and Aguilera, C. M. (2016). Cell Models and Their Application for Studying Adipogenic

Differentiation in Relation to Obesity: A Review. **International Journal of Molecular Sciences**. 17(7).

Scherer, P. E., Williams, S., Fogliano, M., Baldini, G., and Lodish, H. F. (1995). A novel serum protein similar to C1q, produced exclusively in adipocytes. **Journal of Biological Chemistry**. 270(45): 26746-26749.

Schrauwen-Hinderling, V. B., Kooi, M. E., Hesselink, M. K. C., Jeneson, J. A. L., Backes, W. H., Van Echteld, C. J. A., Van Engelshoven, J. M. A., Mensink, M., and Schrauwen, P. (2007). Impaired in vivo mitochondrial function but similar intramyocellular lipid content in patients with type 2 diabetes mellitus and BMI-matched control subjects. **Diabetologia**. 50(1): 113-120.

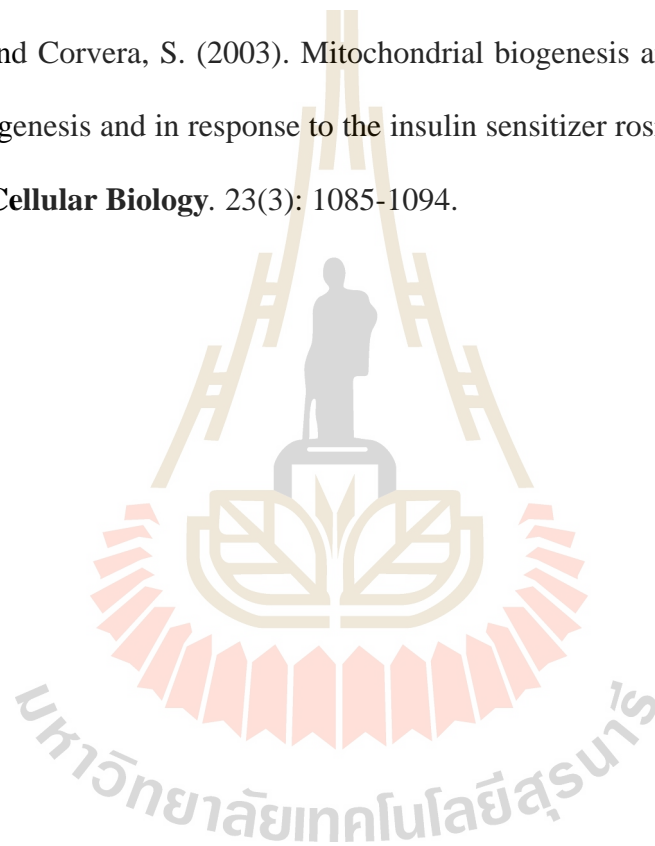
Shetty, M., Loeb, J., Vikstrom, K., and Ismail-Beigi, F. (1993). Rapid activation of GLUT-1 glucose transporter following inhibition of oxidative phosphorylation in clone 9 cells. **Journal of Biological Chemistry**. 268(23): 17225-17232.

Siddle, K. (2012). Molecular basis of signaling specificity of insulin and IGF receptors: neglected corners and recent advances. **Frontiers in Endocrinology (Lausanne)**. 3: 34.

Solow, B. T., Harada, S., Goldstein, B. J., Smith, J. A., White, M. F., and Jarett, L. (1999). Differential Modulation of the Tyrosine Phosphorylation State of the Insulin Receptor by IRS (Insulin Receptor Subunit) Proteins. **Molecular Endocrinology**. 13(10): 1784-1798.

Tae, H. J., Zhang, S., and Kim, K. H. (1995). cAMP activation of CAAT enhancer-binding protein-beta gene expression and promoter I of acetyl-CoA carboxylase. **Journal of Biological Chemistry**. 270(37): 21487-21494.

- Tait, S. W. G., and Green, D. R. (2012). Mitochondria and cell signalling. **Journal of Cell Science**. 125(Pt 4): 807-815.
- Tang, Q. Q., Otto, T. C., and Lane, M. D. (2003). Mitotic clonal expansion: a synchronous process required for adipogenesis. **Proceedings of the National Academy of Sciences of the United States of America**. 100(1): 44-49.
- Wilson-Fritch, L., Burkart, A., Bell, G., Mendelson, K., Leszyk, J., Nicoloso, S., Czech, M., and Corvera, S. (2003). Mitochondrial biogenesis and remodeling during adipogenesis and in response to the insulin sensitizer rosiglitazone. **Molecular and Cellular Biology**. 23(3): 1085-1094.



CHAPTER VII

CONCLUSIONS

To summarize, *O. indicum*, *C. verum*, *T. triandra*, and *P. edulis* ethanolic extracts showed anti-adipogenesis effects. Among 4 types of plants, *O. indicum* extract (OIE) exhibited the highest potential to inhibit the differentiation of pre-adipocytes to adipocytes, which 200 µg/mL OIE-treated adipocytes could reduce lipid accumulation by 52 %. Thus, OIE was selected for further investigation. The main phytochemical composition of OIE at 20 mg/mL was detected by LC-MS and GC-MS including baicalein (657.01 µg/mL), γ -Sitosterol (17.19 %), 2-methyl-2-cyclohexen-1-one (15.28 %), 4-hydroxy-benzene ethanol (13.33 %), 3-hydroxy-2-methylbenzaldehyde (11.18 %). Furthermore, the possible mechanism of the OIE on anti-adipogenesis was investigated. These findings provide evidence that OIE could act as an inhibitor by the following mechanisms; 1) OIE delays cell cycle progression at the early phase of cell differentiation, 2) OIE inhibits adipogenic transcriptional factor including, PPAR γ 2 and SREBP-1c, and 3) OIE decreases IRS-1 and IRS-2 phosphorylation. These results provide compelling evidence that these mechanisms will lead to affect the downstream pathway, including a decrease in Cyclin-dependent kinase 2 (Cdk2), fatty acid synthetase enzyme (FAS), lipid accumulation level, adipokines expression (adiponectin), and glucose uptake level. Furthermore, these results are the first study to my knowledge to investigate that the OIE can improve the mitochondria membrane potential (MMP), which is decreased in mature adipocytes,

and protect mitochondria morphology. In summary, the preliminary mechanism of OIE acted as 3T3-L1 adipogenesis inhibition is summarized in Figure 7.1. So, this research provides novel evidence that OIE contains flavonoid such as Baicalein, and volatile compounds such as γ -sitosterol, etc. that can act as anti-adipogenesis on 3T3-L1 adipocytes. For this reason, OIE has high potential to develop as a novel health food supplement, herbal medicine, or modern drug for the prevention and treatment of hyperlipidemia and obesity. However, further research in animal models and clinical study are still required.

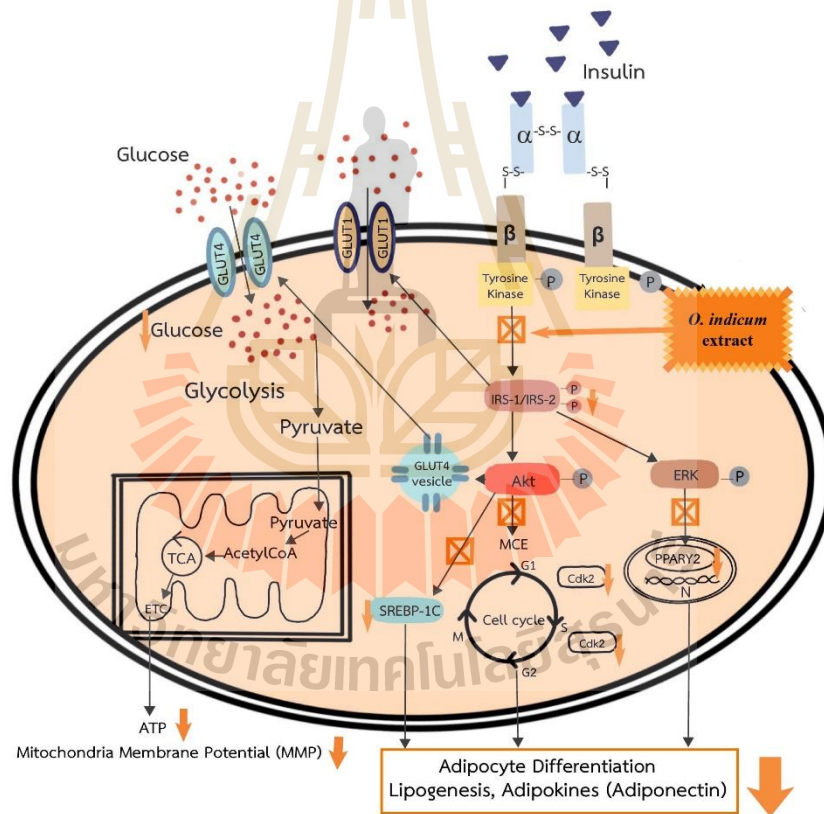
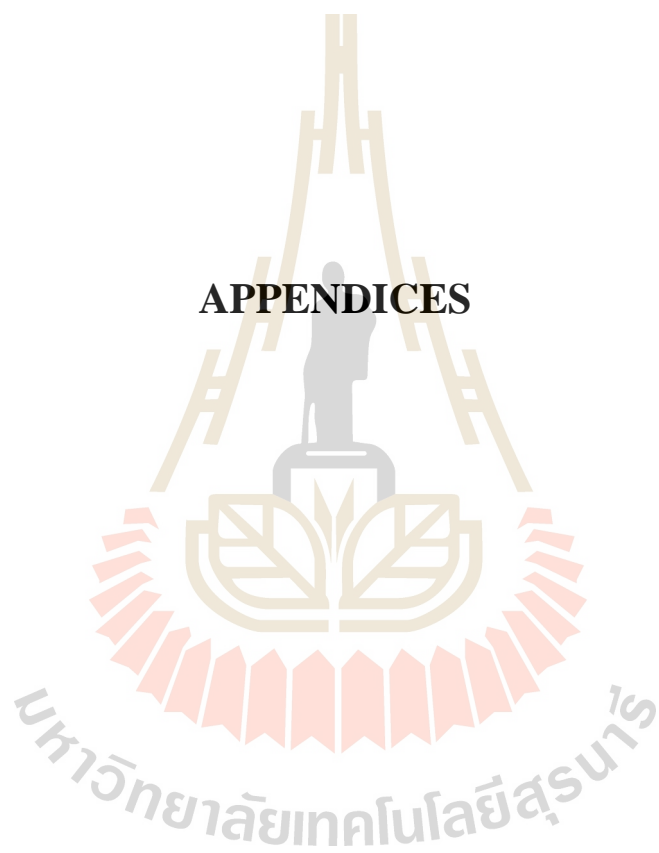


Figure 7.1 Schematic represents the preliminary mechanisms of the anti-adipogenesis of the OIE on 3T3-L1 adipocytes. During adipogenesis, when insulin binds to α -subunit of the insulin receptor, it initiates the phosphorylation of β -subunit (tyrosine kinase domain). These can trigger the phosphorylation of IRS-1/IRS-2, which in turn, start

many protein activations cascades (GLUT4), stimulate the transcriptional factor (PPAR γ 2 and SREBP-1c), and mitotic clonal expansion (MCE). Then, recruit other proteins for adipocytes differentiation and lipogenesis pathway. OIE treats on adipocytes leads to down-regulate adipogenic transcription by a decrease in phosphorylation of IRS-1/IRS-2 (Continued).

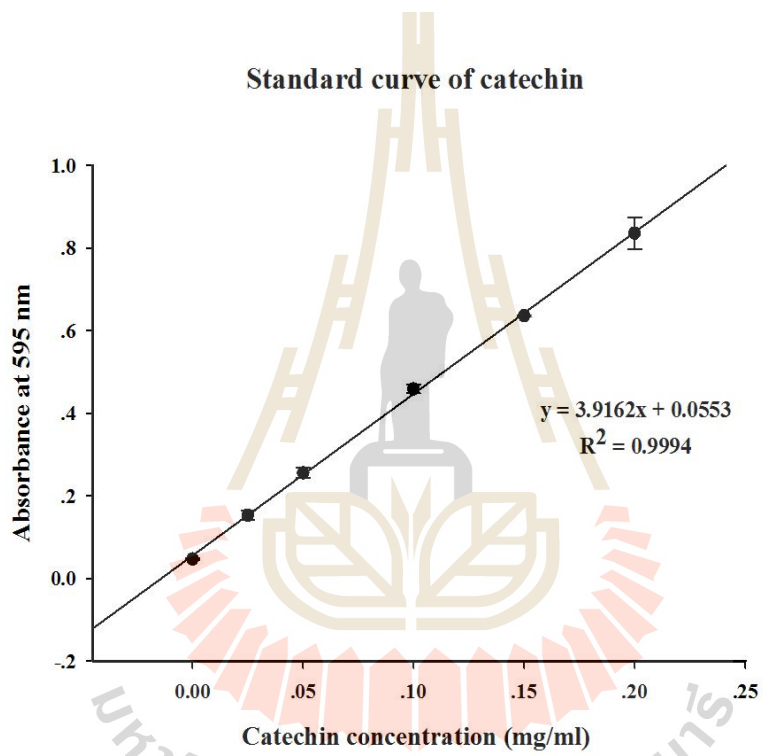


APPENDICES

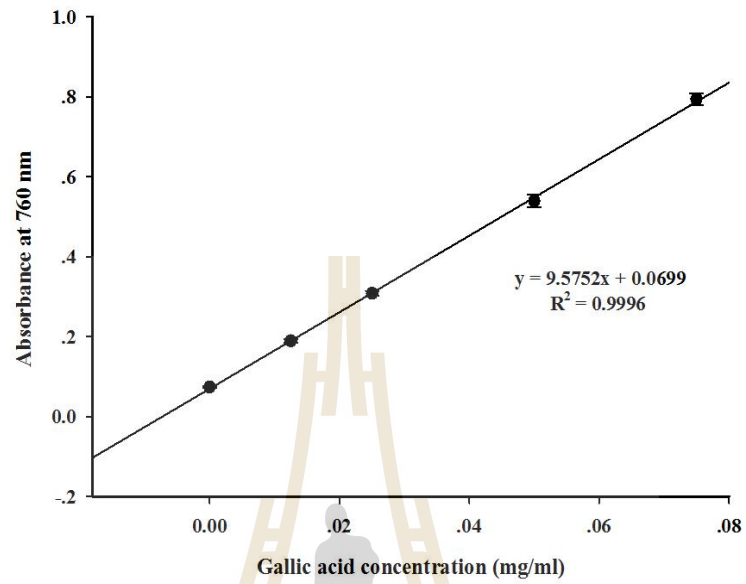


APPENDIX A

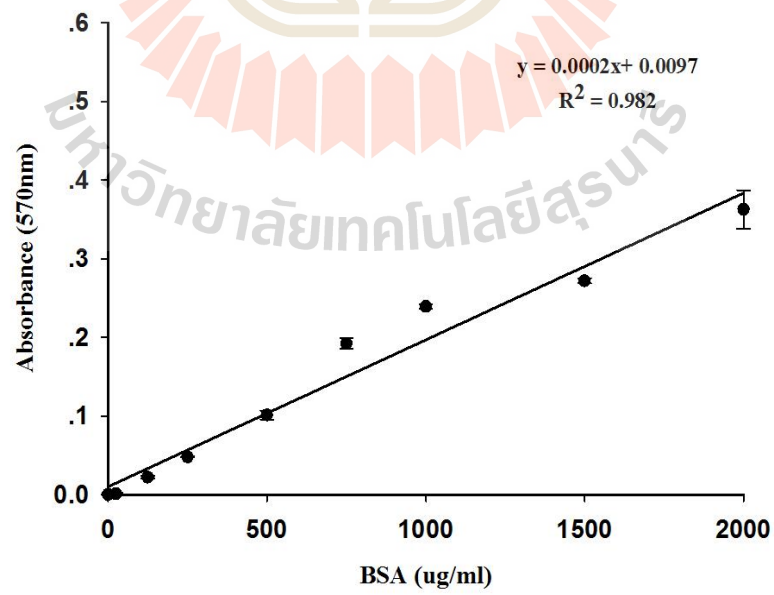
STANDARD CURVE



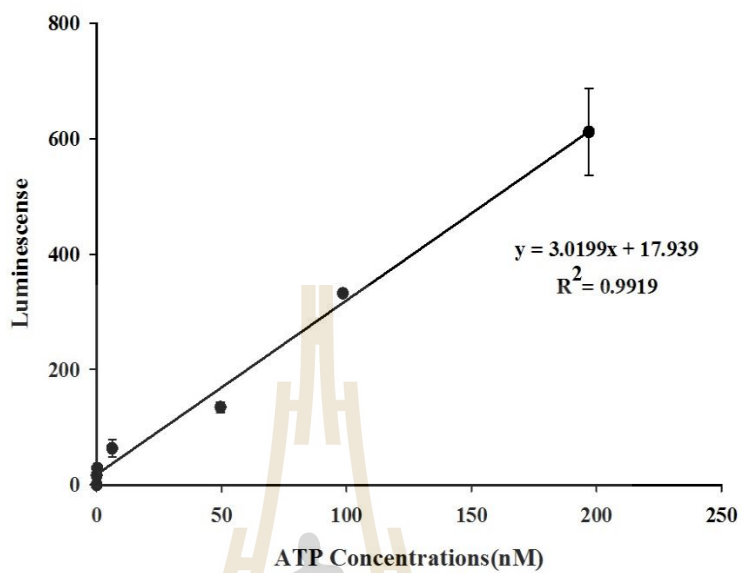
Standard curve of gallic acid



BSA standard curve



ATP standard curve



APPENDIX B

REAGENTS AND BUFFERS

1. Cell culture media

1.1 Media formulations use throughout

1.1.1 Pre-adipocyte Expansion Medium:

	g/liter
Dulbecco's Modified Eagle's Medium (DMEM)	90 %
Bovine Calf Serum	10 %

1.1.2 Differentiation Medium:

	g/liter
Dulbecco's Modified Eagle's Medium (DMEM)	90 %
Fetal Bovine Serum (FBS)	10 %
Dexamethasone	10 μ M
Methylisobutylxanthine (IBMX)	10 mM
Insulin	1.0 μ g/mL

1.1.2 Adipocyte Maintenance Medium:

	g/liter
Dulbecco's Modified Eagle's Medium (DMEM)	90 %
Fetal Bovine Serum (FBS)	10 %
Insulin	1.0 μ g/mL

2 Reagents and Buffers for SDS-PAGE

1.2.1 Tris-lysis buffer pH 8.2 (100 mM NaCl, 50 mM Tris-base, 2 mM EDTA, 0.02% NaN₃)

	g/liter
NaCl (MW.58.44)	2.922 gm
Tris-base (MW.121.1)	3.030 gm
EDTA (C ₁₀ H ₁₆ Na ₂ O ₈ MW.292.25)	0.292 gm
NaN ₃ (MW.65.01)	0.100 gm
ddH ₂ O	200 mL
Adjust pH to 8.2 with 1N HCl	
Adjust volume with ddH ₂ O to	500 mL
Filtrate and store at RT	

1.2.2 Lysis buffer with detergents and protease inhibitors (10 ml)

	g/liter
10% Triton X-100	1 mL
Iodoacetamide (0.5M in ddH ₂ O)	100 µL
Aprotinin (1 mg/mL in PBS)	100 µL
Pepstatin A	10 µL
Phenylmethylsulfonyl fluoride (PMSF; 100 mM in acetone)	100 µL
Tris lysis buffer pH 8.2	8.7 mL
Mix well and aliquot to vial and store at -20 °C	

1.2.3 1.5 M Tris-HCl pH 8.8 (4x Running gel buffer)

	g/liter
Tris-base (MW.121.1)	9.08 gm
ddH ₂ O	20 mL
Adjust pH to 8.8 with HCl	
Adjust volume with ddH ₂ O to	50 mL

1.2.4 0.5 M Tris-HCl pH 6.8 (4x Stacking gel buffer)

	g/liter
Tris-base (MW.121.1)	3 gm
ddH ₂ O	25 mL
Adjust pH to 6.8 with HCl	
Adjust volume with ddH ₂ O to	50 mL

1.2.5 30 % Monomer (30.8 %T, 2.7 % Cbis): (50 mL)

	g/liter
Acrylamide (MW.71.08)	15 gm
Bis-acrylamide (MW. 154.2)	0.4 gm
ddH ₂ O to	50 mL

Filtrate with 0.45 µm filter paper and Degas before use

Store in dark at 4 °C (up to 3 months)

1.2.6 1x Running buffer (1,000 mL)

	g/liter
Glycine (MW. 75.07)	14.413 gm
Tris-base (MW.121.1)	3.028 gm
SDS	1 gm
ddH ₂ O	1,000 mL

1.3 Reagents and Buffers for Western Blotting**1.3.1 Towbin buffer (25 mM Tris; 192 mM Glycine; 20 % Methanol)**

	g/liter
Tris-base (MW.121.1)	3.030 gm
Glycine (MW.74.05)	14.4 gm
Methanol	200 mL
Adjust volume with ddH ₂ O to	1,000 mL
Mix well until dissolved and store at RT	

1.3.2 5 % Skimmed Milk (or BSA)

	g/liter
Skimmed milk	2.5 gm
1X PBS	50 mL
Mix well until dissolved (Freshly prepare before use)	

1.3.3 0.1 % Tween20 in 1X PBS (Prepare before use)

	g/liter
Tween 20	0.5 mL
1X PBS	500 mL
Mix well and store at RT	

1.3.4 0.025 % Coomassie Brilliant blue R250 (40 % methanol, 7 % Acetic acid)

	g/liter
Coomassie brilliant blue R250 (Bio-Rad)	0.0625 gm
Methanol	100 mL
Acetic acid	17.5 mL
Add ddH ₂ O to	250 mL
Mix well until dissolved and store at RT	

1.3.5 De-staining gel solution I (40 % Methanol, 7 % Acetic acid)

	g/liter
Coomassie brilliant blue R250 (Bio-Rad)	0.0625 gm
Methanol	200 mL
Acetic acid	35 mL
Add ddH ₂ O to	500 mL
Mix well until dissolved and store at RT	

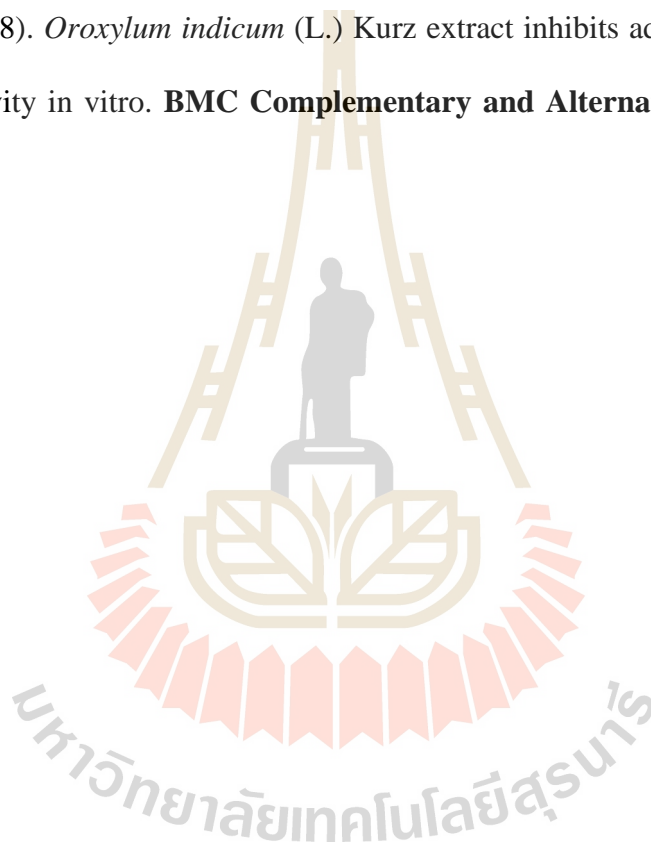
1.3.6 De-staining gel solution II (5 % Methanol, 7 % Acetic acid)

	g/liter
Coomassie brilliant blue R250 (Bio-Rad)	0.0625 gm
Glacial acetic acid	35 mL
Add ddH ₂ O to	500 mL
Mix well until dissolved and store at RT	

APPENDIX C

PUBLICATIONS

- Hengpratom, T.,** Lowe, G., Thumanu, K., Suknasang, S., Tiamyom, K., Eumkeb, G.,
(2018). *Oroxylum indicum* (L.) Kurz extract inhibits adipogenesis and lipase
activity in vitro. **BMC Complementary and Alternative Medicine.** 18(1),
177.



RESEARCH ARTICLE

Open Access

Oroxylum indicum (L.) Kurz extract inhibits adipogenesis and lipase activity in vitro



Tanaporn Hengpratom¹, Gordon M. Lowe², Kanjana Thumanu³, Siriporn Suknasang¹, Kanokwan Tiomyom¹ and Griangsak Eumkeb^{1*}

Abstract

Background: *Oroxylum indicum* (L.) Kurz (*O. indicum*) is found in Thailand. It has been used for the treatment of obesity. This study aimed to investigate the effects of an *O. indicum* extract (OIE) on the adipogenic and biomolecular change in 3T3-L1 adipocytes.

Methods: Initial studies examined the chemical components of OIE. The cell line 3T3-L1 was used to establish potential toxic effects of OIE during the differentiation of pre-adipocytes to adipocytes. The inhibitory effect of OIE on lipid accumulation in 3T3-L1 cells was investigated. Moreover, the impact of OIE on pancreatic lipase activity was determined. In further experiments, Fourier Transform Infrared (FTIR) was used to monitor and discriminate biomolecular changes caused by the potential anti-adipogenic effect of OIE on 3T3-L1 cells.

Results: Chemical screening methods indicated that OIE was composed of flavonoids, alkaloids, steroids, glycosides, and tannins. The percentage viability of 3T3-L1 cells was not significantly decreased after exposure to either 200 or 150 µg/mL of OIE for 2 and 10 days, respectively compared to control cells. The OIE exhibited a dose-dependent reduction of lipid accumulation compared to the control ($p < 0.05$). The extract also demonstrated a dose-dependent inhibitory effect upon lipase activity compared to the control. The inhibitory effect of the OIE on lipid accumulation in 3T3-L1 cells was also confirmed using FTIR microspectroscopy. The signal intensity and the integrated areas relating to lipids, lipid esters, nucleic acids, glycogen and carbohydrates of the OIE-treated 3T3-L1 adipocytes were significantly lower than the non-treated 3T3-L1 adipocytes ($p < 0.05$). Principal component analysis (PCA) indicated four distinct clusters for the FTIR spectra of 3T3-L1 adipocytes based on biomolecular changes (lipids, proteins, nucleic acids, and carbohydrates). This observation was confirmed using Unsupervised hierarchical cluster analysis (UHCA).

Conclusions: These novel findings provide evidence that the OIE derived from the fruit pods of the plant is capable of inhibiting lipid and carbohydrate accumulation in adipocytes and also has the potential to inhibit an enzyme associated with fat absorption. The initial observations indicate that OIE may have important properties which in the future may be exploited for the management of the overweight or obese.

Keywords: *Oroxylum indicum* (L.) Kurz, Adipogenesis, Lipase activity, 3T3-L1 adipocytes, FTIR microspectroscopy, Lipid-lowering drugs

* Correspondence: griang@sut.ac.th

¹School of Preclinic, Institute of Science, Suranaree University of Technology,
Nakhon Ratchasima 3000, Thailand

Full list of author information is available at the end of the article



© The Author(s). 2018 **Open Access** This article is distributed under the terms of the Creative Commons Attribution 4.0 International License (<http://creativecommons.org/licenses/by/4.0/>), which permits unrestricted use, distribution, and reproduction in any medium, provided you give appropriate credit to the original author(s) and the source, provide a link to the Creative Commons license, and indicate if changes were made. The Creative Commons Public Domain Dedication waiver (<http://creativecommons.org/publicdomain/zero/1.0/>) applies to the data made available in this article, unless otherwise stated.

Background

Obesity has become a major global health problem [1]. It is a major contributor to diseases such as diabetes, cardiovascular disease and hypertension [2]. It has been established that being overweight or obese is associated with an increase in both the size and number of adipocytes along with an excessive amount of fat accumulation [3, 4]. Although using appetite suppressant drugs is a common way to treat obesity, long-term pharmacological treatment has been reported to generate many side-effects [5, 6]. This has led to innovative research using natural products to combat obesity in the hope of a safe and novel treatment [7, 8].

O. indicum belongs to Bignoniaceae family, widely found in Tropical Asia including Thailand. The chemical composition of *O. indicum* includes baicalein, chrysin, oroxylin A and oroxylin B [9, 10]. Many previous studies have reported antioxidant [11], anti-inflammatory [12], anti-diabetic [13] and hepatoprotective properties for *O. indicum* and its isolated compounds [14]. Animal studies suggest that *O. indicum* has few toxic effects and oral doses of 250 mg/kg BW for 28 days were tolerated well in rats [13]. It has previously been demonstrated that an extract of *O. indicum* derived from the root of the plant reduced the plasma concentrations of glucose, triglycerides and total cholesterol in diabetic rats [15]. Furthermore, stem bark extracts generated an inhibitory effect on an α -glucosidase enzyme in mature 3T3-L1 adipocytes [13]. Whilst, Oroxylin A, an isolated compound from *O. indicum*, induced both anti-adipogenesis and lipolysis in 3T3-L1 adipocytes. This was largely explained by a down-regulation of many transcriptional factors and an enhanced expression of pro-apoptotic proteins [16].

OIE has varying pharmacological properties depending on which part of the plant it is derived. In this study, we have used an extract from the fruit pods, rather than the stem of the plant which has been previously studied by several groups. The aim of this study was to provide a simple chemical composition of the extract. Initial experiments were performed using 3T3-L1 cells to establish any potential toxic effects of OIE and its impact on lipid accumulation within adipocytes. A further aim was to employ FTIR to examine the biochemical changes observed in the differentiated cells. An in vitro study was also conducted to examine the effect of OIE on pancreatic lipase. The results indicate that OIE can inhibit the development of adipocytes. Both treated and non-treated differentiated adipocytes had distinct biochemical profiles.

Methods

Chemicals

3T3-L1 mouse embryonic fibroblasts and bovine calf serum were purchased from the American Type Culture

Collection (ATCC, CL-173, USA). Insulin solution from bovine, methyl isobutyl xanthine (IBMX), lipase from porcine pancreas type 2, dimethyl sulphoxide (DMSO), 4-Nitrophenyl dodecanoate (pNP), simvastatin and orlistat were purchased from Sigma-Aldrich (St. Louis, USA). Dulbecco's modified Eagle's medium with high glucose (DMEM), penicillin, streptomycin, N-2-hydroxyethylpiperazine-N-2-ethane sulfonic acid (HEPES) and 3-(4,5-Dimethylthiazol-2-yl)-2,5-diphenyltetrazolium bromide (MTT) were purchased from GIBCO Invitrogen (Grand Island, NY). Dexamethasone was acquired from G Bioscience (St. Louis, USA). Oil Red O was purchased from amresco (USA). Fetal bovine serum (FBS) was purchased from Hyclone (Logan, Utah).

Preparation of *O. indicum* extract

O. indicum (fruit pods) fresh samples were purchased from the local market at Wang Nam Khiao district, Nakhon Ratchasima province, Thailand. The voucher specimens (SOI0808U) were deposited at the flora of Suranaree University of Technology (SUT) Herbarium and authenticated by Dr.Santi Wattatana, a lecturer and a plant biologist at Institute of Science, SUT, Thailand. Fresh pods were washed thoroughly with tap water, cut into small pieces and then dried in the oven at 40 °C for 2 days. The dried pieces were pulverised using a mechanical grinder, and the resulting coarse powder was preserved from moisture. The *O. indicum* dry powder (500 g) was extracted with 95% ethanol by a soxhlation for 8 h. The extract was filtered through Whatman filter paper and concentrated using a rotary evaporator at 50 °C under vacuum to remove the ethanol. The remaining extract was stored at -80 °C until required. Subsequently, the sample was lyophilized in a freeze dryer (LAB-CONCO), automatic mode, vacuum 240×10^{-3} mBar, and collector -55 °C. The extracted powder was stored at -20 °C until required. The lyophilized *O. indicum* extract was used within 3 months of preparation. The extract was resuspended in the differentiation medium containing 0.1 v/v DMSO (vehicle) and added to the cells at concentrations ranging from 0 to 1500 μ g/mL.

Phytochemical screening

The stock concentration of the lyophilized extract (10 mg/mL) was prepared and tested for the presence of bioactive phytochemical compounds, including total phenolics, flavonoids, alkaloids, steroids, glycosides, tannin, and saponins.

Test for flavonoids

Briefly, 1 mL of the OIE was mixed with 2 mL of 2% w/v of NaOH. A 2 mL aliquot of 10% w/v lead acetate solution was added to 1 mL of the alkaline extract. The

formation of a yellow colour indicated the presence of flavonoids [17, 18].

Test for alkaloids

The Mayer's and Wagner's test was performed. Briefly, 1 mL of the OIE was added to 2 mL of 1% *v/v* HCl and heated. A few drops of Mayer's and Wagner's reagents was added to the mixture, the presence of a precipitate suggested the presence of alkaloids in the sample [17, 18].

Test for steroids

The steroids containing in OIE were investigated. In short, 1 mL of the OIE was mixed with 2 mL each of chloroform and concentrated H_2SO_4 . A red colour in the lower layer indicated the presence of steroids [17, 18].

Test for glycoside

The detection of glycosides was performed using Salkowski's test. In brief, 2 mg of the OIE was mixed with 2 mL of chloroform and a few drops of concentrated H_2SO_4 . A reddish brown colour was associated with the presence of glycosides [17, 18].

Test for tannin

The Gelatin test was performed to identify tannins in the extract. To summarise, 1 mL of the OIE was added to 2 mL of a 1% *w/v* gelatin solution, the formation of a white precipitate indicated the presence of tannins [17, 18].

Test for saponin

The foam test was performed. Briefly, a 5 mL aliquot of the OIE was shaken for 5 min. If saponins were present, they formed a stable foam in the test tube [17, 18].

Total phenolic content determination (TPC)

The total phenolic content was measured following the method outlined by Kohoude with slight modifications [19]. In brief, 20 μ L of extract (0.625 mg/mL) or a standard solution of gallic acid (0–7.5 μ g/mL) were added into 100 μ L of Folin-Ciocalteu reagent. The mixture was incubated at room temperature for 6 min, prior to the addition of 7.5% *w/v* of Na_2CO_3 . After a 1 h incubation at room temperature, the absorbance was recorded at 760 nm against a DMSO blank. TPC of the sample was expressed as mg of gallic acid equivalents (GAE) per g of dry weight.

Total flavonoid content determination (TFC)

The total flavonoid content was measured according to a previously published method with slight modifications [20]. To summarise, a 25 μ L of extract (3 mg/mL) or a standard solution of catechin (0–200 μ g/mL) were added

to 125 μ L of deionised water, followed by the addition of 10 μ L of 5% *w/v* $NaNO_2$. This mixture was incubated at room temperature, and after 6 min, 15 μ L of 10% $AlCl_3$ was added. Upon mixing the reaction was allowed to proceed for 5 min, then 50 μ L of 1 M NaOH was added. The absorbance of the mixture was determined at 595 nm versus prepared DMSO blank. Total flavonoid of the sample was expressed as mg of catechin equivalent (CE) per g of dry weight.

Cell culture and differentiation procedures

The differentiation procedures of 3T3-L1 preadipocyte were performed as following the ATCC recommended protocol. Briefly, adherent 3T3-L1 cells were cultured in DMEM containing a high glucose concentration, supplemented with 10% of bovine calf serum, 100 U/mL of penicillin and 100 μ g/mL of streptomycin, until they reached 70–80% confluently. Two days after confluence (day 0), the cells were stimulated to differentiate with differentiation medium containing 10% FBS, 1.0 μ M dexamethasone, 0.5 mM of IBMX, and 1.0 μ g/mL of insulin in DMEM. On day 2, the differentiation medium was changed to maintain a medium consisting of 10% of FBS and 1.0 μ g/mL of insulin in DMEM. The maintenance medium was replaced every 48 h for the next 8 days. On day 10, the differentiation of 3T3-L1 pre-adipocytes into adipocytes was observed. The cells were maintained in 5% CO_2 incubator and at 37 °C throughout the whole process. The required doses of OIE were added to the 3T3-L1 cell culture during the differentiation (at day 0, 2, 4, 6, and day 8).

Cytotoxicity assay

The cytotoxic effects of the OIE on the proliferation of preadipocytes and adipocytes were determined by MTT assay largely following the method of Dunkhunthod et al. and Denizot [21, 22]. In brief, the 3T3-L1 cells were seeded in 96-well plates at a density of 5×10^3 cells/well. Two days after reaching confluence, the dividing cells were treated with the OIE at concentrations ranging from 0 to 1500 μ g/mL. Both treated and control cells were incubated for a further 48 h. At the end of the treatment period, the cell viability was assessed by using the MTT assay. The culture medium was removed, and 100 μ L of MTT solution (0.5 mg/mL in phosphate buffer saline) was added, then incubated at 37 °C for 4 h. After incubation, 150 μ L of DMSO was added to dissolve formazan crystal. The absorbance of the intracellular formazan is proportional to the number of viable cells present was determined at 540 nm against a blank medium (Benchmark Plus, Bio-Rad, Japan). The percentage of formazan product was calculated to determine cytotoxicity [23]. OIE at concentrations of 0–200 μ g/mL were used to assess any cytotoxic effects of mature

adipocytes and Oil Red O assay for lipid accumulation. The IC_{50} of the extract was also calculated from a dose-response curve using linear regression analysis.

Oil red O staining

The intracellular triglyceride content was determined using an Oil Red O staining method as previously described [21, 24]. Briefly, on day 10, cells were washed with PBS and fixed with 1 mL/well of 10% (v/v) formalin for 1 h at room temperature. After fixation, the cells were washed, and 500 μ L of 0.5% of the Oil Red O solution was added. The cells were incubated for 30 min at room temperature. The Oil Red O solution was removed by gentle aspiration, and the cells were washed with PBS. The nucleus was then stained with 0.10% (w/v) haematoxylin. Fat droplets were observed under an inverted microscope at an appropriate magnification. To determine the percent of lipid accumulation, the cells were extracted with 250 μ L of isopropanol and 200 μ L of the eluted solution was transferred to a new 96 well plate. The absorbance was measured at 490 nm with a microplate spectrophotometer. The simvastatin at 1.67 μ g/mL was used as a positive control. The 3T3-L1 cells, treated with 200 μ g/mL OIE were selected for FTIR studies.

Fourier-transform infrared spectroscopy

The effect of OIE on 3T3-L1 adipocyte cells using FTIR measurement was performed following the method of Dunkhunthod et al. [21]. Briefly, on day 10, cells were collected and centrifuged at 4000 \times g for 5 min, the medium was removed by gentle aspiration, and the cells were agitated and washed with 0.85% w/v NaCl. The cell suspensions were centrifuged at 4000 \times g for 5 min. The acquired cell pellets were dropped onto a window slide (MirrIR, Kevley Technologies) and dried for 30 min in a desiccator to eliminate the excess water. The dried cells were stored in a desiccator prior to FTIR analysis.

FTIR spectra were obtained at the Synchrotron Light Research Institute (Public Organization), Thailand. FTIR spectra were acquired with a Bruker Vertex 70 spectrometer coupled with a Bruker Hyperion 2000 microscope (Bruker Optics Inc., Ettlin-Gen, Germany) equipped with nitrogen cooled MCT (HgCdTe) detector with a 36 \times IR. The spectra were obtained in the reflection mode with the wavenumber range of 4000–600 cm^{-1} , using an aperture size of 50 μ m \times 50 μ m, with a resolution of 6 cm^{-1} . Each spectrum was produced following 64 scans. OPUS 7.2 software (Bruker Optics Ltd., Ettlingen, Germany) was used to acquire FTIR spectral data and control instrument system.

The spectral ranges of biochemical interest were identified using Principal Component Analysis (PCA) as being between 3000 and 2800 cm^{-1} and 1800–850 cm^{-1} .

The preprocessing of the spectra was performed by second derivative transformations using the Savitzky-Golay algorithm (nine smoothing points) and normalised with extended multiplicative signal correction (EMSC). Score plots (3D) and loading plots were used to represent the different classes of data and relations among variables of the data set, respectively.

The FTIR spectra datasets were submitted for Un-supervised Hierarchical Cluster Analysis (UHCA), to collect similar spectra in groups or clusters, using the OPUS 7.2 software (Bruker). Cluster analysis was performed on the second derivatives, and vector normalises spectra using Ward's algorithm.

Lipase activity

Measurement of lipase activity was performed as previously described by Guo et al. and Dunkhunthod et al. [21, 25]. In brief, lipase of porcine pancreas type 2 was dissolved in distilled water at 5 mg/mL, the solution was centrifuged at 10,000 \times g for 5 min, and the supernatant was used for the assay. A 0.1% w/v solution of pNP laurate was prepared in 5 mM of sodium acetate (pH 5.0) containing 1% v/v Triton X-100. The solution was heated to 80 $^{\circ}C$ and cooled to room temperature prior to use. A 30 μ L volume of the lipase was added to a 96 well plate, followed by 40 μ L of reaction buffer (100 mM of Tris buffer pH 8.2). Either 20 μ L of OIE or 50% v/v DMSO was added prior to the addition 30 μ L of the substrate solution. The mixtures were incubated at 37 $^{\circ}C$ for 6 h and measured at 409 nm using a microplate spectrophotometer. Orlistat at 12.5 to 100 μ g/mL was used as a positive control. The inhibition rate (%) was calculated using the following equation. $[(OD_{control} - blank_{control}) - (OD_{sample} - blank_{sample})] / OD_{control} \times 100$ [26].

Statistical analysis

All the data were expressed as a mean \pm standard error of the mean (SEM). The statistical significances difference between treatment and control groups of cell viability, the amount of lipid accumulation, biomolecular changes, and lipase activity were analysed by One-way analysis of variance (ANOVA) with a Turkey's HSD post-hoc test (SPSS v 23). Values were considered statistically significant when $p < 0.05$ and data were representative of at least three independent experiments ($n \geq 3$). Most experiments were performed in triplicate.

Results

The phytochemical composition, TPC, and TFC

A 1.0 Kg weight of fruit pods from *O. indicum* was processed to obtain a final yield of 18.41% (w/w) OIE (Table 1). Qualitative tests revealed that the extract contained flavonoids, alkaloids, steroids, glycoside, and

Table 1 Extraction yield and phytochemical composition of *Oroxylum indicum* fruit extract. Extraction yield, total phenolic content, total flavonoid content and phytochemical composition of *Oroxylum indicum* fruit extract

Sample	Fresh weight (g)	Dry weight (g)	Yield (g)	Yield (%w/w)	Flavonoids	Alkaloids	Steroids	Glycoside	Tannins	Saponin
<i>Oroxylum indicum</i>	1000	133.40	24.53	18.41	+	+	+	+	+	+
Total phenolic content (TPC)		51.48 ± 0.77 (mg GAE/g) ^a								
Total flavonoids content (TFC)		34.19 ± 2.47 (mg CE/g) ^a								

(+) = positive test; (-) = negative test

Weight and yield of *Oroxylum indicum* was calculated from a 1.0 kg extraction of raw material. ^aThe TPC and TFC were derived from calibration curves using the relevant standard and based on dry weight of *Oroxylum indicum*. The data are expressed as the mean ± SEM of three independent experiments performed in triplicate (n = 9)

tannins, but no saponins were detected. The concentration of TPC and TFC present in OIE were 51.483 ± 0.766 mg GAE/g and 34.191 ± 2.473 mg CE/g of dry weight, respectively (Table 1).

The effect of OIE on the viability of pre- and mature adipocytes

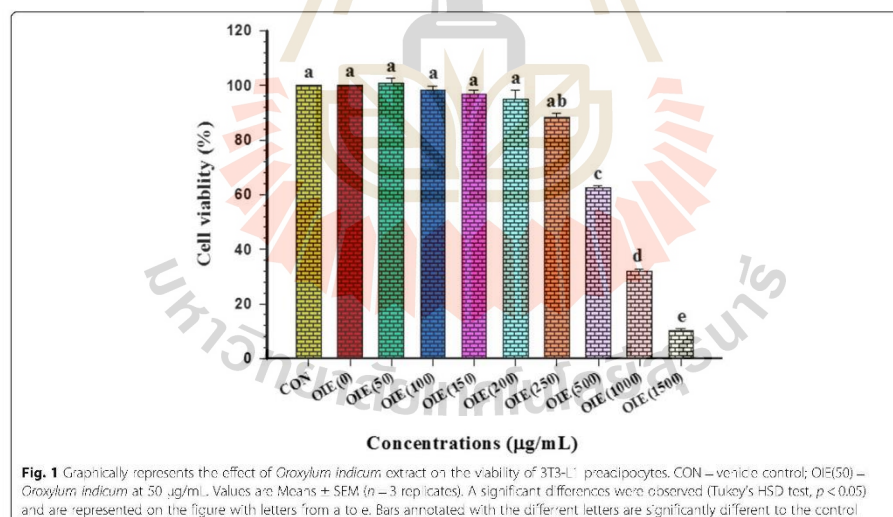
To evaluate the cytotoxicity of OIE on both non-differentiated and differentiated 3T3-L1 cells, an MTT assay was conducted. A concentration of OIE between 250 to 1500 µg/mL showed a significant reduction ($p < 0.05$) in the viability of pre-adipocytes (Fig. 1). However, the viability of cells treated with lower doses of the extract (50 to 200 µg/mL) was not significantly different compared to non-treated cells ($p > 0.05$). The IC_{50} at 48 h for pre-adipocytes was 882.68 ± 47.99 µg/mL. These results suggest that doses of the OIE above 250 µg/mL are detrimental to pre-adipocytes viability. In the light of

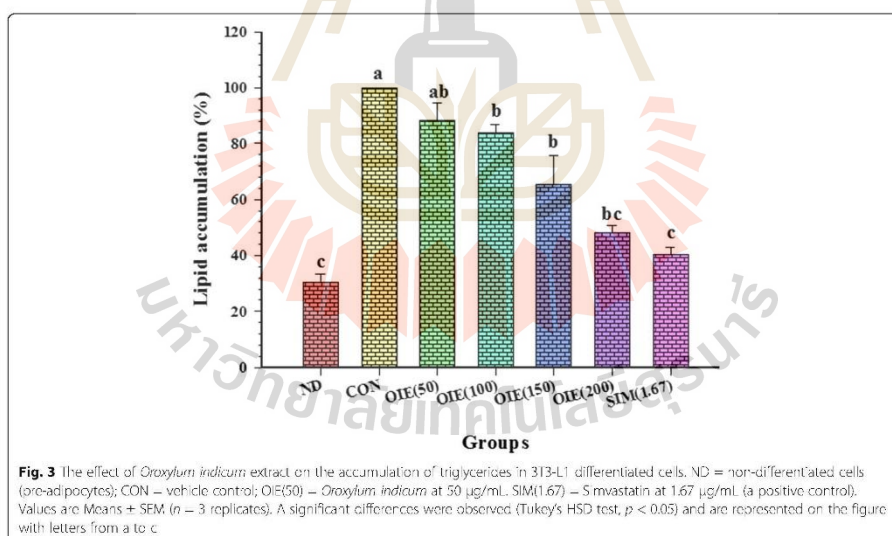
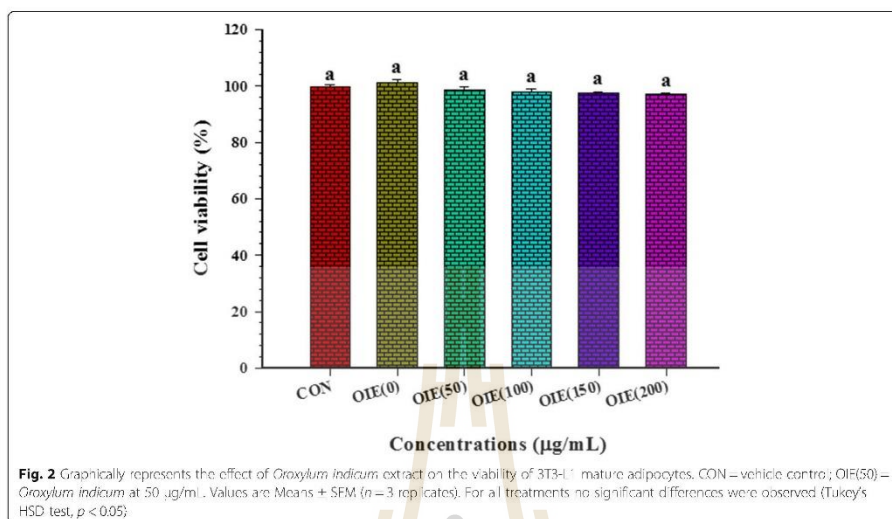
this observation, all subsequent experiments to investigate mature adipocyte viability used a dose of 200 µg/mL or less.

The effect of the OIE on mature adipocytes indicated that doses of OIE at 50 to 200 µg/mL did not reduce the viability of mature cells compared to the control ($p > 0.05$) over a 10 day period (Fig. 2).

The effect of OIE on adipocyte differentiation and lipid accumulation

During the differentiation of 3T3-L1 preadipocytes to adipocytes, the cells were treated with OIE, and the intracellular lipid concentration was determined using Oil Red O staining. The 3T3-L1 pre-adipocytes when exposed to the differentiation medium resulted in a significant increase of lipid accumulation in comparison to pre-adipocytes ($p < 0.05$) (Fig. 3). However, the addition of OIE at 200 µg/mL significantly decreased the





intracellular lipid accumulation by approximately 52%, compared to the 3T3-L1 adipocyte (control) ($p < 0.05$). The IC_{50} and IC_{60} values for OIE on lipid accumulation were determined to be 201.26 ± 10.00 and 237.72 ± 14.96 $\mu\text{g/mL}$, respectively. In addition, the cholesterol-lowering drug, simvastatin exhibited an IC_{60} at a concentration of 1.67 $\mu\text{g/mL}$. The effect of simvastatin is 142 times greater than OIE.

In order to gain more evidence that OIE could affect lipid accumulation in differentiated 3T3-L1 cells, pre-adipocytes and adipocytes were stained with Oil Red O and hematoxylin and observed a light microscope (Fig. 4). Untreated adipocytes displayed an increase in size and number of prominent lipid droplets (Fig. 4b). Whilst adipocytes treated with simvastatin exhibited very

small and diffuse lipid droplets (Fig. 4h). The 200 $\mu\text{g/mL}$ OIE treated adipocytes displayed smaller size and number of lipid droplets that seemed to be focused on one part of the cell (Fig. 4g).

FTIR spectra profiles

FTIR microspectroscopy was used to determine the biochemical composition of pre-adipocytes, adipocytes, and adipocytes treated with either, simvastatin or OIE. For each treatment FTIR spectra between wavelengths 3000 – 950 cm^{-1} were obtained (Fig. 5). The Spectra were converted to second order derivatives to allow a more detailed comparison of the different treatments to the cells (Table 2). The spectra were separated into three distinct areas: (1) lipids (3000 – 2800 cm^{-1}), (2) proteins (1700 – 1500 cm^{-1}) and (3) carbohydrate and nucleic acids (1300 – 950 cm^{-1}).

The second derivative spectra in the lipid region

The spectra in the high-frequency region at 3000 – 2800 cm^{-1} correspond to the symmetrical and asymmetrical vibrations of $-\text{CH}$ groups of the lipid content [27]. The average second derivative spectra of 3T3-L1 cells under different experimental conditions exhibited three characteristic regions at 2962 cm^{-1} , 2924 cm^{-1} and 2854 cm^{-1} which are associated with cellular lipids. Each area is produced as a result of asymmetrical stretching from the methyl and methylene groups of lipids, and also the symmetrical stretching from methylene groups of lipids (Fig. 6a). Further evidence for the presence of lipids occurred at the lower wavenumber region at 1740 cm^{-1} , which is assigned to $\text{C}=\text{O}$ stretches of the ester functional groups from lipids and fatty acids (Fig. 6b) [28]. The relative absorbance at 2924 cm^{-1} and 1740 cm^{-1} of adipocyte were stronger than the treated cells or pre-adipocytes (Fig. 6a and b). To discriminate between non treated and treated adipocytes the ratio of the integrated area of several functional groups was calculated. The selected regions were CH_2 (2938 – 2906 cm^{-1} , centred at 2924 cm^{-1})/ CH_3 (2973 – 2954 cm^{-1} , centred at 2962 cm^{-1}) [29, 30]. The selection of these area was made as they are associated with asymmetric stretching of lipids. The results showed that the ratio of integrated area of the lipids region in the OIE-treated adipocytes displayed significantly less than the untreated adipocytes group ($p < 0.05$) and did not significant from a simvastatin-treated group ($p > 0.05$) (Fig. 7a). Another useful parameter was the integrated area of the ester functional groups from lipids at 1740 cm^{-1} in the OIE-treated adipocytes group indicated significantly lower than the untreated adipocytes group ($p < 0.05$) (Fig. 6b and 7a).

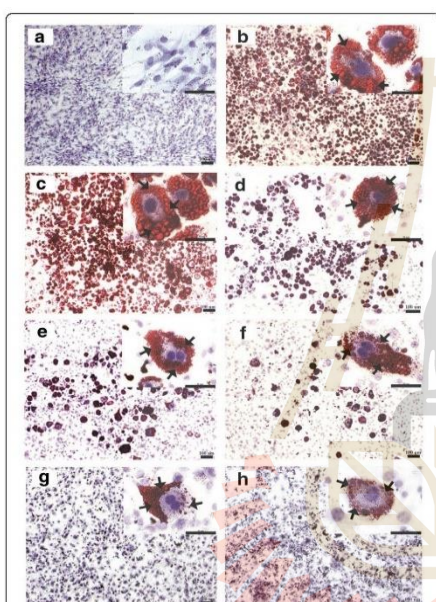


Fig. 4 Microscopic imaging of intracellular lipid after Oil Red O and hematoxylin staining of the samples. 3T3-L1 cells are stained with Oil Red O and hematoxylin. The lipid droplets were red in appearance and the nuclei were blue in colour. The arrows indicate lipid droplets within the adipocytes. The size and the number of lipid droplets appear to be a larger in untreated adipocytes (b and c), a non-differentiated cells (pre-adipocytes), b differentiated cells (untreated adipocytes), c vehicle control, d, e, f and g differentiated cells treated with *Oroxylum indicum* extract at the dose 50 $\mu\text{g/mL}$, 100 $\mu\text{g/mL}$, 150 and 200 $\mu\text{g/mL}$, respectively; h simvastatin at 1.67 $\mu\text{g/mL}$. (original magnification at $\times 40$, scale bar: 100 μm and inset view at $\times 400$, scale bar: 50 μm)

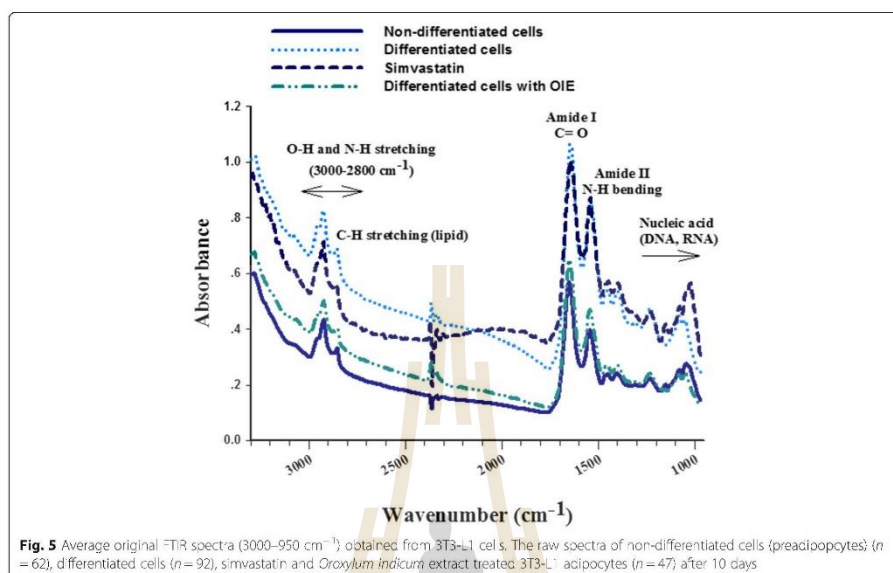


Table 2 FTIR band assignments for functional groups found in the second derivative spectra of 3T3-L1 cells [27, 28]

2nd derivative spectra (cm^{-1})	Band assignment
2962	Asymmetrical stretching (C-H) from methyl ($-\text{CH}_3$) groups of lipids
2924	Asymmetrical stretching (C-H) from methylene ($-\text{CH}_2$) groups of lipids
2854	Symmetrical stretching (C-H) from methylene ($-\text{CH}_2$) groups of lipids
1740	(C=O) of ester functional groups primarily from lipid and fatty acids
1647	Amide I protein (C=O stretching)
1543	Amide II protein (N-H bending, C-H stretching)
1462	Asymmetrical deformation (CH_2) _{scissor} from methylene ($-\text{CH}_2$) groups of lipids
1400	Symmetrical stretching (COO^-) associated with symmetrical in-plane deformation bend (CH_2) of proteins
1234	Asymmetrical stretching (PO_2^-) mainly nucleic acids with the little contribution from phospholipids
1153	Asymmetrical stretching (CO-O-C) of glycogen, other carbohydrates and nucleic acids
1080	Symmetrical stretching (PO_2^-) of the phosphodiester backbone of nucleic acids (DNA and RNA) and phospholipids
1018	(C-O) vibration from glycogen and other carbohydrates

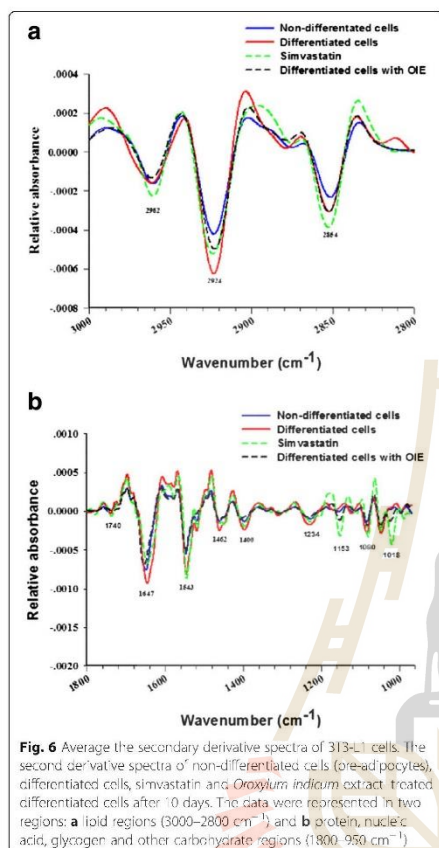
The second derivative spectra in the protein region

Spectra in the areas from 1700 to 1500 cm^{-1} are attributed to an absorption peak of proteins amide I and II. The ratio of the integrated area of several proteins related functional groups, including CH_2 asymmetric stretching (2938–2906 cm^{-1} , centred at 2924 cm^{-1})/amide I (1674–1624 cm^{-1} , centred at 1647 cm^{-1}) was calculated for control and treated adipocytes. In this case there no significant difference between non treated adipocytes and OIE treated adipocytes ($p > 0.05$) (Fig. 7b) [31].

The second derivative spectra in the carbohydrate and nucleic acid region

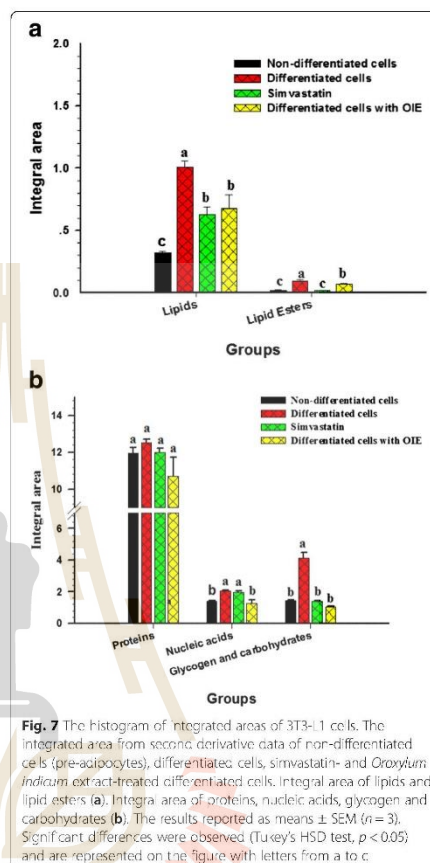
C-O vibrations attributed to glycogen and other carbohydrates were identified at wavelengths of 1153 cm^{-1} and 1018 cm^{-1} [32]. These signal intensity and integral area of the OIE-treated adipocytes displayed significantly less than untreated adipocytes ($p < 0.05$) but not significant different from simvastatin-treated group (Fig. 7b).

The functional group of PO_2^- stretching mode from mainly nucleic acids was located at 1234 cm^{-1} and 1080 cm^{-1} . In this case, the OIE-treated adipocytes displayed signal intensity and integral area significantly less than the untreated and simvastatin-treated adipocytes ($p < 0.05$) (Fig. 6b and 7b) [27].



PCA

Principal Component Analysis (PCA) was performed to further discriminate data acquired from pre-adipocyte, untreated adipocyte, simvastatin- and OIE-treated adipocytes using FTIR. The PCA results were obtained from second-order derivative spectra at 3000–2800 cm^{-1} and 1700–950 cm^{-1} . The results from 2-dimensional PCA clustering (Fig. 8a) clearly reveal distinct separation of differentiated adipocytes from treated adipocytes. The OIE and simvastatin-treated adipocytes would appear to have similar properties. Also, the spectrum band which most influences to the clustering can be examined through the PCA loading plots (Fig. 8b). PC1 loading plot was discriminated by the loading spectra at 2920 cm^{-1} and 2850 cm^{-1} caused by the C-H



stretching, and at 1153 cm^{-1} and 1022 cm^{-1} resulting from the C-O vibrations from glycogen and other carbohydrate [33], which separated the negative score plot of the untreated adipocytes from the positive score plot of simvastatin- and OIE-treated adipocytes. These results illustrated and confirmed that untreated adipocytes had a higher lipid and carbohydrate contents than simvastatin- and OIE-treated adipocytes. Moreover, the negative PC2 loading in the lipids region (centred at 2920 cm^{-1} and 2854 cm^{-1} , 1485 cm^{-1}) suggest that preadipocytes and OIE-treated adipocytes exhibit different properties. These results are consistent with the second derivative spectra results mentioned in the previous section.

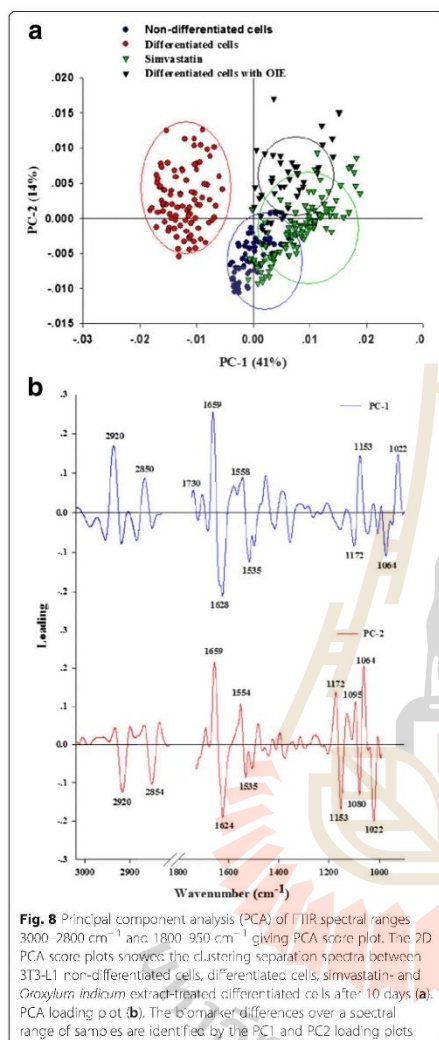


Fig. 8 Principal component analysis (PCA) of FTIR spectral ranges 3000–2800 cm^{-1} and 1800–950 cm^{-1} giving PCA score plot. The 2D PCA score plots showed the clustering separation spectra between 3T3-L1 non-differentiated cells, differentiated cells, simvastatin- and *Crozytum indicum* extract-treated differentiated cells after 10 days (a). PCA loading plot (b). The biomarker differences over a spectral range of samples are identified by the PC1 and PC2 loading plots

UHCA

Unsupervised Hierarchical Cluster Analysis (UHCA) was used to determine the spectral similarity within groups and between groups of preadipocytes, untreated adipocytes, simvastatin- and OIE-treated adipocytes. The spectral similarity regarding relative distance is illustrated in

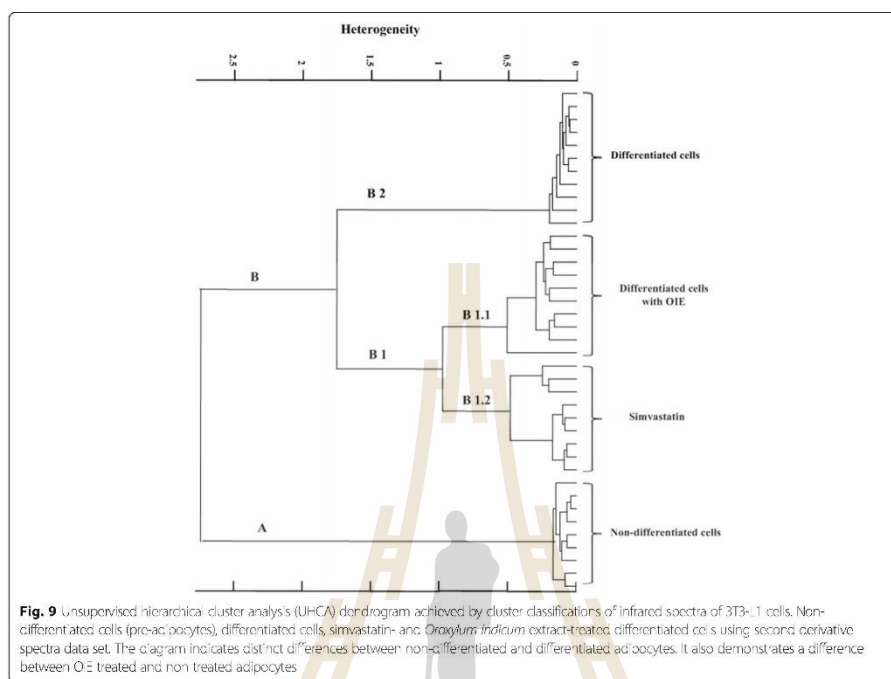
the dendrogram (Fig. 9), which was obtained using second derivative spectral data and Ward's algorithm. In simple terms, the lower the heterogeneity, the more similarity exists between the groups. The UHCA analysis indicates that there is a distinct difference between pre-adipocytes and the other cell types. Further to this, the non-treated adipocytes are different from both OIE and simvastatin-treated cells. The results exhibited that the first cluster of pre-adipocyte, branch A, was clearly separated from other groups (branch B). Additionally, the branch B that was corresponding to spectra of untreated adipocytes (branch B2), OIE-treated- (branch B1.1) and simvastatin-treated (branch B1.2) adipocytes was obviously distinguished. The spectra of branch B1 is composed of two subgroups revealing a closer similarity between OIE- and simvastatin-treated adipocytes. Cluster analysis employed Ward's algorithm using second derivatives, and vector normalization, over the spectral ranges 3000–2800 cm^{-1} and 1800–950 cm^{-1} . Regarding the result in Fig. 7a, the lipid amount of pre-adipocytes as expected was the lowest ($p < 0.05$).

Effect of the OIE on pancreatic lipase activity

Pancreatic lipase is an enzyme responsible for the hydrolysis of lipid into free fatty acids and glycerol. OIE concentrations between 100 to 1250 $\mu\text{g}/\text{mL}$ displayed significantly higher inhibitory lipase activity than those of the controls ($p < 0.05$) (Fig. 10). Moreover, the IC_{50} of OIE for the inhibition of pancreatic lipase was 1062.04 ± 32.21 $\mu\text{g}/\text{mL}$. Whilst the inhibitory effect of the positive control, orlistat at 12.5 to 100 $\mu\text{g}/\text{mL}$, demonstrated an IC_{50} at 38.78 ± 9.55 $\mu\text{g}/\text{mL}$. Under those circumstances, the potential strength of orlistat on lipase activity inhibition is approximately 27 times greater than the OIE. These results suggest that the inhibition of pancreatic lipase activity by OIE increased in a dose-dependent manner.

Discussion

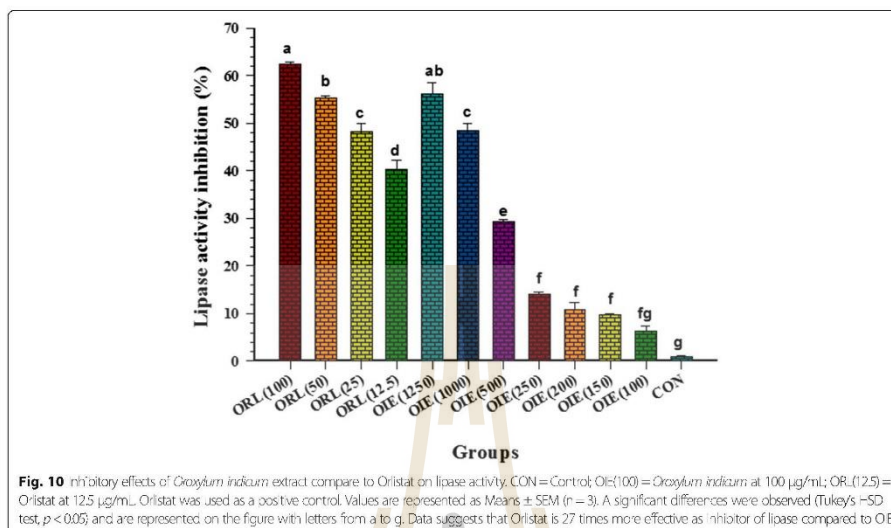
Adipocyte formation and activity appears to play a central role in the development of obesity. The generation and metabolism of adipocytes have become major targets for treating obesity [34]. One area that has increased is the use of natural products to target obesity. Compared to the convenience and cost they are becoming more attractive propositions than synthetic drugs or surgery [35, 36]. In this study, we investigated the effects of an OIE on the anti-adipogenic and biomolecular change in 3T3-L1 cells. Our studies indicated there was a dose-dependent effect of OIE upon the viability of pre-adipocyte ranging from concentrations of 250 $\mu\text{g}/\text{mL}$ to 1500 $\mu\text{g}/\text{mL}$. At lower doses (0–200 $\mu\text{g}/\text{mL}$) there was no significant difference from the control ($p > 0.05$). Although no major impact on the viability of the cells was



observed at lower doses, there may be some toxicological changes to the cells. One further observation was that doses of OIE between 50 to 200 $\mu\text{g}/\text{mL}$ indicated a dose-dependent decrease of lipid accumulation in the adipogenesis assay (Figs. 3 and 4). One explanation for the reduction of lipid could be that the chemical components of OIE may have a potent effect which inhibits the differentiation of 3T3-L1 preadipocytes. A previous study reported that the fruit of *O. indicum* is rich in flavonoids such as baicalein [37]. At a concentration of 20 μM baicalein can prevent the differentiation of preadipocyte to adipocyte during first 4 days of induction [38]. In fact, there is evidence to support that baicalein inhibits a cell cycle regulator, promoting cell cycle arrest at the G0/G1 phase. It was also reported to suppress the m-TOR signaling pathway leading to an inhibition of adipogenic factors such as *PPAR γ* [39]. OIE at 200 $\mu\text{g}/\text{mL}$ lipid accumulation was not significantly different to cells treated with 1.67 $\mu\text{g}/\text{mL}$ (4 μM) of simvastatin (Fig. 3, $p > 0.05$). This was a very interesting observation as it confirms the observations made by Nicholson et al. They demonstrated that statins, such as pitavastatin and

simvastatin at 5 μM could inhibit adipocyte differentiation by blocking *PPAR γ* expression and activating *pref-1* expression [40]. These findings provide evidence that the OIE may also have the capacity to inhibit *PPAR γ* activity.

To further elucidate the biochemical potential of OIE, an in vitro pancreatic lipase assay was performed as part of this study. Lipase became a target for research groups attempting to prevent obesity or metabolic syndrome [21, 25]. Pancreatic lipase is an enzyme responsible for the breakdown of triglycerides into glycerol and fatty acid in the gastrointestinal tract. When lipase activity is inhibited, triacylglycerol cannot cross the intestinal brush border membrane leading to a decrease in the uptake of lipids into the human body. Orlistat, a known lipase inhibitor is a drug for treating obesity was used in this study as a positive control. The results of this study indicated that OIE demonstrates as inhibition of pancreatic lipase between doses of 100–1250 $\mu\text{g}/\text{mL}$ (IC_{50} of 1062.04 ± 32.21 $\mu\text{g}/\text{mL}$), 27 times less potent than orlistat. The dose of OIE that inhibited pancreatic lipase was also a concentration which induced a decrease in



viability of pre-adipocytes (IC_{50} of 882.68 ± 47.99 µg/mL). However, a study by Roh and Jung indicated a number of plant extracts could inhibit pancreatic lipase but had a very little effect on the viability of 3T3-L1 cells [41]. In the light of this publication, it would appear that OIE is not the most effective inhibitor of lipase activity. However, the potential for OIE to inhibit cell cycle progression [39] or its effects on key adipogenic biochemical pathways [16] still requires further investigation.

Although FTIR microspectroscopy has previously been used to characterise biochemical composition in medical research studies [29, 42, 43]. This is the first study using FTIR to demonstrate on the biochemical profile of OIE treated adipocyte. These results indicated that the lipids, lipid esters, nucleic acids, glycogen and carbohydrates of the OIE-treated adipocytes were significantly decreased compared to the untreated adipocytes (Fig. 7a and b). This study indicates that FTIR provided data similar to that obtained using established biochemical assays. This suggests that FTIR is a very useful technique for assessing the impact of plant extracts on established cell lines. Although FTIR supported the preliminary evidence regarding to biochemical changes during the differentiation of 3 T3-L1 cells more research is needed to clarify the mechanism of action of OIE.

Conclusions

This study suggests that the OIE derived from the fruit pods of the plant inhibited both adipogenesis and lipid

accumulation in 3T3-L1 adipocytes. The extract inhibited lipase activity, but this was not as effective as orlistat. FTIR microspectroscopy provides valuable information which supported the biochemical assays used to assess 3T3-L1 cells. The precise mechanism of inhibitory effect on adipogenesis and lipid accumulation is of biochemical interest and requires further investigation.

Abbreviations

ANOVA: One-way analysis of variance; DMEM: Dulbecco's modified eagle's medium with high glucose; DMSO: Dimethyl sulphoxide; EMSC: Extended multiplicative signal correction; FTIR: Fourier transform-Infrared; IBMX: 3-Isobutyl-1-methylxanthine; MTT: 3-(4,5-Dimethylthiazol-2-yl)-2,5-diphenyltetrazolium bromide; OIE: *Croxyllum indicum* extract; PCA: Principal Component Analysis; SEM: The standard error of the mean; TFC: Total flavonoids content; TPC: Total phenolic content; UHCA: Unsupervised Hierarchical Cluster Analysis

Acknowledgements

The authors are grateful to the Synchrotron Light Research Institute (Public Organization), Thailand, for supporting the FTIR microspectroscopy technique.

Funding

The research was supported by the Thailand Research Fund through The Royal Golden Jubilee Ph.D. Program (Grant No. PH-D/0029/2556). The sponsors had no influence in the design of the study, data collection, analysis, and interpretation of the data. They had no influence over the contents or organization of this manuscript and writing the manuscript.

Availability of data and materials

The datasets used and analysed during the current study are available from the corresponding author on reasonable request.

Authors' contributions

TH designed the study, carried out all experiments, analysed and interpreted the data, drafted the initial and revised manuscript. GL conceived and designed the study, supervised data collection, critically reviewed and revised the manuscript. KTH and KTI participated in the designed, performed and interpreted of FTIR data, and wrote a manuscript of FTIR part. SS contributed in plant preparation and extraction, prepared chemical substances, and drafted the manuscript of these parts. GE designed the project, supervised the experiments, wrote and revised the manuscript. All authors have read and approved the final manuscript.

Ethics approval and consent to participate
Not applicable.**Competing interests**

The authors declare that they have no competing interests.

Publisher's Note

Springer Nature remains neutral with regard to jurisdictional claims in published maps and institutional affiliations.

Author details

¹School of Preclinical, Institute of Science, Suranaree University of Technology, Nakhon Ratchasima 3000, Thailand. ²School of Pharmacy and Biomolecular Sciences, Liverpool John Moores University, James Parsons Building, Byrom Street, Liverpool L3 3AF, UK. ³Synchrotron Light Research Institute (Public Organization), Suranaree Subdistrict, Muang District, Nakhon Ratchasima 30000, Thailand.

Received: 26 June 2017 Accepted: 30 May 2018

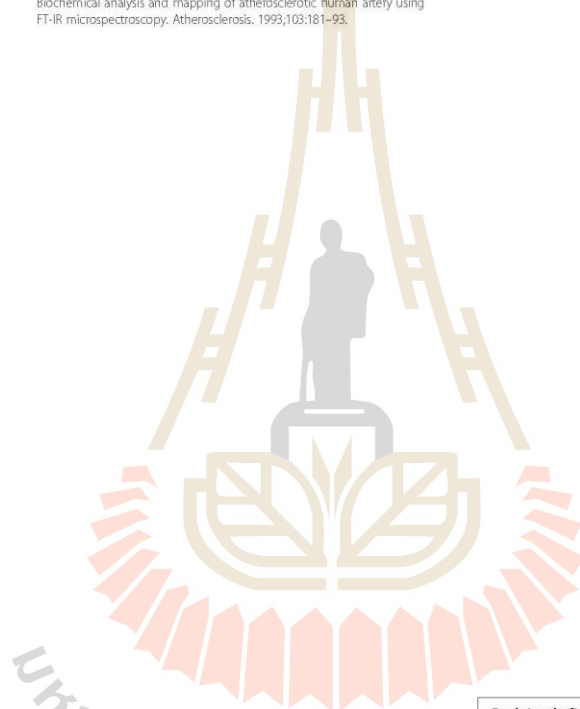
Published online: 08 June 2018

References

- Wang C, Chiang C, Yatsuya H, Hillawe EH, Ikerdeu E, Honjo K, et al. Descriptive epidemiology of hypertension and its association with obesity: based on the WHO STEPwise approach to surveillance in Palau. *Asia Pac J Public Health*. 2017; <https://doi.org/10.1177/1010539517704042>.
- Kopelman PG. Obesity as a medical problem. *Nature*. 2000;404:635–43.
- Ahmadian M, Duncan RE, Jaworski K, Sarkadi-Nagy E, Sul HS. Triacylglycerol metabolism in adipose tissue. *Future Lipidol*. 2007;2:229–37.
- Tchernof A, Despres JP. Pathophysiology of human visceral obesity: an update. *Physiol Rev*. 2013;93:359–404.
- De Simone G, D'Addato G. Sibutramine: balancing weight loss benefit and possible cardiovascular risk. *Nutr Metab Cardiovasc Dis*. 2008;18:337–41.
- Thuraijajah PH, Syn W-K, Nell DA, Stell D, Haydon G, Orlitat (Kenical)-induced subacute liver failure. *Eur J Gastroenterol Hepatol*. 2005;17:1437–8.
- Yun JW. Possible anti-obesity therapeutics from nature—a review. *Phytochemistry*. 2010;71:1625–41.
- Ghorbani A, Hajizadeh MA, Rajaei Z, Zendeabad SB. Effects of fenugreek seeds on adipogenesis and lipolysis in normal and diabetic rats. *Pak J Biol Sci*. 2014;17:523–8.
- Dinda B, Silsarma I, Dinda M, Rudrapaul P. *Oroxylum indicum* (L.) Kurz: an important Asian traditional medicine: from traditional uses to scientific data for its commercial exploitation. *J Ethnopharmacol*. 2015;161:255–78.
- Uddin K, Sayeed A, Islam A, Rahman AA, Ali A, Khan G, et al. Purification, characterization and cytotoxic activity of two flavonoids from *Oroxylum indicum* vent. (Bignoniaceae). *Asian J Plant Sci*. 2003;2:515–8.
- Palaswan A, Soogayun S, Letturm T, Pradnivat P, Wiwanitit V. Inhibition of Heinz body induction in an in vitro model and total antioxidant activity of medicinal Thai plants. *Asian Pac J Cancer Prev*. 2005;6:458–63.
- Tran TV, Malainer C, Schwaiger S, Hung T, Atanasov AG, Heiss EH, et al. Screening of Vietnamese medicinal plants for NF- κ B signaling inhibitors assessing the activity of flavonoids from the stem bark of *Oroxylum indicum*. *J Ethnopharmacol*. 2015;159:36–42.
- Singh J, Kakkar P. Modulation of liver function, antioxidant responses, insulin resistance and glucose transport by *Oroxylum indicum* stem bark in STZ-induced diabetic rats. *Food Chem Toxicol*. 2015;62:221–31.
- Joshi SV, Vyas BA, Shah PD, Shah DR, Shah SA, Gandhi TR. Protective effect of aqueous extract of *Oroxylum indicum* Linn. (root bark) against DNBS-induced colitis in rats. *Indian J Pharmacol*. 2011;43:656–61.
- Tamboli AM, Karpe ST, Shaikh SA, Manikrao AM, Kature DV. Hypoglycemic activity of extracts of *Oroxylum indicum* (L) vent roots in animal models. *Pharmacologyonline*. 2011;2:890–9.
- Singh J, Kakkar P. Oroxylum a, a constituent of *Oroxylum indicum* inhibits adipogenesis and induces apoptosis in 3T3-L1 cells. *Phytomedicine*. 2014;21:1733–41.
- Yadav R, Agarwala M. Phytochemical analysis of some medicinal plants. *J Phytol*. 2011;3:10–4.
- Rauf A, Jan M, Rehman W, Muhammad N. Phytochemical, phytotoxic and antioxidant profile of *Caralluma tuberculata* NE Brown. *J Pharm Pharmacol*. 2013;2:21–5.
- Kohoude MJ, Gbaguidi F, Agbani P, Ayedoun M-A, Cazaux S, Bouajila J. Chemical composition and biological activities of extracts and essential oil of *Boswellia dalzielii* leaves. *Pharm Biol*. 2017;55:33–42.
- Jing LJ, Mohamed M, Rahmat A, Bakar MFA. Phytochemicals, antioxidant properties and anticancer investigations of the different parts of several gingers species (*Boesenbergia rotunda*, *Boesenbergia pulchella* var attenuata and *Boesenbergia armeniaca*). *J Med Plants Res*. 2010;4:27–32.
- Dunkhunthod B, Thumanu K, Eumkeb G. Application of FTIR microspectroscopy for monitoring and discrimination of the anti-adipogenic activity of baicalin in 3T3-L1 adipocytes. *Vib Spectrosc*. 2017;89:92–101.
- Denizot F, Lang R. Rapid colorimetric assay for cell growth and survival: modifications to the tetrazolium dye procedure giving improved sensitivity and reliability. *J Immunol Methods*. 1986;89:271–7.
- Mandlik V, Patil S, Bopanna R, Basu S, Singh S. Biological activity of Coumarin derivatives as anti-leishmanial agents. *PLoS One*. 2016;11:e0164585.
- Ramirez-Zacarias JL, Castro-Munozledo F, Kuri-Harcuch W. Quantitation of adipose conversion and triglycerides by staining intracytoplasmic lipids with oil red O. *Histochemistry*. 1992;97:493–7.
- Guo X, Liu J, Cai S, Wang Q, Ji B. Synergistic interactions of apigenin, naringin, quercetin and emodin on inhibition of 3T3-L1 preadipocyte differentiation and pancreas lipase activity. *Obes Res Clin Pract*. 2016;10:327–39.
- Cai S, Wang Q, Wang M, He J, Wang Y, Zhang D, et al. In vitro inhibitory effect on pancreatic lipase activity of subfractions from ethanolic extracts of fermented oats (*Avena sativa* L.) and synergistic effect of three phenolic acids. *J Agric Food Chem*. 2012;60:7245–51.
- Garip S, Gozen AC, Severcan F. Use of Fourier transform infrared spectroscopy for rapid comparative analysis of *Bacillus* and *Micrococcus* isolates. *Food Chem*. 2009;113:1301–7.
- Baloglu FK, Garip S, Heise S, Brockmann G, Severcan F. FTIR imaging of structural changes in visceral and subcutaneous adiposity and brown to white adipocyte transdifferentiation. *Analyst*. 2015;140:2205–14.
- Vongsvitvut J, Heraud P, Gupta A, Puri M, McNaughton D, Barrow CJ. FTIR microspectroscopy for rapid screening and monitoring of polyunsaturated fatty acid production in commercially valuable marine yeasts and protists. *Analyst*. 2013;138:6016–31.
- Nara M, Okazaki M, Kagi H. Infrared study of human serum very-low-density and low-density lipoproteins. Implication of esterified lipid C=O stretching bands for characterizing lipoproteins. *Chem Phys Lipids*. 2002;117:1–6.
- Srisayam M, Weerapreeyakul N, Barusux S, Tanthanuch W, Thumanu K. Application of FTIR microspectroscopy for characterization of biomolecular changes in human melanoma cells treated by sesamol and kojic acid. *J Dermatol Sci*. 2014;73:241–50.
- Cao J, Ng ES, McNaughton D, Stanley EG, Elefany AG, Tobin MJ, et al. The characterisation of pluripotent and multipotent stem cells using Fourier transform infrared microspectroscopy. *Int J Mol Sci*. 2013;14:17453–76.
- Zohdi V, Whelan DR, Wood BR, Pearson JT, Bamsey KR, Black MJ. Importance of tissue preparation methods in FTIR micro-spectroscopic analysis of biological tissues: traps for new users? *PLoS One*. 2015;10:e0116491.
- Nlawroci AR, Scherer PE. Keynote review: the adipocyte as a drug discovery target. *Drug Discov Today*. 2005;10:219–30.
- Chang J. Medicinal herbs, drugs or dietary supplements? *Biochem Pharmacol*. 2005;92:11–9.
- Cleio A, Colquitt J, Sidhu M, Royle P, Walker A. Clinical and cost effectiveness of surgery for morbid obesity: a systematic review and economic evaluation. *Int J Obesity*. 2003;27:1167–77.
- Roy MK, Nakahara K, Na TV, Talakontavakom G, Takenaka M, Isose S, et al. Baicalin, a flavonoid extracted from a methanolic extract of *Oroxylum*

indicum inhibits proliferation of a cancer cell line in vitro via induction of apoptosis. *Die Pharmazie*. 2007;62:149–53.

38. Madsen L, Petersen RK, Sørensen MB, Jørgensen C, Hallenborg P, Pridal L, et al. Adipocyte differentiation of 3T3-L1 preadipocytes is dependent on lipoxygenase activity during the initial stages of the differentiation process. *Biochem J*. 2003;375:539–49.
39. Seo M-J, Choi H-S, Jeon H-J, Woo M-S, Lee B-Y. Baicalein inhibits lipid accumulation by regulating early adipogenesis and m-TOR signaling. *Food Chem Toxicol*. 2014;67:57–64.
40. Nicholson AC, Hajar DP, Zhou X, He W, Gotto AM Jr, Han J. Anti-adipogenic action of pitavastatin occurs through the coordinate regulation of PPARgamma and Pref-1 expression. *Br J Pharmacol*. 2007;151:807–15.
41. Roh C, Jung U. Screening of crude plant extracts with anti-obesity activity. *Int J Mol Sci*. 2012;13:1710–9.
42. Pijanka JK, Kumar D, Dale T, Yousef I, Parkes G, Untereiner V, et al. Vibrational spectroscopy differentiates between multipotent and pluripotent stem cells. *Analyst*. 2010;135:3126–32.
43. Manoharan R, Baraga JJ, Rava RP, Dasari RR, Fitzmaurice M, Feld MS. Biochemical analysis and mapping of atherosclerotic human artery using FT-IR microspectroscopy. *Atherosclerosis*. 1993;103:181–93.



Ready to submit your research? Choose BMC and benefit from:

- fast, convenient online submission
- thorough peer review by experienced researchers in your field
- rapid publication on acceptance
- support for research data, including large and complex data types
- gold Open Access which fosters wider collaboration and increased citations
- maximum visibility for your research: over 100M website views per year

At BMC, research is always in progress.

Learn more biomedcentral.com/submissions



CURRICULUM VITAE

Name: Miss Tanaporn Hengpratom

Date of Birth: November, 11 1991

Place of Birth: Ratchaburi, Thailand

Education:

2013-Present Ph.D. Candidate (Biomedical Sciences), Institute of Science, Suranaree University of Technology, Nakhon Ratchasima, Thailand (GPA = 3.97)

2009-2013 Bachelor of Health Science (Physical Therapy) (First Class Honors), Mae Fah Lung University, Chiang Rai, Thailand (GPA = 3.92)

Scholarships:

2014-Present The Royal Golden Jubilee Ph.D. Program, The Thailand Research Fund, Thailand

2016-2017 The Newton Fund Ph.D. Placement Scholarship Program, Thailand

Publications:

Hengpratom, T., Lowe, G., Thumanu, K., Suknasang, S., Tiamyom, K., Eumkeb, G., (2018). *Oroxylum indicum* (L.) Kurz extract inhibits adipogenesis and lipase activity in vitro. **BMC Complementary and Alternative Medicine.** 18(1), 177.

(Impact Factor 2018 = 2.479, SCOPUS SJR 18 = Q1, Web of Sci 18 = Q2)